HEAT TRANSFER CHARACTERIZATION DURING RECIPROCATING AGITATION THERMAL PROCESSING OF CANNED PARTICULATES IN A NEWTONIAN FLUID

By:

Anubhav Pratap Singh

Department of Food Science and Agricultural Chemistry
Macdonald Campus, McGill University
Montreal, Canada

May, 2015

A thesis submitted to McGill University in partial fulfillment of the requirements for the degree of Doctor of Philosophy

Suggested short title:

HEAT TRANSFER IN RECIPROCATING AGITATION THERMAL PROCESSING

Dedicated to my beloved parents,
Mrs. Krishna Singh and Mr. Dinesh Pratap Singh,
and my soulmate, Anika.
Your love and support made this thesis possible.

ABSTRACT

A novel method of reciprocating agitation for enhancing heat transfer during thermal processing of canned particulates in Newtonian fluid (glycerin) was investigated in this study. First, a lab-scale reciprocating agitation retort was developed by modifying an existing conventional still retort to include a reciprocating mechanism providing reciprocations at a frequency of 0-5 Hz and amplitude of 0-30 cm. Temperature distribution studies inside the modified retort and inside the reciprocating cans revealed better temperature uniformity during reciprocating agitation as compared to still mode.

Heat penetration studies were subsequently conducted to evaluate the influence of reciprocating agitation on heat transfer coefficients (overall U, and fluid-to-particle h_{fp}), process time and quality loss. Reciprocating agitation resulted in 2-7 times enhancement in U & h_{fp} leading to 52-87% reduction in equilibration time of the cold spot. This enabled 46-62% reduction in process time resulting in 26-36% reduction in quality-deterioration index (cook-value/lethality) as compared to conventional still mode of thermal processing. Thus, reciprocating agitation was shown to have potential to deliver high quality products.

The effect of container orientation on heat transfer during reciprocation agitation thermal processing was then studied by placing experimental cans in one of the three possible orientations viz. horizontally along axis of reciprocation (HA), horizontally perpendicular to axis of reciprocation (HP) & vertically (V). HA orientation provided most rapid heat transfer followed by HP and V orientations, respectively. Here, it was seen that a high reciprocation intensity was not required to decrease process time considerably and a mild reciprocation intensity was sufficient. HA orientation was recommended for processing liquid foods and HP or V orientation was optimal for liquid particulate food mixtures.

Influence of various process variables (operating temperature, reciprocation frequency, reciprocation amplitude, container headspace, liquid viscosity/concentration, particle density & particle concentration) on U and h_{fp} were estimated for two situations: i) cans filled with single particle (liquid-only situation) and ii) cans filled with multiple particles. In single particle study, both U and h_{fp} were influenced significantly by reciprocation frequency, reciprocation amplitude, operating temperature and liquid viscosity. Headspace affected only U, while particle density affected only h_{fp}. In general, higher U and h_{fp} were obtained at lower liquid viscosity and at higher

frequency, amplitude, temperature and headspace. In the multiple particle study, it was generally observed that the magnitude of U and h_{fp} were larger as compared to single-particle (liquid-only) scenario due to higher level of turbulence/mixing inside the cans on account of collisions amongst particles. U & h_{fp} followed the trend: Nylon > polypropylene > Teflon, while, the rate of temperature increase followed the trend: polypropylene > Nylon > Teflon. U & h_{fp} were found to increase on increasing particle concentration, however, beyond an optimal concentration U & h_{fp} decreased due to dominance of conduction based heating.

Based on the results of these studies, simultaneous multi-objective optimization of heat transfer coefficients (U & h_{fp} - to maximize heat transfer) and reciprocation intensity (RI - to minimize agitation losses) was conducted. For this, a composite model was developed using all available data and was then subjected to numerical optimization. High RI (37-45 ms^{-2}) was recommended to maximize U & h_{fp}, whereas lower RI (16-19 ms^{-2}) was found optimal for simultaneous optimization of U, h_{fp} & RI. Product composition containing low viscous liquids filled with 23-27% concentration of particles with density of 1134-1351 kg/m^3 were found most desirable. Optimal conditions were also reported for different operating temperatures, liquid viscosities, particle concentrations and particle densities.

Dimensionless correlations were then developed for predictive modeling and scale-up of reciprocating agitation thermal process using multiple non-linear regressions of significant dimensionless groups. Dimension of can along the axis of reciprocation was found to play a dominant role in the heat transfer phenomenon and was included in the characteristic length formulated for Nusselt number at can wall (from U). On comparing results of this study with literature, it was clear that forced convection effects and turbulence levels during reciprocating agitation were significantly larger than other modes of rotary agitation. Yet, effect of natural convection could not be ignored at lower RI.

Finally, flow visualization studies were carried out to characterize particle motion/mixing behavior of liquid/particle mixtures by videotaping particle motion/mixing in transparent containers under various conditions. The nature of mixing and particle motion was found markedly different for different orientations and particle densities. Mixing time was affected by frequency, liquid viscosity, container orientation, particle concentration and particle density.

RÉSUMÉ

Une nouvelle méthode d'agitation à mouvement alternatif a été investiguée pour améliorer le transfert de chaleur au cours du traitement thermique d'un fluide Newtonien (glycérine) contenant des matières particulaires. Dans un premier temps, un système d'agitation à mouvement alternatif à petite échelle a été développé en modifiant un système conventionnel pour y ajouter un mécanisme réciproque dont la fréquence d'agitation est de 0 à 5 Hz et l'amplitude est de 0 à 30 cm. Une étude de la distribution des températures à l'intérieur de conserves traitée par agitation à mouvement alternatif révéla une meilleure uniformité des températures par rapport au témoin.

La transmission de chaleur a ensuite été étudiée afin de connaitre l'influence de l'agitation à mouvement alternatif sur les coefficients de transfert de chaleur (U global et h_{fp} fluide-particule), sur le temps de traitement et sur la perte de qualité. L'agitation réciproque a augmenté U et h_{fp} d'un facteur de 2 à 7, contribuant à une réduction de 52 à 87% du temps d'équilibre au point froid. Ceci a pour effet une réduction de 46 à 62% et par conséquent une réduction de 26 à 36% de l'index de perte de qualité (valeur de cuisson / léthalité) par rapport à un procédé conventionnel sans agitation. Il a ainsi été observé que l'agitation peut produire des aliments de bonne qualité.

L'effet de l'orientation de la conserve sur le transfert de chaleur au cours du traitement thermique à agitation à mouvement alternatif a ensuite été étudié en plaçant la conserve sur l'une de trois axes: horizontalement selon l'axe de mouvement de va-et-vient (HA); horizontalement perpendiculaire à l'axe de mouvement de va-et-vient (HP); et verticalement (V). L'orientation HA produit le transfert de chaleur le plus rapide, suivi par les orientations HP et V. Il a été observé qu'une amplitude de mouvement éleve n'est pas nécessaire pour une réduction importante du temps de traitement. L'orientation HA est recommandée pour les aliments liquides ou pour des conditions d'agitation modérées tandis que les orientations HP et V étaient ideales pour les aliments mixtes.

L'influence de plusieurs variables de traitement (température d'opération, fréquence de mouvement, amplitude de mouvement, espace de tête, viscosité/concentration du liquide, densité des particules & concentration des particules) sur U et h_{fp} a été estime pour deux cas: i) une conserve contenant une seule particule (entièrement liquide) et ii) une conserve contenant plusieurs particules. Dans le premier cas, la fréquence du mouvement, l'amplitude du mouvement, la température du traitement et la viscosité du liquide ont eu une influence significative sur U et h_{fp}. L'espace de tête a seulement eu une influence sur U alors que la densité des particules a seulement

eu une influence sur h_{fp}. Généralement, un U et h_{fp} plus grands ont été obtenus pour une viscosité plus faible et une fréquence, une amplitude, une température et un espace de tête de valeur plus grande. Dans le cas de la conserve contenant plusieurs particules, il a généralement été observé que les valeurs de U et h_{fp} étaient plus grandes par rapport au groupe à une particule à cause de l'augmentation de l'agitation par turbulence à l'intérieur de la conserve due aux collisions entre particules. U et h_{fp} suivaient la tendance suivante: polypropylène > Nylon > Téflon. U et h_{fp} ont augmenté en fonction de la concentration des particules jusqu'à l'atteinte d'un maximum, suite à quoi U et h_{fp} ont diminué gouverné par la conduction.

Par la suite, une étude d'optimisation multiobjective des coefficients de transfert de chaleur (U et h_{fp} pour maximiser le transfert de chaleur) et de l'intensité d'agitation (RI pour minimiser les pertes d'agitation) a été effectuée. Pour ce faire, un modèle composé a été généré à partir des données précédemment recueilles pour faire une optimisation numérique. Un RI élevé (37 à 45 ms^{-2}) maximise U et h_{fp} alors qu'un RI plus faible (16 à 19 ms^{-2}) permet l'optimisation simultané des paramètres U, h_{fp} et RI. Un produit de faible viscosité ayant une concentration particulaire de 23 à 27% d'une densité de 1134 à 1351 kg/m^3 était plus désirable. Les conditions optimales pour des températures, viscosités, concentrations particulaires et densités particulaires ont également été obtenes.

Des corrélations sans dimension ont ensuite été développées pour la modélisation prédictive et changement d'échelle du processus thermique en utilisant des régressions non-linéaires des groupes significatifs sans dimension. La dimension de la conserve selon l'axe de mouvement d'agitation joue un rôle important dans le phénomène de transfert de chaleur et s'inclut dans la longueur caractéristique servant au calcul du nombre de Nusselt. En comparant avec la littérature, il est clair que les effets de convection forcée et de la turbulence durant l'action d'agitation par mouvement alternatif était plus important que les autres modes d'agitation rotatoire. Toutefois, l'effet de la convection est non-négligeable pour une RI faible.

Enfin, une étude de visualisation du mouvement des fluides a permis la caractérisation du mouvement des particules et des interactions liquide-particule par enregistrement vidéo de conserves transparentes sous traitements différents. Le mouvement des particules s'est révélé très différent pour des orientations et densités de particule différentes. Le temps d'agitation était affecté par la fréquence, par la viscosité du liquide, par l'orientation de la conserve, par la concentration des particules et par la densité des particules.

CONTRIBUTIONS OF AUTHORS

Several journal publications and conference presentations have been made based on this thesis research. Some authors have been involved in the manuscripts and their contributions are detailed as follows:

Anubhav Pratap Singh is the PhD candidate who planned and conducted all the experiments in consultation with his supervisor, gathered and analyzed the results, and drafted all the manuscripts for scientific publications.

Dr. H. S. Ramaswamy is the thesis supervisor, under whose guidance the research was carried out, and who assisted the candidate in planning and conducting the research as well as in correcting, editing, reviewing and processing the manuscripts for publications.

Anika Singh is a PhD candidate under supervision of Dr. Ramaswamy, at McGill University. She helped the candidate in review of literature and in establishment of methodology for evaluating heat transfer coefficients under reciprocating agitation conditions.

LIST OF PUBLICATIONS AND PRESENTATIONS

Part of this thesis has been published or submitted for publications in refereed scientific journals:

Singh, A. P., Singh, A., & Ramaswamy, H. S. (2015). Heat transfer phenomena during thermal processing of liquid particulate mixtures – A Review. *Critical Reviews in Food Science and Nutrition, http://doi.org/10.1080/10408398.2014.989425*

Singh, A., Singh, A. P., & Ramaswamy, H. S. (2015). Computational techniques used in heat transfer studies on canned liquid-particulate mixtures. *Trends in Food Science and Technology*, 43(1), 83–103.

Singh, A. P., Singh, A., & Ramaswamy, H. S. (2015). Modification of a static steam retort for evaluating heat transfer under reciprocation agitation thermal processing. *Journal of Food Engineering*, 153, 63-72.

Singh A. P., & Ramaswamy, H. S. (2015). Effect of can orientation on heat transfer coefficients associated with liquid particulate mixtures during reciprocation agitation thermal processing. *Food and Bioprocess Technology*, 8(7), 1405-1410.

Singh A., Singh A. P., & Ramaswamy, H. S. (2014). A refined methodology for evaluation of heat transfer coefficients in canned particulate fluids under rapid heating conditions. *Food and Bioproducts Processing*, 94, 169-179.

Singh A. P., & Ramaswamy, H. S. (2015). Optimization of heat transfer and reciprocation intensity during thermal processing of liquid particulate mixtures undergoing reciprocating agitation. *Innovative Food Science & Emerging Technologies*, In review.

Singh A. P. & Singh A., & Ramaswamy, H. S. (2015). Dimensionless correlations for heat transfer coefficients during reciprocating agitation thermal processing of Newtonian liquid/particulate mixtures. *Food and Bioproducts Processing*, In review.

Singh A. P., & Ramaswamy, H. S. (2015). Heating behavior of canned liquid during reciprocating agitation thermal processing of liquid-particulate mixtures. *Food and Bioprocess Technology*, Prepared for submission.

Singh A. P., & Ramaswamy, H. S. (2015). Visualization and quantification of particle-motion and particle-mixing during reciprocating mode of agitation. *Journal of Food Engineering*, Prepared for submission.

Part of this thesis have been presented in various scientific conferences:

Oral Presentations

Singh A.P., Singh A., & Ramaswamy H.S. (2015). Multi-variate optimization of reciprocation container agitation thermal processing of liquid particulate mixtures using a hybrid genetic algorithm. 12th International Congress on Engineering and Food (ICEF12), June 14-18, Quebec City, QC, Canada.

Singh A. P., & Ramaswamy, H. S. (2014). Heat transfer during Reciprocation Thermal Processing of Liquid Particulate Foods. Research Feeding Industry Symposium, September 17, Montreal, QC, Canada.

Singh A. P., Singh A., & Ramaswamy, H. S. (2014). Heat Transfer during Reciprocation Thermal Processing of Canned Particulates - A Single versus Multiple Particle Study in a Newtonian Fluid. The Northeast Agricultural and Biological Engineering Conference (NABEC), July 27-30, Kemptville, ON, Canada.

Singh A. P., & Ramaswamy H. S. (2014). High Temperature High Pressure Resistance of Clostridium botulinum - Canadian Study. Institute of Food Technologists (IFT) Annual Conference, June 21-24, New Orleans, LA, USA.

Singh A. P., Singh A., & Ramaswamy H. S. (2014). Retort Modification and Evaluation of Heat Transfer during Thermal Processing under Reciprocating Container Agitation. Institute for Thermal Processing Specialists (IFTPS) Annual Meeting, March 11-14, Orlando, FL, USA. **[won first place in graduate paper competition].**

Conference presentations - Poster

Singh A.P., Singh A., & Ramaswamy H.S. (2015). Reciprocating agitation thermal processing: Heat transfer characterization under different container orientations. Institute of Food Technologists (IFT) Annual Conference, July 11-14, Chicago, IL, USA. **[finalist in AAFSIS Paper Competition & Food Engineering division].**

Singh A.P., Singh A., & Ramaswamy H.S. (2015). Optimization of heat transfer and reciprocation intensity during thermal processing of liquid particulate mixtures undergoing reciprocating agitation. Institute for Thermal Processing Specialists (IFTPS) Annual Meeting, March 3-6, San Antonio, TX, USA. **[won second place in graduate paper competition].**

Singh A. P., Singh A., & Ramaswamy H. S. (2014). Effect of System Parameters on Heat Transfer to Canned Particulate Viscous Newtonian Fluids under Reciprocating Container Agitation Thermal Processing. 17th World Congress of Food Technology & Expo, IUFOST-2014, August 17-21, Montreal, QC, Canada.

Singh A., Singh A. P., & Ramaswamy H. S. (2014). Effect of Can Orientation on Heat Transfer Coefficients associated with Canned Particulate Fluids during Reciprocating Container Agitation Thermal Processing. 17th World Congress of Food Technology & Expo, IUFOST-2014, August 17-21, Montreal, QC, Canada.

Singh A.P., Singh A., & Ramaswamy H.S. (2014). Fabrication and characterization of a reciprocating steam retort and the study of the effect of reciprocation on heat transfer in a single-particle can filled with viscous Newtonian Fluid. Institute of Food Technologists (IFT) Annual Conference, June 21-24, New Orleans, LA, USA. **(finalist in Marketing & Management Division and AAFSIS Paper Competition).**

Singh A., Singh A. P., & Ramaswamy H. S. (2014). A refined method for evaluating heat transfer coefficients in canned particulate fluids under rapid heating conditions. Institute for Thermal Processing Specialists (IFTPS) Annual Meeting, March 11-14, Orlando, FL, USA. **[won second place in graduate paper competition].**

ACKNOWLEDGEMENTS

My first and foremost acknowledgement is to my supervisor, Dr. Hosahalli S. Ramaswamy, without whose faith and encouragement this work wouldn't have happened. I would like to thank him for posing faith in me and allowing me to explore multiple ideas in the field. My research experience at McGill wouldn't have been as enriching and useful without the multiple conversations I had with him. To him, I owe a new sense of direction in my life, and it is from the bottom of my heart that I thank him for all he has done for me over the years.

Next, I would like to thank Dr. Samson Sotocinal for his support and useful advice in the fabrication and maintenance of the reciprocating retort.

I would like to extend my appreciation to Dr. Vijaya Raghavan, Dr. Valerie Orsat, Dr. Inteaz Alli, Dr. Benjamin Simpson and Dr. Varoujan Yaylayan, members of my committee, for their suggestions during my research. Also extended are my sincere thanks to all professors and staff in the Department of Food Science. I would also like to thank our department's secretaries, Ms. Leslie Ann LaDuke and Ms. Patricia Singleton, for their support and helpfulness.

I also would like to thank all my lab-mates and friends, inside and outside the Food Science department, for their encouraging attitude and for their help. I apologise for not naming everyone, I´m sure that everybody is remembered. Yet, I would like to especially thank Mr. Navneet Rattan, Dr. Ajaypal Singh, Dr. Yetenayet Tola and Dr. Derek Wray for their help and support during my initial days at McGill.

I would also like to thank my motivation, my colleague, and my lovely wife Mrs. Anika Singh, for her unconditional love and support. Not only was she a wonderful co-author to many of my papers, but always stuck to my side, even when I was irritable and depressed. She has been the source of inspiration who pushed me to work many late nights. I would also like to extend my thanks to my parent-in-laws, my brother-in-law, my brother and my cousins for being my support group and the source of encouragement when I was down and low.

Last, but not the least, I would like to thank my beloved and very supportive parents (Mr. Dinesh Pratap Singh and Mrs. Krishna Singh) and my beloved uncle (Dr. Akhilesh Singh) for their support, sacrifice and constant encouragement. I want them to know that I am very grateful for their unreserved love and encouragements throughout my studies. Without their love and patience, I would not have become who I am now.

TABLE OF CONTENTS

NOMENCLATURE

α	thermal diffusivity, m^2/s
a	radius of sphere, m
A	total external surface area, m^2
AR	aspect ratio of can,
β	thermal expansion coefficient, K^{-1}
c_p	specific heat capacity, J/kg^{o}C
C_0	cook value, min
d	particle diameter, m
D	D-value, min
ε	particle concentration,
f_h	heating rate index, min
F_0	process lethality, min
$F_{z/T}$	lethality at temperature T for a z-value of z,
Fr	Froude number
g	acceleration due to gravity, ms^{-2}
Gr	Grashoff Number
h_{fp}	fluid to particle heat transfer coefficient, W/m^2^{o}C
h_s	headspace, m
H	height of can, m
j_{ch}	heating lag factor,
k	thermal conductivity, W/m^{o}C
l	crank radius, m
L_c	characteristic length, m
m	mass, kg
n	number of samples
N	final count of TTI,
N_o	initial count of TTI,
ρ	density, kgm^{-3}
Pr	Prandtl number,

Pt	process time, min
Re	Reynold's number,
T	temperature, ^oC
T_o	reference temperature, ^oC
t	time, s
τ	Fourier number,
u	local flow velocity, ms^{-1}
U	overall heat transfer coefficient, $W/m^{2o}C$
ψ	sphericity,
ν	kinematic viscosity, m^2/s
ω	angular velocity, rad/s
x	value of a variable,
$\bar{x}$	mean of the values,
z	z-value, ^oC

Subscripts

ap	apparent,
c	can,
crt	constant/average retort temperature,
HA	cans placed horizontally along the axis of reciprocation,
HP	cans placed horizontally perpendicular to the axis of reciprocation,
i	initial condition,
l	liquid,
p	particle,
ps	particle surface,
pred	predicted,
r	retort,
ref	reference,
s	surface,
V	cans placed vertically perpendicular to the axis of reciprocation

LIST OF TABLES

LIST OF FIGURES

CHAPTER 1

INTRODUCTION

Even after two centuries, the "art" of thermal processing (canning) envisaged by the French confectioner, Nicolas Appert, continues to be the most reliable and safe way of preserving food. Although, the "science" behind this "art" is now well established and thermal processing is one of the best understood and safe process, yet, evolving consumer demands for high quality food drive the need for constant innovations and research. Conventional thermal processing in still retorts involves heating food, packaged in hermetically sealed containers, at high enough temperature for sufficient time to eliminate micro-organisms of public health and spoilage concern. During this process, the phenomenon of natural convection predominates the heating mechanism of food and stand alone natural convection is slow, and thus conventional thermal processing requires a long time to heat the product to the required sterilizing temperatures. As a result, quality of thermally processed food deteriorates considerably, which is a major cause of concern for thermal processing industries. Luckily, natural convection can be easily supplemented with forced convection to reduce process times, increase production efficiency, and in some instances minimizing the ruinous effects of heat (Dwivedi, 2008). This is achieved by agitating the containers during the process by rotational (axial, biaxial or end-over-end) or reciprocating agitation, and in doing so, inducing forced convection currents that mix and heat the food more effectively. Rotary retorts have tremendous advantages over still retorts for processing of food containers containing liquid–particle mixtures such as peas, corn, asparagus, mushrooms, beans etc. in liquid and a variety of semisolid or viscous foods such as sauces or soups containing meat chunks or vegetables (Sablani and Ramaswamy, 1996). Most research on rotary agitation has been done on end-over-end mode and axial mode of rotation. Apart from these two modes, recently, biaxial mode of rotary agitation of containers was proposed and studied by Dwivedi (2008) and was found to be better than other modes of rotation for reduction of process times and improvement in quality of products. This simulates the commercial high speed continuous retorts and turbo type cookers manufactured by FMC (now JBL Corporation USA). Very recently, a new concept of imparting agitation by using high frequency longitudinal agitation has been proposed and this promises to drastically reduce the process times (Walden and Emanuel, 2010). However, there exists a paucity of available

scientific literature on this mode of agitation and there is scope for investigating the reciprocating agitation process.

Thermal processing of canned particulate-liquid foods during agitation processing requires the particle center to receive the predetermined minimum heat treatment in the form of minimum process lethality (F_o). Accurate and reliable prediction of lethality at the slowest point of heating (cold-spot) is the key to the proper design and successful optimization of the agitating retort process. Several studies have carried out the evaluation of heat transfer to canned particulate in Newtonian liquids (Lenz and Lund, 1978; Deniston *et al.*, 1987; Fernandez *et al.*, 1988; Stoforos and Merson, 1990, 1991; Sablani and Ramaswamy, 1995, 1996, 1997, 1999; Meng and Ramaswamy, 2005, 2007a, 2007b and Dwivedi and Ramaswamy, 2010a, 2010b, 2010c, 2010d). These studies have focused on evaluating overall heat transfer coefficient U, which is the heat transfer coefficient between the heating medium in the retort and the liquid in the can, and the fluid-to-particle heat transfer coefficient h_{fp}, which is the heat transfer coefficient between liquid in the can and particle surface. Based on the retort temperature, h_{fp}, and U values, particle lethality can be predicted using computer programming. Thus, knowledge of U and h_{fp} is essential for establishment and control of a thermal process. However, U and h_{fp} depend on various system and product parameters and vary with different processing conditions. The effect of various parameters on U and h_{fp} e.g. process temperature, headspace, agitation speed, liquid viscosity, particle properties and volume fraction occupied by the particles, etc. have been experimentally investigated by Lenz and Lund (1978), Deniston *et al.* (1987), Fernandez *et al.* (1988), Sablani and Ramaswamy (1995, 1996, 1997, 1999), Meng and Ramaswamy, (2005, 2007a, 2007b) and Ramaswamy and Dwivedi (2011). They observed that U and h_{fp} are affected by most of these parameters and a detailed evaluation of the heat transfer with these process variables is imperative to understand the phenomenal behavior of heat transfer occurring during the process.

As mentioned above there are several factors affecting heat transfer coefficients in agitation processing, therefore it is necessary to quantify the influence of these factors. Traditionally, dimensionless correlations have been widely used to predict the heat transfer coefficients in terms of the Nusselt number. There are some dimensionless groups well known and used for correlating experimental heat transfer data, such as Nusselt (Nu), Reynolds (Re), Prandtl (Pr), and Grashof (Gr) numbers. Dimensional analysis gives more insight to the physical phenomena and can also

be used for scale-up purpose. Various researchers (Lenz and Lund, 1978, Deniston *et al.* 1987, Fernandez *et al.* 1988, Sablani *et al.*, 1997, Meng and Ramaswamy, 2007c, and Dwivedi and Ramaswamy, 2010d) have developed dimensionless correlations for U and h_{fp} prediction in various modes of agitations.

Apart from heat transfer analysis and development of correlations, flow visualization studies can be used to gain a better understanding of the mixing behavior of particulate systems and for understanding their influence on associated heat transfer within cans (Rao and Anantheswaran, 1988). Stoforos and Merson (1990) studied the motion of spherical particles in axially rotating cans and characterized the particle-to-liquid relative velocity from the idealized particle motion and liquid velocities. Their flow visualization study revealed more complicated particle motion than idealized in mathematical analyses. Later Stoforos and Merson (1991) attempted to use this technique to explain the decrease of h_{fp} values when increasing rotational speed or decreasing liquid viscosity for a Teflon sphere during axial rotation. Sablani (1996) studied the motion of a single particle in a can subjected to end-over-end rotation and explained the differences in h_{fp} between various experimental conditions. Such a study will be beneficial in understanding the motion of the particles inside the can and in identifying the magnitude and the nature of turbulence created due to the movement of liquid and particles.

Although, the first reciprocating cooker was patented by Gerber (1938), recent interest in reciprocating agitation thermal processing started with a patent by Richard Walden (Walden, 1999) around the beginning of twenty first century and is now popularized as Shaka® technology. The first pilot Shaka retorts were manufactured in 2006 and utilized a current retort system with licensed technology to induce a vigorous shaking motion. The Shaka retort is one of the first major improvements to retorts in over 60 years and is still a relatively new process (Angalet, 2011), which yet, need to be investigated in detail. Apart from the book chapter by Walden and Emanuel (2010), there exists no independent research validation of the claims made by the manufacturers. They claimed that that this process can reduce process times more than 20-fold as compared with a still process and more than 10-fold compared to a rotary process and hence may increase the quality of the thermally processed food. More recently, Allpax introduced a new range of retorts called Gentle Motion retorts which is similar to Shaka® retorts in operation, but employs a less severe reciprocation frequency (< 1 Hz) to process products susceptible to agitation losses (IFTPS,

2015). Independent validation and further investigation of the causes of the tremendous reduction of process times need to be evaluated and understood. A heat transfer study coupled with a particle mixing study of the process is required in order to properly understand and quantify the effects associated with this mode of agitation. Hence, based on the available knowledge and understanding from the studies on other modes of agitations, the following work is undertaken to understand the heat transfer behavior during the thermal processing of cans undergoing reciprocating container agitation.

1.1 Objectives

1.1.1. Overall Objective

The overall objective of this work is to evaluate the associated heat transfer phenomenon during thermal processing of canned particulates in Newtonian fluids under reciprocation mode of container agitation.

1.1.2. Specific Objectives

i. To modify an existing conventional steam retort to accommodate a reciprocating agitation mechanism under a range of process variables.

ii. To evaluate heat transfer, process time and quality loss degradation index associated with reciprocating agitation thermal processing of cans.

iii. To study the effect of container orientation during reciprocating agitation thermal processing of liquid particulate mixtures.

iv. To study the effect of processing conditions and product properties on heat transfer during reciprocating container agitation with a single particle suspended in liquid-only cans.

v. To study the effect of processing conditions and product properties on heat transfer during reciprocating container agitation in liquid containing multliple particles.

vi. To predict optimal processing conditions and different product properties for reciprocating agitation thermal processing.

vii. To develop dimensionless correlations for predicting heat transfer during reciprocating agitation thermal processing of particulate Newtonian fluid mixtures.

viii. To study the particle motion and particle mixing during reciprocating agitation thermal processing of liquid particulate mixtures.

PREFACE TO CHAPTER 2

Process establishment and validation are the two key issues in studies dealing with thermal processing and are necessary when investigating a new system like reciprocating agitation thermal processing. While process establishment involves determination of minimal thermal process time and temperature, process validation ensures that these requirements are met. Determination of this minimal thermal process is a complex procedure with numerous factors involved like pH of the food, type and resistance of the target microorganism, storage conditions after the process, thermo-physical properties of the food, container shape and size etc. Collection of time-temperature data is the first step in such studies and researchers have used various methodologies for data collection depending on the objective of the heat transfer study. Also, various methodologies have been adopted to analyze the time-temperature data collected for estimation of heat transfer coefficients and development of dimensionless correlations to characterize the thermal process.

This chapter reviews the various methods and models available in literature for the collection and analysis of time-temperature data during thermal processing of canned liquid particulate mixtures. The use of dimensionless correlations, the range of heat transfer coefficients and the available knowledge on the effect of various processing variables on heat transfer in other modes of agitation have also been highlighted.

Parts of this chapter have been presented at the Research Feeding Industry (RFI) symposium held on Sep 14, 2014 in Montreal, Quebec.

Parts of this chapter have been accepted for publication as review articles on: *Heat transfer phenomena during thermal processing of liquid particulate mixtures – A Review*. Critical Reviews in Food Science and Nutrition, http://doi.org/10.1080/10408398.2014.989425

Parts of this chapter have been published as review articles on: "*Computational techniques used in heat transfer studies on canned liquid-particulate mixtures – A review*" in Trends in Food Science and Technology. 43(1), 83–103.

The review was carried out by the candidate under the supervision of Dr. H. S. Ramaswamy.

CHAPTER 2

LITERATURE REVIEW

2.1 Abstract

During the past few decades the food industry has been moving towards improved thermal and novel processing technologies as well as non-thermal processing techniques, to minimize the associated high quality loss involved in commercial thermal processing. Among these are the novel agitation systems which permit forced convention in canned particulate fluids to improve heat transfer, reduce process time and minimize heat damage to processed products. These include traditional rotary agitation systems involving end-over-end, axial or biaxial rotation of cans and the more recent reciprocating (lateral) agitation. The invention of thermal processing systems with induced container agitation has made heat transfer studies more difficult due to problems in tracking the particle temperatures due to their dynamic motion during processing and complexities resulting from the effects of forced convection currents within the container. This has prompted active research on modeling and characterization of heat transfer phenomena in such systems. This chapter brings in perspective the current status on thermal processing of particulate foods, within the constraints of lethality requirements from safety view point, and discusses available techniques of data collection, heat transfer coefficient evaluation, various critical processing parameters which affect these heat transfer coefficients, and dimensionless correlations developed for predictive modeling of heat transfer with a focus on agitation processing conditions.

2.2 Introduction

Invented at the beginning of 1800 and scientifically established by early 1900, thermal processing technology has come a long way and is considered to be one of the very mature and scientifically based processes. Up until the 1950s, emphasis of thermal processing has largely remained on food safety, with quality loss barely registering a concern. Common thermal processing techniques are still considered effective for preserving foods and ensure that the product is safe, shelf-stable and devoid of any harmful bacteria. Recently, however, due to increased consumer awareness about importance of food quality, technology has been gearing up to improve better quality retention without compromising safety. Several commercially adapted thermal processes like high-temperature short-time processing, ultra-high temperature processing, aseptic

processing, agitation thermal processing, retort pouch / thin profile processing etc., have largely emerged to meet consumer demands for high quality products.

Thermal processing involves heating foods in hermetically sealed containers for specific time and temperature combinations in order to destroy pathogenic and spoilage micro-organisms (Dwivedi, 2008). In order to properly predict the time and temperature combinations necessary to deliver a safe canning process, it is important to be able to predict the transient temperatures using models based on a thorough understanding of the mechanisms involved in the heat transfer process. Further, the applied thermal treatment not only destroys microorganisms, but also simultaneously results in loss of many nutrients and degrades quality of products appreciably (Awuah *et al.*, 2007a). With the advancement of knowledge and advent of affordable technological concepts, there is a considerable interest in the food industry for adaptation of technologies to satisfy consumer demand for producing high-quality products without compromising safety and shelf stability. Thus, it is necessary to study and understand the heat transfer phenomenon associated with thermal processing for devising a process which not only imparts a minimal thermal treatment for ensuring safety and stability, but also results in minimal overcooking. Additionally, with many new products, new packages, and new processes appearing on the market each day, it is important to have appropriate methodologies for studying these systems for assuring minimal thermal treatments.

Convection is the dominant mechanism for heating of thermally processed foods. In static or batch processes, the phenomenon of natural convection comes into play. Convection heating is beneficial in terms of reducing process times, increasing production efficiency, and in some instances minimizing the ruinous effects of heat (Tucker, 2004). However, it has been observed that the natural convection involved in thermal processing is too slow to be of any benefit, except when dealing with liquid foods, and therefore needs to be supplemented with forced convection. This is achieved by agitating the containers by rotational (axial, biaxial or end-over-end) or reciprocation (lateral) agitation, and in doing so, a forced convection current is induced that helps to mix and heat the food more effectively. Rotary retorts have tremendous advantages over still retorts for processing of viscous foods in large containers (Sablani and Ramaswamy, 1996; Tattiyakul *et al.*, 2002). Such retorts can increase convection in containers containing liquid–particle mixtures such as high-quality peas, corn, asparagus, mushrooms, and a variety of semisolid

or viscous foods such as sauces or soups containing meat chunks or vegetables (Smout *et al.*, 2000). Most research on rotary agitation has been carried out with end-over-end (EOE) and axial modes of rotation. Apart from these two modes, biaxial mode of rotary agitation of containers (as is common in continuous turbo retorts) was studied by Dwivedi (2008) and was found to be better than other modes of rotation for reduction of process times and improvement in quality of products. Recently, a new concept of imparting agitation by using high frequency reciprocating (lateral) agitations has been proposed by Walden and Emanuel (2010). High frequency back-and-forth motion of containers during reciprocating mode of agitation has the potential to drastically reduce process times and to yield very high quality thermally processed food products. However, there exists a paucity of scientific data on the heat transfer phenomenon involved in this mode of agitation.

Validation of a thermal process by processing authorities requires gathering of time-temperature data to ensure that the minimum required lethality is achieved at slowest heating point of the system (particle-center for liquid-particulate foods). Time-temperature data are also required for evaluation of heat transfer coefficients associated with the process. However, with development of newer and faster agitation techniques, the task of collecting these data have become complex. It is difficult to gather center temperature of agitating particles without affecting their free motion. Various techniques have been developed for monitoring particle temperatures during agitation. Depending on the purpose of collection of heat penetration data, these techniques may range from the use of normal thermocouples (Deniston et al, 1987; Sablani, 1996; Meng, 2006) to the use of other technologies like wireless sensors (Lesley, 1987; Wang *et al.*, 2006; Awuah *et al.*, 2007b; Dwivedi and Ramaswamy, 2010c;), time-temperature indicators like liquid crystals (Stoforos and Merson, 1991; Zitoun and Sastry, 1994; Balasubramaniam and Sastry, 1995) and, chemical (Weng *et al.*, 1992; Hendrickx *et al.*, 1995; Van Loey *et al.*, 1995, 1997, 2004) and biochemical indicators (Pflug *et al.*, 1980a, 1980b; Silva *et al.*, 1994).

Most of the earlier heat transfer studies on thermal processing (Clifcorn *et al.*, 1950; Conley *et al.*, 1951; Berry and Bradshaw, 1980; Berry and Kohnhorst, 1983, 1985) dealt with the effect of agitation on specific heat penetration parameters of various products. However, the more recent ones have focused on evaluation of heat transfer coefficients associated with thermal processing. During thermal processing of liquid-particulate mixtures, two heat transfer coefficients are of

interest: i) the overall heat transfer coefficient (U) from heating medium to the can liquid through the can wall, and ii) the fluid-to-particle heat transfer coefficient (h_{fp}) from liquid to particle-surface. Both U and h_{fp} are important parameters influencing the heating rate of liquid-particulate mixtures. Calculation of these heat transfer coefficients is also beneficial, because they can be used in predictive mathematical models and simulation programs for prediction and optimization of the thermal process, and thus reduce time and cost of experiments involved. A number of studies have been published to evaluate the physical parameters that influence these heat transfer coefficients, and it has been recognized that agitation speed, retort temperature, headspace volume, system geometry, liquid viscosity, rotation radius, particle size, and particle density were key factors in influencing U and h_{fp} (Lenz and Lund, 1978; Naveh and Kopelman, 1980; Lekwauwa and Hayakawa, 1986; Rao and Anantheswaran, 1988; Sablani and Ramaswamy, 1995, 1999; Meng, 2006; Dwivedi, 2008).

Gathering of time-temperature data after the development of a new process is a primary task, both for the purpose of validation and for studying associated heat transfer. In this chapter, various methods available in literature for gathering of time-temperature data during thermal processing of liquid-particulate mixture are reviewed. Further, different models used by researchers, to model the heat transfer associated with liquid-particulate mixture during canning, are highlighted. Influence of system and product parameters on associated heat transfer coefficients during different modes of agitation and dimensionless correlations developed for predictive modeling of these heat transfer coefficients are reviewed. In addition to this, this chapter also presents the necessary requirements to impart a minimal process for safe sterilization during thermal processing.

2.3 Requirements for a minimal thermal process

Thermal processing primarily deals with application of heat for eliminating microorganisms which are of public health concern and for extension of shelf-life of foods. Although safety is the paramount consideration for designing a thermal process, yet it is important to preserve the quality of products as well. Hence, it is desirable for canners to be able to predict the amount of heat transferred which would be sufficient to eliminate most microorganisms while

minimizing nutrient destruction. Therefore, understanding of process evaluation and process calculation methodologies is very important.

The phrase "*minimal thermal process*" was introduced by the US Food and Drugs Administration in 1977 and is defined as "*the application of heat to food, either before or after sealing in a hermetically sealed container, for a period of time and at temperature scientifically determined to be adequate to ensure the destruction of microorganisms of public health concern*". Calculating or determining the process schedule required to kill or inactivate heat resistant and pathogenic bacteria in food forms the basis of thermal process calculations. Determination of proper thermal process time and temperature for a can is a complex procedure with numerous factors involved like pH of the food, type and resistance of the target microorganism, storage conditions after the process, heating conditions, thermo-physical properties of the food, container shape and size etc. (Stumbo, 1973).

The operating temperature and pH are the most important factors as thermal resistance of microorganisms in low-acid foods is appreciably higher than the resistance of those found in high-acid foods and in both cases it is highly temperature dependent. Selection of a reference temperature for thermal processing is primarily based on the heat resistance of a target pathogenic microorganism that could be present in the product. Table 2.1 lists the heat resistance of common microorganisms in food at different levels of pH. From Table 2.1, it is clear that operating temperatures (around 250 °F) and decimal reduction times are highest for thermophilic and mesophilic spores in low-acid foods, and lower for mesophilic spores in pH range 4.0 – 4.6 (around 200-212 °F), and lowest for yeasts, molds, and non-spore-forming mesophilic bacteria in high-acid foods (around 150 °F). Thus, for a minimal process, heating low-acid foods at high temperatures under sterilization conditions is necessary, while a lower level of thermal treatment at pasteurization conditions is enough for high-acid foods. Additional details about heat resistance of microbes, level of pH and reference temperatures involved are available in literature (Ball and Olson, 1957; Stumbo, 1973; Odlaug and Pflug, 1978; Montville and Sapers, 1981; Larousse and Brown, 1996; Brown, 2000; Breidt *et al.*, 2007).

Table 2.1. Comparative heat resistance of bacteria important to thermally processed foods (adapted from the works of Odlaug and Pflug, 1978; Larousse and Brown, 1996).

Class of Food	Type of Microbes	Microorganism(s)	Reference Temperature (°F)	D-Value (min)	Z-Value (°F)
Low-acid food (pH > 4.6)	Thermophiles	Flat-sour group (*B. stearothermophilus*)	250	4.0 – 5.0	14-22
	Mesophiles	Putrefactive anaerobes (*C. botulinum* - A and B)	250	0.1–0.2	14-18
		C. sporogenes group (including P.A. 3679)	250	0.1 - 1.5	14-18
Acid food and acidified food (pH 4.0 – 4.6)	Thermophiles	*B. coagulans* (facultatively mesophilic)	250	0.01– 0.07	14-18
	Mesophiles	*B. polymyxa* and *B. macerans*	212	0.10 – 0.50	12-16
		Butyric anaerobes (*C. pasteurianum*)	212	0.10 – 0.50	12-16
		B. licheniformis	200	4.5	27
Acid food and acidified food (pH < 4.0)	Yeasts, molds, and mesophilic bacteria	*Lactobacillus* species, *Leuconostoc* species	150	0.50 – 1.00	8-10

In order to determine the processing time, it is important to understand the concept of process lethality (F_o). Process lethality can be defined as the equivalent time of heating at reference temperature (250 °F for sterilization) which shall produce the same amount of microbial kill as the process. The desired degree of lethality (F_o) in terms of an equivalent time at a reference temperature is generally pre-established for a given product, and processes are designed to deliver a minimum of this preset value at the slowest heating location of the product. Other than the basic mathematical model (Equation 2.1) used for lethality calculations, based on the original work of Ball and Olson (1957), researchers have proposed many other methods to evaluate process lethality and process times for delivering a safe process, ranging from general and improved general methods, to various formula methods like Ball (1923), Gillespy (1953), Hayakawa (1964), Stumbo (1973), Steele and Board (1979), Pham (1989) methods etc.

$$F_0 = \int_0^t 10^{\frac{(T-T_0)}{z}} dt \qquad (2.1)$$

Table 2.2. Principles for minimum lethality requirements for low-acid foods (pH>4.5)

Reference	Minimum Lethality Requirement	Comments
Stumbo *et al.* (1975)	Small cans (54.0 mm dia & 57.2 mm heigh): $F_{10/121.1} \geq 2.8$ min Big cans (157.2 mm dia & 177.8 mm mm height): $F_{10/121.1} \geq 3.1$ min	**Food safety:** To achieve 12 log reduction in *C. botulinum* spores Spoilage still possible.
	Small cans (54.0 mm dia & 57.2 mm height): $F_{10/121.1} \geq 9$ min. Big cans (157.2 mm dia & 177.8 mm height): $F_{10/121.1} \geq 11$ min.	**Shelf life:** To achieve 4 log reduction in *C.sporogenes* spores Organism of concern is spoilage spore *C. sporogenes*
Holdsworth and Simpson (2007)	$F_{10/121.1} \geq 3.0$ min	**Food safety:** To achieve 12-D reduction in *C. botulinum* spores. Spoilage still possible.
	$F_{10/121.1} \geq 6.0$ min	**Shelf life:** To be safe, and to prevent spoilage
	$F_{10/121.1} = 0.5$ - 1.5 min	**For cured meat products:** Curing controls initial spore load & subsequent spore growth
Sielaff (1996)	$F_{10/121.1} = 3$ - 8 min	**Shelf life in moderate climate:** 4 months to 4 years if storage temperature T ≤ 25 °C. Microbial stable; 2-log reduction in thermophilic spoilage spores, which germinate at T > 35 °C
	$F_{10/121.1} = 16$ - 20 min	**Shelf life in tropical climate:** 1 year at storage temperature T ≥ 35-40 °C. Food is microbial stable. 6-log reduction in thermophilic spoilage spores, which germinate at T > 35 °C
	$F_{10/121.1} = 0.65$ - 0.85 min	**For cured meat products:** 1 year storage life, if the product is cured and given this minimal treatment.
Heinz and Hautzinger (2007)	$F_{10/121.1} > 2.52$ min	**Food Safety:** To eliminate most heat resistant spores for pathogens (*C. botulinum*)
	$F_{10/121.1} > 2.58$ min	**Shelf life:** To eliminate most heat resistant spores for pathogens (*C. botulinum*)
	$F_{10/121.1} = 4$ - 5.5 min	**For moderate climate:** Shelf life of up to 4 years at temperature < 25 °C can be achieved
	$F_{10/121.1} = 12$ - 15 min	**For tropical climate:** In tropical countries, F-value have to be increase for safe storage of the finished products under storage temperatures up to 40°C

[a] Minimal Lethality expressed as $F_{z/T}$ where z is the z-value concerned and T is the reference temperature of heating

Various researchers (Stumbo *et al.*, 1975; Nelson and Tressler, 1980; Atherton and Thorpe, 1980; Montville and Sapers, 1981; Brown, 2000; Barrett *et al.*, 2004) and trade associations (National Canners Association Research Laboratories, 1968; NFPA, 1971, 1982, 1985; Institut-Appert, 1979) have provided guidelines on minimal lethality requirements for the thermal processing of canned foods. In general, for low-acid foods, a minimum F_o = 3 min (to achieve book-cook or 12-D reduction of *Clostridium botulinum* spores) is necessary; although, conservatively, a higher lethality is usually applied. Different kinds of products like fish, meat, milk and dairy products etc. require different levels of minimal treatments due to specific statutory laws in place for them. Some of the general principles on which these values must be selected have been highlighted for low-acid foods in Table 2.2.

On the other hand, for high-acid foods, a less severe heat treatment is necessary as it is very unlikely that *C. botulinum* spores will survive in a high-acid environment. A process of F_o = 0.7 min is recommended by Hersom and Hulland (1980) for this purpose. For high-acid products, temperatures below 100 ^oC are usually adequate; however, heat-resistant fungi may survive and germinate to cause structural breakdown in some food products. The target lethality requirements at different operating temperatures for acidified foods at different operating temperatures and temperature-sensitivity (z-value) of target microorganism have been given by various researchers and are presented in Table 2.3.

Table 2.3. Minimum Lethality Requirements for Acidified Foods (pH<4.5)

pH-range	Minimal Lethality[a]	Reference
3.1 – 3.2	$F_{10/195}$ = 0.1 min	Odlaug and Pflug (1978)
3.3 – 3.5	$F_{10/195}$ = 1.0 min	Nelson and Tressler (1980)
3.5 – 4.0	$F_{10/195}$ = 16 - 23 min	Barrett *et al.* (2004)
4.0 – 4.3	$F_{15/200} = F_{8.3/93.3}$ = 5 min	National Canners Association Research Laboratories (1968)
4.3 – 4.4	$F_{15/200}$ = 23 min $F_{15/212}$ = 10 min	Larousse and Brown (1996)
	$F_{15/200} = F_{8.3/93.3}$ = 10 min	National Canners Association Research Laboratories (1968)
4.5 – 4.6	$F_{15/212}$ =10 min $F_{18/230}$ = 1.6 min	Montville and Sapers (1981)
	$F_{8.3/93.3}$ = 10 min	National Canners Association Research Laboratories (1968)

[a] Minimal Lethality expressed as $F_{z/T}$ where z is the z-value concerned and T is the reference temperature of heating

2.4 Methodologies for heat penetration data gathering

2.4.1 Use of thermocouples

Generation of heat penetration profile is important for establishing a thermal process. This involves carrying out experiments for measuring the time-temperature profiles at slowest point of heating for retort, liquid and food particles. Traditionally thermocouples are used for measuring temperature data. Table 2.4 details different types of thermocouple-based methodologies used for liquid and particle temperature measurements in agitating retorts.

Table 2.4. Thermocouple-based temperature measurement techniques.

Liquid [a]	**Agitating retorts** [b]
• Rigid needle type thermocouples are used. • Some researchers have also used wireless sensors. • More than one thermocouple or thermocouples of different lengths (Ex: In No.2 cans, 3 thermocouples of 43 mm, 32 mm and 21 mm length and fixed respectively at 20mm, 56mm and 85mm from the bottom) can be used for temperature uniformity studies. • Procedures for attaching a needle type thermocouple are detailed in literature.	• A slip-ring assembly is used to EOE and axial mode of agitation as there is a possibility of entangling of the thermocouple wires. • The slip-ring detaches the static side of thermocouple wires outside the retort from the thermocouples inside rotating cage, thus preventing the twisting of the wires during cage rotation. • A second slip-ring is attached during biaxial agitation to allow twisting and turning of thermocouple wires in opposing directions during the biaxial rotation of cage
Fixed particles [c]	**Moving particles** [b]
• A rigid thermocouple is attached to the particle-center or the slowest point of heating. • In agitation processing, this does not simulate the real free motion due to agitation. • Results may have inaccuracies due to restricted motion of the particles.	• A flexible thin wire thermocouple attached to the particle-center is used. • To collect the particle-center temperature for spheres, a hole slightly greater than its radius is drilled and the thermocouple tip (commonly duplex Type T copper-constantan thermocouple made of 20, 22 or 24-gauge flexible wires) is fixed at center with epoxy glue.

[a] Lesley (1987); Ramaswamy and Abbatemarco (1996); Sablani (1996); Sablani and Ramaswamy (1996); Pflug (2003); Meng (2006); Wang *et al.* (2006).

[b] Sablani (1996); Sablani and Ramaswamy (1995, 1999); Meng (2006); Meng and Ramaswamy (2005, 2007a, 2007b); Dwivedi and Ramaswamy (2010a, 2010b).

[c] Lenz and Lund (1978); Hassan (1984); Deniston *et al.* (1987); Fernandez *et al.* (1988).

The most common types of thermocouples are duplex T-Type (copper/constantan with Teflon insulation) and K-type (chromel-constantan). Common configurations are flexible wires (20, 22 or 24-gauge) and rigid needle types. There are several other types of rigid and flexible thermocouples available: (a) molded thermocouples made of rigid Bakelite insulation, which are available to suit specific can sizes; (b) stainless-steel needle thermocouples, which are relatively thin and rigid; (c) flexible thin wire thermocouples which can be used for measuring the heat penetration at the center of particulate materials; and (d) custom-made thermocouples, rigid rod-in-tube type, which can be made to any suitable length (Holdsworth and Simpson, 2007). Further details about the type of thermocouples to be used for various thermal processing operations are available in literature (Bee and Park, 1978; Pflug, 2003).

Thermocouple-based approaches for data gathering generally use various thermocouple connectors and extension wires to transport temperature signals to a data logger or data acquisition system. Caution must be exercised to avoid certain sources of error which may be associated with the use of these connectors and extension wires. These include: disparity in thermal emf between thermocouples, connectors and extension wires; temperature differences between two wire junctions; and reversed polarity at thermocouple-extension wire junction. Inaccuracies in temperature measurements may result in errors in process evaluation; hence, frequent calibration is essential to provide reliable data. Thermocouples should be calibrated in place as part of the complete data acquisition system against a traceable calibration standard (thermometer, RTD, thermistor). Factors affecting calibration include: improper junctions, metal oxidation, multiple connectors on single lead, worn or dirty slip-rings, and inadequate data-logger cold junction compensation. Some precautions when using thermocouple-based data acquisition systems include: minimizing multiple connections on the same wire; cleaning all connections; grounding the thermocouples and recording device; slitting thermocouple outer insulation outside the retort to prevent flooding of data-logger or data recording device; and using properly insulated thermocouple wires (Holdsworth and Simpson, 2007). Guidelines for use of thermocouples and thermocouple connection and calibration are detailed in the literature (CFPRA, 1977; IFTPS, 1992; May, 1997).

2.4.2 Data collection via wireless sensors.

Data collection in the biaxial mode of rotation in a Steritort or data collection in hydrostatic sterilizers or rotary tunnels produces great challenges as it is almost impractical to use conventional wired thermocouples because of the haphazard/random motion of particles (Ex. helical motion in biaxial retorts or mixed and variable motions in hydrostatic or continuous sterilizers). For data gathering under such situations, researchers have used self-contained wireless sensors which gather data continuously and transmit signals to a computer. Dwivedi and Ramaswamy (2010c) showed that there were no statistical differences between the performances of wireless systems compared to conventional systems and in fact, the wireless sensors were reported to be relatively more stable for rotary autoclaves especially for free axially rotating cans. By adopting wireless technology, 20-80% of the wiring costs in industrial application can be eliminated and also gives a chance of real time tracking of the free movement of particles (Wang *et al.*, 2006). Some other researchers (Francesco and Vittorio, 2003; Lesley, 1987) have also used wireless sensors and found them useful as a reliable temperature gathering technique.

However, it is not possible to realistically use data from these wireless sensors, even for determining local temperatures in cans, as these sensors are relatively large and occupy significant space resulting in deviations from actual process. Even with miniature wireless sensors, Awuah *et al.* (2007b) observed that process time for a target cumulative lethality was underestimated due to the combined effects of can contents, rotation speed, remote sensor configuration and sensor-mounting fixtures. Also, due to the sensor heat sink effect, recorded temperatures are not accurate. Hence, correction factors are required when wireless sensors (even miniature ones) are used. Ecklund (1956) provided correction factors for heat penetration thermocouples. However, results of Britt *et al.* (1997) revealed that Ellab Tracksense and Datatrace modules did not support Ecklund's correction factor (i.e., multiplying jh value by 1.1) for 300x407 can size. Hence, use of wireless sensor always requires additional work for calculating appropriate correction factors to be used in process calculations and process validation. Some researchers are reluctant to use wireless sensors in heat transfer studies as these correction factors frequently change with variation of process variables affecting thermal processing (discussed in detail in Section 2.6). For temperature measurements of moving particles, these would be of limited use because of the motion restrictions imposed on particle when such devices are attached. Although, in static retorts,

attaching the largest particle to the tip of the wireless sensor of appropriate length might provide reasonable data, and could be used by determining the proper correction factor.

2.4.3 Use of thermochromic liquid crystals (TLCs)

Although particle-surface temperatures can be used to solve simple energy balance models (Equations 2.2 and 2.3) to predict heat transfer coefficients, these temperatures cannot be measured using conventional thermocouple techniques due to difficulties in fixing the thermocouple tip to the surface of a moving particle. In order to solve this problem, thermochromic liquid crystals (TLCs) have been used by different researchers (Stoforos and Merson, 1991; Balasubramaniam and Sastry, 1994a, 1994b, 1994c, 1995; Zitoun and Sastry, 1994). Liquid crystal is a chemical compound which changes its color in response to surface temperature changes due to their unique molecular structure rearrangement. They are coated on a free moving particle and the particle temperature history is generated by image analysis of videotaped color changes of the liquid crystal during heating. Balasubramaniam and Sastry (1995) reviewed the use of thermochromic liquid crystals (TLCs) in heat transfer studies and their applications to food processing research.

Some researchers (Gadonna *et al.*, 1996; Ochoa *et al.*, 2005) have further improved this technique by using a transducer particle made up of two concentric spheres (core of the particle was a polypropylene sphere pre-coated with a black paint and then coated with a liquid-crystal and subsequently coated with a layer of transparent epoxy resin of known thermal diffusivity) or by using a surface with a low thermal mass (a thin tissue embedded with TLCs). Image analysis of hue of liquid crystals reveals surface temperature distributions with positions and time and shows how the local heat transfer coefficients change with time. Dynamic flow behavior, such as vortex shedding etc., can be used to quantify the effect of flow behavior on heat transfer phenomenon occurring during the process. Basics involved in the calibration and the use of TLCs are described in detail in literature (Kakade *et al.*, 2009; Abdullah *et al.*, 2010).

The liquid crystal technique can provide useful information, if properly used, but does have limitations. Color calibration is difficult; and it must be emphasized that each calibration curve between temperature and hue value is unique as color determination depends both on equipment and environment conditions during the experiment (different lightening chambers, light bulbs, dust formation on light bulbs, image processing system etc.). Furthermore, the method can only be used

with optically transparent liquids (Balasubramaniam and Sastry, 1995; Kakade *et al.,* 2009; Abdullah *et al.*, 2010).

2.4.4 Use of melting point indicators (MPIs)

The melting point approach is similar to the use of TLCs, as both involve optical methods, for particle-surface temperature measurements. In this method, a melting point indicator (MPI), made of a polymeric material which changes color at a specific temperature, is used. Hollow spherical particles are used in this method and they are filled with several MPIs with different melting points. Time taken by the surface of the indicator (placed inside the particle) to reach its melting point is measured and their color changes are visually recorded. This method has been used by several researchers (Damay and Pain, 1993; Mwangi *et al.*, 1993) for monitoring flow behavior and spatial heat transfer coefficient distribution during thermal processing. Like other optical methods, the melting point indicator method is also limited to transparent fluids and, therefore, can only be used with model systems.

2.4.5 Use of biological indicator units (BIUs)

Biological indicators have been used simultaneously to monitor temperature and lethality achieved inside a can. This was done by development of biological indicator units (BIUs), by Pflug *et al.* (1980a, 1980b), containing a sample tube filled with spores of *Bacillius stearothermophilus*. This BIU tube is then inserted into the cans at slowest point of heating. These tubes are generally made of plastic. For calibration of BIUs for lethality measurements, a representative sample from a large batch is calibrated by submitting them to a known thermal process, and F_o-value can be determined from heat penetration. Apart from *B. stearothermophilus*, other spores have been used recently. Rönner (2002) developed a technique for studying sterilization systems using BIUs made of *B. stearothermophilus* and *B. subtilis* in an 8 mm diameter microporous bead of modified polyacramide gel with 90% water. They also developed a similar system using ascospores for studying pasteurization. However, because of the associated thermal lag due to the containment material, this technique produces a lag in temperature outputs. Other researchers have also used aluminum containers to improve heat transfer and eliminate thermal lag during temperature measurements (Rodriguez and Teixeira, 1988). These techniques show good agreement between F_0 values from heat penetration compared with F-values from the BIUs, yet, the biological values

tend to be slightly lower than the F_0 from heat penetration measurements. In a more recent study on biaxial rotation processing of liquid particulates cans, Hassan and Ramaswamy (2013) used the biological validation technique to calculate process lethality. In this study, carrot and meat alginate spherical particles, inoculated with spores of *C. sporogenes* and *Geobacillus stearothermophilus*, were filled into cans along with a non-Newtonian liquid (carboxymethyl cellulose). Process times were calculated to achieve an accumulated lethality of 3 and 15 min for carrot and meat alginate fabricated particles. Using spore counts of the particles before and after the given process, the number of log reductions of the bacterial spores and hence the process lethality were determined. They showed that F_0 values obtained from biological validation were statistically same as those computed from numerical simulation thereby demonstrating that the standardized bio-validation technique can be effectively used for establishing/verification of thermal processing schedules

2.4.6 Use of chemical and biochemical indicators.

Apart from BIUs, several researchers have also developed many biochemical (Hendrickx *et al.*, 1995) and chemical indicators (Silva *et al.*, 1994) for collecting heat penetration data inside the can by correlating them with lethality measurements. These are collectively known as time-temperature integrators (TTIs) as they show the accumulated time-temperature history of a product and change properties (like color, degree of microbial kill etc.) when a particular time temperature combination has been reached. Thus, lethality measurements (using Equation 2.1) can be made. Chemical indicators have also been used to determine heat transfer coefficients between food particles and liquids (Weng *et al.*, 1992; Maesmans *et al.*, 1993, 1994; Van Loey *et al.*, 1995). Weng *et al.* (1992) used immobilized peroxidase as a chemical TTI to gather the temperature history of particles in the pasteurization process. Anthocyamins, thiamins, methylmethionine sulfonium and sucrose inversion are some other chemical TTIs which have been used. Ramaswamy *et al.* (1996) also used a chemical marker for process lethality measurement at 110^{o}C in a continuous medium flow holding tube.

Apart from these, α–amylase has been used extensively as a biochemical TTI for studying inactivation kinetics during sterilization and pasteurization processes (Van Loey, 1996; Van Loey *et al.*, 1997; Tucker, 1999). However, α-amylase is unstable at very high temperatures and is hence treated with *Bacillus amyloliquefactens* (Maesmans *et al.*, 1994), *B. licheniformis* (De Cordt *et al.*,

1992) or polyols (De Cordt *et al.*, 1994) to improve its stability. Some researchers (Haentjens *et al.*, 1998; Guiavarc'h *et al.*, 2002a, 2002b; Van Loey *et al.*, 2004) have also developed enzyme systems such as using α-amylase at reduced water content as TTIs and residual denaturation enthalpy as response. A comprehensive list of potential TTIs which can be used for thermal processing is available in literature (Holdsworth and Simpson, 2007; Pflug, 2003; Van Loey *et al.*, 1995).

2.4.7 Use of magnetic thermometry and magnetic resonance imaging techniques

All previous experimental techniques are limited by the need to measure temperature directly by thermocouples or indirectly by using BIU, TTI etc. or by an optical method. But none of them can track the temperature of a freely-moving particle non-invasively. Some progress has been made with `temperature pills' which use a particle with a quartz crystal inside acting as the temperature sensing element. The element resonates at a temperature-dependent frequency and invokes a coil circuit and thus generates a magnetic signal (Balasubramaniam and Sastry, 1994c). An external receiver converts the magnetic signal into a temperature reading. Bhamidipati and Singh (1994, 1995) were the first to exploit this technique in detail. They used a cylindrical particle (22.6 mm length, 10.7 mm diameter) of known density and specific heat capacity, which broadcasts its temperature to an external antenna coil following the motion of particle sensor inside the tube, allowing temperature-time profile of the particle to be obtained. The test fluids were aqueous CMC solutions heated to 82 ºC. Another novel non-invasive technique (Ghiron and Litchfield, 1997) involved measurement of temperature using magnetic resonance technique: the change in temperature of a magnetic particle was detected by change in its magnetization. More recently, researchers have used magnetic resonance imaging to measure temperature and subsequently derive the thermal diffusivity (Gultekin and Gore, 2006) and heat transfer coefficients (Gultekin and Gore, 2008) of products. Being non-invasive, these techniques do not interfere with particle trajectory as temperature is being measured, and has added advantage of yielding local h_{fp} values. However, the large size and density of the broadcasting particle is severely limiting. It is also crucial that sensing particle behaves the same way as the food. This type of technique offers scope for real process measurement, but it is again not yet fully developed.

2.5 Methodologies for evaluating heat transfer coefficients during thermal processing of particulate liquid foods

The heat transfer in a can is characterized by assuming a model in which heat is transferred in two stages: first from the heating medium (steam or water) to the can liquid and then from the can liquid to the particle. The intensity of heat transfer is characterized by heat transfer coefficients existing at these two stages: overall heat transfer coefficient, U (from heating medium to can liquid through the can wall) and fluid to particle heat transfer coefficient h_{fp} (from liquid to particle surface). The values of U and h_{fp} are used to estimate the efficiency of associated heat transfer.

The governing equation for heat transfer in such systems is given by the energy balance equation for a liquid-particulate canned system (Equation 2.2) according to which total heat coming inside the can is equal to the heat energy required for increasing the temperature of liquid and particle.

$$UA_c(T_R - T_l) = m_l c_{pl} \frac{dT_l}{dt} + m_p c_{pp} \frac{dT_p}{dt} \tag{2.2}$$

Second term on the right side of Equation (2.2) is equal to heat transferred to particles across liquid-particle interface, and can be represented as Equation (2.3). Simultaneous solution of these two equations yields the value of U and h_{fp}.

$$m_p . c_{pp} . \frac{dT_p}{dt} = h_{fp} A_p (T_l - T_{ps}) \tag{2.3}$$

2.5.1 From direct particle temperature measurements

Equations (2.2-2.3) form the basic framework which needs to be solved to calculate U and h_{fp}. This evaluation can be independently solved by collecting the time-temperature data of retort, liquid and particle-surface to estimate U and h_{fp}. However, it is difficult to collect particle-surface temperatures and instead, many researchers find it easier to collect particle-center temperatures using thermocouples fixed to the particle-center (Section 2.4.1.). Particle-center temperature collection is also preferred, as cold-spot temperatures are used to determine process lethality (Equation 2.1). On measuring particle-center temperatures, heat transfer coefficients (U and h_{fp}) are back-calculated by comparing experimental lethality (Equation 2.1) to that determined by solving Equations (2.2-2.3) together with the conduction heat transfer equation inside the particle.

Table 2.5. Methodologies for measuring U and h_{fp} using direct temperature measurement techniques.

From particle-center temperature measurements

Analytical method [a]

- Dimensionless temperatures at a specific point of particle is calculated using the following equation and h_{fp} is calculated using iteration: $\frac{T-T_i}{T_l-T_i} = \sum_{n=1}^{\infty} C_n \left[\cos(\gamma_n r/a)\right]$

where, $C_n = (4\sin\gamma_n \exp(-\gamma_n^2 \alpha T/a^2))/(\gamma_n + \sin(2y_n))$,

and $\gamma_n =$ positive roots of $\gamma_n \tan\gamma_n = h_{fp}/k_p$

Semi-Analytical Method [c]

- Some researchers used a semi-analytical approach for fitting the particle temperature and a semi-numerical for fitting the fluid temperature solution using Duhamel's theorem and a numerical Runge-Kutta scheme.

Numerical method [b]

- These methods are based on finite element and difference approximations of Equations (2.2-2.7).
- U and h_{fp} are evaluated using numerical Runge Kutta scheme.
- They work well in the range $0.02<Bi<200$ and $\tau > 0.2$.
- Numerical solutions are satisfactory & less restrictive.

Low biot-number scenario [d]

- When Bi < 0.1 (aluminum or metal particles), a lumped approach is used and U is evaluated as: $U = \frac{2.303 m_l c_{pl}}{f_h A_c}$
- h_{fp} is evaluated from slope of the line: $\ln(T_l - T) = \ln(T_l - T_i) - \frac{h_{fp} A_p}{m_p c_{pp}} t$
- Calculated h_{fp} doesn't represent true h_{fp} due to linear temperature profile assumption.

From particle-surface temperature measurements [e]

- It is based on equation (2.2-2.3) from which h_{fp} can be calculated as: $h_{fp} = \frac{m_p c_{pp}(T_l - T_i)}{A_p \int_0^t (T_l - T_{ps}) dt}$
- For spheres in rotating cans, the following simplification is available: $h_{fp} = \frac{a\rho_p c_{pp}(T_p - T_i)}{3 \int_0^t (T_l - T_{ps}) dt}$
- Only average final and initial particle temperatures and fluid and particle-surface temperature required.

For non-Newtonian and viscous fluids [b]

- U_{ap} and h_{ap} (apparent fluid-to-particle heat transfer coefficient) are calculated using a lumped model.
- Equations (2.2, 2.4-2.7) remain the same but Equation (2.3) changes as: $m_p . c_{pp} . \frac{dT_p}{dt} = h_{ap} A_p (T_R - T_{ps})$
- While h_{fp} is based on transient temperature difference between the canned fluid and particle, h_{ap} is based on that between retort medium & particle.

[a] Chang and Toledo (1989); Chandarana and Gavin (1989, 1990); Stoforos and Merson (1991).

[b] Meng (2006); Dwivedi (2008).

[c] Stoforos *et al.* (1997).

[d] Hassan (1984); Sastry *et al.* (1985); Fernandez *et al.* (1988); Stoforos and Merson (1991); Tattiyakul *et al.* (2002)

[e] Chau and Snyder (1988); Rodriguez and Teixeira (1988); Sastry *et al.* (1989); Alhamdan *et al.* (1990); Stoforos and Reid (1992).

For a spherical particle, heat flow is described by the following partial differential Equation (2.4) and initial and boundary conditions given by Equations (2.5-2.7) (Sablani and Ramaswamy, 1996):

$$\frac{\partial T}{\partial t} = \alpha_p\left(\frac{\partial^2 T}{\partial r^2} + \frac{2}{r}\frac{\partial T}{\partial r}\right) \quad (2.4)$$

$$T(r, 0) = 0 \qquad \text{at } t=0 \quad (2.5)$$

$$\frac{\partial T(r,t)}{\partial r} = 0 \qquad \text{at } r=0 \quad (2.6)$$

$$k_p \frac{\partial T(r,t)}{\partial r} = h_{fp}(T_f - T_{ps}) \qquad \text{at } r=a \quad (2.7)$$

The value of h_{fp} can be back-calculated by solving Equation (2.4) (subject to initial boundary conditions defined by Equations 2.5-2.7), and using this h_{fp}, U values can be obtained by solving Equations (2.2-2.3). This technique describes the basic methodology for evaluating U and h_{fp}. Most researchers have used either a similar or a slight modification of this technique for measuring U and h_{fp} in liquid-particulate food mixtures in a can. There are many numerical, computational and analytical techniques for solving these equations (Table 2.5). On comparing analytical and numerical methodologies, the analytical approach was found to show more accuracy (Cariño-Sarabia and Vélez-Ruiz, 2013).

2.5.2 From indirect particle temperature measurement

Apart from traditional thermocouple-based direct temperature measurement techniques, particle temperature can also be measured by indirect technique like the use of BIU and other TTI and TLC etc. For these types of techniques, researchers (Pflug *et al.*, 1980a, 1980b; De Cordt *et al.*, 1992, 1994; Weng *et al.*, 1992; Maesmans *et al.*, 1993, 1994; Silva *et al.*, 1994; Hendrickx *et al.*, 1995; Van Loey, 1996; Van Loey *et al.*, 1995, 1997, 2004; Haentjens *et al.*, 1998; Tucker, 1999; Guiavarc'h *et al.*, 2002a, 2002b; Hassan and Ramaswamy, 2013) have used lethality or other time-temperature integration models. The model gives lethality as output (F_m) using Equations (2.1-2.7) for different values of U and h_{fp}. Lethality of experimental TTI (F_{TTI}) is calculated using calibration charts or by reading the TTI's initial (N_o) and final (N) status in accordance with Equation (2.8).

$$F_{TTI} = D\log(N_0/N) \quad (2.8)$$

Values of F_{TTI} and F_m are matched by iteration of values of U and h_{fp} to yield the heat transfer coefficient (U and h_{fp}) of the thermal process. Weng *et al.* (1992) named this approach a *Least Absolute Lethality Difference* (LALD) method and also compared it with another common approach called *Least Square temperature difference* (LSTD) in which sum of the squares of temperature differences of the model output is matched with that of the experimental particle. They showed that using the LALD-approach, weight of higher temperatures (more lethal) is more pronounced than that of lower temperatures in their respective contribution to the final processing value, which is in accordance to the concept of higher microbial kill at higher temperatures. However in case of LSTD, weight of all temperatures (low or high) are same. Thus, LALD procedures can be used in agitated conditions where it is difficult to satisfy the Fourier number stability criterion ($\tau < 0.2$) in the initial temperature range (ex. agitation processing or HTST methodologies), and thus accuracy of lower temperatures is limited.

2.5.3 When collection of particle temperature is difficult

Under certain conditions, temperature monitoring using traditional optical or thermocouple-based technologies is difficult. Dwivedi and Ramaswamy (2010a) developed an innovative methodology to measure U and h_{fp} under conditions where temperature monitoring is not possible. This methodology is particularly useful when an alternate mode of processing is available where particle-temperatures can be measured. This methodology is based on the assumption that the ratio of U/h_{fp} falls within a statistically similar range, even if the mode of agitation is changed, because factors influencing U will also influence h_{fp} in a somewhat similar manner. This method involved developing correlations between h_{fp} and U using real time–temperature data gathered from the processing mode in which particle temperatures are measurable. This correlation was then used to calculate h_{fp} from U-value obtained from low Biot-number model described in Table 2.5. Dwivedi and Ramaswamy (2010a) coupled experimentally evaluated U from fluid temperatures (measured using wireless sensors) in the biaxial mode with values of ratio of U/h_{fp} in fixed axial mode to compute h_{fp} for the biaxial mode. This approach gave consistent results with the traditional approach of measuring both liquid and particulate temperature. It is to be noted that h_{fp} values using this methodology are representative values and may deviate from the h_{fp} values computed using other methods, yet they can be used to understand the effect of various process variables on the heat transfer happening during the thermal process.

2.5.4 Using heat-flux instead of temperatures

Apart from techniques involving direct and indirect temperature measurement, other innovative techniques have also been used to predict h_{fp}. In such approaches, heat conduction errors are considered to be negligible. Here, h_{fp} is determined by monitoring the heat flux, e.g., from a heating wire, needed to maintain particle-surface temperature constant. Generally, a good agreement between predicted and experimental data is obtained for fluid temperatures, however, significant variation are observed for particle-surface temperatures using these approaches (Chang and Toledo, 1989, 1990; Stoforos *et al.*, 1997).

2.6 Factors affecting heat transfer coefficients (U and h_{fp}) during thermal processing

There are many studies in which heat transfer coefficients (U and h_{fp}) have been evaluated by researchers. These studies can be clearly divided on the basis of mode of agitation. Some of these have been summarized for non-agitated and agitated systems in Tables 2.6 and 2.7 respectively.

Table 2.6. Heat transfer studies on thermal processing of liquid-particulates in non-agitated systems.

Reference	Liquid	Particle	h_{fp} (W/m^2K)
Chau and Snyder (1988)	Water	Shrimp	1276
		aluminum	1073
Chang and Toledo (1989, 1990)	Water	Potato Cubes	239-303
	Sucrose solution		146
	Sucrose solution (0 m/s)	Carrot Cubes	600-1533
	Sucrose solution (1.58 m/s)		356-735
Chandarana and Gavin (1989), Chandarana *et al.* (1990)	Starch	Silicone Rubber Cube	8.1-86.5
	Water		65.7-107.1
Alhamdan *et al.* (1990)	Water	Mushroom shaped aluminum	652-850
Awuah *et al.* (1995)	CMC	Potato Cylindrical	80 -450
		Carrot Cylindrical	100 -550
Cariño-Sarabia and Vélez-Ruiz (2013)	Water	-	57–248
	CMC	-	28–169
	-	Mushroom	28–132
	-	Tomato Puree	30–183
	-	Potato	31–248

These values have been gathered under various operating conditions and with different particles and liquid. Some researchers have used model food particles for data collection, while others have used real food systems. An analysis of these values gives an idea of the intensity of heat transfer under various modes of operation. In general, any factor which increases agitation or decreases thickness of boundary layers leads to increase in values of U and h_{fp}. Some of these factors affecting heat transfer coefficients during thermal processing of liquid-particulate mixtures have been discussed here.

2.6.1 Mode of agitation

Ultimate objective of agitation thermal processing is to improve the values of these heat transfer coefficients. In general, it is observed that increased agitation leads to increase in heat transfer occurring in the system. It is observed by many researchers that non-agitated (Still process) mode of thermal processing has the lowest values of heat transfer coefficients. Amongst agitated systems, biaxial mode of agitation has the highest heat transfer coefficient, followed by EOE mode and then by fixed axial mode of rotation (Dwivedi and Ramaswamy, 2010b). For oscillatory mode of rotation, when the direction of rotation was reversed every 15–45 s, Hotani and Mihori (1983) reported that heating rates and uniformity were increased and that there was no significant difference between EOE rotation and axial rotation. There is a possibility to increase these values further by using new modes of agitation like reciprocating or lateral agitations, which promises to increase the heat transfer tremendously (Walden and Emanuel, 2010). However, there is no published heat transfer coefficient data available for this mode of agitation. The reason for this increase is that magnitude of U and h_{fp} is governed by particle-to-fluid relative velocity (Chandarana and Gavin, 1989), which is increased by lateral or reciprocating agitation.

2.6.2 Speed of Agitation

As early as 1951, Conley *et al.* (1951) documented the impact of speed of agitation on heat transfer rates and resulting process times. Heat transfer and lethality of canned liquid foods containing particles processed in Steritort have been studied (Lenz and Lund, 1978), and it was found that changing reel speed from 3.5 to 8 rpm resulted in an average increase in U by 33% and in values of h_{fp} by 44%. The effect of rotational speed is more evident at lower speeds. At higher

speeds, effect of rotation generally dies down, and after a certain speed, heat transfer coefficients do not improve much.

Table 2.7. Heat transfer studies on thermal processing of liquid-particulates in agitated systems.

References	Liquid	Particle	U (W/m^2K)	h_{fp} (W/m^2K)	Mode
Lekwauwa and Hayakawa (1986)	Water	Potato (spheroidal)	113-1704	60-2613	Rotary retort
Deniston *et al.* (1987)	Water	Potato Spherical	95-2300	127-200	Rotary retort
	Starch solution	Potato Cube	--	99	
	Water	Mushroom	--	850	
Lenz and Lund (1978)	Water	Lead Particle (Single)	732-970	522-1811	Rotary retort
		Lead Particles (Multiple)	210-330	341-1550	
	Water & Sucrose	Lead Particle (Single)	562-709	539-1175	
		Lead Particle (Multiple)	170-244	431-1198	
Hassan (1984)	Water	Potato Spheres	--	98-165	Rotary retort
		Teflon Spheres	--	32-108	
		Aluminum Spheres	--	139-735	
Stoforos and Merson (1991)	Water	Aluminum (spheres)	142-201	128.7-1296	Rotary retort
		Teflon(sphere)	83-192	410-2071	
		Potato	--	233	
Sablani and Ramaswamy (1995,1996)	Water	Propylene Sphere	480- 880	65-120	EOE
	Oil	Nylon spheres cylinders & cubes	130-200	170-1130	
	Water		520- 800	190-1430	
Meng and Ramaswamy (2005, 2007a, 2007b)	CMC	Nylon sphere	U_{ap}: 36-79	h_{ap}: 210-380	EOE
	Glycerin	Nylon & Teflon (Single)	U_{ap}: 266-347	h_{ap}: 50-65	EOE
		Nylon & Teflon (Multiple)	U_{ap}: 45-61	h_{ap}: 163-276	
Ramaswamy and Dwivedi (2011)	Glycerin	Propylene, Nylon & Teflon spheres	210-350	315-585	Fixed axial
			345-580	495-945	Biaxial
Hassan *et al.* (2012)	CMC	Nylon Sphere	265-455	335-630	Fixed axial
			430-720	605-1010	Biaxial

Hassan (1984) measured convective heat transfer coefficients of Teflon, aluminum and potato spheres in end-over-end rotation, and found that varying rotation speed from 9.3 to 101 rpm had more of an effect on U than on h_{fp}. Other researchers have also found similar trends of inhibited increase in heat transfer coefficients beyond a certain agitation speed (Sablani, 1996; Meng, 2006). This trend has been attributed to smaller relative particle-to-liquid velocity at higher rotational speeds. Under larger centrifugal force at higher speed, particles are forced to clump to one edge of the wall resulting in lower relative velocities. Researchers have confirmed these trends using

particle motion analysis (Stoforos, 1988; Sablani, 1996; Meng, 2006; Dwivedi, 2008) by videotaping motion of particles inside transparent cans. Reciprocating agitations can be used to overcome this drawback associated with rotary agitation, as reciprocating motion is free of the effects of centrifugal forces. Dwivedi (2008) reported in his study that U and h_{fp} in free axial mode and biaxial mode increased from 448-907 and 477-1075 W/m^{2}K, respectively, with increase in revolutions per minute from 4 to 24. Thus, in general, increase in speed of agitations increases heat transfer coefficients in all modes of agitation, however, this increase is more prominent at lower speeds.

2.6.3 Fluid viscosity

With an increase in liquid viscosity, level of turbulence inside the can decreases as Reynold's number is inversely proportional to viscosity. Hence, there is a lower mixing and thereby lower heat transfer coefficients. Various researchers have evaluated U and h_{fp} with liquids of varying viscosities. Lenz and Lund (1978) evaluated the effect of viscosity by comparing water and 60% aqueous sucrose solutions. They found that water had higher heat transfer coefficients, than a 60% aqueous sucrose solution, indicating a role of fluid viscosity in the values of U and h_{fp}. Other researchers (Hassan, 1984; Stoforos and Merson, 1991; Sablani, 1996) also noticed that with an increase in liquid viscosity, heat transfer coefficients decreased, and vice-versa. These trends were later confirmed by particle motion studies (Stoforos, 1988; Sablani, 1996; Meng, 2006; Dwivedi, 2008), which showed that for a more viscous liquid, flow was less turbulent, leading to lower particle mixing and lower liquid-particle velocities.

For non-Newtonian fluids, whose viscosities change with mechanical stress due to agitation or thermal stress due to heating, some researchers have used an alternate methodology (discussed in Table 2.5) to predict U_a and h_{ap} (Meng, 2006, Meng and Ramaswamy, 2007b) instead of U and h_{fp}. Meng and Ramaswamy (2007b) found that for CMC solutions associated h_{ap} values ranged from 215 to 376 W/m^{2}K and U_a values ranged from 112 to 293 W/m^{2}K. Their U_a decreased with an increase in liquid viscosity, which could be explained by the thickness of associated boundary layers. Higher thickness of momentum boundary layer leads to higher heat transfer resistance resulting in lower U and h_{fp}. With high viscosity glycerin concentration, researchers

(Sablani, 1996; Meng, 2006; Dwivedi, 2008; Dwivedi and Ramaswamy, 2010a, 2010b) have reported 20-40% lower values under various rotary modes of agitation.

2.6.4 Container headspace

It is generally expected that headspace might act as an insulator in natural convection scenarios (Mohamed, 2007). However, Ramaswamy and Grabowski (1996) noted that the complex nature of heat transfer in headspace makes theoretical prediction difficult. Heat transfer in headspace is governed by evaporation resulting in significant mass transfer effects leading to more rapid heating of the water surface inside the can right just below the headspace, compared to no headspace situation. Joseph *et al.* (1996) reported faster heating rates with an increase in headspace volume in canned conduction-heated materials. James *et al.* (2006) also reported rapid heating effect in cans with 10% headspace compared to no headspace situation during off-axial rotation of cans. Erdogdu and Tutar (2011), through their computational fluid dynamics analysis, observed that headspace temperature increased rapidly due to lower heat capacity and viscosity of air, and heating rates were faster in cans containing headspace compared to no headspace situation. Thus, it is seen that presence of headspace invariably increases the amount of heat transfer. However, after sufficient headspace (around 7-14 mm), the headspace bubble starts acting as an insulator (Ramaswamy and Grabowski, 1996; Mohamed, 2007), retarding further heat transfer. Mohamed (2007) evaluated the effect on heat transfer coefficients for three levels of headspace (10%, 14% and 20% v/v) and found that calculated average effective heat transfer coefficients to be 54, 53 and 50 W/m^2K for the three headspaces, respectively. Other researchers (Sastry *et al.*, 1985; Lekwauwa and Hayakawa, 1986; Chandarana *et al.*, 1990; Sablani and Ramaswamy, 1995, 1999) have also seen that the increase of headspace first increases heat transfer coefficients; however after an optimum headspace, U and h_{fp} start decreasing. On neglecting headspace, insulating effects will inevitably lead to either over-processing or under-processing both of which may have negative effects on consumer's health and safety.

2.6.5 Particle concentration

Particle concentration (ε) is generally defined as percentage of particle volume to that total liquid-particulate volume. Researchers (Hassan, 1984; Deniston *et al.*, 1987) have studied the effect of particle concentration on heat transfer rates and found that with increase in the particle

concentration, heat transfer coefficients increase up to a maximum value and then start decreasing. This phenomenon is explained by the fact that the presence of additional particulates causes secondary agitation of the liquid due to collisions amongst the particles and affects heat transfer coefficients. This results in better mixing and distribution of heat inside the can, leading to increase in U and h_{fp} values. Hence, U and h_{fp} increase till an optimum concentration is reached. Beyond this concentration, particles become tightly packed in the can and are no longer free to move (Deniston *et al.*, 1987). Hence, functional dependency of U and h_{fp} on particle concentration is different for tightly packed particles as compared to loosely packed particles. Sablani (1996) found that U increased 20% for oil and 5% for water at 30% concentration when compared to a single particle, but a further increase in concentration to 40% resulted in a decrease of h_{fp} by 12% for oil and 7% for water. Dwivedi (2008) also reported that particle concentration has a significant influence ($p < 0.05$) on U and h_{fp}. For a particle size of 25 mm, U increased with an increase in particle concentration from 20% to 30%, while further increasing this concentration to 40% decreased U and h_{fp}.

2.6.6 Particle size

Hassan (1984) found that an increase in diameter of potato spheres processed in water from 2.22-3.49 cm, resulted in greater process times for fluid and particles. It was observed that the effect of rotational speed on particle heating times was higher than for smaller particles than larger particles. The overall heat transfer coefficient, however, was reported to have highest values at all rotational speeds when particles of an intermediate size (2.86 cm) were used. Deniston *et al.* (1987) showed that h_{fp} was not greatly influenced by increasing particle size. Lenz and Lund (1978) reported that increasing particle size resulted in higher overall heat transfer coefficients, but Sablani and Ramaswamy (1996) found that U values decreased by about 9% in oil and 6% in water as the size of nylon particle increased from 19.05 to 25 mm diameter, and concluded that particle size influenced more h_{fp} than it did U. Meng (2006) reported no significant effect of particle size on U_a and h_{ap}. Dwivedi (2008) reported that U values in free axial mode were found to decrease by 29-33% as size of particles increased from 19.05 to 25 mm. Under the same increasing size condition, h_{fp} also decreased, probably due to thicker boundary layers associated with larger particle diameters. They also noticed that an increase in diameter had greater influence on h_{fp} than U (h_{fp} decreased by 32-41% for 19.05 to 25 particles). Thus, we may conclude that, like other

parameters, U and h_{fp} increase to a maximum value with an increase in size of the particle, due to increased turbulence created by larger particles, and then start decreasing possibly due to restricted movements.

2.6.7 Particle shape

Different shapes like spheres, cubes, cylinders etc. contribute to varying void fractions between particles and hence liquid fill would be different which also creates differences in the severity of agitation. Thus, heat transfer coefficients could very well depend on particle shapes. Sablani and Ramaswamy (1995, 1998) found that U-values for the cube-shaped single-particle in oil were about 6% lower than those of the cylinder, and 8% lower than that of the sphere. h_{fp} values for cube were 6% higher than cylinder and 23% higher than sphere. They concluded that the influence of shape is more noticeable on U than h_{fp}. Similar results have also been observed by Meng (2006) and Dwivedi (2008). The particle shape also influences the associated surface area as well as surface to volume ratios. These can also influence the associated heat transfer coefficients during thermal processing under container agitation conditions.

2.6.8 Particle density

Particle density can affect particle fluid motion pattern inside the can, thereby affecting heat transfer coefficients. It has been observed that U and $h_{fp,}$ generally, increase with increase in density. Particles of greater density settle in the can faster, resulting in more motion inside the can due to higher particle-liquid relative velocity, resulting in a higher h_{fp} (Sablani, 1996). Meng, (2006) also reported that h_{fp} values increased with increase in particle density. Dwivedi (2008) studied the influence of particle density on U and h_{fp} in free axial mode and found that at 20% particle concentration, polypropylene particles (lighter than water) have lowest h_{fp} (495 W/ m^2K) and Teflon particles (heavier than water) have the highest (922 W/m^2K), while nylon particles (density almost equal to water) fell in between with h_{fp} of 764 W/ m^2K. However, in a single-particle scenario, Sablani (1996) had found that Teflon particles had lower h_{fp} than nylon as Teflon settled at the bottom of the can.

2.7 Dimensionless correlations

Dimensionless correlations are widely used in the prediction of heat transfer coefficients and have shown great promise with regard to their applicability and reliability (Dwivedi and Ramaswamy, 2010d). Dimensional analysis is a technique to create dimensionless groups for reducing the total number of functional variables of relevant physical properties in heat transfer studies. Some of the dimensionless quantities which have been used to establish correlations between different process and system variables are: Reynolds's number, Nusselt number, Biot Number, Prandtl number, Grashoff number etc. Different dimensionless constants which can be used for the development of such correlations for spherical particles are detailed in literature (Incropera and DeWitt, 2011). The dimensional analysis can be used during scale-up of the process and also to provide average value of heat transfer coefficient over a body during heating and cooling. They also offer the flexibility to predict the heat transfer coefficient without the need of actual experimentation, and can be used in optimization subroutines and other predictive programs. Some of the developed correlations have been compiled and represented in Table 2.8. U and h_{fp} are represented in these correlations in terms of Nusselt number (Equation 2.9).

$$\mathrm{Nu} = \frac{\text{Convective heat transfer from liquid to particle surface}}{\text{Conductive heat transfer inside the liquid}} = h_{fp}L_c/k_l \; or \; UL_c/k_l \tag{2.9}$$

2.7.1 Choice of dimensionless variables

The correct choice of characteristic length is very important for establishing dimensionless correlations. However, the correct characteristic length to be used for various dimensionless numbers requires careful considerations into the geometry of the thermal process. Researchers have tried different variables as the parameter of characteristic length for correlating U and h_{fp} in different thermal processing scenarios. In axial rotation, reel radius was used as the characteristic length. Also, some researchers have used diameter of the can as the characteristic length to describe heating behavior of liquid in presence of multiple particles. Diameter of the particle has also been used as characteristic length in correlation for fluid to particle heat transfer coefficient h_{fp} (Fernandez *et al.*, 1988). Some studies have suggested using the sum of the rotation diameter and the diameter of the can, as the characteristic length, for U correlation, and the particle's shortest dimension for h_{fp} correlations (Sablani *et al.*, 1997).

Table 2.8. Some dimensionless correlations available for predictive modeling of thermal processing systems.

Experimental Conditions	Limitations/Validity	Correlation for:	Dimensionless correlation	Reference
Mushroom shaped particles in CMC	$4.0 < Ra < 8.0$	h_{fp}	Heating:$Nu = 1.88 \times 10^{-3}\ Ra^{0.388} = e^{3.11 - 0.077\ Fo}$ Cooling:$Nu = 1.25 \times 10^{-3}\ Ra^{1.113} = e^{1.59 - 0.037\ Fo}$	Alhamdan and Sastry (1990)
Mushroom shaped particles in water	$2 \times 10^6 < Ra < 3 \times 10^9$		Heating: $Nu = 5.53\ Ra^{0.21} = 630\ Fo^{-0.18}$ Cooling: $Nu = 0.08\ Ra^{0.27} = 100\ Fo^{-0.23}$	Alhamdan *et al.* (1990)
Potatoes, tomatoes and mushrooms in ionized water, NaCl (3%) and CMC	$0.32 \leq Bi \leq 4.78$	h_{fp} (single - potato)	$Nu = 2.0515(GrPr)^{0.0914}$	Cariño-Sarabia and Vélez-Ruiz (2013)
		h_{fp} (mutiple - potato)	$Nu = 1.1075(GrPr)^{0.0887}\ (V_p/V_f)^{-0.1562}$	
		h_{fp} (single - tomato)	$Nu = 2.8450(GrPr)^{0.0455}$	
		h_{fp} (mutiple - tomato)	$Nu = 2.3721(GrPr)^{0.0741}\ (V_p/V_f)^{-0.0110}$	
		h_{fp} (single - mushroom)	$Nu = 2.9411(GrPr)^{0.0514}$	
		h_{fp} (mutiple - mushroom)	$Nu = 2.4158(GrPr)^{0.0523}\ (V_p/V_f)^{-0.0190}$	
Nylon, Teflon and polypropylene spheres in High Viscous Glycerin solution	$0.26 \leq Gr/(Re)^2 \leq 13.51$ (free axial) $0.38 \leq Gr/(Re)^2 \leq 18.07$ (fixed axial)	U (free axial – forced)	$Nu = 52.90\ Re^{0.27}\ Pr^{0.10}\ (\rho_p/\rho_l)^{0.47}\ (\varepsilon/(100-\varepsilon))^{0.015}$	Dwivedi and Ramaswamy (2010d)
		U (free axial – natural)	$Nu = 29(GrPr)^{-0.02} + 0.03306Re^{0.66}\ Pr^{0.49}\ Fr^{-0.1635}\ (\rho_p/\rho_l)^{0.42}\ (\varepsilon/(100-\varepsilon))^{0.009}\ (d_p/D_c)^{-0.7}$	
		U (fixed axial – forced)	$Nu = 7.12\ Re^{0.41}\ Pr^{0.184}(\rho_p/\rho_l)^{0.8}\ (\varepsilon/(100-\varepsilon))^{0.04}$	
		U (fixed axial – natural)	$Nu = 0.07(GrPr)^{0.37} + 0.0379Re^{0.5}\ Pr^{0.43}\ Fr^{-0.06}\ (\rho_p/\rho_l)^{0.6342}\ (\varepsilon/(100-\varepsilon))^{0.012}\ (d_p/D_c)^{-1.27}$	
	$0.22 \leq Gr/(Re)^2 \leq 13.51$ (free axial) $0.27 \leq Gr/(Re)^2 \leq 16.69$ (fixed axial)	h_{fp} (free axial – forced)	$Nu = 0.0723\ Re^{0.69}\ Pr^{0.5}\ (\rho_p/\rho_l)^{0.47}\ (e/(100-e))^{0.015\ 43}\ Fr^{-0.20}$	
		h_{fp} (free axial – natural)	$Nu = 20(GrPr)^{0.01} + 0.00955Re^{0.72}\ Pr^{0.56}\ Fr^{-0.195}\ (\rho_p/\rho_l)^{1.165}\ (\varepsilon/(100-\varepsilon))^{0.022}\ (d_p/D_c)^{-1.05}\ (K_p/K_f)^{2.26}$	
		h_{fp} (fixed axial – forced)	$Nu = 0.0723\ Re^{0.67}\ Pr^{0.57}\ Fr^{-0.03}(\rho_p/\rho_l)^{0.4}\ (\varepsilon/(100-\varepsilon))^{0.01}\ (d_p/D_c)^{-1.1}$	
		h_{fp} (fixed axial – natural)	$Nu = 0.07(GrPr)^{0.37} + 0.078Re^{0.5}\ Pr^{0.045}\ Fr^{-0.06}\ (\rho_p/\rho_l)^{0.619}\ (\varepsilon/(100-\varepsilon))^{0.009}\ (d_p/D_c)^{-1.12}\ (K_p/K_f)^{0.48}$	
Beans & aluminum in water & sucrose under axial agitation	$\pi(6Vp/\pi)^{2/3}/A_p \geq 1$	h_{fp}	$Nu = 2.7 \times 10^4\ Re^{0.294}\ Pr^{0.33}\psi^{6.98}$	Fernandez *et al.* (1988)
Canned green peas in Nacl under EOE mode	$63 \leq Re \leq 205$, $2.39 \leq Pr \leq 2.6$	h_{fp} (multiple particle)	$Nu = 3.98\ Re^{0.612}\ Pr^{-0.35}\ (h_s/H)^{0.655}$	Garrote *et al.* (2006)
		U (multiple particle)	$Nu = 8.07\ Re^{0.331}\ Pr^{-0.30}\ (h_s/H)^{0.350}$	
CFD simulation of model canned foods	$F_o < 0.03$	h_{fp}	Sub-critical regime: $Nu_s = 1.78\ F_o^{-0.45}$	Kannan and Gourisankar Sandaka (2008)
	$F_o > 0.03$; $300 < Ra < 5.5 \times 10^5$		Super-critical regime: $Nu_r = 1.05\ Ra_r^{0.16}$ -0.2 $Ra_r^{7.96}\ F_o^{-0.5}$	

CFD simulation of model canned foods	$3800 < Ra < 7900$	Vertical intermediate	$Nu = 1 + 0.71(Ra_{rv} - 1)^{0.77}$	Kurian *et al.* (2009)
	$7900 < Ra < 31027$	Vertical inversion	$Nu = 1.38(Ra_{ri})^{0.35}$	
	$1034 < Ra < Ra_K$	Inclined intermediate (0-90°)	$Nu = 0.78(Ra_{ri})^{0.36}(1.36 \sin \Theta + \cos \Theta)^{0.46}$	
	$Ra_K < Ra < 31027$	Inclined inversion (0-90°)	$Nu = 0.86(Ra_{ri})^{0.36}(1.11 \sin \Theta + \cos \Theta)^{0.43}$	
	$1034 < Ra < 31027$	Horizontal (90°)	$Nu = 0.915(Ra_{ri})^{0.35}$	
	$1034 < Ra < 31027$	Inclined intermediate (90-180°)	$Nu = 1 + 0.086(Ra_{ri})^{0.71}(\pi - \Theta)^{1.90}$	
Nylon, Teflon and polypropylene spheres in high viscous glycerin and CMC solution in EOE mode	$16 \le Re \le 2.34*10^4$, $51.71 \le Pr \le 513.60$, $1.37*10^{-3} \le Fr \le 0.13$	U (particle in glycerin)	$Nu = 0.09\ Re^{0.57}\ Pr^{0.478}\ Fr^{-0.119}$	Meng and Ramaswamy (2007c)
	$1.21 \le Re \le 1.97*10^4$, $51.71 \le Pr \le 513.60$, $3.83*10^{-4} \le Fr \le 0.11$	h_{fp} (particle in glycerin)	$Nu = 0.020\ Re^{0.53}\ Pr^{0.451}\ Fr^{-0.113}\ (\rho_p/\rho_l)^{0.446}\ (L_c/D_c)^{1.18}$	
	$2.44 \le GRe \le 2.42*10^3$, $2.31*10^2 \le GPr \le 4.32*10^3$, $1.37*10^{-3} \le Fr \le 0.13$	U (particle in CMC)	$Nu = 0.099\ G\ Re^{0.62}\ GPr\ Fr^{0.276}\ (V_p/V_c)^{0.091}\ (\rho_p/\rho_l)^{0.286}$	
	$0.08 \le GRe \le 1.77*10^3$, $3.83*10^{-4} \le Fr \le 0.11$	h_{fp} (particle in CMC)	$Nu = 0.014\ G\ Re^{0.613}\ GPr^{0.383}\ Fr^{-0.213}\ (V_p/V_c)^{0.182}\ (\rho_p/\rho_l)^{0.518}\ (L_c/D_c)^{1.131}$	
Polypropylene, Nylon, Acrylic, Delrin, Teflon in water and oil under EOE mode	$5.2*10^2 \le Re \le 5.4*10^5$, $2.6 \le Pr \le 90.7$	U (single particle)	$Nu = 0.93\ Re^{0.51}\ Pr^{-0.36}\ (h_s/H)^{0.21}$	Sablani *et al.* (1997)
	$5.32*10^{-4} \le Fr \le 2.13*10^{-3}$	h_{fp} (single spherical particle)	$Nu = 2 + 1971Fr^{0.31}\ Pr^{0.33}\ a^{0.34}\ (h_s/H)^{1,56}\ ((Dr + Dc)/Dc)^{0.21}$	
	$44 \le Re \le 1.39*10^3$, $2.6 \le Pr \le 78.3$	h_{fp} (single cylindrical particle)	$Nu = 7.26\ Re^{0.42}\ Pr^{0.33}\ a^{1.12}$	
	$44 \le Re \le 1.39*10^3$, $2.6 \le Pr \le 78.3$	h_{fp} (single cubical particle)	$Nu = 8.03\ Re\ Pr^{0.33}\ a^{1.63}$	
	$1.7*10^4 \le Re \le 5.4*10^5$, $2.6 \le Pr \le 90.7$	U (multiple particle)	$Nu = 0.71Re^{044}\ Pr^{0.36}\ (\varepsilon/(100-\varepsilon))^{0.37}(d_e/D_c)^{-0.11}\ \psi_{0.24}$	
	$28 \le Re \le 1.55*10^5$, $1.18*10^3 \le Pe \le 7.71*10^3$	h_{fp} (multiple particle)	$Nu = 0.71Re^{0.61}\ \psi^{0.23}\ (\varepsilon/(100-\varepsilon))^{0.067}(d_p/D_c)^{-0.70}\ (k_p/k_f)^{1.98}$	

For single particle studies, Nusselt number has been related to Reynolds number (Re), Prandtl number (Pr) and relative can headspace. For multiple particle studies, the ratio of headspace to the height of the can(h_s/H), the ratio of the particle to liquid concentration $[\varepsilon/(100 - \varepsilon)]$, the ratio of the equivalent particle diameter to the diameter of the can (d_c/D_c), particle sphericity (ψ), and the density simplex$((\rho_p - \rho_f)/\rho_f)$ have been used in the correlations for Nu (Meng and Ramaswamy, 2007c). Headspace has been used in these correlations because U and h_{fp} depend on the size of the headspace. Apart from these, Fernandez *et al.* (1988) have used the fluidized bed and packed bed approaches and the modified Stanton number and Colburn j-factor in empirical correlations for h_{fp} in cans with axial rotation. Also, the Froude number, density rate, particle concentration and diameter relationships have been incorporated in more specific correlations, such as those developed by Dwivedi and Ramaswamy (2010d) for food canning in rotary retorts. They also used a combination of reel radius, radius of can and radius of particles as characteristic length.

2.7.2 Forced and Free Convection

There are examples of both forced and natural/free convection in food research (Meng and Ramaswamy, 2007c). Natural convection carries heat by natural means, as in conventional still thermal processing; however, in forced convection, heat transfer is enhanced by external application of energy like rotary or lateral agitations etc., as in agitating retorts. In all forced convection situations, the natural convection phenomenon exists to operate because of presence of buoyant forces. However, in case of mixed convection, buoyant and inertial forces operate simultaneously, and sometimes, have the same order of magnitude (Dwivedi and Ramaswamy, 2010d).

In forced convection, the dimensionless heat transfer coefficient is given as combined function of Reynolds Number (Re) and Rayleigh number (Ra). However, in case of natural/free convection, as there is no agitation, turbulence is generally low and the dimensionless heat transfer coefficient is given as function of only Rayleigh number (Incropera and de Witt, 2011). Here, Reynolds's number is indicative of speed of agitation and the turbulence created during the process and can be used to compare the importance of the effect of the inertial and viscous forces. Rayleigh number, on the other hand, is a product of Grashoff (Gr) and Prandtl (Pr) number and is indicative

of the free or natural convection happening in the system. When the Rayleigh number is below the critical value for a fluid, heat transfer is primarily in the form of conduction; and when it exceeds the critical value, heat transfer is primarily in the form of convection.

$$\textbf{Forced Convection: } \mathrm{Nu} = f(\mathrm{Re}, \mathrm{Ra}) \tag{2.10}$$

$$\textbf{Natural/Free Convection: } \mathrm{Nu} = f(\mathrm{Ra}) \tag{2.11}$$

By fixing the value of free convection for varying forced convection, researchers (Dwivedi and Ramaswamy, 2010d) observed that natural convection has an important role especially during the heating of can subjected to axial rotation. Rao and Anantheswaran (1988) found that major agitation in a rotating can occurs during the bottom 1/3rd part of the rotation cycle. Thus, they concluded that for the upper 2/3rd cycle, agitation is very slow and hence natural/free convection plays major role in heat transfer in a rotating can. Also, in other studies, it was found that forced convection is the dominant mechanism for heat transfer for the canned liquid/particle mixture (Sablani *et al.*, 1997; Meng and Ramaswamy, 2007c; Dwivedi and Ramaswamy, 2010d). Hence, researchers have generally used a sum of natural and forced convection for developing correlations for heat transfer coefficients during rotary agitation. Dwivedi and Ramaswamy (2010d) used Equation (2.12) to develop a correlation by considering both natural and forced convection for analysis.

$$\mathrm{N_u} = \mathrm{A_1}(\mathrm{GrPr})^{\mathrm{A_2}} + \mathrm{A_3}\,(\mathrm{Re})^{\mathrm{A_4}}(\mathrm{Pr})^{\mathrm{A_5}}(\mathrm{Fr})^{\mathrm{A_6}}(\rho_\mathrm{p}/\rho_\mathrm{f})^{\mathrm{A_7}}\left(\frac{\varepsilon}{100-\varepsilon}\right)^{\mathrm{A_8}}(\mathrm{d_p}/\mathrm{D_c})^{\mathrm{A_9}}(\mathrm{k_p}/\mathrm{k}_f)^{\mathrm{A_{10}}} \tag{2.12}$$

Many studies (Table 2.8) have been done on the convective heat transfer coefficient in liquid foods, with incorporated overall heat transfer coefficients (U). Rao and Anantheswaran (1988) presented a detailed review about this in their study. However for liquid particulate foods in can this study is very new. Sablani *et al.* (1997) have established correlations for forced convection heat transfer coefficient in cans containing liquid particulates and subjected to end-over-end rotation. Their model was based on particle settling theory, and the terminal velocities were a combined function of gravity, buoyancy, centrifugal and drag forces. They used a packed bed with multiple particles to model heat transfer to the moving liquid particulate system. Awuah and Ramaswamy (1996) reported that simultaneously considering free/forced convection gave correlations with higher R^2 values. They developed a correlation for heat transfer coefficients using spherical and finite cylinders using multiple regressions of statistically significant dimensionless

groups and concluded the test material had significant effect on the Nusselt number and in developed correlations. They also introduced ratio of particle to fluid diffusivities called diffusivity ratio as one of the parameters in the dimensionless correlations.

For high viscosity fluid and particle mixtures in end-over-end mode of agitation, Meng and Ramaswamy (2007c) developed the dimensionless correlations using apparent heat transfer coefficients h_{ap} and U_a. Dwivedi and Ramaswamy (2010d) used Grashoff and Prandtl numbers to develop the correlations for heat transfer coefficient prediction in canned Newtonian liquids (with and without particles), under mixed and forced convection heat transfers during free axial rotation. They concluded that in the absence of particles, the heat transfer by natural convection took place in both end-over-end (47% of total heat transfer) and in free axial mode (51% of total heat transfer). In a very recent study, Cariño-Sarabia and Vélez-Ruiz (2013) compared the evaluated experimental coefficients with values obtained from the correlations. They found that fittings coefficients were not as high as expected and attributed this to varying particles shape and fluid flow properties. However, they also reported that correlations for single particle were better than for multiple particles in a real food system.

2.8 Conclusions

Thermal processing of liquid particulate mixtures is complex and understanding the associated heat transfer phenomenon requires extensive research. The choice of minimal lethality to be imparted during a thermal process is governed by many factors, product pH being the most important. Ample scientific literature is available to select the value of minimal lethality. However, calculation of time-temperature combinations required to deliver this lethality requires substantial experimental work involving collection of heat penetration data. Researchers have used both thermocouple and non-thermocouple-based methods to collect the heat transfer data, in both still mode of operation and in agitating containers. However, data collection in agitating containers is still troublesome and provides opportunities for improvement. Many numerical and analytical methods have been used by researchers to analyze these data for evaluating U and h_{fp}. All these methods involve solving the same energy balance equation; however, exact treatment differs distinctively for direct and indirect temperature measurement techniques. Various innovative and simpler methodologies are also available in certain conditions of processing. Although recent

studies have attempted to understand the phenomenal behavior of heat transfer in liquid-particle mixtures in still and agitating conditions, several conflicting trends have been reported that need further clarification. It has generally been observed that any configuration which leads to an increase in the intensity of agitation yields higher values of U and h_{fp}. Each processing condition is unique in itself and development of new systems, like reciprocating agitation system, warrants the need of additional heat transfer studies. This also prompts the need for improving thermal processing technology further through constant innovations in the design of retorts and data collection and analysis methodologies.

PREFACE TO CHAPTER 3

Reciprocating agitation thermal processing is the most recent development in the field of thermal processing. This process utilizes rapid back and forth motion of containers to enhance heat transfer using forced convection. Before investigating the complex phenomenon of heat transfer inside a liquid-particulate system, it is important to understand and characterize the temperature distribution studies inside the retort and inside a can containing only liquid. Besides, comparison between reciprocating retort and conventional still retort shall be useful to elucidate the effect of reciprocation on the retort temperature distribution.

Since, a reciprocating retort was not available, the main objective of this work was to develop a lab-scale reciprocating retort by installing a reciprocating cage inside an existing conventional still retort. The developed retort was characterized to ensure that the required reciprocation frequency and amplitude were constantly delivered. Further, heating behavior and temperature uniformity inside the developed retort and in liquid-only cans were characterized and compared with conventional still retorts.

Parts of this chapter won the first prize in the **Charles Stumbo Graduate Student Paper Competition** and an oral presentation was made in the Annual Meeting of the Institute for Thermal Processing Specialists (IFTPS) held on Mar 11-14, 2014 in Orlando, Florida.

Parts of this chapter have been published as an original research article: *Modification of a static steam retort for evaluating heat transfer under reciprocation agitation thermal processing*. Journal of Food Engineering, 153, 63-72.

The experimental work and data analysis was carried out by the candidate under the supervision of Dr. H. S. Ramaswamy.

CHAPTER 3

MODIFICATION OF A STATIC STEAM RETORT FOR STUDYING RECIPROCATING AGITATION THERMAL PROCESSING

3.1 Abstract

A lab-scale reciprocating agitation retort was developed by modifying an existing conventional vertical static retort to include a reciprocating mechanism. For this a reciprocating cage, capable of holding 4 cans, was installed inside the static retort. This reciprocating cage was connected to a slider-crank assembly which was powered by a 0.5 HP magnetic motor. The slider-crank mechanism converted the rotary motion produced by the motor into a reciprocating motion of the cage. A mechanism was provided to control the amplitude (3-30 cm) and frequency of reciprocations (0-5 Hz). During characterization of this retort, it was noticed that the reciprocation frequency decreased at higher temperatures due to expansion of the metal parts and joints on heating. Hence, a calibration chart was developed to set the supply voltage to obtain the required operating frequency. Temperature distribution study of the retort was conducted by collecting temperatures at various locations inside the retort. The average of standard deviation of temperatures across various locations over the first 10 min of heating was varied between 1.29–1.83 ºC during reciprocation, as compared to 2.44 ºC in a still retort. The come-up time of the retort was found to vary between 3-4 min. In-container heating uniformity studies were conducted by collecting liquid temperatures at 3 positions inside a 307x409 can filled with 80% glycerin to 10 mm headspace and processed at various reciprocation frequency and amplitude at 120 ºC. During reciprocation processing, it was found that stabilization to within 1ºC standard deviation occurred in around 2.5-5.0 min, while it required about 11 min under static processing condition. Faster heating rates were also obtained on using reciprocating agitation processing with mean heating rate index of liquid decreasing from approximately 10 min to 1-5 min during reciprocation processing. Thus, this study revealed that there were better heating rates and greater uniformity in both in-container and retort temperatures in reciprocating retorts as compared to conventional retorts.

3.2 Introduction

Owing to the recent surge in consumer demands for high quality foods, thermal processing industry has felt a growing need for developing systems which can provide rapid heating conditions for inactivating microorganisms causing public health and spoilage concerns. This is primarily because rapid and uniform heating conditions permit the product to reach the processing temperatures faster, and thus, the required process can be accomplished in a shorter time. The shorter process time, while satisfying the sterility requirements, reduces the thermal damage to food color, texture and nutrients resulting in a better quality. Moreover, short process cycles also help to increase the process efficiency and enhance the production capacity of the facility.

Forced convection obtained through agitation of the containers during thermal processing, has been used to provide rapid heating conditions, particularly in convection-heating products, to promote better heat transfer and to obtain better quality food products (Anantheswaran and Rao, 1985a, 1985b). Agitation also prevents different ingredients and phases in the food product from separating from each other during thermal processing (Dwivedi, 2008). A number of agitating cookers have been described in the patent literature (Lowe and Poindexter, 1952; Oharenko, 1958; Prickett, 1958; Evans, 1992; Veltman, 1995; Silvestrini, 2008) and they all serve the common objective of increasing the rate of heat penetration and making the temperature distribution within the can more uniform. Commercial rotary retorts, like Sterilmatic (FMC Corp., San Jose, CA), Steristar (Malo Inc., Tulsa, OK), Rotomat (Stock America, Inc., Milwaukee, WI) etc., provide agitation through rotation of cans in end-over-end or axial mode.

Lateral reciprocation agitation of containers during thermal processing can potentially impart agitations that do not subside with an increase in intensity. Although, the first reciprocating cooker was patented by Gerber (1938), not much scientific research has been carried out in this area since then. Much later, Walden (1999) acquired patent for a retort utilizing reciprocation agitation of the containers, after which this technology gained momentum. He used a much higher intensity of reciprocation as compared to Gerber and demonstrated that it helped to reduce the process times and improve product quality. Walden and Emanuel (2010) was claimed that with the new system a 10-fold reduction in process times could achieved, as compared to conventional static process. However, they made no attempt to investigate and understand the phenomenon of

heat transfer occurring during the process. There is also paucity of scientific literature on the effect of reciprocation on the associated heat transfer, processing efficiency and product quality.

Hence, in order to study the reciprocating agitation system, a laboratory scale reciprocating retort was developed by installing a reciprocating mechanism inside an existing conventional static steam retort. This chapter further details the heating uniformity studies conducted inside the retort and inside liquid-only cans in order to analyze and characterize the heat transfer phenomenon in the developed retort.

3.3 Development of the reciprocating retort

3.3.1 Conventional static steam retort

A vertical static steam retort (Loveless Manufacturing Co., Tulsa, OK) located at the pilot plant of Macdonald Campus of McGill University, Ste Anne de Bellevue, Quebec was modified in this study. The retort shown in Fig. 3.1 has an internal diameter of 62 cm, wall thickness of 1 cm, and a depth of 100 cm. Steam, air or water (individually or in an appropriate combination) could be used as an operating medium. In this study, we used steam as the operating medium. The flow of steam was pneumatically controlled using a PID controller (Control & Readout Ltd., Worthing, Sussex, England) to maintain specific temperature and pressure inside the retort. The maximum allowable pressure inside the retort was 308 kPa which corresponded to the maximum operating temperature of around 134 ºC. The come up time of the retort was around 3-4 min, depending on the number of cans in the retort and the operating temperature. This retort was modified to include a reciprocating mechanism for achieving reciprocating container agitation inside the retort. The modification mechanism consisted of a reciprocating cage, a slider-crank assembly and a permanent magnet motor.

3.3.2 Reciprocating Cage Assembly

The schematic of the modified retort is shown in Fig. 3.1. The existing static retort (E) was retrofitted to include a reciprocating cage assembly comprising of a cage (A) reciprocating on horizontal rails (B), by the aid of slip rings (C), as shown in Fig. 3.1c. The steel rails (B) were welded to the interior of the steam retort (E). The slip rings (C) were made from Nylon material. The cage (A) width was 12 cm, length 35 cm and height 17 cm and was designed to hold one level

of 4 cans (No. 2) along the diameter of the retort, 2 cans on each side of the axis of reciprocation for balancing. The cans could be placed in three orientations viz. i) vertically perpendicular, ii) horizontally parallel, or iii) horizontally perpendicular to the axis of reciprocation, as shown in Fig. 3.2. Metallic can holders were provided to securely hold the cans in position during reciprocation. The cage (A) was connected to a reciprocating rod (D) of 65 cm in length and 2 cm diameter. The rod was inserted into the retort by drilling a hole at one-third height from the top of the retort. Any loss of steam through the hole was minimized by using a properly greased reciprocating seal (F).

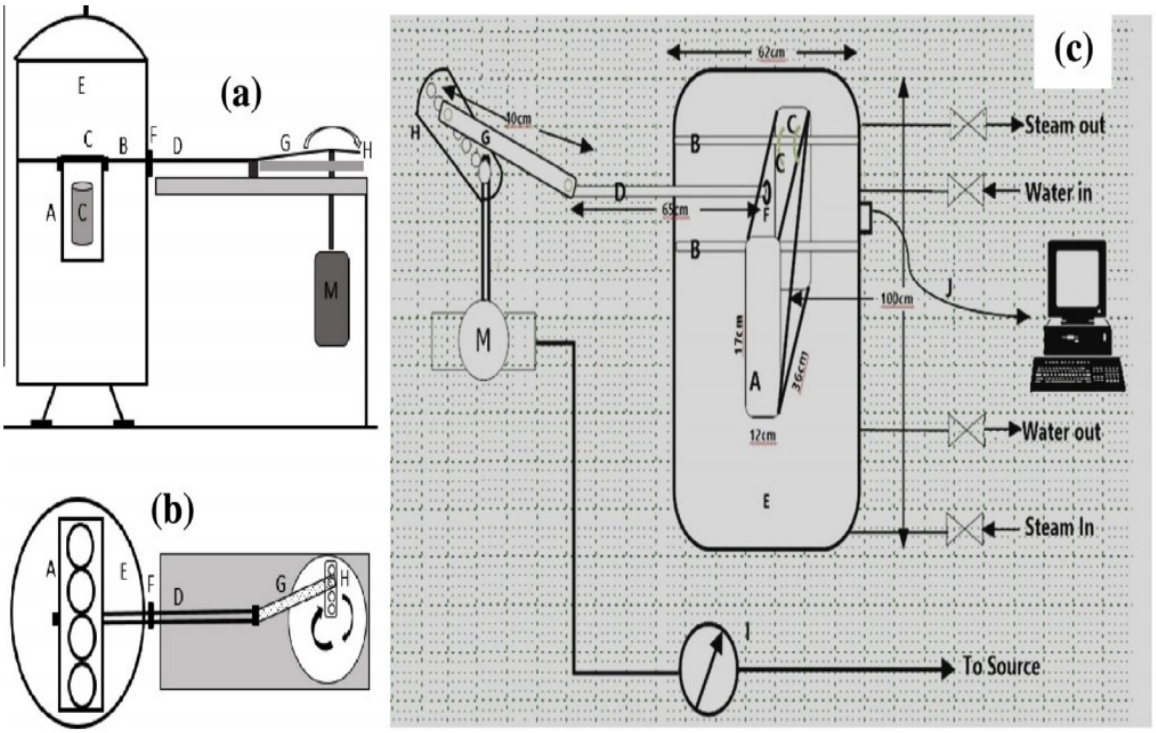

[A: reciprocating cage; B: horizontal rails; C: slip rings; D: reciprocating rod; E: retort; F: reciprocating seals; G: crank arm; H: rotating shaft; I: voltage controller; J: heat penetration cable; M: motor]

Fig. 3.1. a) Side-view of the modified retort. b) Top-view of the modified retort. c) Overall schematic of the experimental setup.

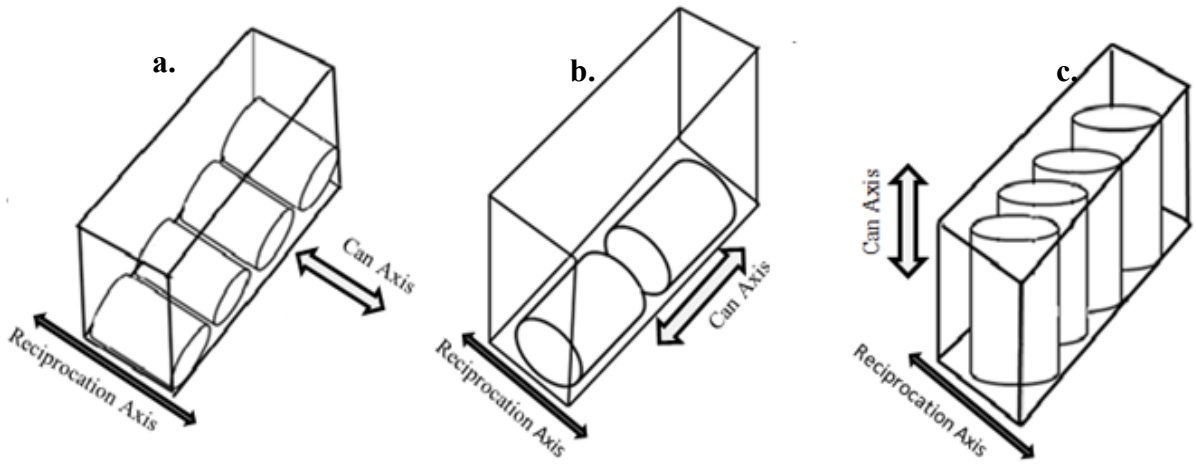

Fig. 3.2. Schematic of the three possible orientations inside the reciprocating cage showing the placement of experimental cans with there longer axis: a) horizontally along the reciprocation axis (HA); b) horizontally perpendicular to reciprocation axis; c) vertical (V).

3.3.3 Slider Crank Assembly

The slider crank assembly consisted of an 18 cm diameter stainless steel rotating shaft (H) and a 40 cm length crank (G). The crank (G) could be attached to different positions through pivots along the radius of the rotating shaft (H). Different positions of the pivot provided the possibility of varying the amplitude of reciprocation. The other end of the crank (G) was connected to the reciprocating rod (D) and was constricted to move in a straight line. On rotation of the shaft, the pivoted end of the crank moved in a circular motion of the required diameter, depending on the position of the pivot. The constricted end of the crank, on the other hand, moved in a linear sliding motion. Thus, through the rotation of the shaft, reciprocating motion was created and was transferred to the reciprocating cage (A) through the reciprocating rod (D). The position of the pivot connecting the rotating end of the crank to the shaft, determined the amplitude of the reciprocation provided by the slider-crank mechanism. 15 pivots were drilled along the radius of the rotating shaft at distances from 1.5 to 15 cm from the center of the shaft. Thus, the amplitude of reciprocation ranging from 3-30 cm could be achieved through this mechanism.

3.3.4 Permanent magnet motor

The rotating shaft was powered through a ½ HP direct current magnetic motor (M) which was connected to the mains through a voltage controller (I). The speed of rotation of the motor was controlled by adjusting the input to the voltage controller. For each rotation of the rotating shaft, one cycle of reciprocation was completed by the reciprocation cage. Thus, the voltage controller (I) was used to control the reciprocation frequency. The rotation speed of the shaft was monitored through a hand-held non-contact photo tachometer and thus the frequency of reciprocations could be determined. The entire set up was rated for a maximum reciprocation frequency of 5 Hz.

3.4 Methodology for retort characterization

In order to calibrate reciprocation frequency obtained in the developed retort, reciprocation frequency obtained at various input voltages (10-30 V) was recorded with respect to time. Subsequently, calibration charts were developed to obtain the desired input voltage to deliver a particular reciprocation frequency at 121.1 ºC. This chart was subsequently used to set the input voltage to obtain the reciprocation frequency in future studies in this thesis.

In order to characterize the heating behavior, heat penetration tests were conducted in the modified reciprocating retort using steam as the heating medium. The temperature distribution in retort was evaluated by placing thin wire thermocouples (wire diameter 0.0762 mm, Omega Engineering Corp., Stamford, CT) at 6 positions (1-top of retort, 2-bottom of retort, 3-cage center,4- cage top, 5-cage bottom, 6-side of cage) inside the retort. In order to quantify the temperature distribution inside the reciprocating cans, test cans of 307x409 size (Home Canning Co., Montreal, QC) were used. The cans were filled with 80% glycerin solution to a 10 mm headspace and closed using a manual double seaming machine (Home Canning Co., Montreal, QC). Liquid temperatures were collected using CNS copper-constantan needle-type thermocouples fitted to the can using C-10 locking connectors (Ecklund-Harrison Technologies Inc., Fort Myers, FL) at three locations (P1- 20 mm above can-bottom-center; P2- 56 mm above can-bottom-center; P3- 85 mm above can-bottom-center).

The thermocouples used for temperature collection inside the retort and inside the can had miniature male connectors which were plugged into the female connectors of the heat penetration cable (J) introduced into the retort (E). The thermocouple outputs were recorded at one second intervals using a data acquisition system (HP34970A, Hewlett, Packard, Loveland, CO). Further details on the temperature measurement techniques are available elsewhere (Sablani and Ramaswamy, 1996; Dwivedi and Ramaswamy, 2010b).

During each experimental run, the reciprocating cage was loaded with duplicate experimental cans and the remaining spaces were filled with dummy cans to provide ballast. Each experimental run was repeated twice. The experimental cans were kept in vertical orientation equidistant from the axis of reciprocation in opposite directions. The crank was pivoted to the desired pivot on the shaft according to the required amplitude. The motor was turned on at the required frequency. Steam was used as the heating medium and operating temperature was set at 120 ^{o}C for all temperature uniformity studies. Cold water was used as the cooling medium. Reciprocations were imparted until all temperatures in both experimental cans reached 30 ^{o}C during cooling.

Retort temperature uniformity was characterized by computing the average standard deviations among the six thermocouples during the first 10 min of heating. Similarly, for liquid temperature uniformity, standard deviations between the 3 liquid thermocouples were plotted with respect to time. Heating rate indices of the liquid (f_{h-l}) was also calculated as they are indicative of the heat transfer resistance between heating medium and can liquid and temperature uniformity was also characterized by difference between the f_{h-l} of three locations.

3.5 Results and discussions

The modified retort was characterized for its ability to deliver a constant frequency of reciprocation throughout the process. Further, temperature distribution studies were conducted inside the retort and inside the can to analyze the heating uniformity at various reciprocation frequencies and amplitudes.

3.5.1 Calibration of reciprocation frequency and input voltage

The control of frequency of reciprocations was achieved by controlling the input voltage to the motor through the voltage controller. Fig. 3.3 shows how the frequency of reciprocation of the cage varied with retort temperature at a particular input voltage. It was observed that if the input voltage was kept constant, the frequency of reciprocations decreased during the come-up time of the retort, as the retort was being heated.

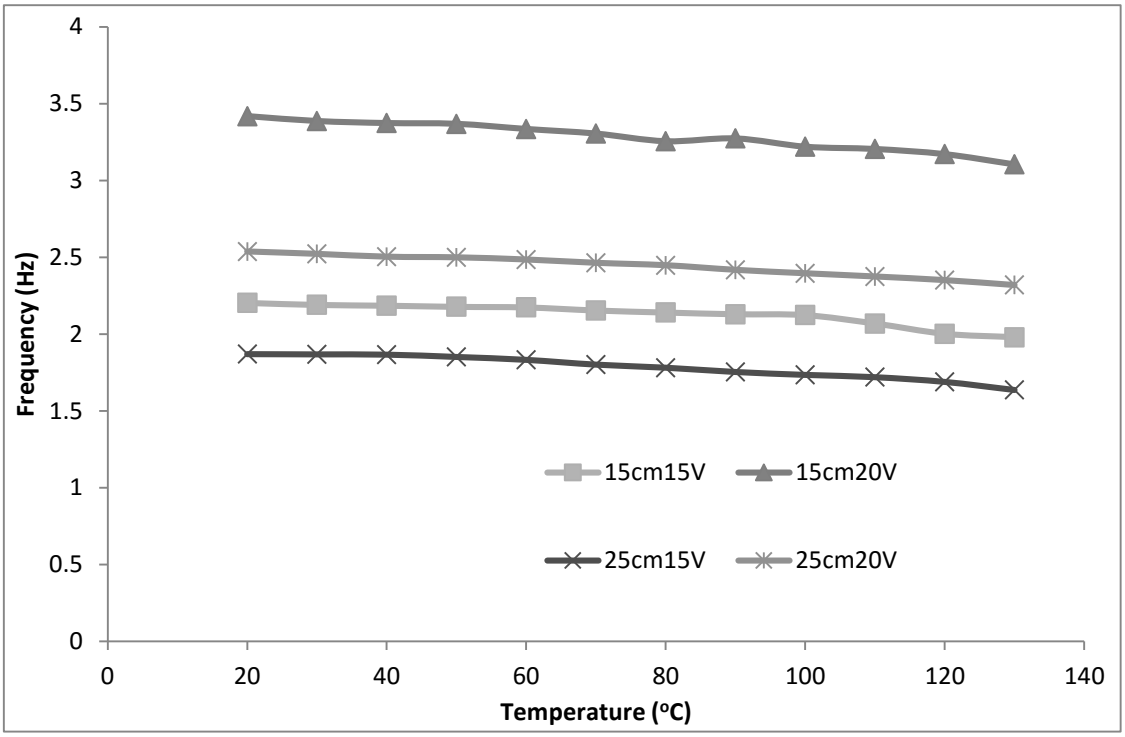

Fig. 3.3. Variations in frequency of the reciprocating cage during come-up time of the retort at various input voltages and amplitudes.

The frequency of reciprocation was highest at the start of the experiment at room temperature. However, as the temperature of the retort increased, the frequency of reciprocation subsided due to thermal expansion of the cage, the rod, the shaft, the crank and other metallic parts in the retort. Thereby, it was necessary to either keep adjusting the input voltage regularly for maintaining a constant frequency or to develop a calibration chart of the input voltage which shall produce a particular frequency at 121.1 °C. Since regularly changing the input voltage was tedious

and non-desirable, it was decided to adopt the later approach. Thus, a calibration chart was developed for setting the input voltage to obtain a particular frequency. For this, the input voltage required to maintain a particular frequency at 121.1 ºC, was chosen as the set voltage.

Table 3.1 presents the calibration chart, according to which the input voltage were set in order to achieve a particular frequency of reciprocation at particular amplitude. Although, this meant that the cage may reciprocate at a slightly higher frequency during the initial stages of heating, but since the come-up time of the retort was very short as compared to the total processing time, this slightly higher frequency was assumed not to affect the processing appreciably.

Table 3.1. Calibration chart for setting the input voltage to the voltage controller for obtaining a particular reciprocation frequency when the retort reaches the operating temperature.

Operating Frequency (Hz)	**Input voltage at a particular amplitude (V)**				
	5 cm	**10 cm**	**15 cm**	**20 cm**	**25 cm**
1	10.3	10.8	11.3	11.9	13.1
2	15.8	14.9	15.8	16.9	19.1
3	18.9	18.6	19.3	20.3	22.9
4	21.1	21.8	22.4	23.6	24.7
5	23.1	23.9	24.5	25.1	25.8

3.5.2 Temperature distribution in the retort

The temperature distribution in the retort was evaluated by placing thin wire thermocouples at 6 positions (1-top of retort, 2-bottom of retort, 3-cage center, 4- cage top, 5-cage bottom, 6-side of cage) in the retort. Fig. 3.4 gives the temperature distribution in the retort during the first 10 min of heating at 2 Hz frequency and 15 cm amplitude. The observed temperature variations were small and indicated that the temperature distribution in the retort was uniform. The average of the standard deviation of data-points over the 10 min heating profile for this frequency and amplitude was around 1.78 ºC. This value under various reciprocating conditions studied varied between 1.29–1.83 ºC. Under non-agitated condition, this value was 2.44 ºC. Thus, it was found that the temperature distribution in the retort was more uniform than under conventional static conditions. The better uniformity resulted from the intense agitation and turbulence in steam created by the

back and forth motion of the reciprocating cage, which prevented the build-up of any local pressure zones across the retort. However, it was also observed that the thermocouples located at the top of the retort recorded the lowest temperature amongst all the thermocouples at temperatures less than 100 ºC. Beyond 100 ºC, all the thermocouples gave almost the same temperature. This may be because the top of the retort was just behind the cage, and at higher frequencies of reciprocation, the shielding effect created due to the motion of the cage may have obstructed the flow of steam to the top during initial phase of heating. Further it was also observed that the come-up time varied roughly between 3-4 min for all the reciprocation frequencies and amplitudes studied.

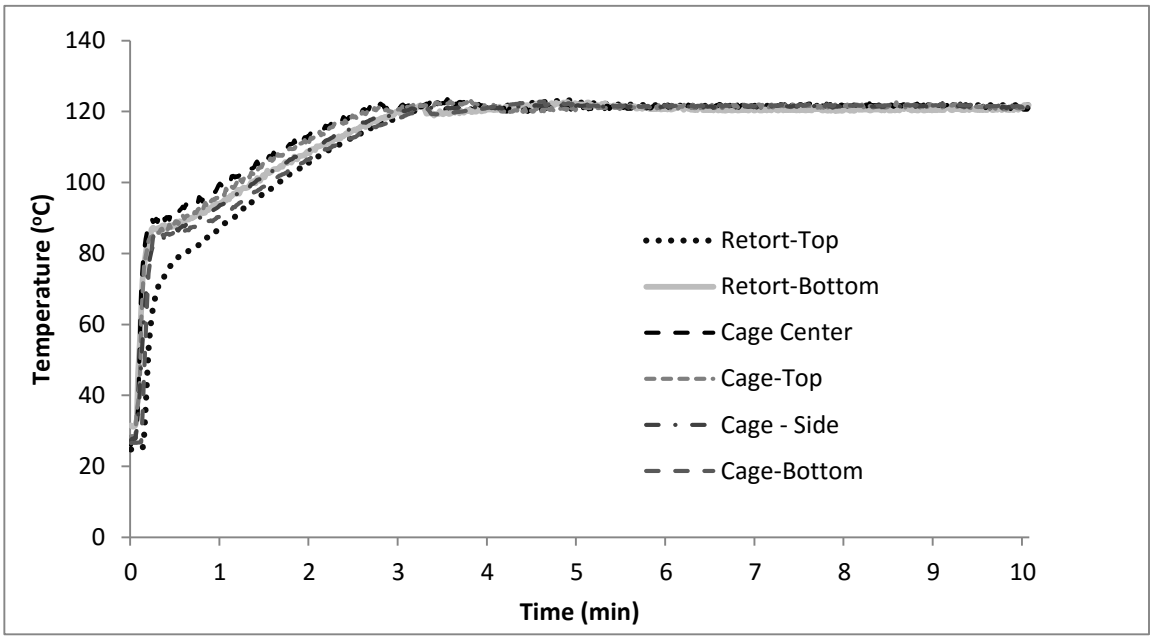

Fig. 3.4. Temperature distribution during the first 10 min of heating at various locations inside the retort at an operating temperature of 120 ºC, frequency of 2 Hz and amplitude of 15 cm.

3.5.3 Temperature profiles during non-agitated thermal processing

Conventional thermal processing in static retort is the lower end limiting case of reciprocation agitation at 0 Hz frequency and 0 cm amplitude. So, static case scenario can be considered as the control. Fig. 3.5 shows the typical profiles for the retort temperature and liquid temperatures at the 3 positions of the can (P1- 20 mm above can-bottom-center; P2- 56 mm above can-bottom-center; P3- 85 mm above can-bottom-center) during the conventional non-agitated

mode of processing. It was observed that the temperature gathered by the thermocouples for the 3 positions for liquid was much lower than that of the retort initially. This was because of the heat transfer resistance between heating medium (steam) and the liquid (glycerin) due to the can wall (Dwivedi and Ramaswamy, 2010b). However, the differences between the temperatures decreased rather fast, almost logarithmically.

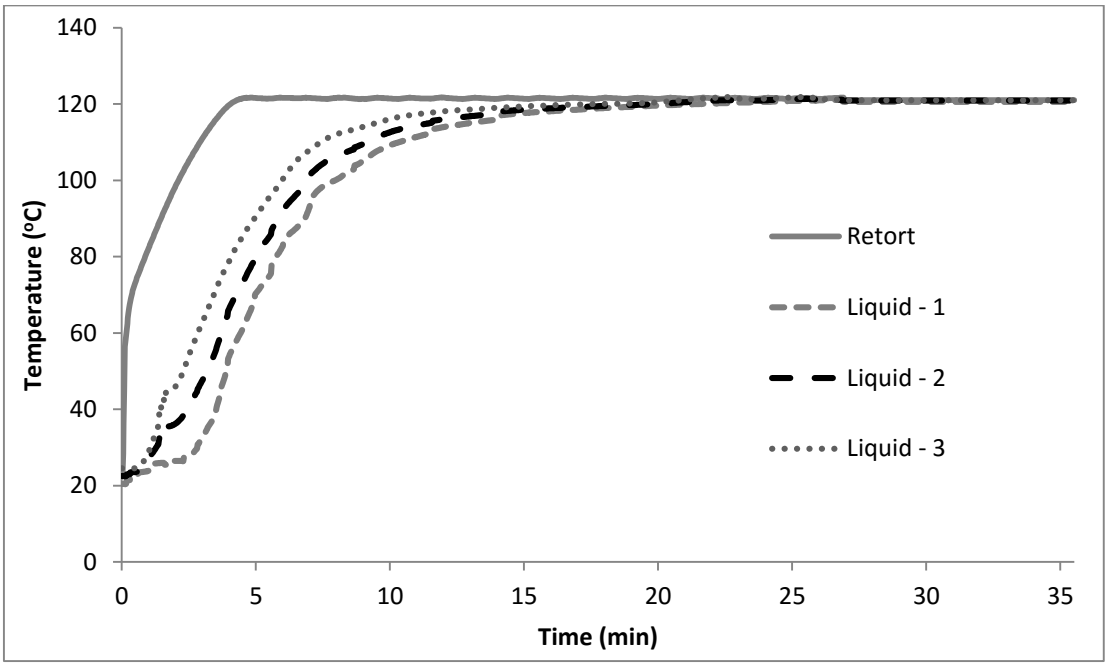

Fig. 3.5. Time-temperature profiles for a can, processed at 120 °C showing the retort and liquid temperature profiles at 3 positions (P1 - 20 mm above can bottom center; P2 - 56 mm above can bottom center; P3 - 85 mm above can bottom center) of the can and processed under still mode of processing.

Fig. 3.5 also shows that the time required for the liquid temperatures to reach the operating temperature was almost around 20 min, although there was a wide variation between the temperatures of three thermocouples. Generally, this time was largest at highest point in the can which is consistent with the assertion that the heat transfer was dominated by viscous forces. Under such heating scenario, even before the cold-spot reaches the operating temperature, the bulk of the can would have stayed at the processing temperature for a long time. This shall result in inadvertent over-processing and huge quality losses associated with conventional static thermal processing (Anantheswaran and Rao, 1985a).

It is also seen from Fig. 3.5 that there were appreciable differences between the 3 liquid-temperature profiles. This is because the prevailing mode of heat transfer during non-agitated processing is mostly natural convection (Meng and Ramaswamy, 2007c), which is insufficient to remove the temperature differences. Thus, non-uniformity exists in the temperature distribution inside the can in non-agitated thermal processing. Hence, the main objective of reciprocating agitation is to remove these non-uniformities in liquid temperature, by incorporating forced convection through rapid back and forth motion of the containers.

3.5.4 Temperature profiles during reciprocating agitation thermal processing

Fig. 3.6 shows the typical profiles for the retort temperature and liquid temperatures at the 3 positions of the can (P1- 20 mm above can-bottom-center; P2- 56 mm above can-bottom-center; P3- 85 mm above can-bottom-center) during the reciprocating agitation thermal processing at 2 Hz frequency and 15 cm amplitude. It was observed that the temperature gathered by the thermocouples for the 3 positions for liquid was almost similar. The variation between the temperatures were higher at initial stages, although very low compared to still mode of processing (Fig. 3.5) and subsided very fast with time. This demonstrated that there was extensive turbulence produced inside the can as a result of forced convection produced on account of rapid back and forth motion of containers. However, the differences between the temperatures decreased rather fast, almost logarithmically. Even, the time required for the temperatures to reach operating temperature decreased to almost 8 min from 20 min in still mode of processing. On increasing the reciprocation frequency or reciprocation amplitude, the time taken for the temperatures to become uniform decreased further. This uniform and faster heating rate would be beneficial for products as it would result in lower process times. These trends are similar to those observed on introduction of rotary agitation in studies on rotary thermal processing (Sablani, 1996). Another interesting observation was that the top temperatures were slightly higher and the center and bottom temperatures were similar. This meant that cold-spot location moved towards the center slightly (Fig. 3.6), from near bottom location during still mode (Fig. 3.5), on account of onset of agitation.

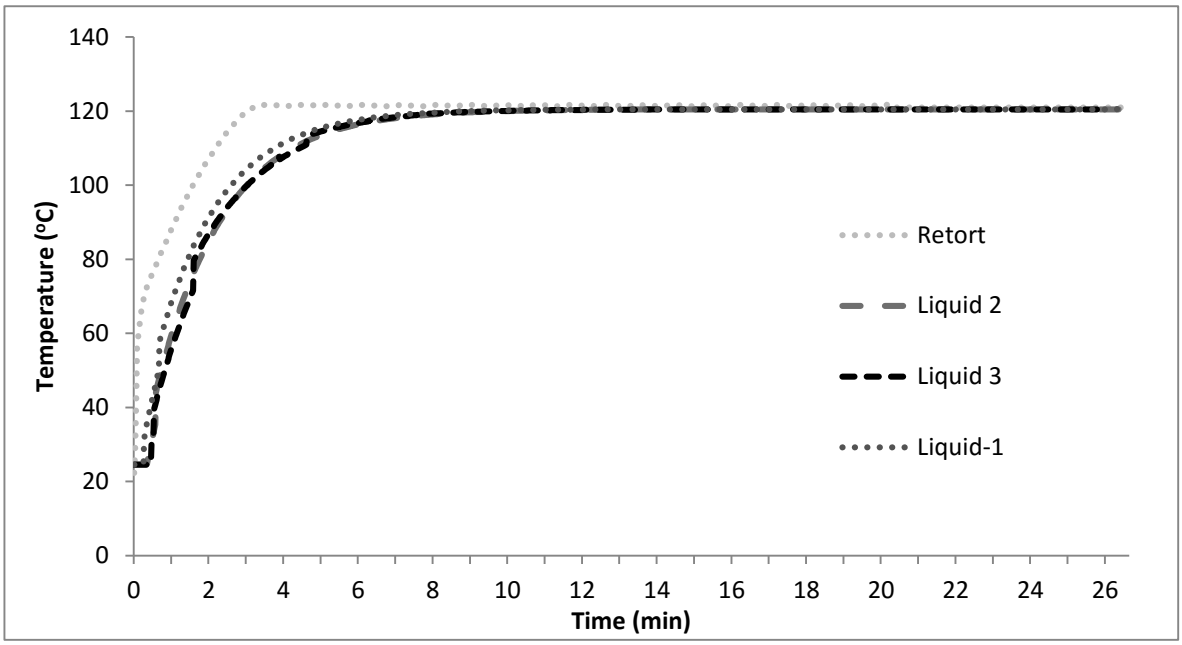

Fig. 3.6. Time-temperature profiles for a can, processed at 120 °C showing the retort and liquid temperature profiles at 3 positions (P1 - 20 mm above can bottom center; P2 - 56 mm above can bottom center; P3 - 85 mm above can bottom center) of the can and processed during reciprocating mode of processing at 2 Hz frequency and 15 cm amplitude.

3.5.5 Liquid temperature uniformity during reciprocation processing

Temperature uniformity in cans during reciprocating agitation was measured in terms of the heating rate index of liquid ($f_{h\text{-}l}$). Table 3.2 presents the $f_{h\text{-}l}$ values calculated from the data collected by the 3 thermocouples at various processing parameters. For static scenario, the $f_{h\text{-}l}$ value for location No. 1 (bottom-center) was nearly double, when compared to location No. 3 which was near the top center of the can. However, with the onset of reciprocation, the temperature gradients in the liquid inside the cans became almost non-existent (Fig. 3.6). This is further supported by the small differences in heat penetration parameters between different locations under the various frequencies and amplitudes of reciprocation (Table 3.2). This implied that the forced convection due to reciprocation resulted in better mixing of the liquid inside the can, which helped the liquid to achieve better temperature uniformity. Similar results were obtained by Sablani and Ramaswamy (1996) in end-over-end mode of rotation.

Table 3.2. Temperature uniformity of the liquid temperature at a can processing temperature of 120 ºC as a function of frequency and amplitude.

Processing Condition		Heating rate index of liquid, f_{h-l} (min)			f_{h-l} (mean±sd)[c] (min)
		Location 1	Location 2	Location 3	
Static Mode		13.8	8.2	7.1	9.7±3.6
Frequency[a] (Hz)	**1**	5.1	4.9	5.2	5.1±0.1
	2	3.1	2.8	3.0	3.0±0.1
	3	2.1	2.5	2.4	2.3±0.2
	4	1.0	1.2	1.1	1.1±0.1
Amplitude[b] (cm)	**5**	4.9	4.9	5.2	5.0±0.2
	10	3.9	3.4	3.5	3.6±0.2
	15	3.1	2.8	3.0	3.0±0.1
	20	3.4	2.8	3.7	3.0±0.3
	25	2.6	3.8	2.9	3.1±0.6

[a] At constant reciprocation amplitude of 15 cm

[b] At constant reciprocation frequency of 2 Hz

[c] sd stands for standard deviation

The gradual tightening of the temperature distribution, under different test runs, is shown as standard deviations in temperature of the liquid as a function of time, in Fig. 3.7. During reciprocation processing, it was found that stabilization to within 1ºC standard deviation occurred in around 2.5-5.0 min, while it required about 11 min under static processing condition. With come-up time of the retort being 3-4 min, temperatures under reciprocation became uniform in less than a minute after come-up. Sablani and Ramaswamy (1996) and Dwivedi and Ramaswamy (2010b) also reported similar trends and found that the time for the standard deviations to reach 1 ºC decreased from 20 min in static mode to 5 min in end-over-end and axial modes, in a water-immersion retort. Thus, an increase in agitation due to reciprocation helped in an early stabilization, resulting in more uniform temperatures within the can.

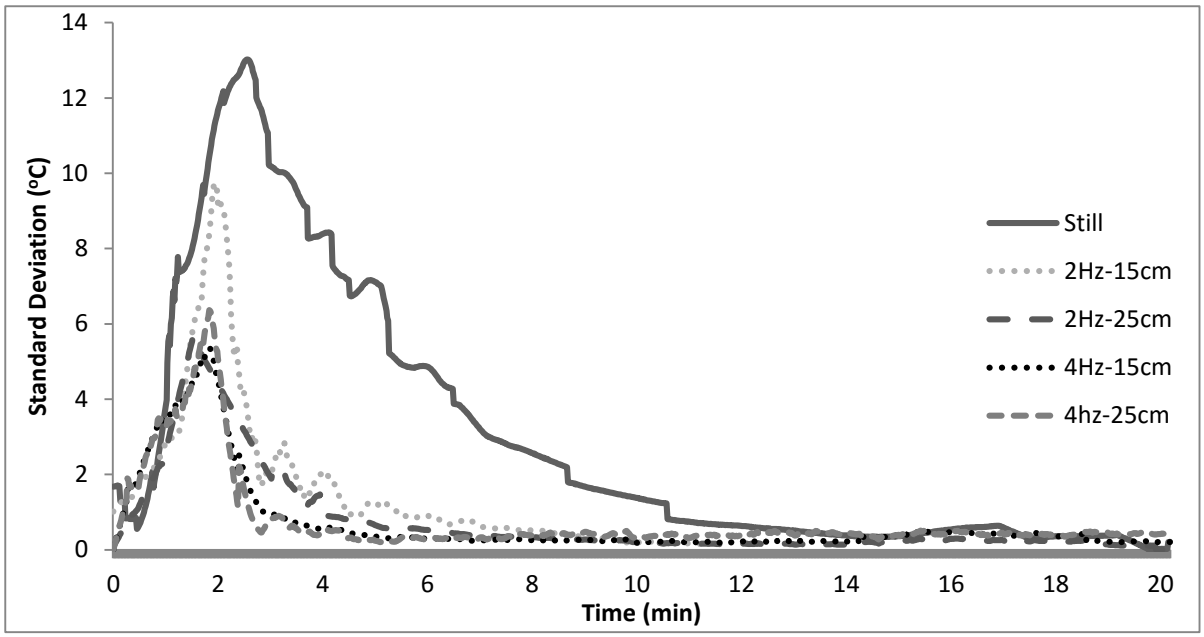

Fig. 3.7. Standard deviations in liquid temperatures of a can processed at 120 °C, as a function of heating time with respect to three thermocouple locations (20 mm; 56 mm; and 85 mm, from the can bottom center) in cans subjected to processing at various reciprocation frequencies and amplitudes.

3.6 Conclusions

The main purpose of this chapter was to modify an existing static retort to facilitate the study of reciprocation agitation thermal processing. It has been demonstrated that the system works well within the range of conditions important for thermal processing applications. The key variables such as frequency and amplitude as well as temperature stability issues have been addressed. Further, the temperature distribution studies inside the retort and in the can revealed that the temperature distribution inside the retort became more uniform due to reciprocation. Also, on increasing the intensity of reciprocation by increasing amplitude or frequency of reciprocation, the temperature uniformity and heat transfer rate improved. The developed retort was suitable to be used to carry out further heat transfer studies on reciprocating agitation thermal processing.

PREFACE TO CHAPTER 4

In Chapter 3, a reciprocating agitation retort was developed and was shown to have better temperature uniformity. Promoters of Shaka® processing have claimed that reciprocating agitation can result in 10-fold reduction in process time leading to better product quality. However, the effect of reciprocating agitations on process time and quality degradation have not been verified independently.

In chapter 4, heat penetration studies were conducted on cans subjected to reciprocating agitation. This study shall be useful in evaluating the effect of operating temperature, reciprocation frequency and reciprocation amplitude on heat penetration parameters, heat transfer coefficient, process time and a quality degradation index. This shall help to understand the effect of reciprocation on the heat transfer phenomenon in food systems.

Parts of this chapter have been presented in the form of a poster presentation at Institute of Food Technologists (IFT) Annual Conference held from June 21-24 in New Orleans, Louisiana.

Parts of this chapter won the first prize in **Charles Stumbo Graduate Student Paper Competition** award and was presented at the Annual Meeting of the Institute for Thermal Processing Specialists (IFTPS) held on Mar 11-14, 2014 in Orlando, Florida.

Parts of this chapter have been published as an original research article: *Modification of a static steam retort for evaluating heat transfer under reciprocation agitation thermal processing*. Journal of Food Engineering, 153, 63-72.

The experimental work and data analysis was carried out by the candidate under the supervision of Dr. H. S. Ramaswamy.

CHAPTER 4

EVALUATION OF HEAT TRANSFER, PROCESS TIME AND QUALITY LOSS DEGRADATION ASSOCIATED WITH RECIPROCATING AGITATION THERMAL PROCESSING

4.1 Abstract

Container agitation during thermal processing results in rapid heat transfer leading to a reduction in process time and improvement in quality of processed food. Reciprocating agitation provides back and forth motion and has the potential to provide rapid container agitation to enhance heat transfer rates. In this chapter, the lab-scale reciprocating retort, developed in previous chapter, was used to characterize the heating behavior of canned particulates during reciprocating agitation. For this, 307x409 cans, filled to a headspace of 10 mm with Nylon particles in a Newtonian fluid (80% glycerin), were processed under various reciprocating conditions at different temperatures. The operating temperature was varied between 110-130^{o}C, while reciprocation frequency was varied between 0-4 Hz and reciprocation amplitude was varied between 5-25 cm. Heat penetration studies on these experimental cans placed in vertical orientation inside the reciprocating cage revealed 52-87 % reduction in the equilibration time of the cold-spot during reciprocating agitation, as compared to still mode of processing. This was due to 50-80 % reduction in the heating rate index of liquid and particle. Consequently, process time, required to achieve lethality of 10 min was reduced from 45 min to 17-24 min. This became possible mainly due to 2-7 times enhancement in the values of heat transfer coefficients. During reciprocation process, the U and h_{fp} values ranged from 232-860 W/m^{2}K and 494-921 W/m^{2}K respectively. The corresponding values during the still mode were 107 W/m^{2}K and 188 W/m^{2}K respectively. The better heating conditions during reciprocation processing, resulted in 26-36 % reduction in quality-deterioration index (cook-value/lethality) and thereby demonstrated the better potential of reciprocating agitation thermal processing in delivering high quality products.

4.2 Introduction

Canned food products heat by conduction, convection or a combination of both. With convection-heating products, the rate of heat penetration can be increased by inducing forced convection through mechanical agitation (Anantheswaran and Rao, 1985b). This invariably results in more uniform temperature distribution and faster heating rates. Thus, agitation can help the

slowest heating point in the can to reach the processing temperature faster, and hence the required lethality can be achieved in a shorter time. Coupled with better temperature uniformity, lower processing times help to ensure lower overall cooking of the food, yielding the potential to produce better quality food products. Agitating these cans can also prevent different ingredients and phases in the food product from separating from each other during thermal processing. These advantages make the use of agitation very desirable during thermal processing.

Clifcorn *et al.* (1950) first suggested the use of agitation in the form of end-over-end rotation to increase heat transfer to canned foods. In EOE (end-over-end) mode of agitation, cans rotate around a circle in a vertical plane. Apart from EOE mode, axial mode of rotation has also been used tremendously, in which cans are moved through a rotating helical coil moving continuously from one to the other end of the retort. The cans must have a headspace for effective agitation. As the can rotates, the headspace bubble moves along the length of the can and brings about agitation of the can's contents. Sablani and Ramaswamy (1996) noted that after a certain speed, when centrifugal and gravitational forces acting on the can were equal, particles inside the can start accumulating at the edge of the can and thus reduce the movement of the headspace within the can. Hence, rotary agitation suffers from the disadvantage that after a certain speed of rotation, the overall heat transfer coefficient (U) and fluid-to-particle heat transfer coefficient (h_{fp}) start decreasing. Biaxial mode of agitation was evaluated by Dwivedi and Ramaswamy (2010a), in which the cans changed the direction of rotation twice during one revolution of the cage. This neutralizes the effect of centrifugal forces by the extra turbulence created due to changing of the direction of motion. Thus some improvement in heat transfer was possible using rotary agitation, although centrifugal forces were a limiting factor.

Rotary agitation has been extensively used in industry and various rotary retorts, like Sterilmatic (FMC Corp., San Jose, CA) etc., have been used industrially to provide in end-over-end or axial modes of agitation. Moreover, with a wide variety of literature available on rotary agitation, they are well established and accepted. However, reciprocating retort, like Shaka® retorts, are relatively new and are still in the development phase. Apart from a few works from the promoters of the Shaka® retorts (Walden and Emanuel, 2010), no independent scientific literature is available to validate the extent of quality improvement and reduction of process time during reciprocating agitation thermal processing.

Hence, the objective of this chapter was to use the lab-scale reciprocating retort, developed in Chapter 3, to investigate the effect of reciprocating agitation on process time reduction, improvement in heat transfer and lowering of quality degradation. This chapter shall attempt to demonstrate the usefulness of reciprocating agitation thermal processing to achieve better quality products.

4.3 Materials and Methods

4.3.1 Simulated Food Heating Model

Instead of using a real food, a simulating food heating model was chosen to conduct thermal studies for the evaluation of a developed reciprocating mechanism. Real foods are difficult to work with especially for performance testing of equipment because of the uncertainties in size, stability, thermo-physical properties etc. With simulated inert particles like Nylon, the fabricated particles could be used repeatedly which is not possible with real foods. Further, a Newtonian fluid was used as the liquid in order to simplify the heat transfer model by removing the changes in viscosity due to the applied stress.

Glycerin (Fisher Scientific, Montreal, PQ) at 80% (v/v) concentration was used as the model fluid to simulate a medium viscosity Newtonian fluid. Nylon spherical particles 19 mm in diameter were used to simulate food particulates as their heating behavior lie in the range of common food materials. As food models, Nylon and glycerin combinations have been used earlier in a number of studies and their thermal properties have been summarized in Table 4.1 (Sablani and Ramaswamy, 1996; Dwivedi and Ramaswamy, 2010b).

Table 4.1. Thermo-physical properties of test materials.

Material	Density (kg/m^3)	Heat capacity (J/kg K)	Thermal conductivity (W/m K)	Thermal diffusivity (m^2/s)
Nylon	1130	2070	0.37	1.5×10^{-7}
Glycerin (80%)	1210	2730	0.33	1.0×10^{-7}

4.3.2 Thermal Processing

The modified reciprocating retort, developed in Chapter 3, was used in this study. Test cans of 307x409 size (Home Canning Co., Montreal, QC) were filled to 10 mm headspace with 80% glycerin solution and Nylon particle. Nylon particle was equipped with the flexible-wire thermocouple by drilling a fine hole reaching the center using a horizontal lathe. Flexible thin-wire thermocouples (wire diameter 0.076 mm, Omega Engineering Corp., Stamford, CT) was then introduced and fixed by a small amount of epoxy glue. The flexible wire were attached to the Nylon particle was inserted inside the can through a C-5.2 stuffing box (Ecklund-Harrison Technologies Inc., Fort Myers, FL).CNS copper-constantan needle-type thermocouples (Ecklund-Harrison Technologies Inc., Fort Myers, FL) were used to measure liquid temperatures. Cans were closed using a manual double seaming machine (Home Canning Co., Montreal, QC). Small fluctuations during temperature collection were normalized using the techniques described in literature (Sablani and Ramaswamy, 1996; Dwivedi and Ramaswamy, 2010b).

The experimental design consisted of different operating temperatures, frequencies and amplitudes. In one set of experiments, a 5-level temperature range between 110 and 130ºC was used with 2 Hz frequency and 15 cm amplitude. Similarly, experiments were conducted at 4 levels of reciprocation frequency from 1-4 Hz at 15 cm amplitude and 120 ºC and at 5 levels of amplitude from 5-25 cm at a constant frequency of 2 Hz and operating temperature of 120 ºC. A separate experiment was carried out under conventional static mode at 120 ºC, by keeping the motor off, for comparing the modified retort with the static retort.

During each experimental run, the reciprocating cage was loaded with duplicate experimental cans at positions B and C (Fig. 3.1b) in vertical orientation and the remaining spaces were filled with dummy cans to provide ballast. The duplicate experimental cans were kept equidistant from the axis of reciprocation on either side of the cage for symmetry. Each experimental run was repeated twice. The crank was pivoted to the desired pivot on the shaft according to the required amplitude. The motor was turned on at the required frequency. Steam was used as the heating medium and was kept on till 30 min or till the lethality reached 10min, whichever was later. Cold water was used as the cooling medium. Reciprocations were imparted until the particle-center temperatures of both experimental cans reached 30 ºC during cooling.

4.3.3 Data Analysis

Heating rate index and Equilibration time: After collection of time-temperature data of the retort, can liquid and particle center, the data was plotted on a semi-logarithmic heat penetration curve. The negative reciprocal of the slope of the straight-line portion of this curve represents the heating rate index, f_h. Heating rate index of the liquid ($f_{h\text{-}l}$) and heating rate index of particle-center ($f_{h\text{-}p}$) were calculated as they are indicative of the heat transfer resistance between heating medium and can liquid, and between the can liquid and particle-center respectively. The rate of heating was also measured using the concept of equilibration time. It was defined as the time required for the cold-spot (particle-center) to reach within 1 ºC of the operating temperature and was used to compare the relative speed with which the cold-spot in the can reached the operating temperature. It was calculated by computing the time required for the heat penetration curve of the particle to touch the x-axis or zero-value.

Heat transfer coefficient: Overall heat transfer coefficient (U) and fluid to particle heat transfer coefficient (h_{fp}) were evaluated according to the methodology detailed in literature (Sablani and Ramaswamy, 1996; Dwivedi and Ramaswamy, 2010a). While U represents the heat transfer occurring at the can-liquid interface, h_{fp} conveys information about the heat transfer at the particle-liquid interface. Knowledge of both U and h_{fp} is imperative to enable a proper understanding of the heat transfer phenomenon.

For this, a predicted particle-center temperature profile was generated from the experimental liquid temperature profile by solving a partial differential equation (Equations 4.1-4.4) for heat flow in a spherical particle immersed in liquid.

$$\frac{\partial T}{\partial t} = \alpha_p\left(\frac{\partial^2 T}{\partial r^2} + \frac{2}{r}\frac{\partial T}{\partial r}\right) \tag{4.1}$$

$$T(r, 0) = 0 \qquad \text{at t=0} \tag{4.2}$$

$$\frac{\partial T(r,t)}{\partial r} = 0 \qquad \text{at r=0} \tag{4.3}$$

$$k_p \frac{\partial T(r,t)}{\partial r} = h_{fp}(T_l - T_{ps}) \qquad \text{at r=a} \tag{4.4}$$

where, T is the temperature of the particle at any position r at any time t, α_p is the thermal diffusivity of the particle, k_p is the thermal conductivity of the particle, T_l and T_{ps} are the

temperature of liquid and particle-surface respectively, and a is the radius of the particle. Thus, knowledge of h_{fp} is required to get the predicted particle-center temperature profile (as h_{fp} is necessary in Equation 4.4). Hence, a value of h_{fp} was first assumed, and predicted F_0 was calculated from the predicted particle-center temperature profile, using Equation (4.5).

$$F_0 = \int_0^{Pt} 10^{\frac{T-\mathrm{T_{ref}}}{z}} dt \tag{4.5}$$

where, T is the temperature of the coldspot, T_{ref} is the reference temperature for microbial destruction (121.1 ^oC), z is z-value for microbial spores (13^oC), and P_t is the process time for which the value of F_o = 10 min. Predicted F_0 was then matched with the actual calculated F_0 at the particle-center based on the experimental particle-center temperature profile. Objective function (difference between predicted and experimental F_0) was minimized through iteration, by sequentially changing the values of h_{fp}. The final h_{fp} for which the predicted and experimental F_0 matches to a preset value of 10 min was used to represent the processing conditions.

Once, the value of h_{fp} and the corresponding predicted particle surface temperatures were known, U was calculated by solving the energy balance equation (Equation 4.6), derived by assuming that the heat transferred across the can wall is equal to the heat absorbed by the particle and can liquid (Sablani and Ramaswamy, 1996):

$$UA_c \int_0^{Pt} (T_R - T_l)\, dt = m_l c_{pl} \int_0^{Pt} dT_l + h_{fp} A_p \int_0^{Pt} (T_l - T_{ps}) dt \tag{4.6}$$

where, A_c and A_p are the surface area of the can and particle respectively, T_R, T_l, and T_{ps} are the temperature of retort, liquid and particle-surface, Pt is the process time for F_o=10 min, and, m_l and c_{pl} are the mass and specific heat capacity of the liquid.

Process time and Cook value: To evaluate the effect of the thermal process on the microbial kill and nutrient destruction, the conventional process lethality (F_o) and cook-value (C_o) were used as indicators (Abbatemarco and Ramaswamy, 1993) and calculated using Equations (4.5) and (4.7) respectively.

$$C_0 = \sum_{t=0}^{Pt} 10^{\frac{T-T_{refn}}{z_n}} \Delta t \qquad (4.7)$$

where, T is the temperature of the coldspot, T_{refn} is the reference temperature for nutrient destruction (100°C), z_n is z-value of a typical nutrient (33 °C), and Pt is the process time for which the value of F_o = 10 min. This process time can be used to compare the effectiveness of reciprocation in reducing the time of processing required. Further, to study the effect of reciprocating container agitation on quality loss, ratio of cook-value to lethality, C_o/F_o, was evaluated. This ratio has been used by researchers (Abbatemarco and Ramaswamy, 1993; Dwivedi, 2008) to measure the degree of cooking and has been used as a quality loss indicator.

4.4 Results and discussions

The heating profile of Nylon particles in glycerin was studied under various reciprocating conditions to achieve a lethality value of 10 min. The analysis of heating behavior is important to understand the effect of the reciprocation on heat transfer. For this, the heat penetration parameters were evaluated for glycerin in presence of a single Nylon particle. Although, there is rarely a real life scenario of a single particle in a can, yet the analysis would be useful in estimating the process times, heat penetration parameters, and the heat transfer coefficients (U and h_{fp}). This approach has been used by other researchers (Ramaswamy, *et al.*, 1993; Sablani and Ramaswamy, 1995; Ramaswamy and Sablani, 1997; Meng and Ramaswamy, 2007a) for predicting heat transfer rates in other modes of agitation, and provides a means of comparison with earlier work. This shall give a thorough insight into the effect of reciprocation on the heat transfer from the heating medium (steam) through the can liquid to the particle and shall help in understanding the phenomenal behavior of heat transfer during reciprocation thermal processing.

4.4.1 Effect of reciprocation on particle equilibration time

Fig. 4.1 shows the linear and semi-logarithmic temperature profiles of the particle-center for static retort at 120 °C, and compares it with other reciprocation frequencies and amplitudes.

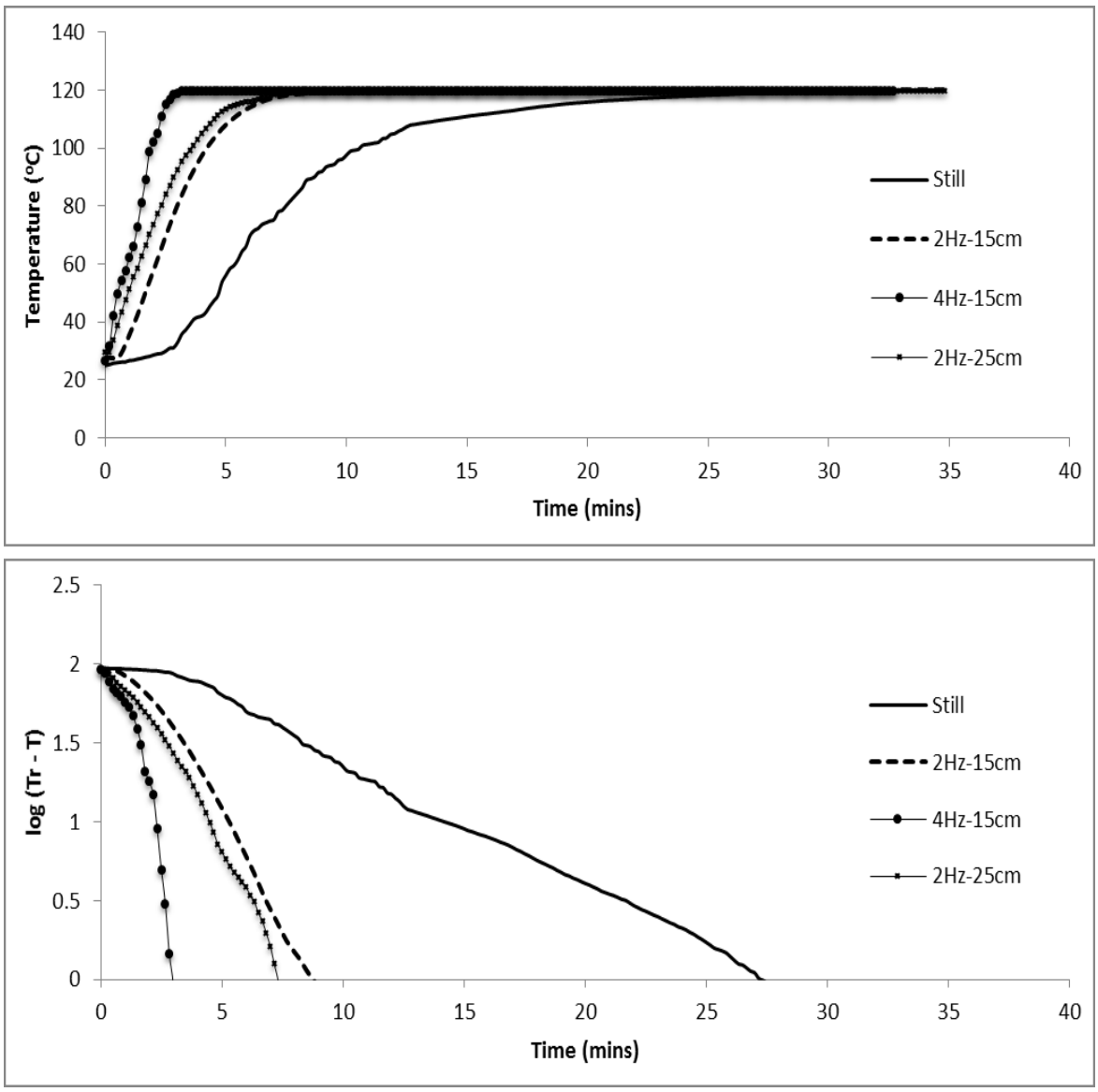

Fig. 4.1. a) Particle center temperature profiles for cans processed at 120 °C under static and various reciprocating conditions; b) semi-logarithmic plot of the particle-center temperature profiles for cans processed at 120 °C under static and various reciprocating conditions.

It is observed from Fig. 4.1a that the particle center temperatures during reciprocation reached the target temperature much earlier than the conventional static conditions. This implies a faster rate of heating during reciprocation. This is because the amount of heat transfer during reciprocation was enhanced to a large extent due to rapid mixing of the liquid and due to increase in the relative velocity between the liquid and the particle (Meng and Ramaswamy, 2005, 2007a). As a result of the high heat transfer condition, the time taken for the particles to reach the operating temperatures was greatly reduced.

In order to compare the time taken to reach operating conditions, Fig. 4.1b is very useful. In addition to the heating rate index (f_h), Fig. 4.1b also shows the equilibration time (when the curve touches the x-axis) for the particle. During the static mode, the time taken was around 27 min. However, when the containers were reciprocated at 2 Hz and 15 cm amplitude, the time taken reduced 3 folds to around 9 min. When the reciprocation frequency was doubled to 4 Hz, this time reduced 3 folds again to around 3.5 min. When the amplitude of reciprocations was increased from 15 to 25 cm, keeping the reciprocation frequency at 2 Hz, the equilibration time decreased from 9 to 7 min. Thus, it was seen that the cold-spot in the cans reached the operating temperatures 3-8 times faster during reciprocation as compared to static operations.

These trends are similar to the works of Walden and Emanuel (2010), who claimed that the heat up times decreased from 50 min in static mode to 2 min at high intensity reciprocation (~100 ms^{-2} reciprocation intensity) for 8% bentonite in aqueous solution. They, however, observed such a high decrease because they calculated the heat-up times to 120 ºC by keeping the retort set-point to 130 ºC. However, in this work the equilibration time was calculated as time to heat up to 1ºC below the retort-set point.

From the published data by Dwivedi and Ramaswamy (2010b), it was found that the equilibration time was around 24 min, 19 min and 15 min at 16 rpm rotations in fixed-axial, end-over-end and biaxial mode of agitation respectively. Thus, on comparison with our results, it is observed that reciprocation agitation was more efficient in decreasing the equilibration time of the particle, as compared to other modes of agitation.

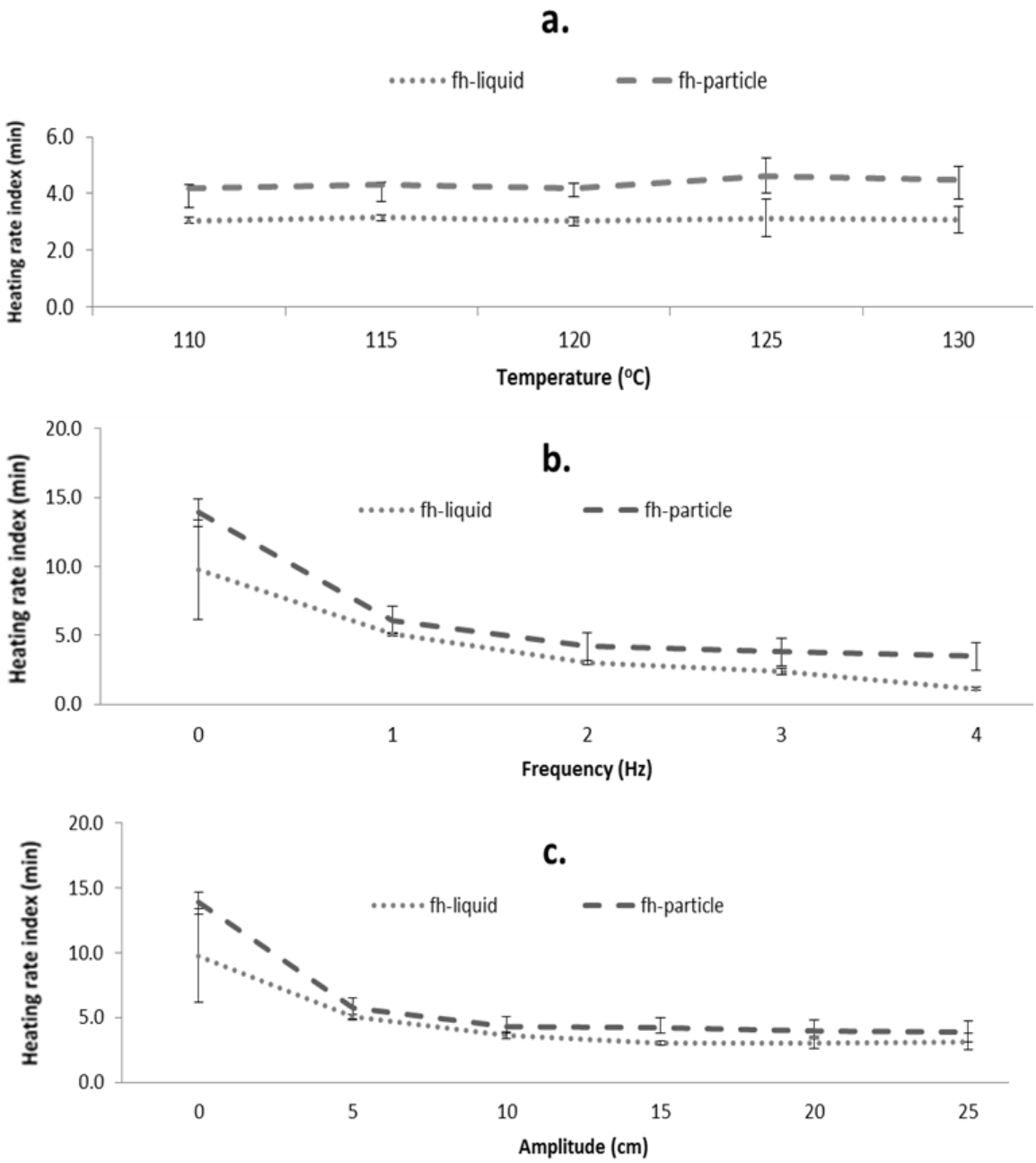

Fig. 4.2. Heating rate index of liquid and particle as affected by: a) operating temperature at 2 Hz frequency and 15 cm amplitude; b) reciprocation frequency at 120 °C operating temperature and 15 cm amplitude; c) reciprocation amplitude at 120 °C operating temperature and 2 Hz frequency.

4.4.2 Effect of reciprocation on the heating rate index

Fig. 4.2 shows the variation of heating rate indices, f_{h-l} and f_{h-p} with temperature, frequency and amplitude. It was observed that there was no appreciable effect of operating temperature on the values of f_{h-p} and f_{h-l}. On increasing the reciprocation frequency and reciprocation amplitude, f_{h-l} decreased. However, the effect of frequency was much more pronounced.

For static mode, f_{h-l} was 9.1 min and it ranged between 5.1-1.1 min for reciprocating agitation. Similar trends were obtained for end-over-end agitation by Sablani and Ramaswamy (1995). Meng and Ramaswamy (2005) reported also similar trends for non-Newtonian fluids in end-over-end mode of rotation.

Fig. 4.2 also shows that the rate of increase in the heat transfer to both the liquid and the particle got slower at higher intensities of reciprocation. Increasing the amplitude from 15-25 cm, did not influence the f_{h-l} much and the values average between 3.0-3.1 min. Ramaswamy and Sablani (1997) explained the inhibition in the increase of heat transfer beyond a certain agitation speed, in a single-particle study by attributing it to the absence of a bulk of particles. A large number of particles would imply higher turbulence due to the increased collisions amongst the particles because of rapid changes in their course of motion on reciprocation.

Similar effects were observed for f_{h-p} and the decrease in f_{h-p} was also not very appreciable after a particular frequency and amplitude. During reciprocation processing, f_{h-p} varied between 3.1-6.5 min while it was around 13.9 min for the static mode. Dwivedi and Ramaswamy (2010b) reported that f_{h-p} varied from 4.2-9.2 min for free axial mode, 6.1-10.9 min for end-over-end mode and 7.2-11.0 min for fixed axial mode.

Thus, on an overall basis, an increase in the intensity of agitation by increasing either the frequency or amplitude of reciprocation led to decrease in the heating rate indices and thereby, indicates larger agitation and presence of higher heat transfer coefficients. Also, this decrease was greater than that observed in other modes of agitation.

4.4.3 Heat transfer coefficients (U and h_{fp})

The amount of heat transfer occurring during the process was calculated by evaluating U and h_{fp}, and they are summarized in Table 4.2. Both U and h_{fp} were found to increase due to reciprocation. During reciprocation process, the U and h_{fp} values ranged from 232-860 W/m^{2}K and 494-921 W/m^{2}K respectively. The corresponding values during the still mode were 107 W/m^{2}K and 188 W/m^{2}K respectively. Thus, reciprocation in general, was found to enhance the heat transfer both at the can-liquid and liquid-particle interfaces.

Other researchers have also obtained similar effects of agitation on the heat transfer coefficients. Ramaswamy and Sablani (1997) reported that U and h_{fp} values varied for a single propylene particle from 118-195 W/m^{2}K and 36-114 W/m^{2}K in oil during end-over-end rotation respectively. Meng and Ramaswamy (2007a) evaluated the value of U for 75-100% glycerin and found them to range between 191-336 W/m^{2}K for end-over-end rotation, while the h_{fp} for the single nylon particle was found to range between 50-75 W/m^{2}K. Dwivedi and Ramaswamy (2010b) reported that for cans filled with 30% (v/v) nylon particles and 80% glycerin, U and h_{fp} values ranged from 345-580 W/m^{2}K and 495-945 W/m^{2}K for biaxial mode of agitation and were highest amongst the three modes of rotary agitation. We found that the U-values during reciprocation were even higher. However, we saw that h_{fp} were comparable to the biaxial mode of agitation. However, our experiments were conducted under a single particle scenario. Increase in the number of particles in actual can shall increase h_{fp} even further, and thus, h_{fp} can also be expected to be highest. Thus, it can be observed that reciprocating agitation leads to better heat transfer situation inside the can than other modes of agitation.

U and h_{fp} increased with an increase in reciprocation frequency and reciprocation amplitude, however, the effect of increase in frequency was more pronounced than the effect of increase in amplitude. U and h_{fp} increased by 150% and 20% on doubling frequency from 2-4 Hz. However, on doubling the amplitude from 10-20 cm, 75% and 7% increase in the values of U & h_{fp} was observed. Thus, an increase in agitation led to increase in the heat transfer depicted by increase in values of U and h_{fp}.

Table 4.2. Heat Transfer Coefficients (U & h_{fp}) as influenced by various operating temperatures, reciprocation frequency and amplitude of reciprocation.

Run no	Temperature (°C)	Frequency (Hz)	Amplitude (cm)	U ($W/m^2 K$)	h_{fp} ($W/m^2 K$)
1	120	Static	Static	107 (±28)	188 (±24)
2	110	2	15	324 (±12)	765 (±19)
3	115	2	15	311 (± 8)	707 (±17)
4	120	1	15	226 (±45)	307 (±59)
5	120	2	5	231 (±35)	493 (±58)
6	120	2	10	307 (±44)	749 (±71)
7	120	2	20	330 (±31)	799 (±63)
8	120	2	25	378 (±37)	776 (±19)
9	120	2	15	325 (±13)	771 (±61)
10	120	3	15	416 (±33)	815 (±84)
11	120	4	15	859 (±49)	921 (±63)
12	125	2	15	321 (±19)	704 (±77)
13	130	2	15	324 (± 36)	737 (±59)

Similar effects have been reported by other researchers (Ramaswamy and Sablani, 1997; Dwivedi and Ramaswamy, 2010b) on increasing agitation in other modes of agitation. They have also reported a greater effect of rotation speed, corresponding to reciprocation frequency, than reel radius, corresponding to amplitude. However, it is evident that the effect of amplitude on U and h_{fp} was certainly higher than the effect of reel-radius in rotary agitation. Sablani and Ramaswamy (1996) had reported only 2-3% increase in value of U and h_{fp} on doubling the reel-radius. However, in our study, the corresponding effect of amplitude was much more prominent.

The operating temperature, however, did not affect the U & h_{fp} values much, although they increased slightly at higher temperatures. The values of U & h_{fp} ranged in between 311-325 W/m^2 K and 704-765 W/m^2K for all experiments at 110-130 °C at a constant agitation of 2Hz-1 5cm. Sablani and Ramaswamy (1995) also reported that the compared with rotation speed and rotation radius, the influence of retort temperature on U was relatively weak, only accounting for 3-6% of

total variability. They attributed to the marginal improvements in the values of U with increase in temperature to the reduction of the liquid viscosity with increase in temperature.

Overall heat transfer coefficient (U) is affected mainly by three factors: the external heat transfer coefficient between the heating medium (steam) and the can wall, the thermal conductivity of the can wall and the internal heat transfer coefficient between the can wall and the can liquid (glycerin). Due to increased reciprocation at higher frequencies and amplitudes, there is increased agitation of both steam and the can liquid. The steam is agitated because of the movement of the cage, while the liquid is agitated because of the movement of the can. Thus, although the thermal conductivity of the can wall remains same, both the external and internal heat transfer coefficients are greatly enhanced. As a result, the overall heat transfer coefficient U is also increased appreciably.

Fluid-to-particle heat transfer coefficient (h_{fp}), on the other hand, is affected mainly by the fluid-particle relative velocity and the number of direction changes in the momentum of the particle. At higher frequency, the number of direction changes and fluid-particle relative velocity are increased. However, at higher amplitudes only the fluid-particle relative velocity is enhanced, as the can has to move a greater distance during the same interval of time, while the number of direction changes remain the same. This may be one of the reasons that the increase of frequency was found to have a larger effect than amplitude. In presence of many particles, the collisions happening within the can shall be an additional factor on which h_{fp} depends.

4.4.4 Process times and cook value

The equilibration time of the particles and process times for 10 min lethality are shown in Fig. 4.3, and the variation of the quality deterioration index (C_o/F_o) with operating conditions are shown in Fig. 4.4. With increase in temperature from 110-130 ºC at 2 Hz frequency and 15 cm amplitude, Fig. 4.3a shows that the equilibration times of the particles increased slightly, as more time was required to reach a higher operating temperature. However, the process times required to reach a lethality of 10 min decreased drastically from 136 min to 11 min. This was because, at higher temperatures, the lethality contribution was much higher, and as a result, the time taken to reach the required lethality was short.

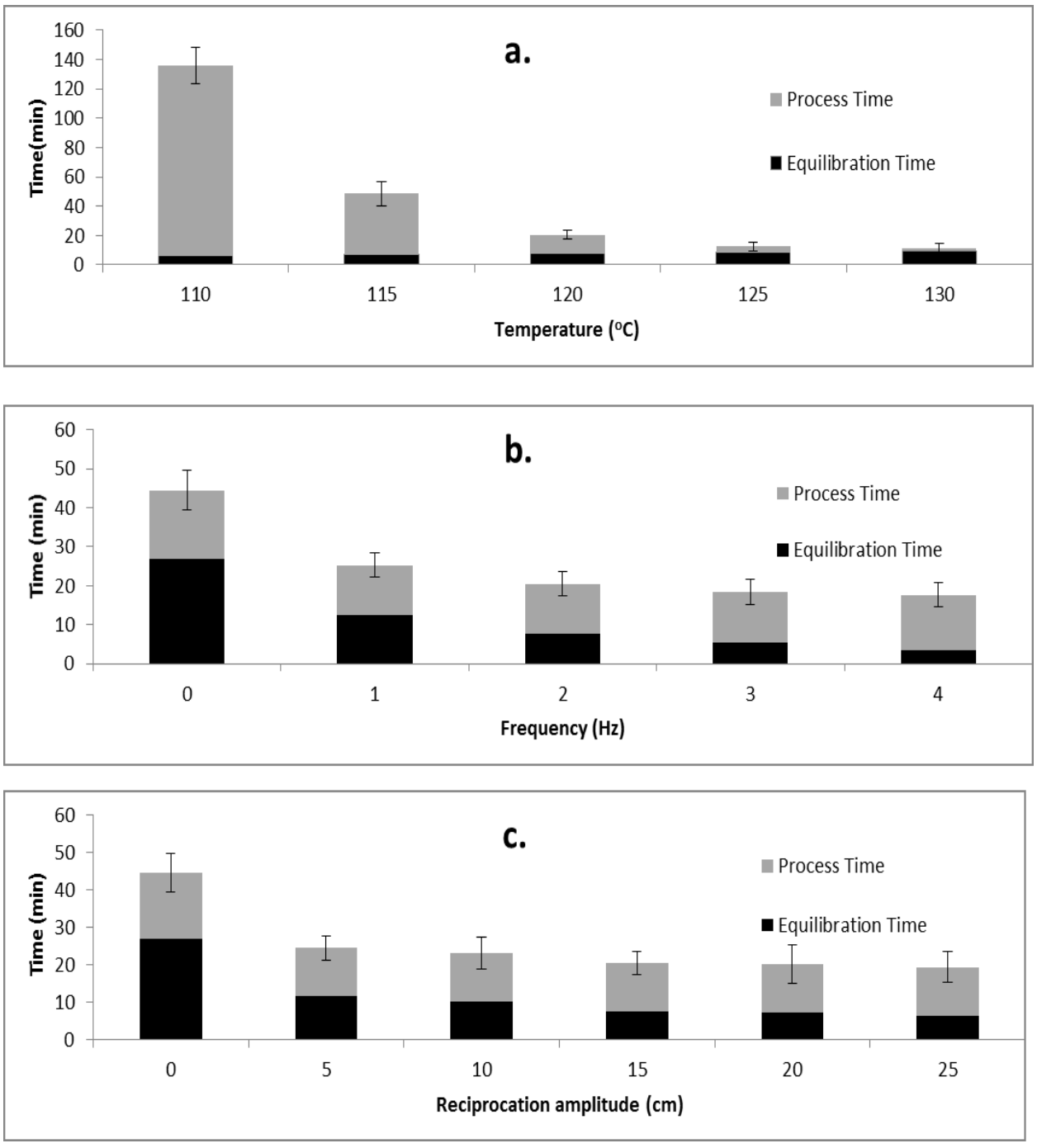

Fig. 4.3. Particle equilibration time and process time required to achieve a lethality of 10 min as affected by: a) operating temperature at 2 Hz frequency and 15 cm amplitude; b) reciprocation frequency at 12 0°C operating temperature and 15 cm amplitude; c) reciprocation amplitude at 120 °C operating temperature and 2 Hz frequency.

This is in accordance with the concepts of HTST treatments, wherein less time is required at a higher temperature to achieve a particular lethality (Anantheswaran and Rao, 1985a). C_o/F_o decreased by 96%, for reciprocation processing, when temperature was changed from 110 to 130 ^oC, as shown in Fig. 4.4a. Dwivedi and Ramaswamy (2010b) also reported a 94% and 82% drop in the value of C_o/F_o for free-axial and end-over-end modes with increase of temperature from 111.6 to 128.4 ^oC. This demonstrates that with the use of high temperatures, lethality can be reached in shorter time, with lower quality losses, and that reciprocation processing is more advantageous than other modes of agitation in achieving this decrease.

The effect of frequency and amplitude on process times are demonstrated in Fig. 4.3b and 4.3c respectively. From Fig. 4.3b, it is clear that at a constant temperature of 120 ^oC, the time required to reach a lethality of 10 min decreased considerably in the case of reciprocation (17-24 min), as compared to the static mode (45 min). This was because of increase in heat transfer occurring due to increased agitation, which led to a decrease in equilibration times, as explained earlier. This led to a decrease in processing times as well.

As compared to the frequency of reciprocation, the reciprocation amplitude had a lower effect on the process times and equilibration times. A doubling of reciprocation amplitude from 10 cm to 20 cm led to only a slight decrease in processing times from 23 min to 20 min, as shown in Fig. 4.3c. It is also observed that the decrease in process times became less severe at higher frequencies and amplitudes due to the presence of only a single particle in can. As explained earlier, if a bulk of particles were present in the can, the process times can be expected to lower further, due to increase of turbulence in the liquid caused by the collision of many particles with each other and with the can wall.

Similar trends were reported by Walden and Emanuel (2010) on the effect of reciprocating agitation on process time. They reported a 20-fold (85 min to 3.5 min) reduction in the process time in static mode as compared to reciprocating agitation (2 Hz frequency and 15 cm amplitude) for achieving a lethality of 6 min. However, their operating temperature during reciprocation was 130 ^oC and during static mode was 121 ^oC. For present study, a similar comparison would lead to the reduction in process time from 45 min (static at 120 ^oC) to 11 min (2 Hz and 15 cm reciprocation at 130 ^oC) for achieving a lethality of 10 min.

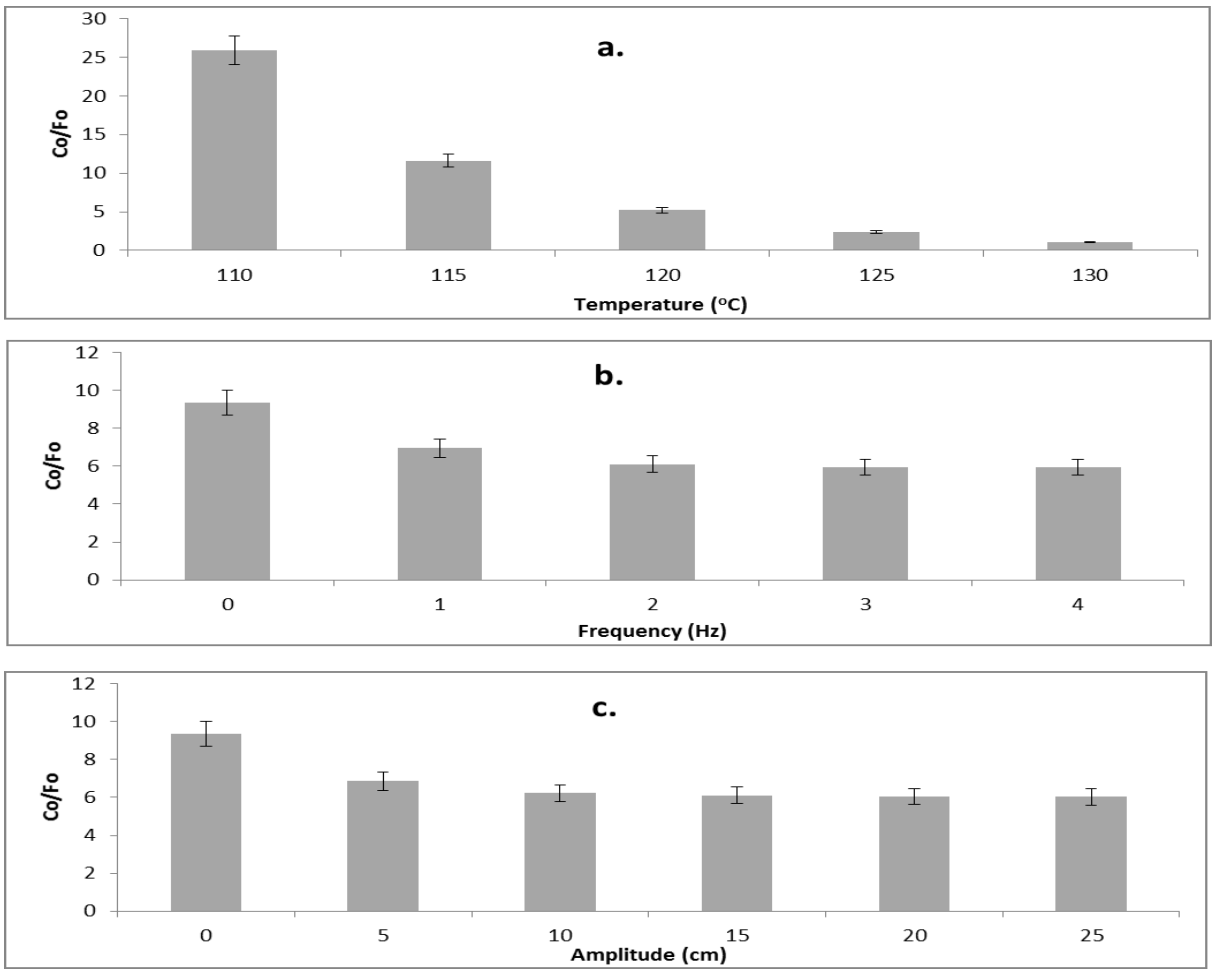

Fig. 4.4: Quality degradation (Co/Fo) as affected by: a) operating temperature at 2 Hz frequency and 15 cm amplitude; b) reciprocation frequency at 120 °C operating temperature and 15 cm amplitude; c) reciprocation amplitude at 120 °C operating temperature and 2 Hz frequency.

.

With regards to quality degradation shown in Fig. 4.4b and 4.4c, quality loss index depicted as C_o/F_o, was lower in case of reciprocation regime, as compared to the static mode. C_o/F_o values were around 9.3 under static mode and decreased to 5.9-6.9 during reciprocation processing. C_o/F_o values were observed to decrease at higher frequencies and amplitudes, thereby suggesting that a higher frequency and amplitude of reciprocation shall result in a lower quality loss and a better quality product. These trends are in agreement with the works of Abbatemarco and Ramaswamy (1993), Ramaswamy *et al.* (1993) and Dwivedi and Ramaswamy (2010b) for other modes of

agitation. Thus, it is seen that reciprocating agitation is effective in providing a process which would deliver lower quality deterioration.

The primary purpose of thermal processing is to achieve the required minimal lethality. Quality is a secondary consideration which has now become the driving force for the industry. The values of C_o/F_o can be used to select the optimal conditions. Thus, a HTST process at 130^{o}C is the most optimum condition for processing. At a particular temperature, the heat transfer can be enhanced by agitation. Since, frequency was the more dominant factor, the scenario of 4Hz-15cm can be considered to be the optimum processing condition at a particular temperature. However, the optimum conditions may depend on additional considerations during processing. For example, at very high frequency, real food products may break or there may be unwanted leaching of nutrients or the energy requirements may be too high etc. Thus, under such scenarios, optimum conditions may vary.

4.5 Conclusions

It was found that reciprocating agitation thermal processing resulted in 3-8 times reduction in the equilibration time of the particle. This was because of the increased heat transfer and lower $f_{h\text{-}p}$ and $f_{h\text{-}l}$ values. Heat transfer coefficients showed 2-7 times improvements in the modified retort as compared to the conventional static retort. Due to these faster heat transfer conditions, process times required to achieve a lethality of 10 min at 120 ^{o}C also reduced by 46-62 % during reciprocating container agitation as compared to static mode of processing. It was also observed that the quality deterioration was 26-36 % lower for reciprocating cans. Thus, overall, it can be concluded that reciprocation thermal processing has tremendous potential to provide high quality safe products due to the rapid heat transfer rates involved during the process.

PREFACE TO CHAPTER 5

In Chapter 4, the effect of reciprocating agitation of containers on the heat transfer phenomenon and process times during thermal processing were demonstrated for vertical orientation. However, during reciprocating agitation thermal processing, containers can be placed in any of the three orientations: along the axis of reciprocation, horizontally perpendicular to axis of reciprocation and vertically perpendicular to axis of reciprocation. The orientation of container with respect to the axis of reciprocation is a critical factor which will affect the amount of heat transfer taking place in the system and needs to be investigated.

Chapter 5 studies the effect of various container orientations on process time, equilibration time and heat transfer coefficients. Subsequently, the optimal orientation configurations for different food mixtures have been considered. This study shall be helpful in understanding the changes in the heat transfer phenomenon on changes in container orientation.

Parts of this chapter have been presented in the form of a poster presentation at 17th World Congress of Food Technology & Expo, IUFOST-2014 held on August 17-21, 2014 in Montreal, Quebec.

Parts of this chapter have been published as an original research article: *Effect of can orientation on heat transfer coefficients associated with liquid particulate mixtures during reciprocation agitation thermal processing*. Food and Bioprocess Technology, 8(7), 1405-1410.

The experimental work and data analysis was carried out by the candidate under the supervision of Dr. H. S. Ramaswamy.

CHAPTER 5

EFFECT OF CAN ORIENTATION DURING RECIPROCATING AGITATION THERMAL PROCESSING

5.1 Abstract

The objective of this chapter was to study the effect of container orientation on heat transfer during reciprocation agitation thermal processing of cans filled with liquid particulate mixtures. Cans of size 307x409, filled with 30 % (v/v) Nylon particles in a Newtonian fluid (100 % glycerin), were placed inside the reciprocating cage of the lab-scale reciprocating retort developed in Chapter 3, with longer axis in one of the three possible orientations viz. horizontal along axis of reciprocation (HA), horizontal perpendicular to axis of reciprocation (HP), or vertical (V). Reciprocation frequency (1-4 Hz) and amplitude (5-25 cm), and container headspace (2-12 mm) were varied according to a full-factorial experimental design, and heat transfer coefficients and process times associated with each orientation were calculated. Additional experiments were also carried out in still mode to study the effect of container orientation in static processing mode. Results showed that for the static mode, horizontal orientations (HA & HP) provided more rapid heating than vertical (V). For agitation processing, HA provided more rapid heat transfer followed by HP and then V, respectively. Reciprocation frequency and amplitude affected the heat transfer significantly ($p < 0.05$) in all orientations, while headspace was significant only for HA. A reciprocation intensity (RI) parameter was defined based on reciprocation frequency and amplitude. A RI value of 30 ms^{-2} was found sufficient for HA cans, while HP and V cans required a higher RI of 60 ms^{-2} for maximum heat transfer. This study could be used in designing of reciprocation thermal processes with optimal heat transfer delivery.

5.2 Introduction

Rapidly changing consumer demand and stiff competition in thermal processing industry has given impetus to the development of retorts and thermal processes which can deliver short sterilization time and maximum quality retention (Ramaswamy and Dwivedi, 2011). Rotary agitation during thermal processing has been found effective in producing turbulence inside the can through forced convection currents generated due to rotary motion. This reduces the process time by shortening the time required for cold spot to reach the operating temperature (Stoforos and

Merson, 1990). Researchers have developed various modes of rotation such as end over end (cans placed with longer axis along the plane of rotation) which is common in batch agitation retorts, fixed axial (cans are locked in with longer axis perpendicular to the plane of rotation), and biaxial rotation (cans changing the direction of rotation twice by rolling on edge of the rotating chamber with its longer axis perpendicular to the plane of rotation) (Dwivedi and Ramaswamy, 2010a). The biaxial rotation is common in continuous processing of cans in turbo cookers. Rotary agitation induces centrifugal force and at high rotation speeds due to which can contents tend to clump against the container wall and agitation efficiency is severely reduced (Hassan *et al.*, 2012). Recently, reciprocation agitation (agitation in form of rapid back and forth motion of containers) has been proposed as an effective way to increase the intensity of heat transfer for reducing process time and improving quality retention (Walden and Emanuel, 2010). However, no major work has been carried out evaluating this mode of agitation.

Can orientation has been found to be an important parameter in studies in still mode of agitation as the heat transfer phenomenon is different in vertical and horizontal cans due to differences in aspect ratio (Kannan and Sandaka, 2008; Boz and Erdogdu, 2013). Ghani *et al.* (2003) and Farid and Ghani (2004) found higher heat transfer rate in vertical cans and attributed it to the enhancement of natural convection due to longer height. On the other hand, Dhayal *et al.* (2013) recently found opposing trends in the horizontal cans depicted a better heat transfer rate than vertical cans for sterilization of canned milk using CFD simulation and experimental validation. However, these studies were conducted only with liquid foods. Recently, Dimou *et al.* (2014) studied the effect of particle orientation (peach halves) in non-agitated liquid-particulate cans placed horizontally and vertically and found the horizontal cans to exhibit faster heating rate, a trend opposite to that of previous literature. Thus, the effect of orientation in static mode also needs further investigation. Even during rotary agitation, where the concept of can orientation is irrelevant, placement of cans in different ways gives rise to different modes of rotary agitation viz. end-over-end, fixed axial or free axial mode of agitation. Heat transfer phenomenon has also been found very different in these three modes of agitation (Dwivedi and Ramaswamy, 2010b) with biaxial agitation giving the highest rate of heat transfer. Hence, the investigation of container orientation is very important for heat transfer studies on any new mode of agitation like reciprocating agitation.

For reciprocating agitation, cans can be placed in one of the three ways. If the reciprocation agitation is transmitted horizontally, horizontal cans can be placed with their longer axis either along axis of reciprocation (HA) or perpendicular to axis of reciprocation (HP). In addition to HA and HP orientations, cans can also be placed vertically (V). Similarly, if reciprocation is transmitted vertically, horizontal orientation (H), vertical orientation along axis of reciprocation (VA) and perpendicular to axis of reciprocation (VP) form the three orientations.

In this chapter, the horizontal reciprocating mechanism, developed in Chapter 3, was used to study the effect of container orientation (V, HA or HP) on extent of heat transfer taking place during thermal processing of liquid-particulate mixtures. Frequency and amplitude of reciprocations, and can headspace were varied to calculate U and h_{fp} during these three orientations. Optimum agitation conditions were reported for each orientation.

5.3 Materials and Methods

5.3.1 Reciprocating Agitation Retort

The lab-scale reciprocating agitation retort, developed in Chapter 3, by retrofitting an existing vertical still steam retort (Loveless Manufacturing Co., Tulsa, OK) to include a reciprocating cage capable of moving back and forth on horizontal rails, was used in this study. Experimental cans could be placed inside the reciprocating cage in three orientations (Fig. 5.1) viz. i) vertically (V), ii) horizontally perpendicular to axis of reciprocation (HP), or iii) horizontally along axis of reciprocation (HA). Further details about the development and specifications of this retort are available in Section 3.2.

5.3.2 Experimental setup

Real foods have considerable variability in size, stability and thermo-physical properties, and are difficult to work with when evaluating associated heat transfer coefficients. Since, the objective of our study was to compare different orientations in terms of heat transfer (not quality), inert materials with uniform thermo-physical properties and heating characteristics similar to foods provide a better alternative.

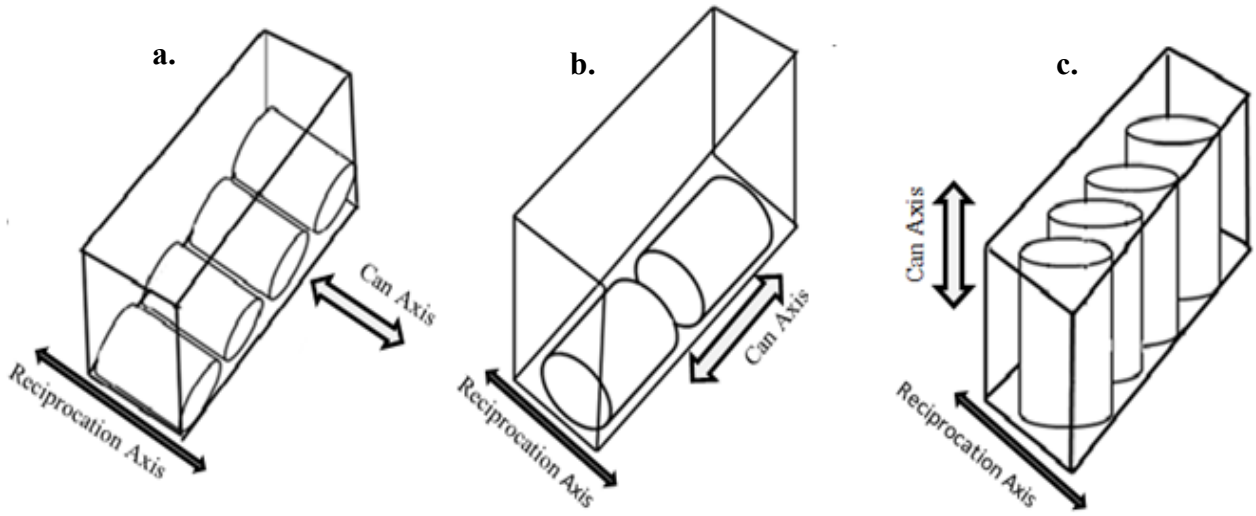

Fig. 5.1. Schematic of the three possible orientations inside the reciprocating cage showing the placement of experimental can with its longer axis: a) horizontally along the reciprocation axis (HA); b) horizontally perpendicular to reciprocation axis (HP); c) vertical (V).

Nylon spheres (Small Parts Inc., Miami, FL) of 19 mm diameter were used as food simulating particles and pure glycerin (Fisher Scientific, Montreal, PQ) was used as a model fluid with Newtonian flow characteristics. Nylon and glycerin have been used as food simulator models in a number of earlier studies on thermal processing (Sablani and Ramaswamy, 1996, 1999; Ramaswamy *et al.*, 1993; Meng and Ramaswamy, 2007a; Dwivedi and Ramaswamy, 2010b; Ramaswamy and Dwivedi, 2011, Hassan *et al.*, 2012) because their thermo-physical properties lie in the range common to foods. The thermo-physical property values were obtained from Ramaswamy and Dwivedi (2011) and are detailed in Table 5.1.

Metal cans of size 307x409 (Home Canning Co., Montreal, QC) were filled with 30% v/v Nylon particles and glycerin to the required headspace and sealed using a manual double seaming machine (Home Canning Co., Montreal, QC). Flexible thin-wire thermocouples (wire diameter 0.0762 mm, Omega Engineering Corp., Stamford, CT) were used to measure center temperature of three Nylon spheres in each can by inserting them to the particle center through a drilled hole and sealing it with a small amount of epoxy glue, while CNS copper-constantan needle-type thermocouples (diameter 1.6 mm, Ecklund-Harrison Technologies Inc., Fort Myers, FL) placed at

the geometric center of the can were used to measure liquid temperatures. All particles (including thermocouple-equipped ones) were free to move throughout the container. Temperature outputs were recorded at one second intervals using a data acquisition system (HP34970A, Hewlett, Packard, Loveland, CO). Particle assembly, can preparation and data gathering are described in further details in literature (Meng and Ramaswamy, 2007a; Ramaswamy and Dwivedi, 2011).

Table 5.1. Thermo-physical properties of test materials.

Material	Density (kg/m^3)	Heat capacity (J/kg K)	Thermal conductivity (W/m K)	Thermal diffusivity (m^2/s)
Nylon	1130	2070	0.37	1.5×10^{-7}
Glycerin (100%)	1260	2430	0.28	0.9×10^{-7}

5.3.3 Thermal Processing

Thermal processing of prepared cans was done according to two full factorial designs. In the first design, 5 levels of frequency (0, 1, 2, 3, 4 Hz) and 3 levels of amplitude (5, 15, 25 cm) were selected, and in the second design, 3 levels of frequency (0, 2, 4 Hz) and 3 levels of headspace (2, 7, 12 mm) were selected to study the effect of reciprocation frequency, amplitude and can headspace. All experimental runs were repeated for each orientation (HA, HP and V). Headspace was fixed at 12 mm in the former design and amplitude of reciprocation was fixed at 15 cm in the latter. It is to be noted that 0 Hz frequency signifies the non-agitated/still mode of processing. Although, HA and HP orientations are essentially same (both signify horizontal can) for still mode, yet, experiments were conducted for each of the three orientation. Also, amplitude is ambiguous in absence of reciprocation at 0 Hz; yet, separate experiments were conducted to satisfy the design requirements. All experimental runs were repeated twice.

In each experimental run, two identical test cans were placed inside reciprocating cage equidistant from axis of reciprocation, in the required orientation. Two additional dummy cans containing water were placed for filling the remaining space in the cage to provide ballast. Retort was then closed, crank was attached to desired pivot for the required amplitude, frequency of reciprocation was set at desired level, set-point for operating temperature in the PID controller was adjusted to 121.1°C, and steam was turned on. Frequency of reciprocation was continuously

monitored throughout the experiment using a hand-held non-contact photo tachometer. After 40 min, steam was turned off and water was turned on for cooling. Temperatures were collected till all temperatures reached below 30^{o}C.

5.3.4 Data Analysis

The time-temperature data (Fig. 5.2a) till steam off was considered for analysis. Average retort temperature during cook period (excluding come-up period) was taken as the average operating temperature (T_{crt}). Logarithmic of temperature difference with average operating temperature (T_{crt}-T) was plotted against time to generate a semi-logarithmic heat penetration curve, as shown in Fig. 5.2b. Heating rate index of liquid ($f_{h\text{-}l}$) and particle-center ($f_{h\text{-}p}$) were calculated as negative reciprocal of slope of straight-line portion of respective curves (Fig. 5.2b). Particle with highest heating rate index ($f_{h\text{-}p}$) was considered to be represent cold-spot conditions and was used to further analysis. Equilibration time of cold-spot (EQT) was estimated from the x-intercept of straight line portion of heat penetration curve of particle-center (Fig. 5.2b) as the time taken for the particle to reach a temperature one degree below the retort temperature.

The values of $f_{h\text{-}l}$ and $f_{h\text{-}p}$ were used to compute the overall heat transfer coefficient (U) and the fluid-to-particle heat transfer coefficient (h_{fp}) using a new methodology. In this methodology, values of h_{fp} were estimated by fitting the predicted temperature profile of cold-spot (particle-center) under constant retort temperature conditions for Fourier number greater than 0.2 with simulated temperature profile of cold spot obtained from a finite difference simulation. Predicted temperature profile of liquid ($T_{pred\text{-}l}$) and particle-center ($T_{pred\text{-}p}$) was generated using Equation (5.1) from heating rate index (f_h) of liquid and particles respectively under constant retort operating conditions.

$$\begin{aligned} T_{pred} &= T_{crt} - (T_{crt} - T_i) * 10^{\left(-\frac{t-t_0}{f_h}\right)} && \forall\, \tau > 0.2 \\ &= T_i && \forall\, \tau < 0.2 \end{aligned} \tag{5.1}$$

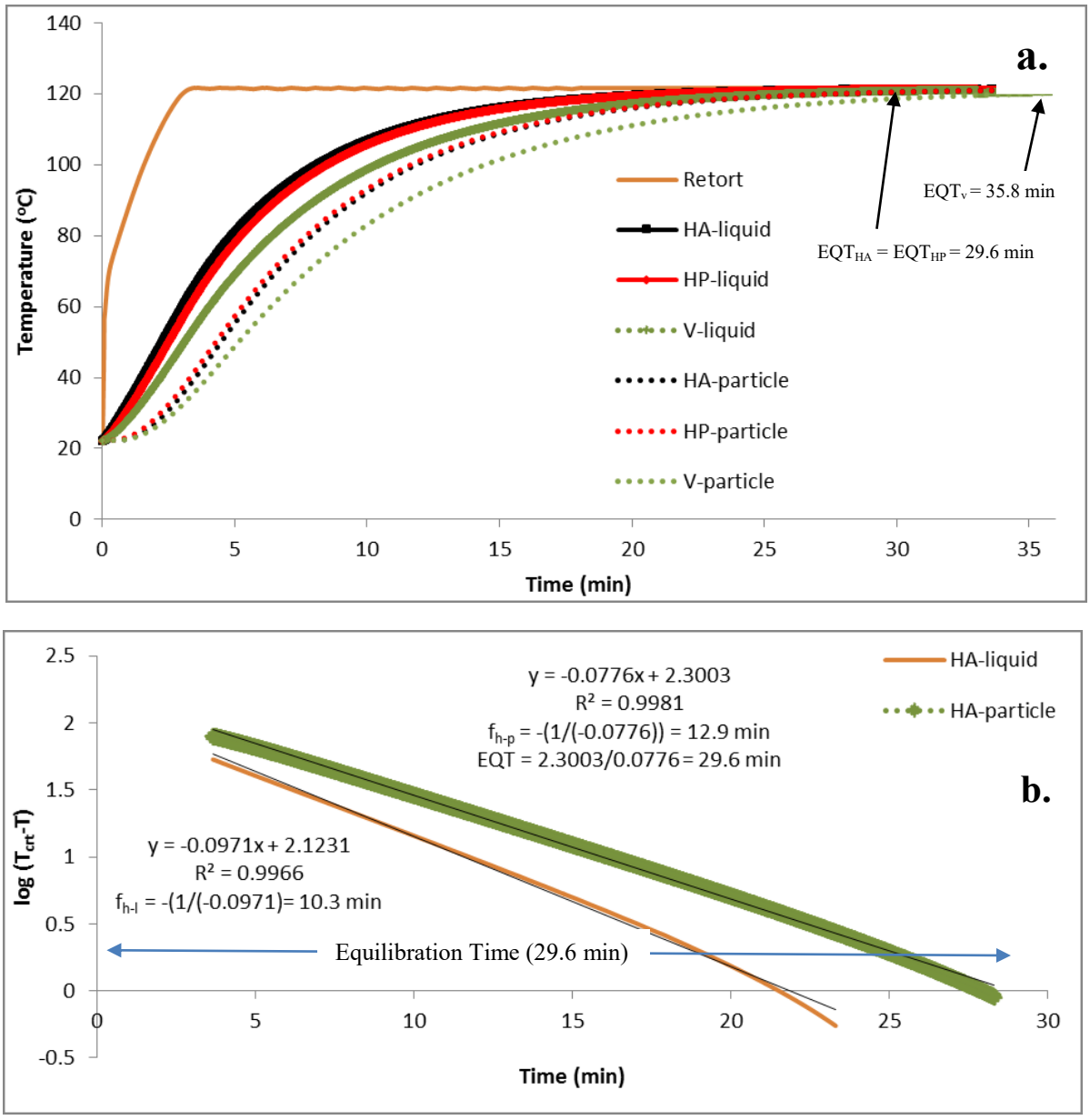

Fig. 5.2. a) Retort, liquid and particle-center temperature profiles for experimental cans with 12 mm headspace and processed under still mode in one of the three orientations i.e. horizontally along the reciprocation axis (HA), horizontally perpendicular to axis of reciprocation (HP), or vertically (V). b) Semi-logarithmic plot showing the equilibration time (EQT) and heating rate indices of liquid and particle (f_{h-l} and f_{h-p}) for experimental cans with 12 mm headspace and processed in HA orientation.

Equation (5.1) is the simplified form of the one-term approximation solution of a transient heat conduction problem and is valid for Fourier number $\tau > 0.2$. Simulated temperature profile of particle-center was generated from predicted liquid profile ($T_{pred\text{-}l}$) using a finite difference simulation of the unsteady state heat conduction problem (Equation 5.2) of a spherical particle immersed in liquid with prescribed initial (Equation 5.3) and symmetrical boundary conditions (Equations 5.4 and 5.5).

$$\frac{\partial T}{\partial t} = \alpha_p\left(\frac{\partial^2 T}{\partial r^2} + \frac{2}{r}\frac{\partial T}{\partial r}\right) \tag{5.2}$$

$$T(r, 0) = 0 \qquad \text{at } t=0 \tag{5.3}$$

$$\frac{\partial T(r,t)}{\partial r} = 0 \qquad \text{at } r=0 \tag{5.4}$$

$$k_p \frac{\partial T(r,t)}{\partial r} = h_{fp}(T_{pred-l} - T_{ps}) \qquad \text{at } r=a \tag{5.5}$$

where, T_{pred} is the predicted temperature of liquid/particle in ^oC, T_{crt} is the average operating temperature in ^oC, T_i is the initial temperature of liquid/particle in ^oC, t is the time in s, t_o is the time at which fourier number $\tau = 0.2$ in s, f_h is the corresponding heating rate index of liquid/particle in s, T is the temperature in ^oC, α_p is the thermal diffusivity of particle in m^2/s, r is the distance from center in m, a is the radius of particle in m, k_p is the thermal conductivity of particle in W/mK, h_{fp} is the fluid-to-particle heat transfer coefficient in W/m^2K, $T_{pred\text{-}l}$ is the predicted liquid temperature in ^oC, and T_{ps} is the particle surface temperature estimated using the finite difference simulation, in ^oC.

For fitting predicted and simulated profiles, an initial guess of h_{fp} was assumed and then difference between the F_0 values (Equation 5.6) of predicted and simulated cold spot (particle-center) temperature profiles were minimized by sequentially changing the value of h_{fp} such that both matched a preset value of 10 min using least accumulated lethality difference (LALD) approach. LALD approach was earlier proposed by Weng *et al.* (1992) for matching time-temperature profiles for predicting h_{fp} and was found more relevant to be used in thermal processing scenarios than least squared temperature difference (LSTD) approach due to higher contribution of higher temperatures towards lethality (Sablani and Ramaswamy, 1996). U was then calculated using energy balance equation derived by assuming that heat transferred across the can wall is equal to heat absorbed by particle and can liquid (Equation 5.7). Although, Equation (5.7) assumes uniform liquid temperatures, it was seen that during liquid temperatures at various

locations inside the can attained uniformity very fast under reciprocating agitation. This equation has also been used by several researchers (Stoforos and Merson, 1991; Sablani and Ramaswamy, 1996; Dwivedi and Ramaswamy, 2010b) in other modes of agitation.

$$F_0 = \int_0^{pt} 10^{\frac{T-121.1}{z}} dt \tag{5.6}$$

$$UA_c \int_0^{pt} (T_{crt} - T_{pred-l})\, dt = m_l\, c_{pl} \int_0^{pt} dT_{pred-l} + h_{fp} A_p \int_{t=0}^{pt} (T_{pred-l} - T_{ps}) dt \tag{5.7}$$

where, F_o is the lethality in s, T is the temperature in ^oC, z is the z-value of microorganism (=10 ^oC), pt is the process time in s, A_c and A_p are the area of can and particle respectively in m^2, m_l and c_{pl} are the mass of liquid in kg and specific heat of liquid in J/(kgK), T_{crt} is the average operating temperature in ^oC, t is the time in s, U and h_{fp} are the overall and fluid-to-particle heat transfer coefficient respectively in W/m^2K, T_{pred-l} is the predicted liquid temperature in ^oC, and T_{ps} is the particle surface temperature in ^oC.

Mean values of parameters from four readings (two replicates of each experiment containing two duplicate cans each) of each experimental run were taken. Students' T-test was conducted to determine if sets of data for each orientation were significantly different from each other. Regression analysis and analysis of variance (ANOVA) were carried out using Design Expert v 6.1 (Stat-Ease Inc, Minneapolis, Minnesota, USA).

5.4 Results and Discussion

5.4.1 Effect of can-orientation on heat transfer in absence of agitation

Fig. 5.2a shows that the temperature rise in liquid and particle-center was almost similar for both horizontal orientations (HA and HP) during still mode of processing. This is because HA and HP orientations are essentially same in absence of agitation as cans are placed perpendicular to the flow of steam in both cases. It was also seen that temperature rise in horizontal cans (HA and HP) was faster than vertical can (V). Vertical orientation was thus seen to have the slowest rate of heat transfer which was also evident from lowest values of U and h_{fp} (Table 5.2). This is similar to the experimental trends of Dhayal *et al.* (2013). However, Ghani *et al.* (2003) reported that heat transfer was faster in vertical orientation using computer fluid dynamics (CFD)

based numerical simulation of still mode. Their CFD analysis was based on the assumption that the can reached operating temperature instantly, however this is not the case in reality and considerable heat transfer occurs during come-up time of retort.

Table 5.2. Values of heat transfer coefficients at various reciprocation frequencies and amplitudes.

Reciprocation Frequency (Hz)	Reciprocation Amplitude (cm)	U_{HA} [a] (W/m^2K)	$h_{fp\text{-}HA}$ [a] (W/m^2K)	U_{HP} [b] (W/m^2K)	$h_{fp\text{-}HP}$ [b] (W/m^2K)	U_V [c] (W/m^2K)	$h_{fp\text{-}V}$ [c] (W/m^2K)
0	0	137±1	235±18	135±7	239±13	106±2	193±16
1	5	290±2	352±13	201±2	329±22	158±6	289±23
	15	395±5	486±21	221±5	426±35	183±10	345±15
	25	471±9	69±46	311±16	522±47	287±8	453±35
2	5	523±5	640±42	197±30	567±39	222±3	506±36
	15	709±8	995±70	350±12	722±56	328±8	770±90
	25	793±9	1090±73	416±8	866±91	402±5	825±59
3	5	776±9	913±22	380±16	821±71	361±32	729±76
	15	898±4	1210±88	513±43	906±34	476±12	890±32
	25	937±14	1340±64	680±30	980±61	658±28	981±57
4	5	877±22	1140±36	706±15	916±50	691±19	895±63
	15	957±36	1370±54	784±13	1020±30	791±1	993±59
	25	987±12	1390±67	852±7	989±87	833±20	1040±24

[a] mean±s.d. for horizontal cans placed along the axis of reciprocation

[b] mean±s.d. for horizontal cans placed perpendicular to the axis of reciprocation

[c] mean±s.d. for cans placed vertically

During the come-up of retort, flow of steam was from bottom to top and thus, heat transfer from can-bottom was more dominating. As bottom film is thicker, it is more turbulent and moves with a higher velocity, giving a higher heat transfer coefficient (Sun *et al.*, 1994). Also, area of cross-section of bottom of the horizontal can is larger leading to better heat transfer. Even during cook period (come-up), a positive flow is generally maintained within the retort leading to disparity in heat transfer capabilities of steam between the top and bottom of can, contrary to the assumption of uniform temperature distribution in a CFD analysis. Jet of steam coming from bottom comes in direct contact with smaller area at base of a vertical can, before getting dispersed by its edges;

while the steam makes contact with longer axis of horizontal can and gets dispersed more smoothly due to its curved bottom surface, resulting in better heat transfer at the wall (higher U).

Under still mode of processing, the prevalent mode of heat transfer is generally natural convection. For natural convection, Rayleigh number (Ra) and Grashoff number (Gr) are the prominent parameters which govern the intensity of heat transfer and amount of turbulence in buoyancy driven flow. An analysis of these numbers will be helpful in further explaining the trends observed in this study (Farid and Ghani, 2004). Since, heat transfer is more dominant from bottom surface; our case can be considered similar to that of convective heat transfer from a horizontal surface (Incropera and DeWitt, 2000). In such a case, radius of can may be used as the characteristic dimension for vertical cans and half of the height of can may be considered as the characteristic dimension for horizontal cans (Farid and Ghani, 2004). Using same parameters in our case, the characteristic length for Ra and Gr calculation would be 44 and 58 mm for vertical and horizontal cans respectively. Thus, due to higher characteristic length, Ra and Gr are higher for horizontal cans (HA and HP) as compared to vertical can (V). This suggests that flow in horizontal cans would be more turbulent leading to a better heat transfer at the liquid particle interface (higher h_{fp}).

The headspace bubble played a critical role in heat transfer during the non-agitated mode of processing. Student's t-test showed that there was significant difference ($p<0.05$) between heat transfer coefficients (Table 5.3) at 2 and 7 mm headspace for both horizontal and vertical cans and presence of headspace resulted in better heat transfer condition. It is generally expected that headspace might act as an insulator in natural convection scenarios (Mohammed, 2007). However, Ramaswamy and Grabowski (1996) noted that the complex nature of heat transfer in headspace makes theoretical prediction difficult. Heat transfer in headspace should be expected to be governed by evaporation resulting in significant mass transfer effects. This should even result in a more rapid heating of the water surface inside the can right below the headspace compared to the no headspace situation. Joseph *et al.* (1996) reported faster heating rates with an increase in the headspace volume in canned conduction-heated materials which is in accordance with the observations in this study. James *et al.* (2006) also reported rapid heating effect in cans with 10% headspace compared to no headspace situation during off-axial rotation of cans. Erdogdu and Tutar (2011), through their CFD analysis, observed that headspace temperature increased rapidly due to

lower heat capacity and viscosity of air as a result of natural convection heating, and heating rates were faster compared to the situation where there was no headspace. On the other hand, values of U and h_{fp} were not significantly different ($p<0.05$) between 7 and 12 mm headspace for both vertical and horizontal cans, which can be explained by the fact that above a sufficient headspace, the headspace bubble started acting as an insulator (Ramaswamy and Grabowski, 1996; Mohammed, 2007).

Table 5.3. Values of heat transfer coefficients at various headspaces and reciprocating frequency.

Reciprocation Frequency (Hz)	Headspace (mm)	U_{HA} [a] (W/m^2K)	$h_{fp\text{-}HA}$ [a] (W/m^2K)	U_{HP} [b] (W/m^2K)	$h_{fp\text{-}HP}$ [b] (W/m^2K)	U_V [c] (W/m^2K)	$h_{fp\text{-}V}$ [c] (W/m^2K)
0	2	119±4	178±12	117±8	210±23	81±2	162±35
	7	110±3	221±46	137±5	241±35	105±5	214±21
	12	137±1	235±18	135±7	239±13	106±2	193±16
2	2	673±7	750±38	307±11	771±54	287±46	759±28
	7	718±4	930±53	317±38	790±31	274±27	798±34
	12	709±8	994±70	350±12	722±56	328±8	770±90
4	2	908±8	999±76	760±75	982±99	764±11	875±91
	7	943±34	1310±77	774±37	1130±97	803±26	881±18
	12	957±36	1370±54	784±13	1020±30	791±1	993±59

[a] mean±s.d. for horizontal cans placed along the axis of reciprocation
[a] mean±s.d. for horizontal cans placed perpendicular to the axis of reciprocation
[a] mean±s.d. for horizontal cans placed vertically

5.4.2 Effect of can-orientation on heat transfer during reciprocating agitation

Fig. 5.3 shows the temperature rise of liquid and particle-center for the three orientations (V, HA and HP) at 2 Hz-15 cm reciprocation. It is seen that forced convection produced through reciprocating motion of cans resulted in faster heat transfer than still mode. This is because in still mode, there is little relative motion of liquids and particles (Deniston *et al.*, 1987) and on agitation, relative motion is increased. As a result, heat transfer inside the can was enhanced resulting in higher liquid and particle-center (cold spot) temperatures as compared to non-agitated processing (Fig. 5.2a). Thus, all orientations of reciprocating thermal processing were found to produce way

faster rate of heating than natural convection. The temperature rise was fastest in HA cans, followed by HP and V cans respectively.

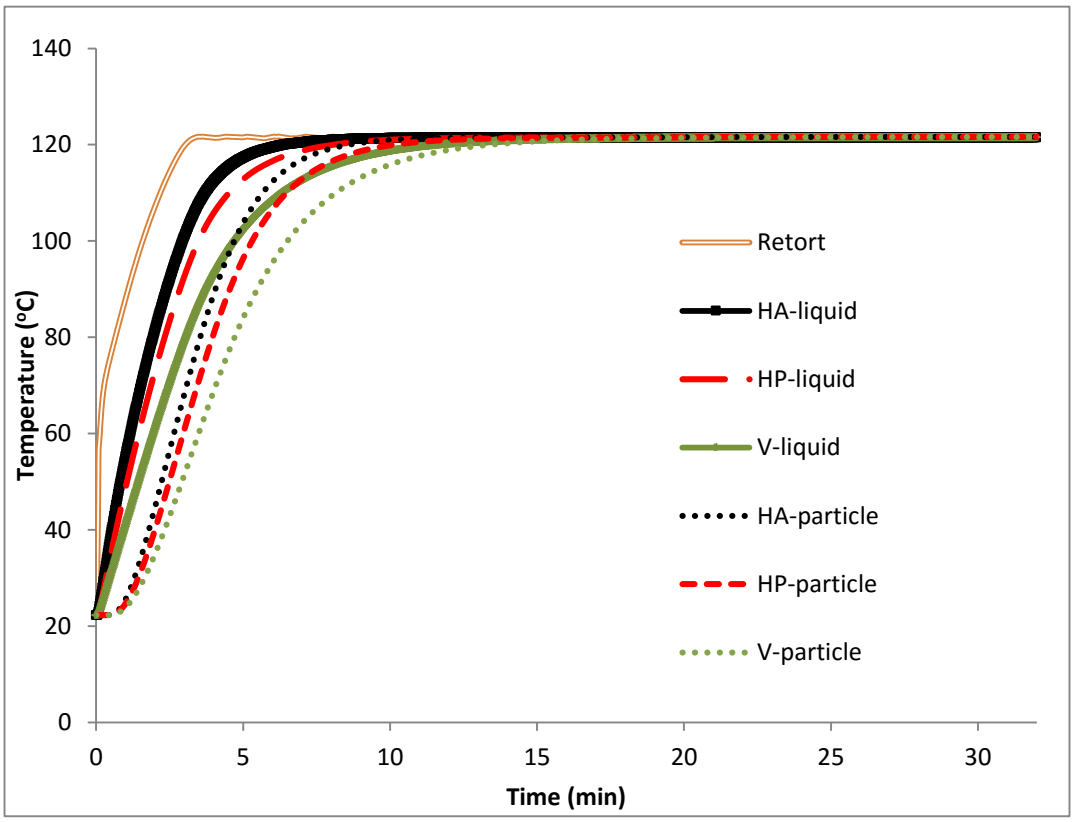

Fig. 5.3. Retort, liquid and particle-center temperature profiles for experimental cans with 12 mm headspace and processed at 2 Hz reciprocation frequency and 15 cm amplitude in one of the three orientations i.e. horizontally along the reciprocation axis (HA), horizontally perpendicular to axis of reciprocation (HP), or vertically (V)

The rate of heating was calculated as U and h_{fp} and is reported with standard deviations for different experimental conditions in Tables 5.2 and 5.3. Student's t-test showed a significant difference ($p< 0.05$) between values of U and h_{fp} in the three orientations (overall mean of U_{HA}, U_{HP} and U_v was 637 W/m^{2}K, 430 W/m^{2}K, and 411 W/m^{2}K respectively; while overall mean of $h_{fp\text{-}HA}$, $h_{fp\text{-}HP}$ and $h_{fp\text{-}V}$ was 857 W/m^{2}K, 700 W/m^{2}K, and 661 W/m^{2}K respectively). Heat transfer coefficients of cans placed along axis of reciprocation (HA) were significantly larger ($p< 10^{-5}$) than those placed perpendicular to axis of reciprocation (HP and V). HA orientation had highest heat transfer probably because movement of the can contents was different than for HP and V cans.

Can contents, in HA orientation, moved back and forth along the length (longer axis) for each reciprocation cycle, and had a perpendicular flat surface on both ends thereby causing direct back and forth reversal of the motion during the reciprocal agitation. However, with HP and V orientations, the particle/liquid motion is limited to shorter axis (equal to the can diameter) as opposed to the height and the opposing surfaces are concave providing some cushion &/or radial rather than the reciprocal movement to the fluid and particles. Thus, liquid-particle relative velocities and particle collision frequency were higher for HA cans resulting in increased turbulence (higher mixing) and higher Reynold's number. Hence, mixing in HA cans was considerably higher, resulting in higher heat transfer coefficients.

Amongst cans placed perpendicular to axis of reciprocation (HP and V), difference in values of heat transfer coefficients were not too significant ($0.05 < p < 0.005$). In order to compare heat transfer in these two orientations, it is important to understand that at any particular reciprocation frequency and amplitude, heat transfer is governed by both natural and forced convection. Since forced convection effects were same at high reciprocation frequency and amplitude, values were almost similar. However, for lower frequency and amplitude of reciprocation, HP cans have slightly higher values of heat transfer coefficients. This difference may be due to the fact that natural convection is more dominant along the radial direction in HP cans (Boz and Erdogdu, 2013), and thus the length scale of heat transfer is lower. Consequently, liquid-particulate mixtures in horizontal can (HP) tend to have higher heat transfer coefficients with higher Rayleigh and Grashoff number (Dimou *et al.*, 2014). However, as amount of agitation increased, forced convection became predominant, due to which difference between the two orientations decreased. Even under rotary agitation, at higher speeds of rotation, values of U and h_{fp} were found to be similar (Ramaswamy and Dwivedi, 2011). Ghani *et al.* (2003), through numerical simulation of rotary agitation, also found that slowest heating zone in the liquid became smaller with increase in agitation. Thus, V and HP cans had similar heat transfer rates at high reciprocation intensity.

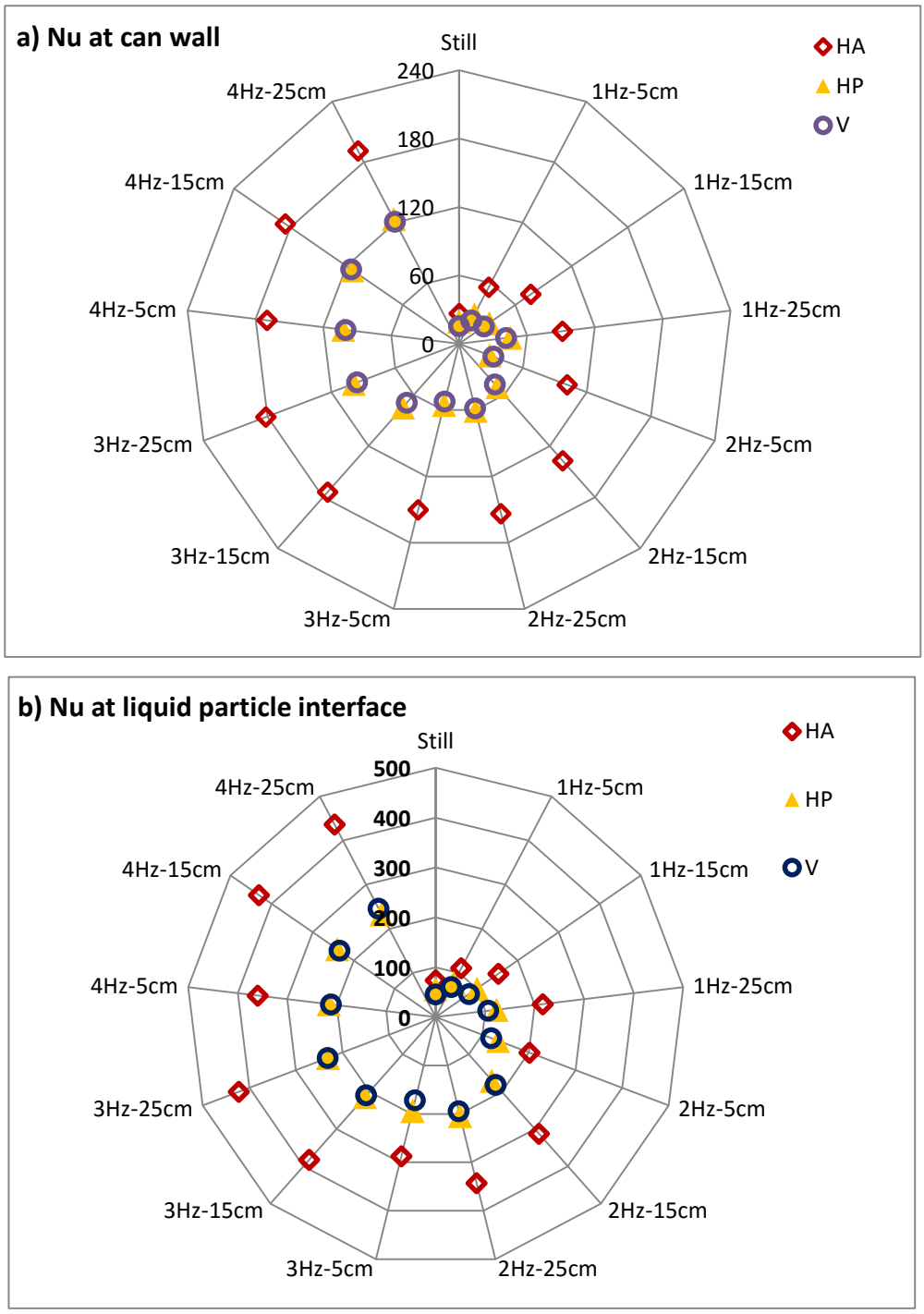

Fig. 5.4. Effect of the three can orientations (HA, HP, V) on the Nusselt number at the two interfaces i.e. a) Nu calculated from overall heat transfer coefficient at can wall; b) Nu calculated from fluid-to-particle heat transfer coefficient at liquid particle interface

Both overall heat transfer coefficient (U) and fluid-to-particle heat transfer coefficient (h_{fp}) ware seen to increase with reciprocation frequency (Tables 5.2 and 5.3) due to enhanced mixing at higher agitation. At higher frequency, direction of motion of liquid and particles changed rapidly resulting in a higher Reynold's number situation, which led to increased heat transfer. Thus, Nusselt number at can wall (Fig. 5.4a) and at liquid particle interface (Fig. 5.4b) increased with frequency, which is similar to the results of Garrote *et al.* (2006) on canned peas subjected to end over end sterilization. Another interesting observation was that, for HA cans, rise in values of Nu was more prominent at lower reciprocation frequencies and magnitude of increase subsided at higher frequency (except h_{fp} at 5 cm amplitude); while for HP and V orientation, opposite was true. This indicates that heat transfer in HA cans was very high even at lower agitation; while for HP and V cans, higher heat transfer could be observed only at higher frequency.

Increase in amplitude of reciprocation also leads to improvement in U and h_{fp} values. At same frequency, higher amplitude results in larger acceleration of particles (to sustain the same frequency) leading to increase in fluid-to-particle relative velocity. From Table 5.2 and Fig. 5.4, it is also clear that effect of increase of reciprocation amplitude was lower at higher reciprocation frequencies. It was also observed that amongst the two parameters, reciprocation frequency has more pronounced effects, consistent with results presented in Chapter 4. Similar results were also obtained for rotary (Sablani and Ramaswamy, 1996) and oscillatory (Sablani and Ramaswamy, 1999) agitation, where rotation speed (analogous to reciprocation frequency) had a more dominant effect on heat transfer than rotation diameter (analogous to reciprocation amplitude).

It was also found that an increase in headspace from 2 to 7 mm improved U and h_{fp} values for all can orientations at all reciprocation frequency (Table 5.3). However, increase from 7 to 12 mm did not have a prominent effect in all cases. Student's T-test on values of U and h_{fp} at different headspaces revealed that there was a significant difference ($p<0.05$) between values at 2 and 7 mm headspace for all orientations. Also, for HA orientation, there was a significant difference ($p<0.05$) between values at 7 and 12 mm headspace; however for HP and V cans, there was no significant difference ($p>0.05$). When headspace was very small (2 mm), there was very little bubble present in can. Hence, U and h_{fp} were lower than that for 7 or 12 mm headspace, where movement of bubble augmented the amount of mixing in the can. Little difference between values of U and h_{fp} of HP and V orientation for 7 and 12 mm headspace could be explained by the fact that movement

of headspace bubble due to reciprocation was along the diameter (shorter axis) of can and hence produced less significant mixing than when it was along the length (longer axis) in HA can. Also, due to gravity effects, chances of air bubble accumulation at top of the can is more prominent in HP and V orientation. Thus, due to lower level of turbulence, heat transfer in cans placed perpendicular to reciprocation axis (HP and V) was not significantly different between 7 and 12 mm headspace. On the other hand, cans placed along reciprocation axis (HA) recorded significant increase in heat transfer on increase of headspace from 7 to 12 mm.

5.4.3 Interaction between can-orientation and operating parameters

Analysis of variance of U and h_{fp} at various reciprocation frequency and amplitude is presented in Table 5.4. Data was fitted to a quadratic model for both U and h_{fp}. It was observed that both frequency and amplitude significantly affected ($p < 0.05$) values of U and h_{fp} for all can orientations. The two way interaction of reciprocation frequency and amplitude was significant ($p < 0.05$) only for U_{HP} and U_v and was not significant ($p > 0.1$) for U_{HA} and h_{fp} values of all orientations. Further, the interaction of square of reciprocation frequency was significant ($p < 0.05$) for U values of all orientations and $h_{fp\text{-}HA}$ and $h_{fp\text{-}HP}$, but was not significant ($p > 0.1$) for $h_{fp\text{-}V}$. The interaction of square of amplitude was not significant ($p > 0.1$) for any of U and h_{fp} values. Developed models with their R^2 values are given in Equations (5.8-5.13) in terms of actual values of reciprocation frequency (F in Hz) and amplitude (A in cm).

$$U_{HA} = -1.262 + 323.024 * F + 13.140 * A + 1.000 * F * A - 32.214 * F^2 - 0.264 * A^2 \quad R^2=0.98 \quad (5.8)$$

$$U_{HP} = 104.054 + 0.793 * F + 2.720 * A + 2.410 * F * A + 30.047 * F^2 - 0.007 * A^2 \quad R^2=0.97 \quad (5.9)$$

$$U_V = 79.933 + 10.133 * F + 1.280 * A + 2.260 * F * A + 29.500 * F^2 + 0.056 * A^2 \quad R^2=0.98 \quad (5.10)$$

$$h_{fp-HA} = -15.094 + 352.038 * F + 25.960 * A + 2.920 * F * A - 29.476 * F^2 - 0.573 * A^2 \quad R^2=0.97 \quad (5.11)$$

$$h_{fp-HP} = 98.285 + 283.028 * F + 10.680 * A + 0.560 * F * A - 24.190 * F^2 - 0.152 * A^2 \quad R^2=0.96 \quad (5.12)$$

$$h_{fp-V} = 44.953 + 261.742 * F + 13.320 * A + 1.900 * F * A - 20.785 * F^2 - 0.277 * A^2 \quad R^2=0.96 \quad (5.13)$$

Table 5.4. Analysis of variance for effect of reciprocation frequency and amplitude on U and h_{fp} for the three can orientations: a) horizontally along the reciprocation axis (HA); b) horizontally perpendicular to axis of reciprocation (HP); c) vertically (V).

a) HA orientation		U_{HA}			h_{fp-HA}	
Parameter	**Type III SS**	**F Value**	**Pr>F**	**Type III SS**	**F Value**	**Pr>F**
F	1312520	427	< 0.0001	2317408	249	< 0.0001
A	52128	16	0.0026	213452	23	0.0010
F*A	2000	0.6	0.4404	17052	2	0.2082
F^2	43585	14	0.0044	36491	4	0.0496
A^2	2323	0.7	0.4070	10944	1	0.3056
b) HP orientation		U_{HP}			h_{fp-HP}	
Parameter	**Type III SS**	**F Value**	**Pr>F**	**Type III SS**	**F Value**	**Pr>F**
F	740726	320	< 0.0001	1136853	233	< 0.0001
A	60062	25	0.0006	52417	10	0.0095
F*A	11616	8	0.0318	627	0.1	0.7280
F^2	37920	16	0.0029	24577	5	0.0493
A^2	1	0.0007	0.9794	770	0.1	0.7002
c) V orientation		U_V			h_{fp-V}	
Parameter	**Type III SS**	**F Value**	**Pr>F**	**Type III SS**	**F Value**	**Pr>F**
F	787644	408	< 0.0001	1286712	220	< 0.0001
A	55950	28	0.0004	77616	13	0.0053
F*A	10215	5	0.0469	7220	1	0.2944
F^2	36550	18	0.0018	18145	3	0.1114
A^2	104	0.05	0.8212	2557	0.4	0.5242

Analysis of variance of data (Table 5.5) on interaction between headspace and frequency revealed that while frequency and its square significantly affected ($p < 0.05$) values of U and h_{fp}

in all orientations, the effect of headspace was significant ($p<0.05$) for U and h_{fp} in only HA cans. For h_{fp} of HA cans, the interaction of frequency and headspace and the effect of square of headspace were also significant. Obviously, effect of frequency was much more predominant than any other factor (highest mean square). Developed quadratic models in terms of actual values of frequency (F, in Hz) and headspace (H, in mm) are given in Equations (5.14-5.19).

Table 5.5. Analysis of variance for effect of headspace and reciprocation frequency on U and h_{fp} for the three can orientations: a) horizontally along the reciprocation axis (HA); b) horizontally perpendicular to axis of reciprocation (HP); c) vertically (V).

a) HA orientation	U_{HA}			$h_{fp\text{-}HA}$		
Parameter	**Type III SS**	**F Value**	**Pr>F**	**Type III SS**	**F Value**	**Pr>F**
F	993894	7719	< 0.0001	1544323	2216	< 0.0001
H	1768	13	0.0076	75264	108	< 0.0001
F*H	240	2	0.2142	24649	35	0.0006
F^2	83089	645	< 0.0001	83586	119	< 0.0001
H^2	221	1	0.2314	12385	17	0.0040
b) HP orientation	U_{HP}			$h_{fp\text{-}HP}$		
Parameter	**Type III SS**	**F Value**	**Pr>F**	**Type III SS**	**F Value**	**Pr>F**
F	620173	1993	< 0.0001	990640	668	< 0.0001
H	1204	4	0.0899	37	0.02	0.8781
F*H	9	0.03	0.8698	9	0.006	0.9401
F^2	39213	126	< 0.0001	35741	24	0.0017
H^2	169	0.5	0.4839	7542	5	0.0587
c) V orientation	U_V			$h_{fp\text{-}V}$		
Parameter	**Type III SS**	**F Value**	**Pr>F**	**Type III SS**	**F Value**	**Pr>F**
F	711392	2646	< 0.0001	792066	934	< 0.0001
H	1441	5	0.0537	4266	5	0.0598
F*H	1	0.003	0.9531	1892	2	0.1788
F^2	59206	220	< 0.0001	123566	145	< 0.0001
H^2	0.02	< 0.0001	0.9933	83	0.09	0.7635

$$U_{HA} = 97.243 + 371.523 * F + 6.894 * H + +0.775 * F * H - 43.362 * F^2 - 0.358 * H^2 \qquad R^2=0.99 \qquad (5.14)$$

$$U_{HP} = 101.787 + 40.545 * F + 6.926 * H + 0.150 * F * H + 29.789 * F^2 - 0.314 * H^2 \qquad R^2 = 0.99 \qquad (5.15)$$

$$U_V = 76.221 + 25.403 * F + 3.048 * H + 0.050 * F * H + 36.603 * F^2 - 0.003 * A^2 \quad R^2 = 0.99 \quad (5.16)$$

$$h_{fp-HA} = 77.825 + 372.682 * F + 44.200 * H + 7.850 * F * H - 43.491 * F^2 - 2.679 * H^2 \quad R^2 = 0.99 \quad (5.17)$$

$$h_{fp-HP} = 161.012 + 315.875 * F + 29.465 * H + 0.150 * F * H - 28.440 * F^2 - 2.090 * H^2 \quad R^2 = 0.99 \quad (5.18)$$

$$h_{fp-V} = 189.874 + 377.959 * F - 2.087 * H + 2.175 * F * H - 52.879 * F^2 + 0.219 * H^2 \quad R^2 = 0.99 \quad (5.19)$$

5.4.4 Equilibration time and process time under HA, HP and V orientation

The objective of agitation thermal processing is to reduce the time required for the cold spot to reach operating temperatures (Meng and Ramaswamy, 2007a). This time is estimated as equilibration time (Fig. 5.2b), as the time required to decrease difference between operating temperature and cold spot temperature to 1° C.

Beyond this equilibration point of heating (after cold spot reaches operating temperature) all orientations impart nearly the same lethality and lethality imparted for remainder of the process time is equal for reciprocating, rotary and still thermal processing. In line with earlier works, equilibration time was found to drastically decrease on reciprocation, as forced convection enhanced the extent of heat transfer inside the can. This tremendous reduction in equilibration time was also due to extensive turbulence created by rapid changes in direction of motion of liquid and particles, resulting in faster heat transfer at liquid-particle interface.

Equilibration time was found to be lowest for HA cans, followed by HP and highest for V orientation (Fig. 5.5). Equilibration time of cold spot reduced from 30 min in still mode to 9 min at 2 Hz-15 cm reciprocation in HA orientation and corresponding decrease in HP and V orientation was from 30 min to 14 min, and from 36 min to 15min respectively. Equilibration time at higher reciprocation frequency and amplitude are further lower as depicted in Fig. 5.5. From the published data (Dwivedi and Ramaswamy, 2010b), equilibration time was found to be around 24 min, 19 min and 15 min at 16 rpm rotations in fixed-axial, end-over-end and biaxial mode of rotary agitation respectively. Thus, reciprocating agitation in either of three orientations provided a better heat transfer scenario than rotary modes of agitation.

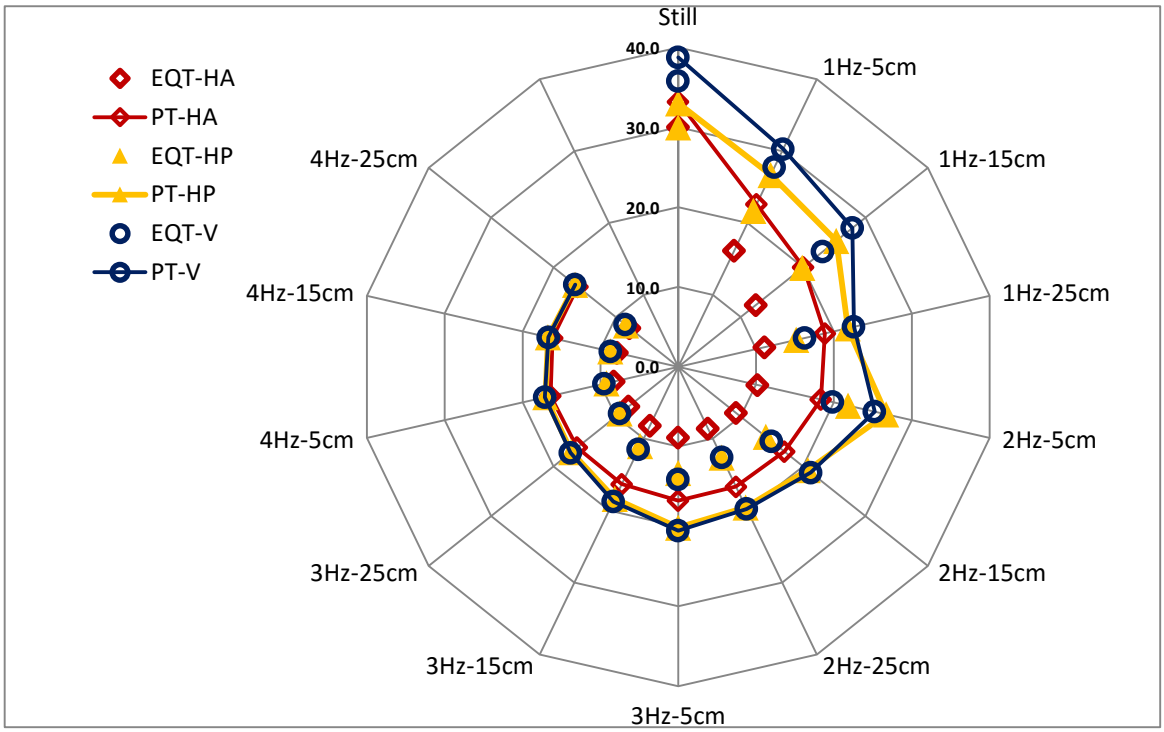

Fig. 5.5. Effect of the three can orientations (HA, HP, V) on equilibration time (EQT) and process time (PT) to attain lethality of 10 min at various reciprocation frequency and amplitude

Lower equilibration times resulted in reduction of process time to achieve lethality of 10 min. Process time decreased from 33-39 min at still mode to 16-17 min at highest reciprocation frequency (Fig. 5.5). It is seen that at higher reciprocation frequency and amplitude, average process time was same for all orientations. However, at milder reciprocation frequency and amplitude combination, HA orientation depicted lowest process time and V cans depicted largest process time (but much lower than still mode). A lower process time effectively means lower overall cooking of the product and thus better quality retention. Thus, in terms of overall cooking, HA orientation can be considered to deliver best quality of product, followed by HP and V orientation respectively under mild agitation scenarios, while at higher reciprocation intensities, the three orientations are almost similar.

5.4.5 Optimum reciprocation intensity and can orientation

In order to present the best quality products, it is essential to select optimum reciprocation intensity and can orientation to impart reciprocation thermal processing. It is seen that, although

reciprocation amplitude and reciprocation frequency are both important parameters in terms of increasing the extent of mixing in a liquid-particulate system, can orientation also plays a very significant role. Reduction in process time and magnitude of breakage of particles due to reciprocation are two important factors to be considered for optimization during reciprocation thermal processing. Lower process time is desirable to lower the overall cooking of product. Lower reciprocation intensity is also desired as shear breakage of particles under high agitation will be significant. Proper combination of can orientation and reciprocation intensity has to be selected to minimize the breakage of particle and to decrease process time.

During reciprocation, reciprocation frequency and reciprocation amplitude affect amount of reciprocation intensity (RI) present in the system. A change in either of the two parameters affects reciprocation intensity. RI can conveniently be expressed as a single value by calculating maximum acceleration for each combination of amplitude and frequency of reciprocation (Walden and Emanuel, 2010), and can be represented by Equation (5.20).

$$Agitation\ Intensity\ (RI) = \omega^2 r(1 + {}^{r}/_{l}) \tag{5.20}$$

where, ω = angular velocity in radian/s = 2* π*frequency (s), r = crank radius (half amplitude) in m, and l = length of connecting rod (M) in m.

Fig. 5.6 shows the variation of heat transfer coefficients (U and h_{fp}) with changes in RI. From Fig. 5.6a, it can be observed that there was a steep rise in values of U for all the three can orientations to around 1.0 g. Beyond 30 ms^{-2}, for HA orientation there was little change. Similarly, beyond 60 ms^{-2}, there was little change in values of U for HP and V orientations. Fig. 5.6b also shows a similar effect of agitation on h_{fp}. Thus, once past 60 ms^{-2}, there is very little subsequent change. This indicates that the process is stable, meaning that small variations in either stroke or frequency will tend to have little effect on rate of heating and hence process time. Similarly, with other combinations of product variables and headspace, the form of the graph will be similar, although the position where the steep fall changes to the stable zone can move. This is similar to the recommendation of Walden and Emanuel (2010) on operating at optimum reciprocation intensity. Thus, from the results in this study, while 60 ms^{-2} reciprocation intensity is sufficient for HP and V orientations, 30 ms^{-2} reciprocation intensity is sufficient for HA orientation to obtain

highest heat transfer coefficient and any higher reciprocation frequency does not create any appreciable effect on the thermal process. Too high agitation speed may be detrimental to the quality of food products as texture loss would be significant due to rapid collisions of particles, and hence reciprocation intensity of 60 ms^{-2} and 30 ms^{-2} is recommended as the higher bound of choice of reciprocation intensity. The exact magnitude of recommended reciprocation intensity may vary with choice of can size and product properties, but the overall trend is expected to be similar.

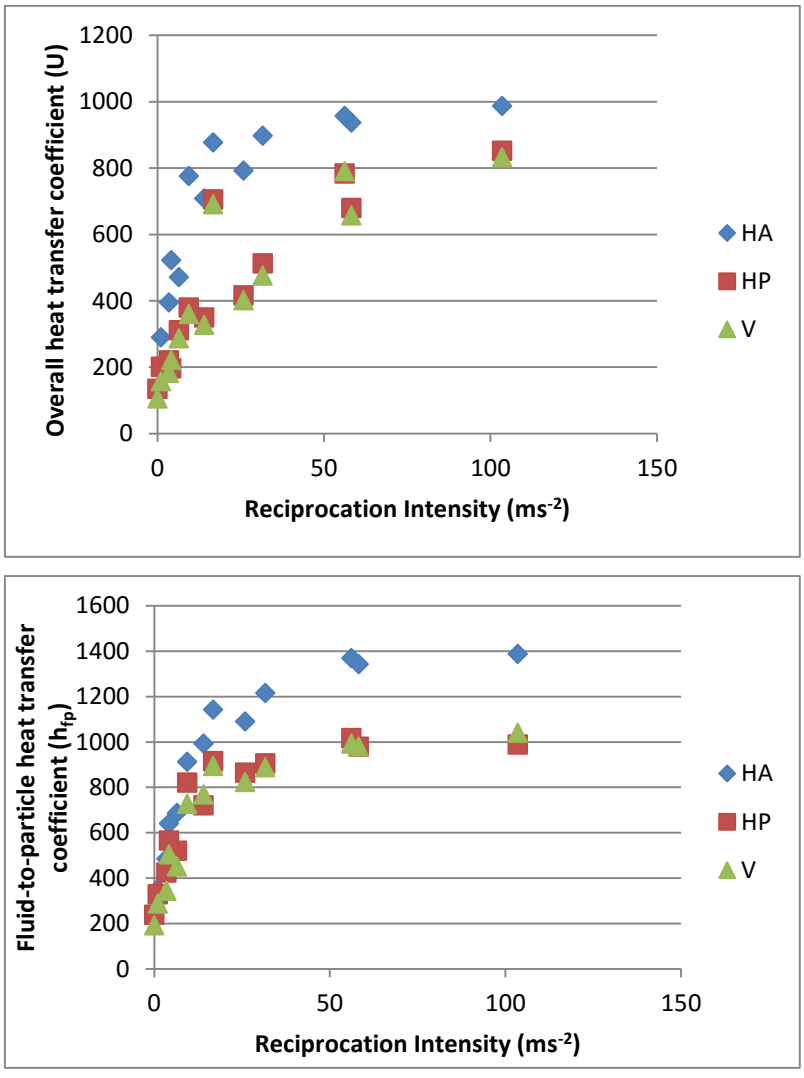

Fig. 5.6. Effect of reciprocation intensity on a) overall heat transfer coefficient (U); and b) fluid-to-particle heat transfer coefficient (h_{fp})

Process time was also seen to be lower at mild reciprocation intensity for HA orientation. Almost similar process time at higher agitation frequency and amplitude (Fig. 5.5) also suggests that too high agitation speed is not required. Since, reciprocation along axis of can shall produce more breakage of particles; HP or V orientations (perpendicular to axis of reciprocation) are preferred for products that cannot tolerate high reciprocation intensities. HA orientation is preferable only for those liquid/liquid-particulate foods (such as thick soups, baby and pet foods etc.), where high intensity reciprocation would not affect the quality of the product.

5.5 Conclusions

Can orientation had a significant effect on nature of heat transfer occurring in the liquid particulate system. HA orientation was the most effective for enhancing the level of heat transfer due to reciprocation of can contents along the longer axis of can, followed by HP and V orientation respectively where the can contents reciprocated along a shorter axis. Although HP and V orientation depicted similar trend, HP was slightly better as heat transfer was better in horizontal orientation. Even under natural convection in still mode, horizontal cans had higher heat transfer rate. Increasing reciprocation speed had most significant effect, followed by reciprocation amplitude in all three orientation. Headspace on the other hand, affected values significantly only for HA orientation. Some amount of headspace was necessary to obtain a better heat transfer rate, although large headspace bubble retarded heat transfer due to the insulation effect of air. Too high reciprocation intensity may not be preferable since quality loss might result due to excessive collisions amongst the particles leading to particle breakage. A reciprocation intensity of 30 ms^{-2} was found optimum for HA cans and of 60 ms^{-2} was found optimum for HP and V cans from maximizing the heat transfer. Each of these values were obtained for 25 cm amplitude. At lower amplitude, the value would be proportionately lower. This enhancement in heat transfer resulted in lower process times as well. Here, it was again seen that too high reciprocation intensity was not required to decrease process time considerably and mild reciprocation intensity is sufficient to decrease the process time. Hence, HA orientation must be selected for achieving lowest process times, however there might be considerable agitation induced losses. HP and V orientations are more suitable for processing such liquid particulate food mixtures where this might be a concern.

PREFACE TO CHAPTER 6

In Chapters 3-5, the effect of various reciprocating conditions like reciprocation frequency, reciprocation amplitude, container orientation etc. on the process time and heat transfer coefficients was discussed in detail. However, there are many other parameters of interest which will affect heat transfer during any agitation processing conditions. These include operating conditions like operating temperature, container headspace etc. or product dependent parameters like liquid viscosity, particle density etc.

Chapter 6 elucidates the effect of various processing conditions and product properties on heat transfer in reciprocating cans using a single particle almost simulating conditions for a liquid-only situation. At the same time, it offers uninhibited exposure of the single particle to free liquid, a situation that has been studied many times in the past for dermining the primary effects of agitation on fluid to particle heat transfer. A single-particle was also placed inside the can to study single-particle scenario. Although, there is rarely a real life scenario of a single particle in can, yet this analysis would be useful in estimating the heat transfer through the can wall in liquid-particulate cans by providing fairly uninhibited heat transfer conditions at liquid-particle interface. More importantly, this study shall help in finding the extent of heat transfer in liquid-only cans, as presence of single particle would not create appreciable difference in the nature of heat transfer.

Parts of this chapter have been presented in form of oral presentation at The Northeast Agricultural and Biological Engineering Conference (NABEC) held on July 27-30 at Kemptville, Ontario.

Parts of this chapter have been submitted for publication as an article "*Heating behavior of canned liquid during reciprocating agitation thermal processing of liquid-particulate mixtures*" in Food and Bioprocess Technology.

The experimental work and data analysis was carried out by the candidate under the supervision of Dr. H. S. Ramaswamy.

CHAPTER 6

EFFECT OF PROCESSING CONDITION AND PRODUCT PROPERTIES ON HEAT TRANSFER COEFFICIENTS DURING RECIPROCATING AGITATION THERMAL PROCESSING: STUDIES WITH A SINGLE PARTICLE SUSPENDED IN A LIQUID-ONLY CAN

6.1 Abstract

The effect of various reciprocating agitation processing conditions and product properties on heat transfer in cans filled with a Newtonian fluid (glycerin) and fitted with a single spherical particle (diameter = 19 mm) was studied. Experimental cans were processed in the modified retort, detailed in Chapter 3, and heat transfer coefficients (U and h_{fp}) were evaluated. The processing conditions included: various levels of retort temperature (110 to 130 ^{O}C), reciprocation frequency (1 to 4 Hz), reciprocation amplitude (5 to 25 cm) and can headspace (6 and 12 mm) using a full factorial designs. Effect of product properties such as density of particle and liquid viscosity on associated heat transfer coefficients were subsequently investigated at different reciprocation frequencies (1 to 4 Hz) using another full-factorial design. Higher heat transfer coefficients were obtained with increasing values of all four processing variables, and the effects of reciprocation frequency and reciprocation amplitude were more significant than those of retort temperature and amplitude of reciprocation. In terms of product properties, U values were enhanced with decreasing liquid viscosity and increasing reciprocation frequency; however they were unaffected by the particle density. The h_{fp} values were affected in a similar fashion, increasing with reciprocation frequency and decreasing with liquid viscosity. However, unlike U, h_{fp} was also significantly affected by particle density.

6.2 Introduction

Mathematical modeling of heat sterilization of canned liquids with suspended food particles requires data on thermo-physical properties of both liquids and solid food particles, and associated heat transfer coefficients. In such systems, the overall heat transfer coefficient, U, and the fluid-to-particle heat transfer coefficient, h_{fp}, are needed to predict heat transferred to solid food particles. No information is available on U and h_{fp} in cans during reciprocation agitation processing, as this mode of agitation is relatively new. However, earlier studies have reported U and h_{fp} values for processing using still mode and different rotational modes of agitation viz. end-

over-end mode, fixed axial mode and biaxial mode (Stoforos and Merson, 1991; Ramaswamy *et al.*, 1993; Garrote *et al.*, 2006; Meng and Ramaswamy, 2007a; Sablani and Ramaswamy, 1999; Dwivedi and Ramaswamy, 2010; Ramaswamy and Dwivedi, 2011; Hassan *et al.*, 2012). These researchers have found that mechanical agitation of cans in rotary autoclaves enhances heat transfer rates to both liquid and particle, and has the potential of improving the quality retention, compared with those foods processed in still autoclaves. However, there is a need to quantify the effect of agitation and other parameters influencing U and h_{fp} for the reciprocating mode of agitation.

The effect of various parameters on U and h_{fp} e.g. process temperature, headspace, rotational speed, radius of rotation, liquid viscosity, particle properties and volume fraction occupied by the particles, etc. have been experimentally investigated by Lenz and Lund (1978), Deniston *et al.* (1987), Femandez *et al.* (1988), Sablani and Ramaswamy (1998, 1999), Meng and Ramaswamy, (2005, 2006) and Dwivedi and Ramaswamy (2010). Most of these studies involved studying multiple particles. However, before studying the effect of agitation on multiple particles, it is imperative to study the effect of reciprocation on a single particle in a can. Sablani (1996) studied the effect of system & product parameters on single particle in can and found that the effect of agitation on heat transfer in such a scenario is markedly different from the effects in presence of multiple particles in can. He found that in a single particle scenario, generally, the U values are higher, while h_{fp} values are lower than the multiple particle case. It was also observed that such a study helps to quantify the effects of agitation on the heat transfer through the liquid inside the can, and can also be used to assess the heat transfer situations in cans filled with only liquid. More importantly, this study shall help in finding the extent of heat transfer in liquid-only cans, as the presence of single particle would not create appreciable difference in the nature of heat transfer.

This chapter focusses on using the reciprocating retort detailed in Chapter 3 to quantify the effect of i) processing conditions, such as retort temperature, reciprocation frequency, amplitude of rotation and can headspace; and ii) product properties such as particle density and liquid viscosity, on both U and h_{fp}, during reciprocating agitation of cans filled with single particle in a Newtonian fluid. This study can also be used to determine the values of U for liquid-only cans, since the effect on U of a single small spherical particle present in the can would be nearly insignificant.

6.3 Materials and Methods

6.3.1 Test Materials

Glycerin (Fisher Scientific, Montreal, PQ) at different levels of concentrations (0-100%) giving different viscosity levels, were used as test liquids. Spherical particles (diameter 19 mm) made of polypropylene, Nylon, and Teflon (Small Parts Inc., Miami, FL), covering a wide range of density (830 kg/m^3 to 2210 kg/m^3), were used as the test particles. The thermo-physical properties of the liquids and particles were measured experimentally and are summarized in Table 6.1. Can liquid temperatures were measured at the geometric center of the cans, using needle type thermocouples. For the purpose of measuring particle transient temperatures, a thermocouple equipped particle was mounted inside the can. The particle assembly, can preparation and data gathering are described in Chapter 5.

6.3.2 Thermal Processing

Cans of size 307 x 409 containing glycerin of required concentration were filled to the required headspace and the thermocouple equipped particle and were processed in the lab-scale reciprocating retort detailed in Chapter 3. Only one particle per can was used. In each test run, two test cans were placed in the reciprocating cage equidistant from the axis of reciprocation with the longer axis along the direction of reciprocation (HA orientation). The remaining space in the cage was filled with dummy cans containing water to provide ballast.

Three retort temperatures (110, 120 and 130 ^{O}C), five reciprocation frequencies (0, 1, 2, 3 and 4 Hz), three amplitudes of reciprocation (5, 15 and 25 cm) and two can headspaces (6 and 12 mm) were employed as processing conditions. In the first set of experiments, a 3 x 3 x 4 full-factorial design was employed with the three retort temperatures, three amplitudes of reciprocation and four reciprocation frequencies (1, 2, 3 and 4 Hz), with a can headspace of 12 mm. Experiments were also carried out at 0 Hz (still retort processing condition) at the three retort temperatures.

In order to study the effect of can headspace, a 3 x 4 x 2 full-factorial design was used with the three retort temperatures, the four reciprocation frequencies (1, 2, 3 and 4 Hz), and the two can headspaces at a constant amplitude of reciprocation of 15 cm. Glycerin concentration of 80% was used to study the effect of processing conditions. All test runs were repeated twice.

Table 6.1. Thermo-physical Properties of Test materials

Material	Density (kg/m^3)	Heat capacity (J/Kg.K)	Thermal conductivity (W/m.K)	Thermal diffusivity (m^2/s)	Thermal effusivity ($J/m^2Ks^{0.5}$)	Viscosity (Pa.s)
Nylon	1130	2070	0.37	$1.5x10^{-7}$	929	-
Polypropylene	830	1840	0.36	$2.3x10^{-7}$	791	-
Teflon	2210	980	0.29	$1.3x10^{-7}$	794	-
Glycerin (100%)	1260	2430	0.28	$0.9x10^{-7}$	-	0.94
Glycerin (80%)	1210	2720	0.33	$1.0x10^{-7}$	-	0.070
Glycerin (50%)	1130	3340	0.41	$1.1x10^{-7}$	-	0.011
Glycerin (20%)	1050	3760	0.53	$1.3x10^{-7}$	-	0.003
Glycerin (0%) / Water	1000	4180	0.60	$1.4x10^{-7}$	-	0.001

In order to study the effect of product properties, three particle densities, five liquid viscosities and four reciprocation frequencies were considered as experimental variables. A 3 x 5 x 2 full-factorial design was employed with the three particle types giving 3 particle densities (polypropylene - 830, Nylon - 1130 and Teflon - 2210 kg/m^3), five glycerin concentrations giving five liquid viscosities (0%-0.001, 20%-0.003, 50%-0.011, 80%-0.070 and 100%-0.94 Pa.s) and two reciprocation frequencies (2 and 4 Hz) with a can headspace of 12 mm, amplitude of reciprocation of 15 cm and 120 ^oC retort temperature. All experiments were repeated twice.

6.3.3 Data Analysis

Details are given in Chapter 4 regarding time-temperature data gathering, normalizations and the subsequent evaluation of liquid (f_{h-l}) and particle (f_{h-p}) heating rate indices. Using the f_{h-l} and f_{h-p}, the overall heat transfer coefficient (U) and the fluid-to-particle heat transfer coefficient (h_{fp}) were evaluated from the equilibrated profiles using the methodology detailed in section 5.3.4. All test results were analyzed using Analysis of Variance (ANOVA) to evaluate the level of significance of all the variables and their interactions.

6.4 Results and Discussions

6.4.1 Influence of processing conditions on U

Tables 6.2 and 6.3 summarize the overall heat transfer coefficients obtained under the different experimental conditions. U values varied from 200-749 W/m^{2}K during reciprocation. Increasing the retort temperature from 110-130 ^{O}C at 2 Hz improved the mean U values by 6-7%. This was probably due to the lowering of liquid viscosity at a higher retort temperature. The overall heat transfer coefficient also increased with the increasing reciprocation frequencies: mean U values increased by 43% from 1 Hz to 2 Hz, by 104% from 1 Hz to 3 Hz, and by 162% from 1 Hz to 4 Hz. Again, this was possibly due to enhanced mixing, resulting in a higher degree of turbulence, which led to increased heat transfer. The influence of reciprocation frequency on U was more pronounced than any other parameters studied.

At 0 Hz (still retort processing condition), the overall heat transfer coefficient was calculated just as with the agitated processing condition in which temperature uniformity of the liquid within the can was achieved in a short time. Since the temperature was not uniform for still conditions, the process time was long and natural convection was the predominant mode of heat transfer, the calculated U may not be a true representation of convection heat transfer. However, since the objective was to evaluate the quantum of improvement in heat transfer rate during agitated processing, a limited number of experiments were carried out with 0 Hz and the data were treated in a similar fashion. These data were only used for the purpose of comparison and not included in the statistical analysis of variance. U values ranged between 114-119 W/m^{2}K during still mode, and were clearly much lower when compared to the U values during reciprocation agitation (200-750 W/m^{2}K). Thus, reciprocation led to a better heat transfer situation as compared to the still mode of operation.

Increase in amplitude of reciprocation also led to some improvement in U values, because of the larger acceleration of cage required to sustain the same reciprocation frequency. Thus, a larger acceleration and thereby greater turbulence was encountered by the liquid at higher amplitude of reciprocation. Increasing the amplitude of reciprocation from 5 to 15 cm improved the mean U value by 31%, and from 15 to 25 cm, it improved by 22%; however, the effect of increase of reciprocation amplitude was lower at higher reciprocation frequencies. Thus, it can be

observed that both reciprocation amplitude and frequency are governing parameters in terms of the increase in the value of U. Both of them together should be considered while designing a thermal process. Reciprocation frequency on one hand increases the speed of cage directly by increasing the number of cycles per second, and the reciprocation amplitude leads to increase in the velocity of the reciprocating cage and its reversing, after the develoment of a fuller velocity profile. Thus, an increase of either of the parameters leads to an increase in the relative velocity between the liquid and the particles and the Reynold's number, thereby increasing turbulence. However, it is observed that amongst the two parameters, reciprocation frequency has more pronounced effects.

Table 6.2. Mean heat transfer coefficients (U and h_{fp}) for cans processed with single particle as influenced by operating temperature, reciprocation frequency and amplitude of reciprocation.

Retort Temp. (°C)	**Reciprocation Frequency (Hz)**	**Reciprocation amplitude (cm)**	**Overall Heat Transfer Coefficient, U[a] (W/m²K)**	**Fluid to particle heat transfer coefficient, h_{fp}[a] (W/m²K)**
110	Still		114 (0.7)	227 (0.9)
	1	5	197 (1.6)	324 (1.2)
		15	216 (0.8)	414 (0.7)
		25	267 (3.1)	450 (0.8)
	2	5	229 (0.7)	463 (2.1)
		15	340 (1.2)	543 (1.1)
		25	401 (0.8)	621 (0.7)
	3	5	295 (0.4)	519 (1.3)
		15	467 (0.7)	619 (1.6)
		25	590 (0.2)	687 (0.2)
	4	5	467 (1.8)	664 (0.8)
		15	590 (2.1)	882 (3.1)
		25	623 (1.1)	1010 (0.7)
120	Still		115 (4.1)	228 (1.4)
	1	5	204 (0.7)	330 (4.2)

		15	220 (1.6)	428 (1.2)
		25	280 (3.5)	472 (3.1)
		5	234 (2.7)	482 (0.7)
	2	15	351 (0.8)	575 (2.1)
		25	415 (1.6)	665 (1.8)
		5	320 (0.7)	521 (1.2)
	3	15	467 (1.2)	651 (3.1)
		25	660 (3.1)	915 (0.9)
		5	534 (1.1)	750 (0.8)
	4	15	623 (0.6)	985 (0.7)
		25	701 (2.1)	1190 (0.5)
	Still		119 (3.9)	233 (1.6)
		5	208 (0.7)	326 (0.4)
	1	15	224 (2.5)	421 (1.2)
		25	274 (0.8)	461 (1.3)
		5	244 (1.6)	507 (0.4)
	2	15	362 (0.7)	614 (0.2)
130		25	432 (1.7)	721 (0.6)
		5	312 (2.4)	580 (1.1)
	3	15	467 (1.2)	690 (0.8)
		25	700 (1.6)	846 (0.7)
		5	534 (0.9)	803 (1.5)
	4	15	660 (1.6)	996 (0.4)
		25	748 (0.7)	1410 (0.8)

[a] values in parentheses are the coefficients of variation (%)

Table 6.3. Mean heat transfer coefficients (U and h_{fp}) for cans processed with single particle as influenced by operating temperature, reciprocation frequency and headspace.

Retort Temp. (°C)	**Frequency (Hz)**	**Headspace (mm)**	**Overall Heat Transfer Coefficient, U[a] (W/m^2K)**	**Fluid to particle heat transfer coefficient, h_{fp}[a] (W/m^2K)**
110	1	6	212 (1.2)	394 (1.1)
		12	216 (0.8)	414 (0.7)
	2	6	340 (2.1)	483 (3.7)
		12	340 (1.2)	543 (1.1)
	3	6	449 (4.1)	570 (3.1)
		12	467 (0.7)	619 (1.6)
	4	6	534 (3.3)	766 (4.2)
		12	590 (2.1)	882 (3.1)
120	1	6	216 (1.1)	427 (0.4)
		12	220 (1.6)	428 (1.2)
	2	6	330 (1.1)	605 (0.9)
		12	351 (0.8)	575 (2.1)
	3	6	449 (1.9)	596 (3.6)
		12	467 (1.2)	651 (3.1)
	4	6	590 (0.3)	956 (0.1)
		12	623 (0.6)	985 (0.7)
130	1	6	220 (4.2)	421 (3.1)
		12	224 (2.5)	421 (1.2)
	2	6	340 (0.4)	558 (0.9)
		12	362 (0.7)	614 (0.2)
	3	6	448 (1.9)	383 (0.4)
		12	467 (1.2)	690 (0.8)
	4	6	659 (1.9)	956 (3.1)
		12	660 (1.6)	996 (0.4)

[a] values in parentheses are the coefficients of variation (%)

It was also found that an increase in headspace also improved the mean U values. This is probably due to an increase in bubble size, resulting in more efficient mixing. However, bubble size beyond a critical level may have a dampening effect on the efficiency of mixing, due to increased drag on the can wall; thus resulting in disturbance in bubble-liquid phenomena (Naveh and Kopelman, 1980). In this study, the effect of headspace was not very pronounced on the values of U and an increase in headspace from 6 mm to 12 mm increased the mean U value by only 4%.

Analysis of variance of data (Tables 6.4 and 6.5) revealed that while reciprocation frequency and reciprocation amplitude were highly significant terms, ($p < 0.0001$), temperature and headspace were also significant ($p<0.05$). The two way interactions of reciprocation frequency and reciprocation amplitude was found significant for the first study, while on evaluating the headspace, the interaction of reciprocation frequency and operating temperature was also found significant. However, the contributions of the two way interactions were low as compared to the main effects, and hence only main effects are plotted in Fig. 6.1 for U.

For the first study, the data fitted a quadratic model (adjusted $R^2 = 0.98$) while in the study on headspace, a 2 factor-interaction model gave the best fit (adjusted $R^2 = 0.94$). The developed correlations are given in Equations (6.1-6.2).

$$U\left(\frac{W}{m^2K}\right) = 224.32 - 1.11T - 36.60F + 7.63H + 1.26(T.F) - 0.069(T.H) + 1.38(F.H) \qquad R^2 = 0.91 \quad (6.1)$$

$$U\left(\frac{W}{m^2K}\right) = -633.56 + 14.58T - 101.40F - 7.37A - 0.072T^2 + 7.56F^2 - 0.044A^2 + 1.26(T.F) + 0.10(T.A) + 2.40(F.A) \qquad R^2 = 0.97 \quad (6.2)$$

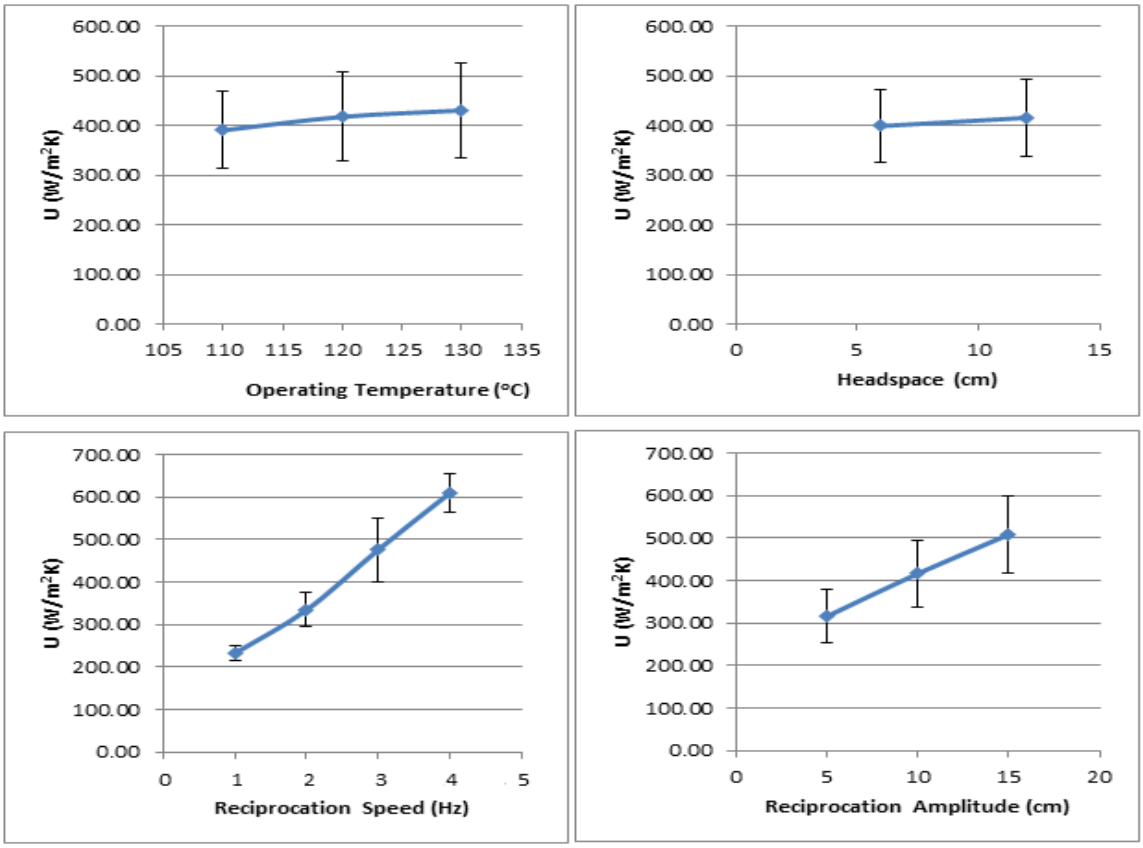

Fig. 6.1. Overall heat transfer coefficient (U), as influenced by retort temperature, reciprocation speed, reciprocation amplitude and headspace in cans filled with single particle

6.4.2 Influence of processing conditions on h_{fp}

Depending on experimental conditions, the fluid-to-particle heat transfer coefficient, h_{fp}, ranged from 320 to 1410 W/m^{2}K. Tables 6.2 and 6.3 summarize average h_{fp}, values for all the processing conditions. Analysis of variance showed that except for headspace, all other factors studied affected h_{fp}, values significantly (Tables 6.4 and 6.5). Two-way interaction effects of only reciprocation frequency with itself, retort temperature and reciprocation amplitude were significant in this case. Also, like U, the effects of interactions were of a lower magnitude and hence, only main effects are shown in Fig. 6.2. Higher h_{fp} values were obtained at higher levels of all four parameters. The mean h_{fp}, value increased by about 16% with an increase in the retort temperature from 110 to 130 ºC. Increasing reciprocation frequency from 1 to 2 Hz improved the mean h_{fp} value by 40%, and by about 137% from 1 to 4 Hz, probably due to increased particle-liquid relative velocity at the higher reciprocation frequency.

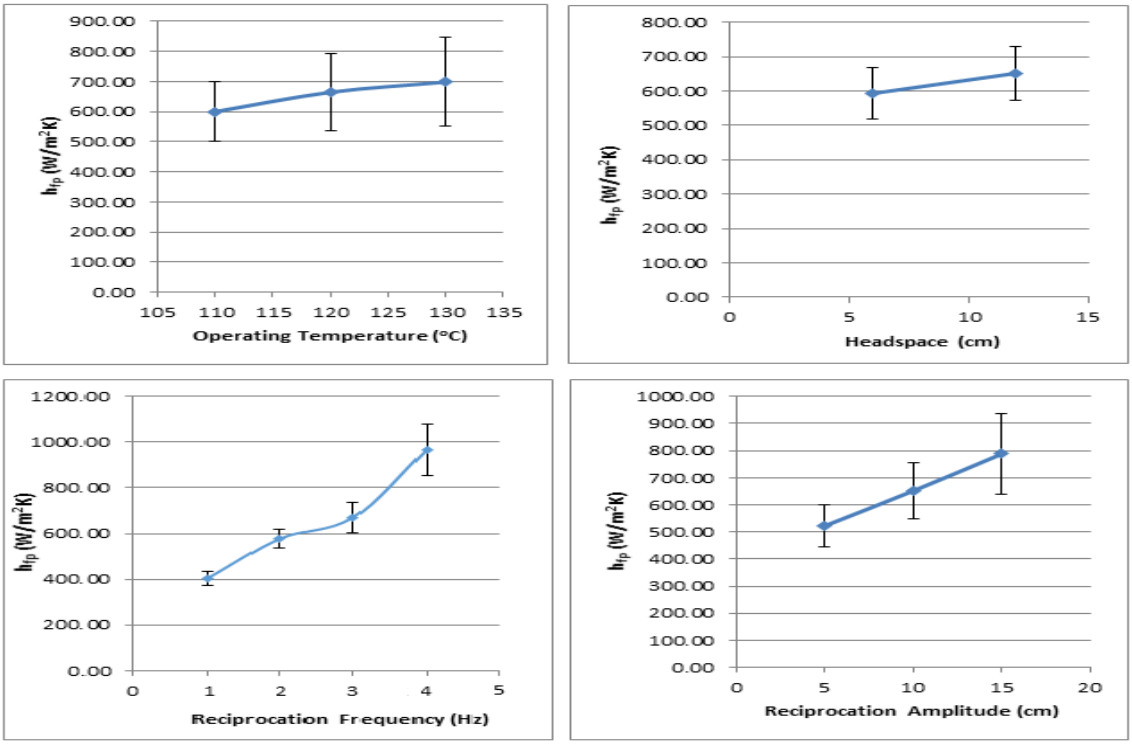

Fig. 6.2 Fluid-to-particle heat transfer coefficient (h_{fp}), as influenced by retort temperature, reciprocation speed, reciprocation amplitude and headspace in cans filled with single particle

The effect of amplitude of reciprocation on h_{fp} was also prominent, though less than reciprocation frequency. Increasing the amplitude of reciprocation from 5 to 15 cm improved the mean h_{fp} values by about 24% and a further increase from 15 to 25cm improved the h_{fp} by about 20%. The headspace and its interactions did not have a significant effect ($p>0.05$) on the h_{fp} values, unlike U. This may be because the particle-liquid relative velocity was not affected by the bubble space to a large extent. In most of the cases, the increase of headspace from 6 to 12 mm showed a very marginal increase in the value of h_{fp}. This is because, with an increase in headspace, the size of the bubble increased, leading to increase in the liquid velocity and turbulence. However, this resulted in increased values of U, although it was not reflected much on the h_{fp} values. The developed correlations are given as Equations (6.3-6.4).

$$h_{fp}\left(\frac{W}{m^2K}\right) = -942.93 + 29.32T - 449.40F - 32.92A - 0.152T^2 + 30.60F^2 - 0.034A^2 + 3.30(T.F) + 0.26(T.A) + 5.41(F.A) \qquad R^2 = 0.92 \qquad (6.3)$$

$$h_{fp}\left(\frac{W}{m^2K}\right) = 749.11 - 4.14T - 52.27F - 41.50H + 1.38(T.F) - 0.033(T.H) + 4.56(F.H) \qquad R^2 = 0.87 \qquad (6.4)$$

Table 6.4. Analysis of variance showing the influence of retort temperature, reciprocation frequency and reciprocation amplitude on U and $h_{fp.}$ of cans filled with single particle

Source	U			h_{fp}		
	Type III SS	**F Value**	**Pr > F**	**Type III SS**	**F Value**	**Pr > F**
Model	9.8E+05	61.43	< 0.0001 **	2.0E+06	72.62	< 0.0001 **
Temp. (T)	9689	5	0.027 *	57878	18	0.0002 *
Freq. (F)	7.2E+05	407	< 0.0001 **	1.4E+06	450	< 0.0001 **
Amp. (A)	2.2E+05	124	< 0.0001 **	4.2E+05	132	< 0.0001 **
TXT	415	0.2	0.63	1856	0.5	0.45
FXF	2250	1.2	0.27	33480	10	0.0032 *
AXA	156	0.08	0.76	93	0.03	0.86
TXF	4871	2	0.11	32303	10	0.0037 *
TXA	1676	0.9	0.34	11087	3	0.072
FXA	17621	9	0.0042 *	88229	27	< 0.0001 **

**** p<0.0001 * p<0.05**

Table 6.5. Analysis of variance showing the influence of retort temperature, reciprocation frequency and headspace on U and h_{fp} of cans filled with single particle

Source	U			h_{fp}		
	Type III SS	**F Value**	**Pr > F**	**Type III SS**	**F Value**	**Pr > F**
Model	5.0E+05	255	< 0.0001 **	7.5E+05	11.70	< 0.0001 **
Temp. (T)	3398	10	0.0052 *	8381	0.7	0.38
Freq. (F)	4.9E+05	1506	< 0.0001 **	7.1E+05	66	< 0.0001 *
Head. (H)	1.6E+03	5	0.037 *	20704	1	0.18
TXF	3250	9	0.0060 *	3779	0.3	0.55
TXA	67	0.2	0.65	1593	0.1	0.70
FXA	500	1	0.23	5594	0.5	0.47

**** p<0.0001 * p<0.05**

6.4.3 Influence of product properties on U

Fig. 6.3a summarizes the mean overall heat transfer coefficients for propylene, Teflon and Nylon obtained at different reciprocation frequencies using fluids of different concentrations. U values for propylene varied from 270 - 1150 W/m^{2}K, for nylon from 300-1240 W/m^{2}K and for Teflon from 290-1110 W/m^{2}K, depending on the concentration/viscosity of the glycerin used and reciprocation frequency. Analysis of variance of data depicted in Table 6.6 revealed that both liquid viscosity/concentration and reciprocation frequency effects were highly significant ($p<0.0001$). Particle density effects (achieved based on using different spherical particles) and interactions involving particle density were however, not significant ($p>0.05$). The viscosity-reciprocation frequency interaction effect was significant (Table 6.6) and their relative effects are shown in Fig. 6.4.

Table 6.6. Analysis of Variance Results for U and h_{fp} of cans filled with single particle as affected by particle density, reciprocation frequency and liquid viscosity

Source	U			h_{fp}		
	Type III SS	**F Value**	**Pr > F**	**Type III SS**	**F Value**	**Pr > F**
Model	1.9E+06	110	< 0.0001 **	8.79E+06	9	< 0.0001 **
Particle Type (P)	4736	1	0.32	1.77E+06	8	0.0022 *
Frequency (F)	8.2E+05	417	< 0.0001 **	3.10E+06	29	< 0.0001 **
Liquid Conc. (LC)	1.0E+06	507	< 0.0001**	1.96E+06	18	0.0003 *
PXF	3358	0.8	0.44	5.75E+05	2	0.08
PXLC	1151	0.3	0.75	5.95E+05	2	0.08
FXLC	1.3E+05	69	< 0.0001 **	7.80E+05	7	0.0132 *

**** p<0.0001 * p<0.05**

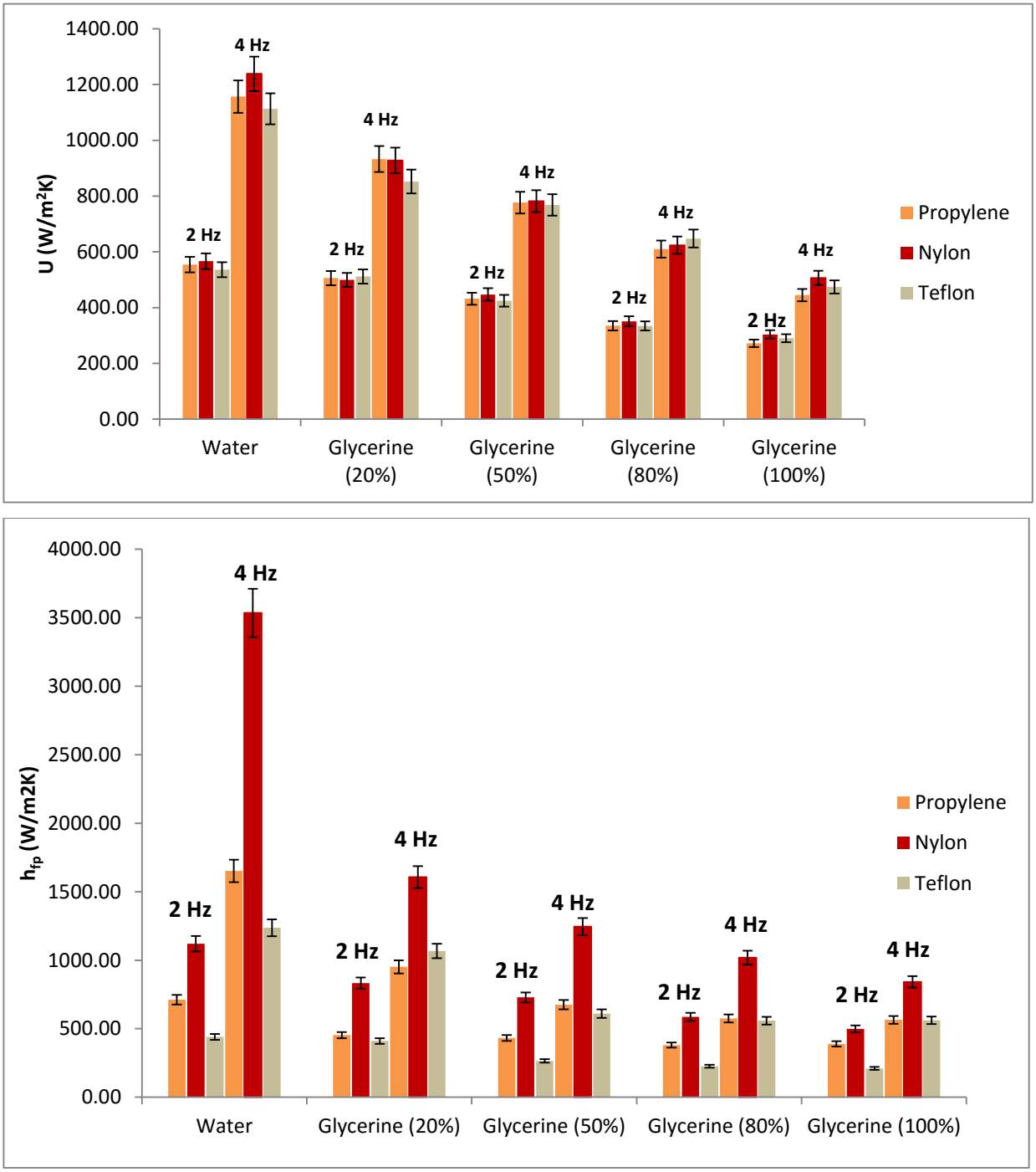

Fig. 6.3. Effect of particle type, liquid concentration/viscosity and reciprocation speed in cans filled with single particle on a) Overall Heat Transfer Coefficient (U), b) Fluid-to-particle Heat Coefficient (h_{fp})

From Fig. 6.4, it is clear that the overall heat transfer coefficient increases with an increase in the reciprocation frequency and a decrease in liquid viscosity (glycerin concentration). The increase in overall heat transfer coefficient, with increasing reciprocation frequencies, can be explained by the enhanced mixing (caused by the rapid back and forth motion of the reciprocating cage) which results in a higher degree of turbulence. When the reciprocation frequency increased from 2 to 4 Hz, the U value increased by 53% for water and by 39% for pure glycerin (100%). This suggested that higher reciprocation frequency led to a better heat transfer situation, and thereby a faster heat transfer situation could be achieved.

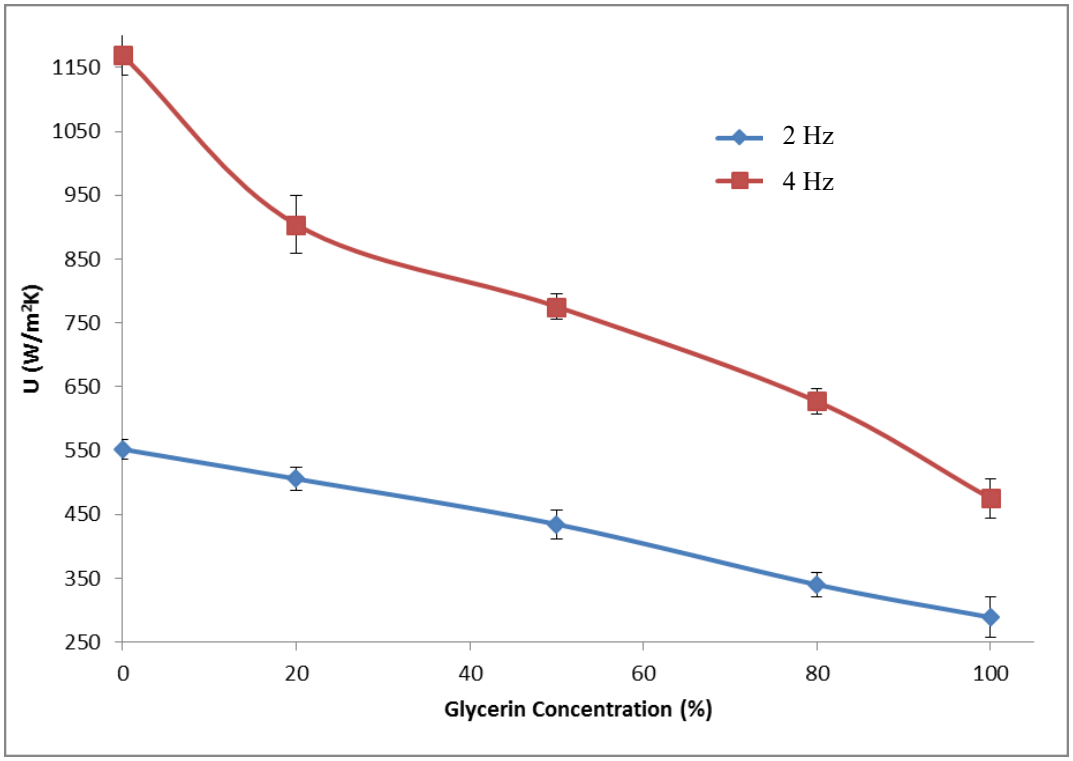

Fig. 6.4. Overall heat transfer coefficient (U) as affected by the liquid viscosity and reciprocation frequency in cans filled with single particle.

The fluids of higher viscosity generally had lower heat transfer coefficient. U value for water (0% glycerin) was the highest and the average U values for the three types of particles studied were recorded around 552 W/m^{2}K at 2 Hz reciprocation frequency. With increase in viscosity from 0.001 Pa.s (0% glycerin) to 0.011 Pa.s (50% glycerin), the U values decreased by 21%. Further increase of liquid viscosity from 0.011 Pa.s to 0.94 Pa.s (100% glycerin) led to 34%

reduction in U values. For low viscosity liquids like water and 20% glycerin, the higher values of U can be attributed to the presence of a smaller thickness of boundary layer with water.

It was found that the U-values were almost same for the different densities of particles. Although, the particle motion has an important effect on the overall heat transfer coefficient, and particles with different density and volume fractions may alter the flow pattern of the can liquid. However, in the present case particle density did not influence U; this was possibly due to the presence of a single particle, which did not affect the mixing much. Hence, the overall heat transfer coefficients were unaffected.

The developed correlations for U for the three particles are given in Equations (6.5-6.7):

Polypropylene: $U\left(\frac{W}{m^2K}\right) = 18.03 + 0.75LC + 273.63F - 1.81(LC.F)$ $R^2 = 0.95$ (6.5)

Nylon: $U\left(\frac{W}{m^2K}\right) = 9.94 + 0.83LC + 282.69F - 1.78(LC.F)$ $R^2 = 0.94$ (6.6)

Teflon: $U\left(\frac{W}{m^2K}\right) = -2.23 + 1.39LC + 267.08F - 1.83(LC.F)$ $R^2 = 0.98$ (6.7)

6.4.4 Influence of product properties on h_{fp}

Depending on experimental conditions, the fluid-to-particle heat transfer coefficient, h_{fp}, ranged from 380-1650 W/m^{2}K, 499-3530 W/m^{2}K and 210-1230 W/m^{2}K for propylene, nylon and Teflon respectively. Figure 6.3b summarizes average h_{fp} values under different processing conditions. Analysis of variance showed that while reciprocation frequency affected h_{fp} very significantly ($p < 0.001$), liquid viscosity and particle density also affected it slightly ($p<0.05$) (Table 6.6). Two-way interaction effects of viscosity and reciprocation were also slightly significant ($p < 0.05$).

The effect of viscosity and reciprocation frequency on h_{fp} values was similar to that observed with U. Fig. 6.3b demonstrates that, under all processing conditions, h_{fp} values were higher with the lower viscosity liquid; again this is possibly due to the associated lower thickness of the boundary layer. The increase in the h_{fp} values, as liquid viscosity decreased, can also be

associated with a higher particle-to-liquid relative velocity. With decrease in viscosity, the relative velocity increases because in a lower viscosity fluid, the particles can move more freely inside the liquid. Hence, higher rate of heat transfer takes place from the liquid to the particle, thereby resulting in higher values of h_{fp}. However, the decrease of h_{fp} with increasing viscosity was more pronounced with Nylon, yet it had higher values than PP and Teflon under all conditions. However, for Teflon and propylene, at higher viscosities (between 80% and 100% glycerin), the h_{fp} values were almost the same.

Fig. 6.5 presents a plot of variation of h_{fp} with glycerin concentration as affected by the particle type. Amongst the three particle densities studied, it was observed that h_{fp} followed the following trend: Nylon > Polypropylene> Teflon. It is also shown that the heating rate index of the particles, $f_{h\text{-}p}$ followed the following trend: polypropylene < Nylon < Teflon. Thus, it is seen that although polypropylene was heated fastest, Nylon particles had the highest heat transfer coefficient. These discrepancies between the trends in the heat transfer coefficient and the heating rate was explained by their correlation with thermal diffusivity and thermal effusivity of the particles. The value of thermal diffusivity depicts the rate at which a particle adjust to the external temperature change, while thermal effusivity is its ability to exchange thermal energy with its surroundings. It is clear from the values of thermal diffusivity of the substances given in Table 6.1 that the thermal diffusivity of polypropylene is the highest and that of Teflon is the lowest. Hence, since the thermal diffusivity of propylene is highest, its heating rate was fastest and thereby it exhibited the lowest heating rate index. Also, due to the same reason, Teflon exhibited the highest heating rate index or the slowest heating rate. However, h_{fp} is indicative of the heat flux which is flowing through the body. It is not necessary that a body with the highest heating rate will be the body with the highest heat transfer coefficient. The trend in heat transfer coefficient correlated better with thermal effusivity. Thermal effusivity is given as square root of the product of heat capacity, thermal conductivity and particle density, and measures the rate at which a material can absorb heat. Thus, it can be seen that Nylon (=929 $J/m^2Ks^{0.5}$) has the highest thermal effusivity. It must be mentioned that, although heat transfer coefficient is independent of material properties, its apparent dependence on thermal effusivity may be attributed to the fact that U and h_{fp} measured here are not instantenous, but depict an average value derived from a lumped model. Some factors such as surface-liquid interactions vary with particle type and are often included into the value of

U and h_{fp}. Hence U and h_{fp} are found a function of some particle properties. Further, other particles observed some obstruction in the free heat transfer as their motion were restricted due to the density difference existing between them and the liquid used. Teflon, which is denser than glycerin, sunk at the bottom; while polypropylene, which is lighter, floated at the top. Thus, there motion was inhibited. However, in a multiple particle scenario, a different trend can be observed, as the presence of a bulk of particles will affect the motion of the particles.

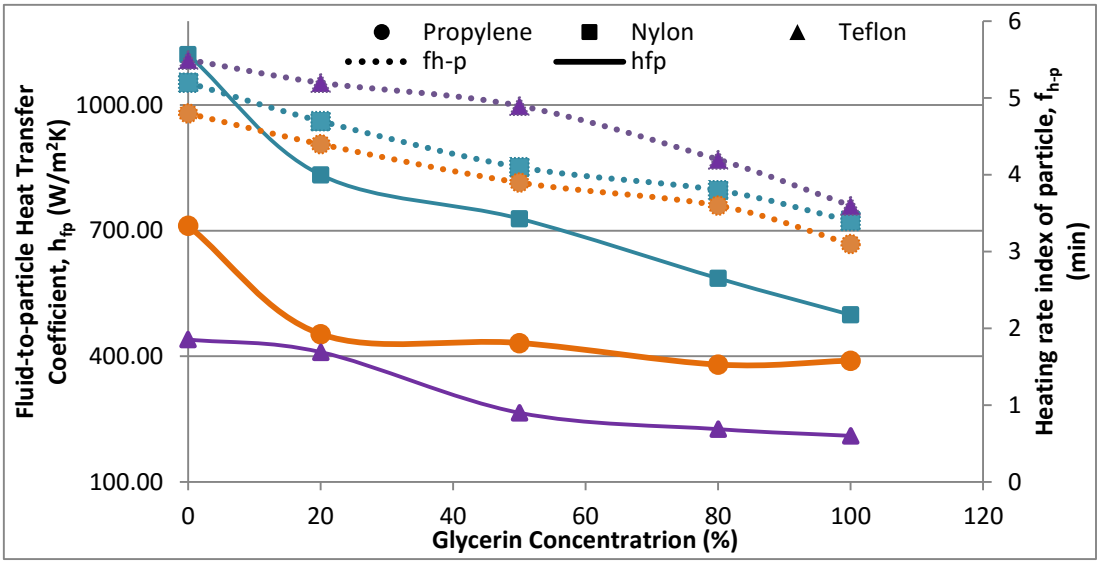

Fig. 6.5. Effect of liquid viscosity and particle density on fluid-to-particle heat transfer coefficient, h_{fp} and heating rate index of particle $f_{h\text{-}p}$ for cans filled with single particle and processed at 2 Hz frequency.

The developed correlations for U for the three particles are given in Equations (6.8-6.10):

$$\text{Polypropylene: } h_{fp}\left(\frac{W}{m^2K}\right) = -283.89 + 6.93LC + 423.6F - 4.28(LC.F) \quad R^2 = 0.83 \quad (6.8)$$

$$\text{Nylon: } h_{fp}\left(\frac{W}{m^2K}\right) = -96.37 - 0.92LC + 666.67F - 4.33(LC.F) \quad R^2 = 0.82 \quad (6.9)$$

$$\text{Teflon: } h_{fp}\left(\frac{W}{m^2K}\right) = -7.78 + 7.15LC + 333.33F - 4.38(LC.F) \quad R^2 = 0.87 \quad (6.10)$$

6.5 Conclusions

Both heat transfer coefficients (U and h_{fp}) were influenced significantly by reciprocation frequency, reciprocation amplitude, operating temperature and liquid viscosity. Headspace affected only U, while particle density affected only h_{fp}. It was observed that reciprocation frequency followed by reciprocation amplitude and liquid viscosity was the most significant parameter affecting the values of U and h_{fp}. The relative magnitude of U and h_{fp} value, under the different processing conditions, varied depending on the combined effect of particle motion, particle-to-liquid relative velocity, and level of liquid mixing during reciprocation. In general, higher U and h_{fp} values were obtained at lower liquid viscosity, higher reciprocation frequency, higher reciprocation amplitude, higher operating temperature, and higher headspace. Nylon particles had highest fluid-to-particle heat transfer coefficient, h_{fp}, as it was free to move throughout the can due to similar density with that of the medium. On the other hand, U values for different particle types was not significantly different, as a single particle within the can did not affect the heat transfer at the can wall significantly. However, these results, particularly the effect of particle type, may vary significantly in case of multiple particles. Yet, this study helped in obtaining an overall understanding of the phenomenon of heat transfer at the can wall, and some insight into the heat transfer at liquid-particle interface. The overall heat transfer coefficient (U) obtained in this study can be directly utilized for modeling liquid-only scenarios, as a single particle would not create noticeable difference in the U values.

PREFACE TO CHAPTER 7

In Chapter 6, the effect of various processing conditions and product properties on cans filled with a single particle was discussed so as to get information for liquid only-type of situation and at the same time providing unlimited heat transfer conditions for the single particle used in the can. Chapter 7 focusses on the scenario when cans are filled with multiple particles (more practical).

Effects of various processing conditions (temperature, frequency, headspace) and product properties (liquid viscosity, particle concentration, particle density) on heat transfer coefficients (U and h_{fp}) are studied for cans filled with multiple particles and subjected to reciprocating agitation thermal processing. This study will be helpful in understanding the effect of various processing scenarios for different types of products on the amount of heat transfer occurring in the system.

Parts of this chapter have been presented in the the form of an oral presentation at The Northeast Agricultural and Biological Engineering Conference (NABEC) held on July 27-30 at Kemptville, Ontario.

Parts of this chapter have been presented in the form of a poster presentation at 17th World Congress of Food Technology & Expo, IUFOST-2014 held on August 17-21, 2014 in Montreal, Quebec.

Parts of this chapter have been submitted for publication as an article "*Optimization of heat transfer and reciprocation intensity during thermal processing of liquid particulate mixtures undergoing reciprocating agitation*" in Innovative Food Science & Emerging Technologies.

The experimental work and data analysis was carried out by the candidate under the supervision of Dr. H. S. Ramaswamy.

CHAPTER 7

EFFECT OF PROCESSING CONDITION AND PRODUCT PROPERTIES ON HEAT TRANSFER COEFFICIENTS DURING RECIPROCATING AGITATION THERMAL PROCESSING: STUDIES WITH PARTICULATE MIXTURES INVOLVING MULTIPLE PARTICLES

7.1 Abstract

Effects of various processing conditions (temperature, frequency, and headspace) and product properties (liquid viscosity, particle concentration, and particle density) on heat transfer coefficients (U and h_{fp}) during sterilization of reciprocating cans with multiple particle - fluid mixtures were studied. To study the effect of processing conditions, different operating temperatures (110-130 ^{o}C), reciprocating frequencies (0.3-3.6 Hz) and can headspace (5-15 mm) were employed according to a central composite rotatable design. Effect of product properties was studied using a full-factorial design comprising 3 levels of liquid viscosity (obtained from 0, 50 & 100% glycerin concentration), 4 levels of particle concentration (single, 15, 30 & 45% v/v), 3 levels of particle density (830, 1130 & 2210 kg/m^3 for polypropylene, Nylon and Teflon particles respectivelly) and 3 levels of reciprocating frequency (1, 2 & 3 Hz). In general, U & h_{fp} values were found to be higher than those with single particle scenario discussed in Chapter 6. Reciprocating frequency had the most significant impact on extent of heat transfer, followed by headspace and operating temperature respectively. For different particle densities studied, U & h_{fp} followed the trend: Nylon>polypropylene>Teflon. For different liquid viscosities, U & h_{fp} were higher for thinner fluids due to lower effects of viscous forces as compared to inertial forces. U & h_{fp} were found to increase with increasing particle concentration, however, beyond a certain concentration, U & h_{fp} decreased pehaps due to dominance of conduction based heating.

7.2 Introduction

Heat transfer rates to canned food products, such as liquid containing discrete particles, can be increased by mechanical agitation. This has permitted the use of high temperature short time (HTST) concepts for particulate fluids by employing agitation processing. Thermal processing schedule for canned foods has been traditionally established using experimental heat penetration data. In recent years, increased interest in mathematical modeling has prompted further attention to the mechanism of heat transfer in particulate food systems. Theoretical models can be used for

the design, optimization and validation of such food systems. However, the usefulness of theoretical models depends on the accuracy of the input physical parameters. The overall heat transfer coefficient from the heating medium to the can liquid (U) and the fluid-to-particle heat transfer coefficient (h_{fp}) are two important parameters, along with thermo-physical properties of food materials that are needed for these predictions.

The overall heat transfer coefficient (U) and the fluid-to-particle heat transfer coefficient (h_{fp}) in cans are influenced by various environmental conditions and physical properties of the liquid and particles. Several researchers have quantified the effect of various processing conditions and product properties on U and h_{fp} in still mode of thermal processing (Alhamdan and Sastry, 1990; Awuah *et al.*, 1995; Cariño-Sarabia and Vélez-Ruiz, 2013) and in various other modes of agitation such as during end-over-end rotation (Stoforos and Merson, 1991; Ramaswamy *et al.*, 1993; Garrote *et al.*, 2006; Meng and Ramaswamy, 2007a), oscillatory rotation (Sablani and Ramaswamy, 1999), and axial and biaxial rotation (Dwivedi and Ramaswamy, 2010; Ramaswamy and Dwivedi, 2011; Hassan *et al.*, 2012) of the containers. These studies have found that operating temperature, agitation speed, mode of agitation, container headspace, liquid viscosity, particle concentrations, particle density, particle shapes, particle sizes etc. significantly affect U and h_{fp} and therefore are important parameters for which data need to be evaluated under practical conditions in order to be considered for predicting optimal conditions for any mode of thermal processing. However, for reciprocating agitation, there are limited number of studies available. Although, some work has been conducted for evaluating the effects of some process variables during reciprocating agitation thermal processing in Chapter 5 (reciprocating frequency, reciprocating amplitude, container orientation, headspace etc.), yet a more detailed and extensive study is needed to understand the effect of other processing conditions and product properties.

Systematic effect of processing conditions and product properties on associated convective heat transfer coefficient, in liquid-only cans fitted with a single particle, was reported in Chapter 6. This chapter shall highlight the effect of these processing conditions (temperature, frequency, and headspace) and product properties (liquid viscosity, particle concentration, and particle density) on the associated heat transfer coefficients with multiple particles in liquid filled cans subjected to reciprocating agitation processing.

7.3 Materials and Methods

7.3.1 Materials

The vertical retort, modified in Chapter 3 to include a reciprocating mechanism, was used in this study. Sterilization studies were conducted on 307x409 cans (Home Canning Co., Montreal, QC) placed in the reciprocating cage with horizontal axis along the axis of reciprocation. Various concentrations of Glycerin (Fisher Scientific, Montreal, PQ) were used to simulate various levels of liquid viscosity encountered in real liquid foods. 19 mm spheres of Teflon, Nylon and Polypropylene (Small Parts Inc., Miami, FL) were used as model food particles simulating the heating behavior of real foods. The thermo-physical properties of these model materials were listed in Chapter 6. Flexible thin-wire thermocouples were used to measure particle-center temperatures, while needle-type thermocouples placed at can's geometric center were used to measure liquid temperatures. The thermocouple outputs were recorded at one second intervals using a data acquisition system (HP34970A, Hewlett, Packard, Loveland, CO). The particle assembly, can preparation and data gathering were described in further details in Chapter 5.

7.3.2 Experimental Design

Test cans were subjected to thermal processing under different conditions selected by a Design Expert software based experimental design (Stat-Ease Inc, Minneapolis, Minnesota, USA). In Chapter 5, the effects of reciprocation amplitude and container orientation were highlighted; in this study, all experiments were conducted at 15 cm amplitude with cans placed horizontally with their longer axis along the axis of reciprocation.

To study the effect of processing conditions, different levels of operating temperature (110-130 ^{o}C), reciprocation frequency (0.3-3.6 Hz) and can headspace (5-15 mm) were selected according to a central composite rotatable design (CCRD) design. These experiments were conducted with 50% glycerin concentration and 19 mm Nylon spheres at 30% (v/v) particle concentration.

Effect of product properties was studied using a full-factorial designs comprising of 108 experiments by varying liquid viscosities/concentration (viz. 0.001, 0.011 & 0.94 Pa.s liquid viscosity obtained from 0, 50 & 100% glycerin concentration, respectively); particle concentration

(single, 15, 30 & 45% v/v particle concentration); reciprocation frequency (1, 2 & 3 Hz) and particle density (830, 1130 & 2210 kg/m^3 particle density obtained from Teflon, Nylon and Polypropylene particles). These experiments were performed at 121.1 ºC operating temperature and can headspace was kept as 10 mm. All experimental runs in both designs were done with duplicate experimental cans placed equidistant from the axis of reciprocation and were repeated twice.

7.3.3 Data Analysis

The U and h_{fp} values were calculated using the methodology detailed in Section 5.3.4. Mean values of the parameters from four readings (two replicates of each experiment containing two duplicate cans each) of each experimental run were taken. Regression analysis and analysis of variance (ANOVA) were carried out using Design Expert (Stat-Ease Inc, Minneapolis, Minnesota, USA) software. For this, the experimental data were fitted using a quadratic model for best fit.

7.4 Results and Discussions

7.4.1 Effect of processing conditions

Quality deterioration in a particular liquid-particulate mixture is strongly influenced by operating temperature, agitation speed and can headspace during both rotary (Sablani and Ramaswamy, 1996; Meng and Ramaswamy, 2007a, 2007b; Dwivedi and Ramaswamy, 2010b) and reciprocating (Walden and Emanuel, 2010) mode of agitation. In this study, the overall range U and h_{fp} were found to vary between 187-692 W/m^{2}K and 299-1402 W/m^{2}K respectively for 30% v/v Nylon spheres in 50% glycerin (Table 7.1). Both U and h_{fp} were significantly higher than those observed in various modes of rotary agitation (Dwivedi and Ramaswamy, 2010b). This suggests that reciprocating agitation is more effective than rotary agitation in terms of enhancing heat transfer due to strong turbulence created by rapid back and forth motion of the cans.

Table 7.1. Values of heat transfer coefficients as affected by operating temperature, headspace and frequency for cans filled with multiple particles.

Run	Operating Temperature (^oC)	Reciprocation Frequency (Hz)	Can Headspace (mm)	U [a] (W/m^2K)	h_{fp} [a] (W/m^2K)
1	120	0.3	10	187±15	299±19
2	114	1	7	354±16	490±25
3	126	1	7	368±12	502±39
4	114	1	13	336±27	472±27
5	126	1	13	350±21	487±19
6	120	2	5	545±16	813±42
7	110	2	10	518±23	749±41
8	120	2	10	526±23	762±22
9	120	2	10	523±10	763±45
10	120	2	10	527±39	779±26
11	120	2	10	525±14	780±37
12	120	2	10	527±37	763±14
13	120	2	10	523±13	776±32
14	130	2	10	515±12	776±25
15	120	2	15	501±36	735±44
16	114	3	7	664±22	1150±41
17	126	3	7	689±22	1190±65
18	114	3	13	629±25	1100±34
19	126	3	13	669±17	1140±41
20	120	3.6	10	692±32	1400±55

[a] Values presented as mean ± standard deviation

Analysis of variance of various interactions of these process parameters are presented in Table 7.2. Individual interactions of reciprocation frequency (F) and can headspace (H) and square of frequency significantly affected ($p<0.005$) both heat transfer coefficients (U and h_{fp}). Interaction of reciprocation frequency and can headspace were also significant ($p<0.05$) for h_{fp} but was not significant ($p>0.05$) for U. Individual interaction of operating temperature (T) also had a highly significant effect ($p<0.005$) on h_{fp}, but was also significant for U ($p<0.05$). Other interactions were not significant ($p>0.05$) for both U and h_{fp}. The two-way interaction of these parameters have been plotted in Figs. 7.1 and 7.2 for U and h_{fp}, respectively. Based on the total sum of squares, the order of the effects of individual variables were found to be: reciprocation frequency > can headspace > operating temperature for both U and h_{fp}.

Table 7.2. Analysis of variance for temperature, headspace and frequency effects on U and h_{fp} for cans filled with multiple particles.

Parameter	**U**			**h_{fp}**		
	Type III SS	**F Value**	**Pr>F**	**Type III SS**	**F Value**	**Pr>F**
T-Temperature	549	4.1	0.0201[b]	1466	11	0.0013[c]
F-Frequency	3.1E+05	2366	< 0.0001[c]	1.4E+06	11341	< 0.0001[c]
H-Headspace	1986	14.8	0.0032 [c]	5289	40	< 0.0001[c]
T*F	174	1.3	0.2796[a]	230	1.7	0.2130[a]
T*H	28	0.2	0.6540[a]	18	0.1	0.7155 [a]
F*H	40	0.3	0.5932[a]	610	4	0.0258[b]
T^2	0.08	0.0006	0.9805[a]	3	0.02	0.8759[a]
F^2	8618	64	< 0.0001[c]	19536	149	< 0.0001[c]
H^2	81	0.6	0.4540[a]	204	1	0.2393[a]

[a] **non-significant interaction (p>0.05)**

[b] **slightly significant interaction (0.005<p<0.05)**

[c] **significant interaction (p<0.005)**

Similar trends have also been found with end-over-end (Sablani and Ramaswamy, 1996) and axial/bi-axial modes of agitation (Dwivedi and Ramaswamy, 2010b), although some studies (Anantheswaran and Rao, 1985a; Meng and Ramaswamy, 2007a) have found headspace to be non-significant when varied over a smaller range. However, in line with this study, other researchers

(Sablani and Ramaswamy, 1996; Dwivedi and Ramaswamy, 2010a, 2010b) have also found that when headspace was varied over a larger range, it had a more significant effect than operating temperature.

A quadratic model fitted well with the experimental results with coefficient of variation of 2.27% and 1.43% for U (Equation 7.1) and h_{fp} (Equation 7.2) respectively.

$$U = 385.10 - 2.06T + 168.22F - 20.46H + 0.78(T.F) + 0.10(T.H) - 0.75(F.H) + 0.0021T^2 - 25.14F^2 + 0.27H^2 \qquad R^2 = 0.99 \qquad (7.1)$$

$$h_{fp} = 219.60 + 2.36\,T + 102.51\,F - 19.34 * H + 0.89(T.F) + 0.084(T.H) - 2.91(F.H) - 0.014T^2 + 37.86F^2 + 0.42H^2 \qquad R^2 = 0.99 \qquad (7.2)$$

Operating temperature was the most important parameter that should be taken into consideration while designing a thermal process. It is well established that lower temperatures correspond to longer process times while higher temperatures result in lower process times for achieving a target lethality, thus directly affecting the process time efficiency and quality of the final product. It was observed that the operating temperature, in addition to its effect on final process time, also significantly affected h_{fp} but had less significant effect on U. At 120 ^{o}C, 2 Hz frequency and 10 mm headspace, U and h_{fp} increased by 1-3% on increasing the temperature by 5 ^{o}C and decreased by 2-4% on a similar decrease (Figs. 7.1 and 7.2), thus showing that variation of temperature did not affect the values much. Similar enhancements in U and h_{fp} with increase in temperature have been observed in other modes of agitation (Sablani and Ramaswamy, 1996; Ramaswamy and Dwivedi, 2011) due to increase in convection at higher temperatures. It must be noted that for real fluid foods (other than juices and beverages), which are thixotropic non-Newtonian fluids, the magnitude of increase of U and h_{fp} at higher temperatures during reciprocating agitation will be larger compared to this study (using glycerin a Newtonian fluid), due to reduction in viscosity of such fluids under agitation (Meng and Ramaswamy, 2007a). Thus, intensive turbulence during reciprocation will further aid heat transfer coefficient enhancement associated with temperature increase.

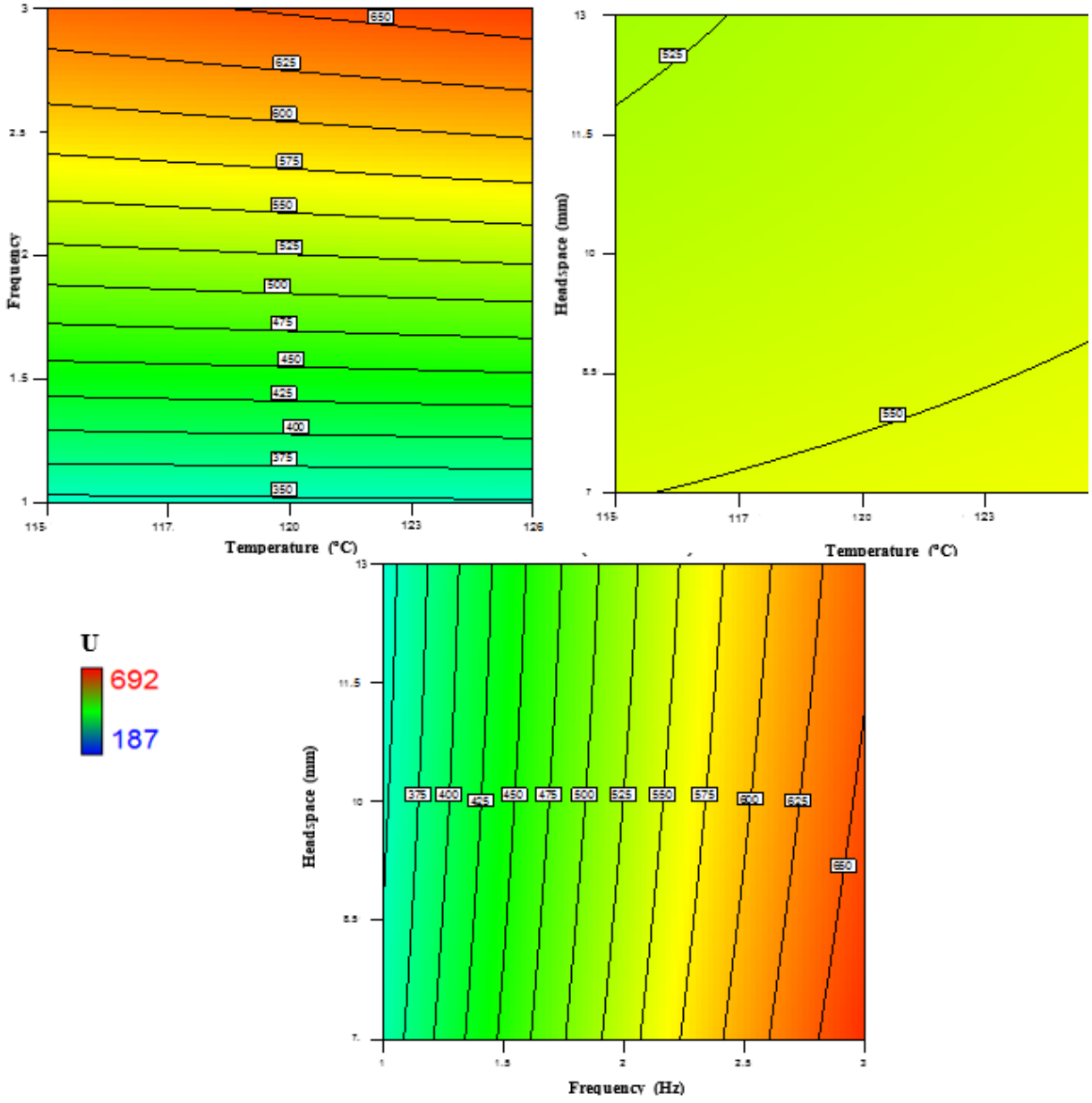

Fig. 7.1. Effect of operating temperature, reciprocation frequency and can headspace on overall heat transfer coefficient (U) for cans filled with multiple particles.

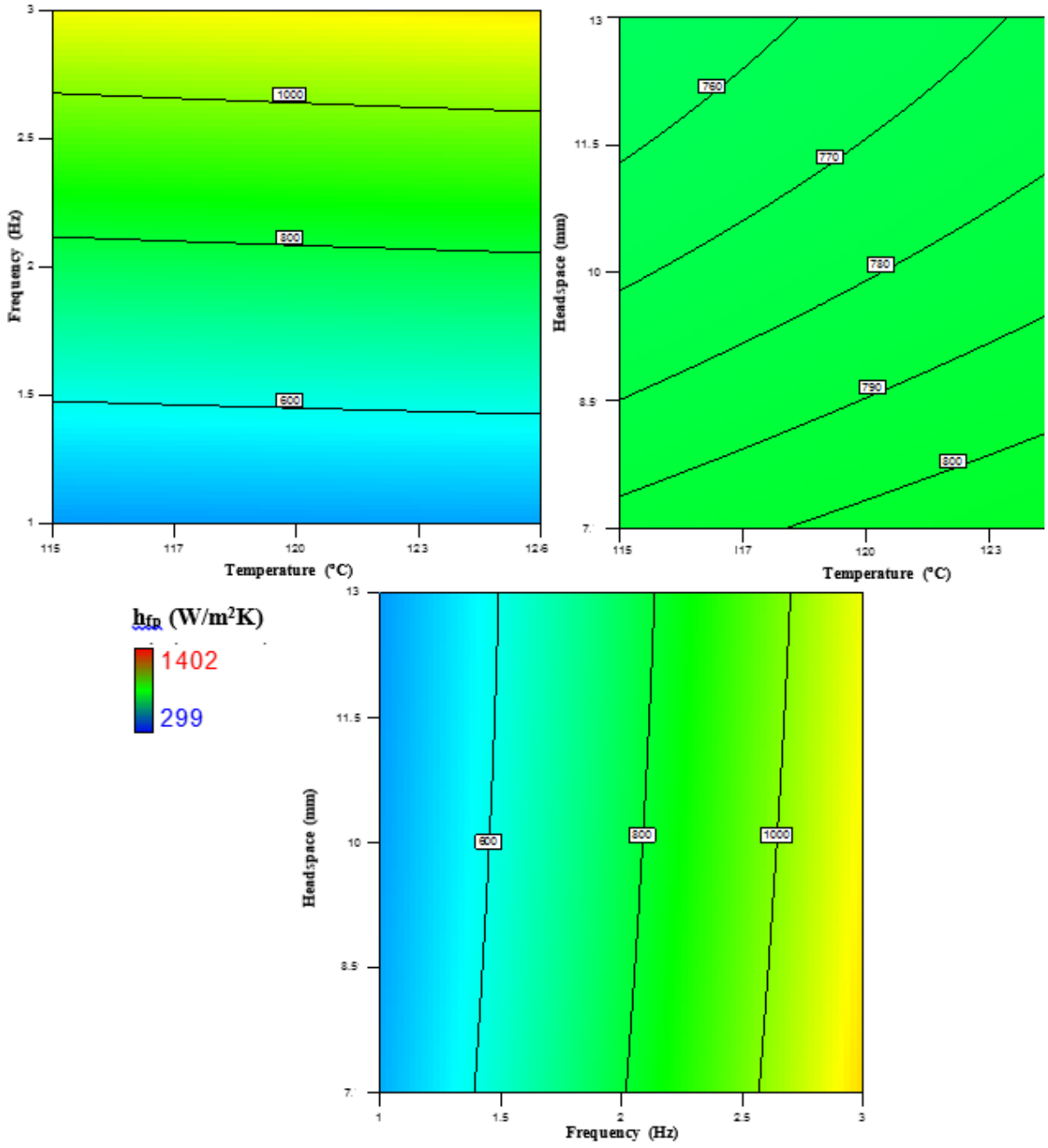

Fig. 7.2. Effect of operating temperature, reciprocation frequency and can headspace on fluid to particle heat transfer coefficient (h_{fp}) for cans filled with multiple particles.

As expected, an increase in agitation frequency resulted in an increase in U and h_{fp}, due to increased turbulence created by higher collisions amongst particles and resulting in an increase in the associated Reynold's number. Doubling of reciprocation frequency from 1 to 2 Hz, resulted in 45-54% increase in U and 58-63% increase in h_{fp}, and tripling from 1 to 3 Hz, resulted in 88% increase in U and 139% increase in h_{fp}. The extent of increase in U and h_{fp} on doubling and tripling of agitation speed is larger in reciprocating agitation than rotary modes of agitation (Sablani and Ramaswamy, 1996; Dwivedi and Ramaswamy, 2010b). At higher frequency, the direction of motion of the liquid and particles changed rapidly resulting in a higher degree of turbulence, which led to increased heat transfer. Thus, the Nusselt number at the can wall and at the liquid particle interface increases with frequency, which is similar to the results of Garrote *et al.* (2006) on canned peas subjected to end over end sterilization.

With an increase in can headspace, on the other hand, U and h_{fp} values generally decreased. This decrease was more prominent at lower reciprocation frequency and lower temperatures (Figs. 7.1 and 7.2). Similar effect of increasing headspace have been obtained by other researchers (Ramaswamy and Grabowski, 1996; Mohamed, 2007; Erdogdu and Tutar 2011). This happens mainly due to the insulating effect of air in the headspace bubble (Mohamed, 2007). However, it must be noted that compared to no headspace situation, heat transfer in presence of headspace is higher, as headspace is necessary for effective agitation of liquid inside the container (Ramaswamy and Grabowski, 1996). Headspace effect was less significant at higher frequency as the role of headspace decreased on intensive shaking produced by rapid back and forth motion of containers. Effect of headspace was more significant on h_{fp}, than on U, as increase of particle motion (due to turbulence created in liquid in presence of headspace) augmented heat transfer better at liquid-particle interface than that at the can wall.

7.4.2 Effect of product properties

Table 7.3 summarizes mean overall heat transfer coefficients (U) and fluid to particle heat transfer coefficients (h_{fp}) for propylene, Teflon and Nylon obtained at different frequencies (F) for different glycerin concentration (LC) and particle concentrations (PC) studied. U values for propylene, Nylon and Teflon varied from 175-915 W/m^{2}K, 185-1089 W/m^{2}K and 95-545 W/m^{2}K respectively depending on experimental conditions. Thus, the order of values generally followed

the trend: Nylon>polypropylene>Teflon. A similar trend was observed, with higher values, for h_{fp} which ranged from 252-1040 W/m^{2}K, 267-1190 W/m^{2}K and 143-654 W/m^{2}K for polypropylene, Nylon and Teflon, respectively. Analysis of variance (Table 7.4) revealed that for U, individual and squares of interactions of liquid viscosity/concentration (LC) and particle concentration (PC) were significant ($p<0.05$) for all three particle densities (PD) studied. Apart from this, individual interaction of frequency and its two-way interaction with LC were also significant ($p<0.05$). Similar trends were observed with h_{fp} for all three PD, the only exception being that individual interaction of PC was not significant ($p > 0.05$). A quadratic model fitted well with the experimental results with coefficient of variation of 7.31%, 8.37% and 5.78% for U values of polypropylene (Equation 7.3), Nylon (Equation 7.4) and Teflon (Equation 7.5) respectively, and that of 5.91%, 6.35% and 5.89% for h_{fp} values of polypropylene (Equation 7.6), Nylon (Equation 7.7) and Teflon (Equation 7.8) respectively.

$$U_{polypropylene} = 179.76 - 4.97\mathrm{LC} + 12.84\mathrm{PC} + 165.59\mathrm{F} - 0.006(\mathrm{LC.PC}) - 0.96(\mathrm{LC.F}) + 0.21(\mathrm{PC.F}) + 0.04LC^2 - 0.26PC^2 + 3.28F^2 \qquad R^2 = 0.98 \qquad (7.3)$$

$$U_{Nylon} = 156.256 - 5.14\mathrm{LC} + 17.44\mathrm{PC} + 207.71\mathrm{F} - 0.01(\mathrm{LC.PC}) - 1.13(\mathrm{LC.F}) - 0.04(\mathrm{PC.F}) + 0.04LC^2 - 0.35PC^2 + 0.68F^2 \qquad R^2 = 0.97 \qquad (7.4)$$

$$U_{Teflon} = 79.69 - 3.02\mathrm{LC} + 6.86\mathrm{PC} + 131.15\mathrm{F} - 0.01(\mathrm{LC.PC}) - 0.54(\mathrm{LC.F}) + 0.11(\mathrm{PC.F}) + 0.02LC^2 - 0.14PC^2 - 4.26F^2 \qquad R^2 = 0.98 \qquad (7.5)$$

$$h_{fp-polypropylene} = 389.07 - 7.02\mathrm{LC} + 11.53\mathrm{PC} + 145.14\mathrm{F} - 0.01(\mathrm{LC.PC}) - 0.91(\mathrm{LC.F}) + 0.11(\mathrm{PC.F}) + 0.05LC^2 - 0.25PC^2 + 4.64F^2 \qquad R^2 = 0.98 \qquad (7.6)$$

$$h_{fp-Nylon} = 359.78 - 7.48\mathrm{LC} + 15.89\mathrm{PC} + 229.62\mathrm{F} + 0.01(\mathrm{LC.PC}) - 1.07(\mathrm{LC.F}) - 0.57(\mathrm{PC.F}) + 0.05LC^2 - 0.33PC^2 - 5.59F^2 \qquad R^2 = 0.97 \qquad (7.7)$$

$$h_{fp-Teflon} = 191.30 - 4.24\mathrm{LC} + 5.11\mathrm{PC} + 137.43\mathrm{F} + 0.01(\mathrm{LC.PC}) - 0.58(\mathrm{LC.F}) - 0.02(\mathrm{PC.F}) + 0.03LC^2 - 0.12PC^2 - 3.07F^2 \qquad R^2 = 0.97 \qquad (7.8)$$

Table 7.3. Values of heat transfer coefficients as affected by liquid viscosity (from different glycerin concentrations), particle concentration and frequency for different particle densities (from Polypropylene, Nylon, Teflon) studied.

No.	Glycerin conc. (%)	Particle Conc. (%v/v)	Frequency (Hz)	Polypropylene		Nylon		Teflon	
				U (W/m^2K)	h_{fp} (W/m^2K)	U (W/m^2K)	h_{fp} (W/m^2K)	U (W/m^2K)	h_{fp} (W/m^2K)
1	0	Single	1	338±23	512±26	357±35	553±44	195±2	305±14
2	0	Single	2	502±11	690±40	536±7	766±17	307±24	440±64
3	0	Single	3	675±17	834±65	765±28	996±20	428±6	563±64
4	0	15	1	463±30	648±42	517±29	719±49	274±11	373±24
5	0	15	2	678±22	849±37	748±3	921±37	416±19	520±10
6	0	15	3	899±11	1010±43	1005±15	1190±64	523±34	655±25
7	0	30	1	499±35	677±38	584±13	792±48	284±33	358±34
8	0	30	2	724±13	881±32	809±20	989±26	417±16	508±41
9	0	30	3	915±20	1040±43	1090±39	1190±17	545±9	640±19
10	0	45	1	390±14	526±55	443±19	601±64	226±25	308±36
11	0	45	2	576±11	698±60	592±16	739±56	352±13	429±23
12	0	45	3	759±24	877±53	811±24	925±22	466±14	542±34
13	50	Single	1	218±11	319±30	222±32	333±14	113±6	174±22
14	50	Single	2	285±19	373±45	341±26	475±25	186±26	265±44
15	50	Single	3	394±29	483±43	443±9	564±59	254±29	337±18
16	50	15	1	266±25	360±39	317±28	420±46	165±4	218±33
17	50	15	2	402±28	476±62	468±24	574±41	260±11	320±50
18	50	15	3	536±38	615±41	607±20	683±13	342±18	398±35

19	50	30	1	306±38	394±27	346±2	453±57	166±5	216±22
20	50	30	2	436±15	507±14	526±4	618±27	258±17	310±10
21	50	30	3	572±22	630±12	655±33	732±11	331±17	391±41
22	50	45	1	231±23	315±29	236±32	326±26	127±33	178±39
23	50	45	2	316±38	383±29	353±15	437±66	201±2	249±51
24	50	45	3	422±27	490±15	451±30	527±29	263±28	310±55
25	100	Single	1	175±27	252±21	185±24	262±30	96±35	143±46
26	100	Single	2	241±30	304±1	283±31	356±14	160±28	210±22
27	100	Single	3	326±19	393±4	358±39	437±54	211±6	270±53
28	100	15	1	221±17	288±8	263±30	336±23	139±35	179±70
29	100	15	2	337±21	381±37	400±26	454±20	223±19	254±58
30	100	15	3	449±38	490±3	499±16	542±11	292±16	323±35
31	100	30	1	254±22	317±32	299±10	357±70	147±7	177±34
32	100	30	2	370±23	397±33	436±19	488±44	222±39	249±20
33	100	30	3	491±38	497±37	564±26	581±28	284±8	317±27
34	100	45	1	201±24	264±17	209±32	272±66	114±38	155±55
35	100	45	2	280±14	327±17	310±3	363±64	177±15	213±57
36	100	45	3	373±12	411±15	396±38	439±27	266±12	332±51

Table 7.4. Analysis of variance for effect of temperature, headspace and frequency on U and h_{fp} for cans filled with multiple particles.

Parameter	U			h_{fp}		
	Type III SS	F Value	Pr>F	Type III SS	F Value	Pr>F
	U (polypropylene)			**h_{fp} (polypropylene)**		
LC-Glycerin conc.	5.7E+05	575	<0.0001[c]	1.0E+006	1046	<0.0001[c]
PC-Particle Conc	12418	12	0.0015 [c]	2112	2	0.1506 [a]
F-Frequency	4.4E+05	443	<0.0001[c]	3.5E+005	363	<0.0001[c]
LC*PC	664	0.6	0.4206[a]	48	0.05	0.8248 [a]
LC*F	36989	37	<0.0001[c]	33086	34	<0.0001[c]
PC*F	307	0.3	0.5827 [a]	85	0.08	0.7678 [a]
LC^2	78045	78	<0.0001[c]	1.1E+05	118	<0.0001[c]
PC^2	1.2E+05	125	<0.0001[c]	1.1E+05	115	<0.0001[c]
F^2	85	0.08	0.7710 [a]	172	0.2	0.6757[a]
	U (Nylon)			**h_{fp} (Nylon)**		
LC-Glycerin conc.	6.8E+05	417	<0.0001[c]	1.2E+06	880	<0.0001[c]
PC-Particle Conc	10996	6	0.0156[b]	1	0.001	0.9750[a]
F-Frequency	5.6E+05	341	<0.0001[c]	4.7E+05	333	<0.0001[c]
LC*PC	1130	0.6	0.4141[a]	223	0.1	0.6956 [a]
LC*F	51553	31	<0.0001[c]	46061	32	<0.0001[c]
PC*F	10	0.006	0.9361[a]	2190	1	0.2261[a]
LC^2	89093	54	<0.0001[c]	1.23E+05	86	<0.0001[c]
PC^2	2.2E+05	136	<0.0001[c]	1.97E+05	138	<0.0001[c]
F^2	3	0.002	0.9625[a]	249	0.1	0.6789[a]
	U (Teflon)			**h_{fp} (Teflon)**		
LC-Glycerin conc.	1.8E+05	805	<0.0001[c]	3.313E+05	883	<0.0001[c]
PC-Particle Conc	304	13	0.0012[c]	12	0.03	0.8569[a]
F-Frequency	1.9E+05	846	<0.0001[c]	2.191E+05	584	<0.0001[c]
LC*PC	82	0.3	0.5541[a]	1011	2	0.1125[a]
LC*F	11399	49	<0.0001[c]	13595	36	<0.0001[c]
PC*F	82	0.3	0.5527[a]	3	0.008	0.9285[a]
LC^2	28441	124	<0.0001[c]	41620	111	<0.0001[c]
PC^2	36548	159	<0.0001[c]	26723	71	<0.0001[c]
F^2	145	0.6	0.4328[a]	75	0.2	0.6579[a]

[a] **non-significant interaction (p>0.05);** [b] **slightly significant interaction (0.005<p<0.05);** [c] **significant interaction (p<0.005)**

Fig. 7.3 shows the time-temperature profile for cans filled with polypropylene, Nylon and Teflon particles at 30% (v/v) particle concentration and 50% glycerin solution, and reciprocating at 2 Hz frequency. It was seen that polypropylene particles had highest temperature rise for particle-center temperatures followed by Nylon particles; while, Teflon particles exhibited slowest heating rate. This is in sharp contrast with the observations in rotary modes of agitation (Sablani and Ramaswamy, 1997; Ramaswamy and Dwivedi, 2011), where Teflon particles were found to have highest heating rates. During end-over-end or axial rotation of cans, heavier particles like Teflon continuously fell from top to bottom of can during rotation of cage in vertical plane due to effects of gravity. However, during reciprocating motion, there was no influence of gravity, due to which Teflon particles formed clumps at the bottom of the can, even when the can was shaking at high intensity. In fact, high intensity reciprocations may further aid the formation of clumps. Thus, the heating rate for Teflon particles was observed to be lowest. On the hand, polypropylene and Nylon particles (of lower density) did not sink at bottom and were able to move freely throughout the can, and thus created higher turbulence and heating rates.

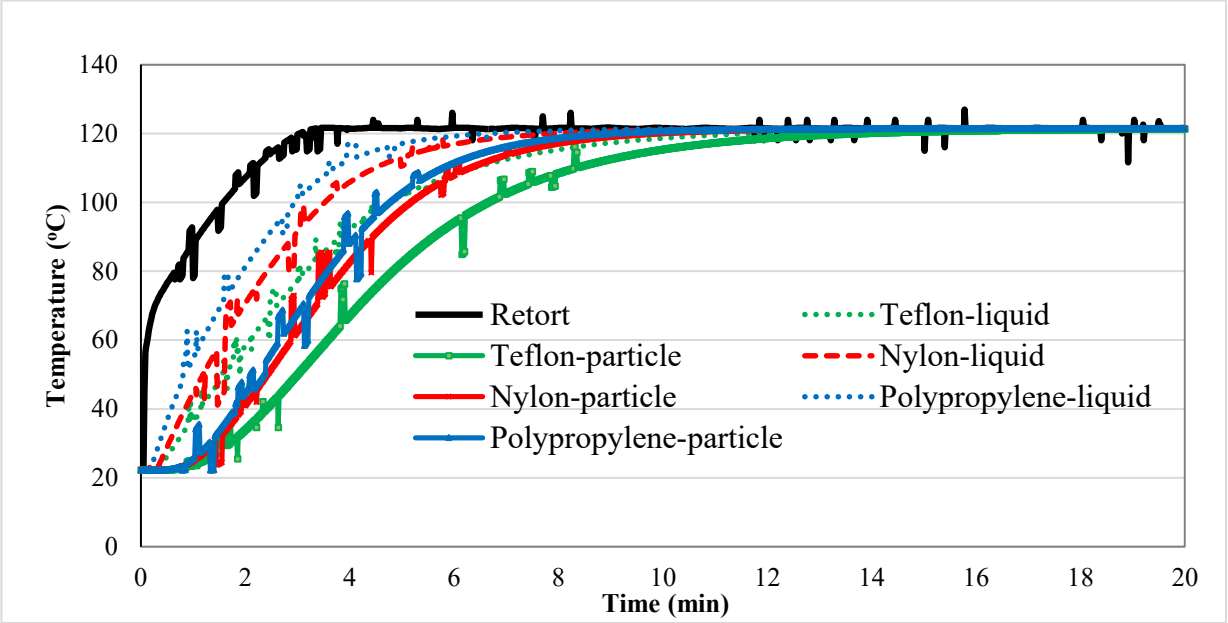

Fig. 7.3. Time-temperature profile for cans filled to 10 mm headspace with 30% (v/v) concentration of polypropylene, Nylon and Teflon particles and 50% glycerin and processed at 2 Hz reciprocating frequency and 121.1 ºC.

It was seen that rate of temperature rise followed the trend: polypropylene > Nylon > Teflon. However, this trend was not the same as that for U and h_{fp}. Figs. 7.4 and 7.5 show the values of the heat transfer coefficients of Nylon, polypropylene and Teflon particles for different liquid viscosity and particle concentration respectively. From these figures and on the basis of sum of squares in ANOVA analysis (Table 7.4), it is seen that U and h_{fp} followed the trend: Nylon > polypropylene > Teflon. Thus, it is seen that although polypropylene heated fastest, it had lower h_{fp} as compared to Nylon. This discrepancy between the trends in heat transfer coefficient and heating rates can be explained by looking into the thermal diffusivity and thermal effusivity of particles, as with the case with the single particle study in Chapter 6. As discussed in Chapter 6, the value of thermal diffusivity depicts the rate at which a particle adjusts to the external temperature change, while thermal effusivity depicts its ability to exchange thermal energy with its surroundings. It is clear from the values of thermal diffusivity of the substances given in Table 6.1 that thermal diffusivity of polypropylene is highest and that of Teflon is lowest, which explains their respective heating rates. However, h_{fp} is indicative of the heat flux absorbed by the body and hence correlated better with values of thermal effusivity, which measure the rate at which a material can absorb heat.

Fig. 7.4 demonstrates the effect of liquid viscosity and frequency on U and h_{fp} of three particle types studied at 30% (v/v) particle concentration. As expected from the results in Section 7.4.1, both coefficients increased with increase in reciprocation frequency. With increase in liquid viscosity, U and h_{fp} values decreased for all particle types. Higher viscous fluids generally had lower heat transfer coefficient. With increase in viscosity from 0.001 Pa.s (0% glycerin) to 0.011 Pa.s (50% glycerin), U values decreased by 21%. Further increase of liquid viscosity from 0.011 Pa.s to 0.94 Pas (100% glycerin) led to 34% reduction in U values. For a fluid of low viscosity, the Reynolds number is large due to lower effect of viscous term, which results in higher turbulence and hence greater heat transfer coefficients. This is consistent with observation by other researchers (Ramaswamy *et al.*, 1993; Farid and Ghani, 2004) in other modes of agitation. Also, the liquid-particle relative velocity is reduced due to the increase in resistance to flow at higher viscosities.

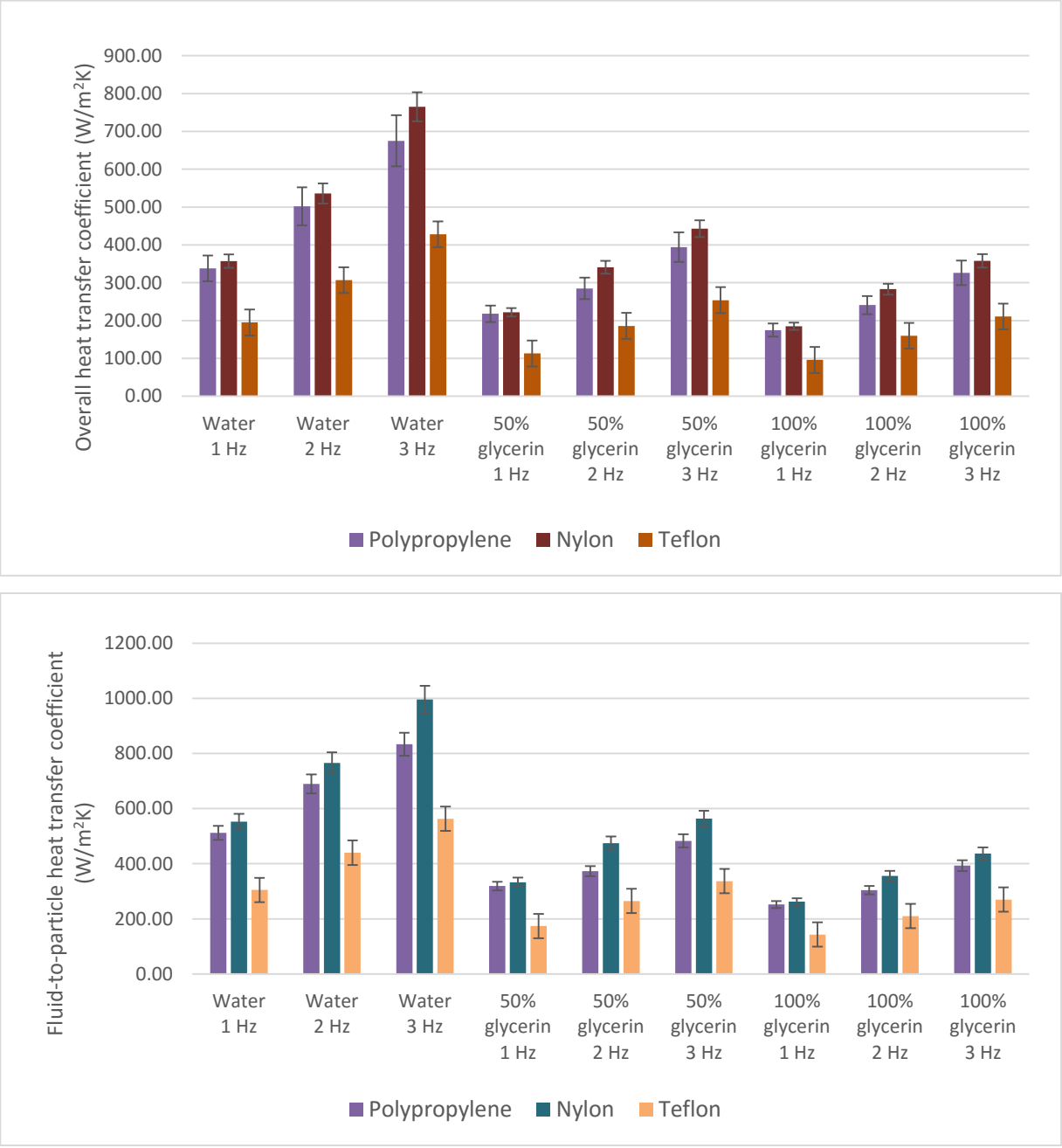

Fig. 7.4. Overall heat transfer coefficient (U) and fluid-to-particle heat transfer coefficient (h_{fp}) as affected by liquid viscosity and reciprocation frequency for the three particle types studied for cans filled with 30% v/v particle concentration.

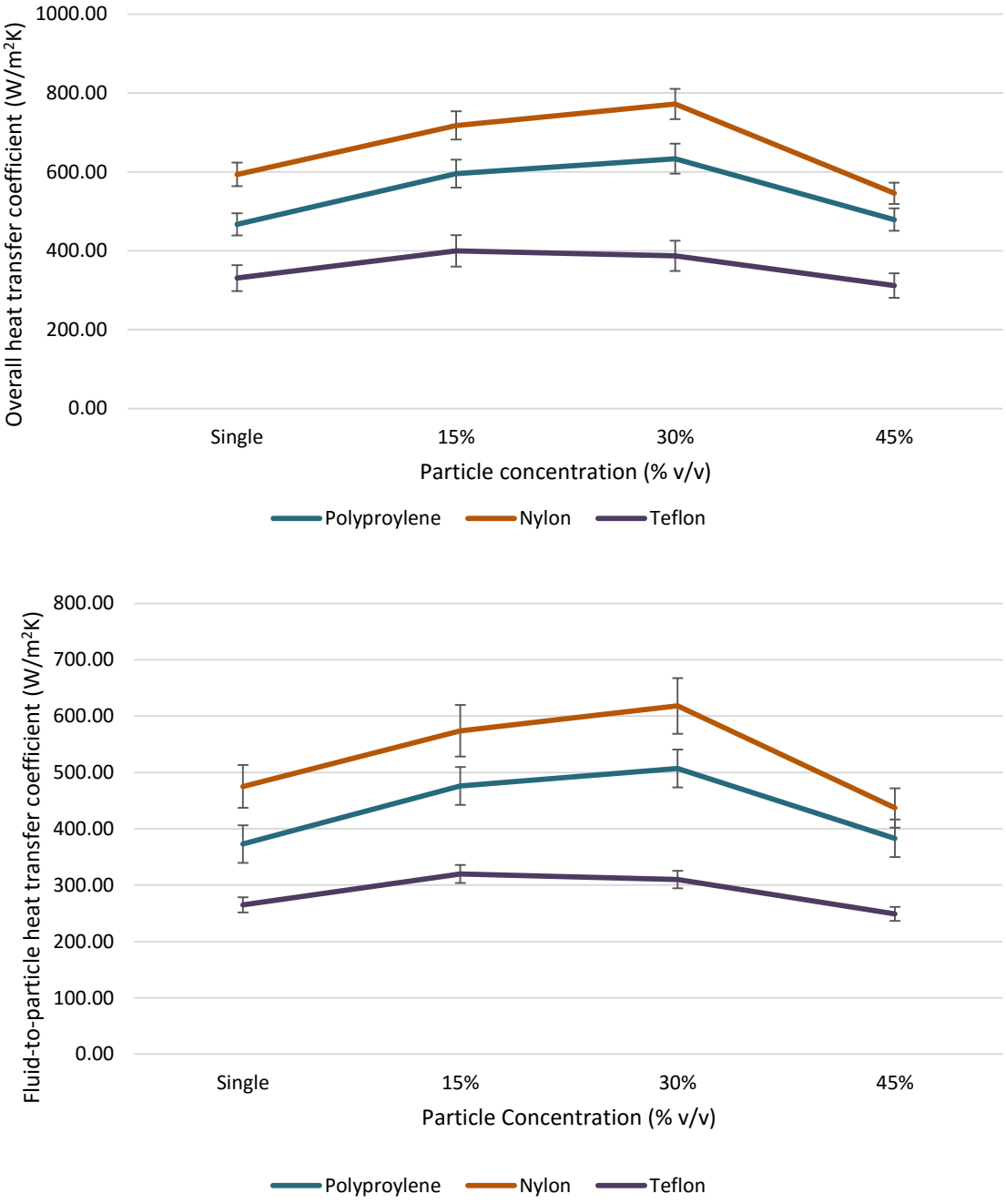

Fig. 7.5. a) Overall Heat Transfer Coefficient (U), b) fluid-to-particle Heat Coefficient (h_{fp}) for cans processed with polypropylene, Nylon and Teflon spheres with 50% glycerin concentration at various particle concentrations at 2 Hz reciprocation frequency.

Fig. 7.5, above, shows the effect of particle concentration for cans processed with polypropylene, Nylon and Teflon spheres with 50% glycerin concentration. It was observed that values of both U and h_{fp} for all three particles increased with increase in the concentration of particles inside the can. However, after a certain concentration, U and h_{fp} started decreasing. Initial increase in heat transfer coefficients on increasing the number of particles has been attributed to better mixing produced by movement of large number of particles (Sablani and Ramaswamy, 1997). However, clumps formed on high concentration of particles resulting in inhibition of heat transfer beyond a certain particle concentration due to dominance of conduction-based heating.

7.5 Conclusions

Effects of various processing conditions and product properties on heat transfer coefficients (U and h_{fp}) associated with reciprocation agitation thermal processing of liquid particulates was analyzed. In general, U and h_{fp} values were found to be higher than for other modes of agitated and non-agitated thermal processing. In terms of process variables, reciprocation frequency had the most significant impact on extent of heat transfer. The effect of headspace was less significant at higher reciprocation intensities, while operating temperature had the least significant effect. In terms of product properties, U and h_{fp} followed the trend: Nylon>polypropylene>Teflon. However, the rate of temperature increase followed the trend: polypropylene > Nylon > Teflon. Heat transfer coefficients were better correlated by thermal effusivity of particles than thermal diffusivity. U and h_{fp} were found to increase on increasing particle concentration, however, beyond an optimal concentration, U and h_{fp} decreased due to dominance of conduction based heating. Higher liquid viscosity resulted in inhibition of movement of particles due to viscous forces and hence agitation and heat transfer decreased.

PREFACE TO CHAPTER 8

Optimization of a thermal processes may have multiple objectives. Maximizing the amount of heat transferred to minimize processing times for achieving the targeted lethality is the primary objective of any optimization study on thermal processing. Apart from this, reciprocating agitation thermal processing presents additional constraints like minimization of reciprocation intensity to minimize product damage due to severe agitation. This study focusses on simultaneous optimization of both these objectives.

In chapter 8, data from chapters 6 and 7 were utilized to develop a composite model using regression analysis. This model was subsequently used for simultaneous maximization of heat transfer coefficients (U and h_{fp}) and minimization of reciprocation intensity (RI). Various other constraints were included in the analysis to formulate optimal conditions under selected processing scenarios. This study shall be helpful for the thermal processing industry in finding optimal processing conditions and prescribe desirable product properties for reciprocating agitation thermal processing.

Parts of this chapter won the second prize in **Charles Stumbo Graduate Student Paper Competition** and a poster presentation was made in the Annual Meeting of the Institute for Thermal Processing Specialists (IFTPS) held on Mar 3-6, 2015 in San Antonio, Texas.

Parts of this chapter have been submitted for publication as an original research article "*Optimization of heat transfer and reciprocation intensity during thermal processing of liquid particulate mixtures undergoing reciprocating agitation*" in Innovative Food Science & Emerging Technologies.

The experimental work and data analysis was carried out by the candidate under the supervision of Dr. H. S. Ramaswamy.

CHAPTER 8

OPTIMIZATION OF HEAT TRANSFER AND AGITATION INTENSITY DURING RECIPROCATING AGITATION THERMAL PROCESSING

8.1 Abstract

Simultaneous optimization of heat transfer and reciprocation intensity was carried out for reciprocating agitation thermal processing of liquid-particulate foods. Data on the effects of various processing conditions (temperature, frequency, and headspace) and product properties (liquid viscosity, particle concentration, and particle density) on heat transfer coefficients (U and h_{fp}) during sterilization were utilized to develop a composite model describing the effect of all variables. Heat transfer coefficients (U and h_{fp}) were maximized individually and simultaneously with minimal reciprocation intensities (RI) using numerical optimization procedures. High RI (37-45 ms^{-2}) was recommended to maximize U and h_{fp}, whereas lower RI (16-19 ms^{-2}) was found optimal for simultaneous optimization of U, h_{fp} and RI. Product properties containing low viscous liquids filled with 23-27 % concentration of particles with density of 1134-1351 kg/m^3 were found most desirable. Optimal conditions were also reported for different operating temperatures, liquid viscosities, particle concentrations and particle densities.

8.2 Introduction

Recent innovations in food processing driven by increased consumer awareness and demands for high quality products has inspired rapid development in the principles and processes in thermal processing industry (Awuah *et al.*, 2007a). With developments of new modes of agitation like reciprocating agitation thermal processing, optimization studies on thermal processing have become not only more desirable but also a necessity, and have to cover various situations and constraints. The food processing industry should aim to achieve balance between the conducive and harmful effects of thermal processing (Balsa-Canto *et al.*, 2002). Hence the basis for optimization of thermal process should be to impart required lethal effect to ensure microbiological safety and to simultaneously reduce the extent of thermal damage on color, texture and nutritional attributes (Awuah *et al.*, 2007a). The general principles involved during optimization of thermal processing have been reviewed by Holdsworth (1985).

Optimization of thermal processing is bound by many constraints as every process has different quality attributes, which further have different criterion and each constraint added, tends to give different results (Silva *et al.*, 1994). Optimization of a thermal process can be done to maximize the heat transfer rate for maximum quality retention after processing (Awuah *et al.*, 2007a; Lund, 1982; Rattan and Ramaswamy, 2014). Apart from maximizing heat transfer, during reciprocating agitation, there is an additional factor which needs to be considered. Very rapid back and forth motion of cans warrants the choice of lower reciprocation intensities as they may damage some products in form of nutrient leaching, texture degradation etc. (Walden and Emanuel, 2010). Minimization of reciprocation intensity (RI) is also desirable for optimizing energy requirements. Thus, a combined effect of maximization of heat transfer and minimization of reciprocation intensity was considered in this work, for predicting optimal processing conditions and product properties.

In this study, a composite model was developed using data generated and included in Chapters 6 and 7 for generating optimal conditions for imparting reciprocating agitation. Optimization was conducted for three objective functions (max U, max h_{fp} and min RI) and under various constraints determined by various levels of operating temperatures, liquid viscosity, particle concentrations and particle densities. The results of optimization are presented and the implications on optimal processing conditions and product properties are discussed.

8.3 Materials and Methods

8.3.1 Composite Model

A composite model was first developed for predicting modeling of U and h_{fp} using a single equation containing effects of all variables, viz. operating temperature (T), reciprocation intensity (RI), container headspace (H), liquid viscosity (LV), particle concentration (PC) and particle density (PD). Since amplitude and container orientation were fixed in Chapter 7, only data from Chapters 6 and 7 for cans placed along the axis of reciprocation and reciprocating at an amplitude of 15 cm were considered in this study. For this, a quadratic model was evaluated from available data in using stepwise regression, which involves removal of non-significant ($p>0.05$) model terms, and hence the composite model equation contained only significant effects.

Reciprocation intensity (RI) used in composite model was obtained from corresponding reciprocation frequency (F) by calculating maximum acceleration from position analysis of a can during its motion (Walden and Emanuel, 2010), and can be represented by Equation (8.1). This parameter depicts acceleration and hence can be used to depict both the force of impact amongst particles and the energy requirements at a particular reciprocation frequency and amplitude, and hence is useful for optimization of reciprocating agitation thermal processing.

$$Reciprocation\ Intensity\ (RI) = \omega^2 a(1 + (a/2l))/2 \quad (8.1)$$

where, RI= reciprocation intensity (ms^{-2}), ω = angular velocity in radian/s = 2* π*frequency (s), a = amplitude = 0.15 m, and l = length of connecting rod = 0.4 m.

8.3.2 Optimization objectives and constraints

Subsequently numerical optimization was conducted using the built-in functionality of Design Expert software. Optimization procedure was carried out for predicting processing conditions and product properties for obtaining maximum heat transfer by maximizing U and h_{fp} individually and simultaneously. Optimization was also conducted for maximizing U and h_{fp} and minimizing RI simultaneously. Thus, the three objectives of the multi-objective optimization were summarized as:

i) max (U) – maximum heat transfer at can wall,
ii) max (h_{fp}) – maximum heat transfer at fluid-to-particle interface,
iii) min (RI) – minimum reciprocation intensity for minimal product impact and energy requirement.

Some other constraints were also considered during the analysis for predicting optimal conditions under various processing scenarios. The constraints and their applicability in case of reals foods is summarized below:

i) T=110 ºC – low temperature sterilization,
ii) T=130ºC – high temperature sterilization,
iii) LV = 0.001 Pa.s –low viscosity liquid
iv) LV=0.011 Pa.s – medium viscosity liquid,

v) LV=0.94 Pa.s – high viscosity liquid,

vi) PC = 0.1 v/v – liquid-only (single-particle scenario for h_{fp}),

vii) PC = 45% v/v – tightly packed can with little movement of particles simulating conduction dominated heat transfer regime,

viii) PD = 830 kg/m^3 – particles lighter than liquid (polypropylene),

ix) PD = 1130 kg/m^3 – particle with density comparable to liquid (Nylon),

x) PD = 2210 kg/m^3 – particle heavier than liquid (Teflon).

8.4 Results and Discussions

8.4.1 Composite effect of all processing conditions

The effect of six process variables has been discussed in Chapters 6 and 7 for the single and mulitple particle case scenario in detail. Although Equations (6.2, 6.4-6.10) and (7.1-7.8) depict the values of U and h_{fp}, but they only valid for certain conditions (constant values of variables not included in respective models). Hence, for optimization of all processing conditions and product properties, a single composite model was developed using combined data from Table 6.3, Fig. 6.3, Table 7.1 and Table 7.3. For this, a quadratic model was evaluated via stepwise regression by replacing reciprocation frequency with reciprocation intensity (RI), liquid concentration with corresponding liquid viscosity (LV) and particle type with particle density (PD).

During stepwise regression, based on ANOVA analysis of the model terms which are not significant ($p>0.05$) were removed from final regression equation, and hence the regression equation contains only significant effects. Individual interaction and interaction of square of LV, particle concentration (PC) and PD, and two way interaction of LV and PD were significant ($p<0.05$) for both U and h_{fp}. Individual effect of RI and its two-way interactions with LV and PD also significantly affected ($p<0.05$) both U and h_{fp}; however, interaction of its square significantly affected ($p<0.05$) only U. For U, all interactions of temperature (T) and headspace (H) were non-significant ($p>0.05$), while for h_{fp} individual and square of interactions of temperature and headspace were significant ($p<0.05$). The developed regression equations for U and h_{fp} (in terms of actual variables), are given as Equations (8.2) and (8.3) respectively, and were found to fit the experimental data adequately with R^2 of 0.95 and 0.90 respectively (Fig. 8.1).

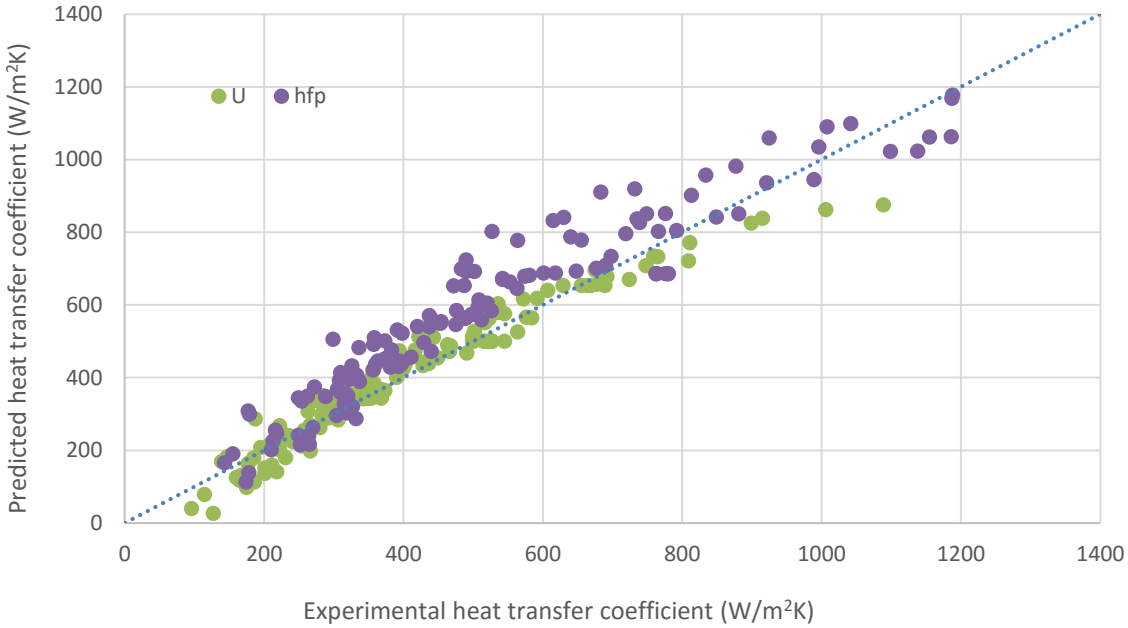

Fig. 8.1. Comparison of composite model values and experimental data for overall heat transfer coefficient (U) and fluid-to-particle heat transfer coefficient (h_{fp}).

$$U_{model} = -130.63 + 21.95\text{RI} - 22414.80\text{LV} + 12.59\text{PC} + 0.78\text{PD} - 4.02(\text{RI.LV}) - 0.0028(\text{RI.PD}) + 0.074(\text{LV.PD}) - 0.22\text{RI}^2 + 23421.98\text{LV}^2 - 0.26\text{PC}^2 - 0.00029\text{PD}^2 \quad R^2 = 0.95 \quad (8.2)$$

$$h_{fp-model} = 24364.47 - 395.94\text{T} - 153.12\text{H} + 16.74\text{RI} - 26014.24\text{LV} + 13.18\text{PC} + 1.24\text{PD} - 6.86(\text{RI.LV}) - 0.0031(\text{RI.PD}) + 0.11(\text{LV.PD}) - 1.65\text{T}^2 + 7.33\text{H}^2 + 27126.81\text{LV}^2 - 0.28\text{PC}^2 - 0.00045\text{PD}^2 \quad R^2 = 0.90 \quad (8.3)$$

8.4.2 Individual maximization of U and h_{fp}

The developed composite model was used to evaluate optimal processing conditions and product properties to be used during reciprocation thermal processing of liquid particulate mixtures. Enhancement in heat transfer is the most important factor to be considered for optimization during agitation thermal processing (Rattan and Ramaswamy, 2014). Maximum

values of U and h_{fp} represent best heating scenario with minimum process time for achieving the same degree of microbial kill with minimum quality degradation due to heat (Awuah *et al.*, 2007a). The results of optimization of heat transfer in terms of maximization of U and h_{fp} individually and simultaneously are presented in Table 8.1. All parameters were varied between the experimental ranges considered in Chapters 6 and 7.

Table 8.1. Optimal processing conditions and product properties for individual and simultaneous optimization of U and h_{fp}.

Operating Temperature (°C)	**Reciprocation Intensity (ms^{-2})**	**Can Headspace (mm)**	**Liquid Viscosity (Pa.s)**	**Particle Concentration (%)**	**Particle Density (kg/m^3)**	**U**	**h_{fp} (W/m^2K)**
	i.)	**Maximum U**					
129	44	7	0.001	24	1134	911	1480
124	45	7	0.001	24	1134	909	1480
127	43	9	0.001	24	1134	910	1440
	i.)	**Maximum h_{fp}**					
118	45	6	0.002	22	1235	882	1600
117	44	6	0.002	14	1366	844	1660
111	37	5	0.001	0.2	1303	750	1560
	i.)	**Maximum U**					
	ii.)	**Maximum h_{fp}**					
128	45	13	0.001	24	1134	909	1520
124	45	6	0.001	24	1134	909	1540
111	45	6	0.001	24	1134	909	1650

Individual maxima of U and h_{fp} were found at lower headspace ranges (5-9 mm), lower viscosities (0.001-0.002 Pa.s) given by lower concentrations of glycerin and were depicted by particles with densities (1134-1366 kg/m^3) comparable to that of the fluid used (glycerin). This is in accordance with the earlier results that low headspace, low viscosity, and particle densities closer to fluid had higher heat transfer. U was maximized for higher operating temperatures (124-129°C), maximum reciprocation intensity (45 ms^{-2}) and 24% (v/v) particle concentration, while h_{fp} was maximized at 117-118 °C for highest reciprocation intensity of 45 ms^{-2} at 23-14% particle concentration.

However, for single particle scenario, h_{fp} was maximized at lower temperature (111 ºC) and at lower reciprocation intensity (37 ms^{-2}). At higher temperatures, the liquid inside became thin and consequently heat transfer was increased inside the liquid leading to higher overall heat transfer coefficients (U). Surprisingly, h_{fp} was maximized at lower temperatures for single particle scenario, although, it can be explained by some observations in Chapters 4 and 6. While using single particle in can, we found that the operating temperature did not affect U and h_{fp} very significantly and that after a certain reciprocation frequency, the enhancement in heat transfer was not appreciable. The minimum of the optimal reciprocation intensity was around 37 ms^{-2}, which is close to the recommendations of Walden and Emanuel (2010) for obtaining maximum heat transfer under reciprocating agitation.

8.4.3 Simultaneous maximization of U and h_{fp}

The results produced in the previous section represented individual maximization of U and h_{fp}. However, during thermal processing, simultaneous maximization of U and h_{fp} is important to decrease process time and improve quality of product. Hence, optimization was conducted for maximizing U and h_{fp} simultaneously. The optimum conditions were obtained for maximum reciprocation intensity (45 ms^{-2}), medium particle concentration (24% v/v), particle density close to that of Nylon (1134 kg/m^3) and lowest viscosity levels (0.001 Pa.s). These conditions are similar to optimal conditions for maximization of U alone.

Optimal values were available for all operating temperature ranges (111-128 ºC) and headspace (6-13 mm) considered, and thus temperature and headspace did not affect optimization results. It must be noted that the correlation for U (Equation 8.2) also did not contain terms for temperature and headspace. Thus, it is seen that simultaneous maximization of U and h_{fp} followed similar trends as that of individual maximization of U. Hence, it can be concluded that maximizing U alone might be sufficient for establishing optimal processing conditions for reciprocation thermal processing.

8.4.4 Simultaneous optimization of heat transfer and reciprocation intensity

Traditionally, maximization of heat transfer in terms of optimization of U and h_{fp}, process times and quality degradation has been the sole focus of optimization studies on various modes of thermal processing. However, the very rapid high intensity reciprocations during reciprocating

agitation has been a cause of some concern for some commodities (Higgins, 2012). Although, reciprocation intensity increases heat transfer rates, it also may affect the product quality due to leaching of nutrients and texture degradation, particularly for soft products. Additionally, it also results in increased energy and maintenance requirements for equipment used during reciprocating agitation thermal processing. Hence, a minimal reciprocation intensity is another parameter of optimization which might be considered in optimization studies on reciprocation thermal processing. Table 8.2 depicts the optimal conditions for simultaneous optimization of heat transfer and reciprocation intensity subjected to various constraints for different product types.

For overall optimization (without any constraints), optimal conditions were obtained at lowest operating temperature (110 ºC) and minimal headspace (5 mm) for a product filled with liquid of minimal viscosity (0.001 Pas) with a medium concentration (23-27%) of particles with density of 1305-1351 kgm^{-3}. Reciprocation intensity in the range 16-19 ms^{-2} was found to be ideal for reciprocating agitation thermal processing of products susceptible to high intensity agitations. Thus reciprocation intensity is a critical factor from energy point of view as well, since product of reciprocation intensity with mass depicts force and energy requirements of the system.

8.4.5 Constrained optimization under different processing conditions

Optimization was also conducted by applying constraints on various processing variables for studying optimization under various conditions. It is seen that for low operating temperature (T=110 ºC), optimal results were obtained at 18 ms^{-2} reciprocation intensity, and for higher temperatures (T=130 ºC) a slightly higher reciprocation intensity (20-21 ms^{-2}) was desirable. This slight increase in intensity requirement is due to the reduction in equilibration time at higher reciprocation intensity. Yet, temperature was not found to affect the optimization very significantly. Similarly, headspace was not found significant for simultaneous optimization of U, h_{fp} and reciprocation intensity.

All optimization results show that the use of a liquid of low viscosity is highly desirable for maximizing heat transfer. However, many products use liquid of higher viscosity. Hence, a constraint of various levels of liquid viscosity was applied to study optimal configurations for viscous products. For a liquid viscosity of 0.01 Pa.s (medium viscosity i.e. close to that of 50% glycerin), a higher reciprocation intensity of 23-24 ms^{-2} was desirable, other parameters being the

same as that for unconstrained optimization. This is because higher intensity shaking aided heat transfer in viscous liquids.

However for very high viscosity liquids (close to that of 100% glycerin), a lower reciprocation intensity of 15-17 ms^{-2} was desirable. This may be attributed to the formation of lumps on very high intensity agitations of very thick liquids. Instead, use of lower intensity agitation is preferred for such liquids as it may accelerate the heat transfer at lower temperatures. This is similar to suggestion of 10 ms^{-2} reciprocation intensity for high viscous bentonite solution (Walden and Emanuel, 2010).

Unconstrained optimization of U, h_{fp} and reciprocation intensity suggests use of 23-27% (v/v) particle concentration for product design. However, some products may be mostly liquid (single-particle scenario), while some other may have such very high particle concentration resulting in conduction-dominated heating (45% particle concentration scenario). For single-particle scenario, 20-23 ms^{-2} reciprocation intensity was optimal, however, for conduction-dominated products, a higher reciprocation intensity of 28-32 ms^{-2} was considered desirable. This is because, higher reciprocation intensity would aid heat transfer in such conduction dominated products, by attempting to enhance convection currents.

For the three particles types considered in this study, optimization results revealed that lower operating temperatures (110 ^{o}C), higher reciprocation intensity (23-24 ms^{-2}) and lower particle concentrations (19-22% v/v) were more desirable for polypropylene particles, with other parameters similar to that for unconstrained optimization. However, Nylon and Teflon, which were heavier than water, required higher operating temperatures (130 ^{o}C), lower reciprocation intensity (18-21 ms^{-2}) and higher particle concentrations (22-35% v/v). Particle concentration requirements for very heavy particles like that of Teflon were much higher (28-35 %) than that for Nylon (22-25 %). This is mainly because, higher concentration of particles in Teflon ensured that some concentration of particles were free to move and did not form clumps at the bottom, and thus aided the amount of heat transfer. This is similar to results in Chapter 7 that showed that higher concentration of particles may assist heat transfer.

Table 8.2. Optimal processing conditions and product properties for simultaneous optimization of heat transfer coefficients (U and h_{fp}) and reciprocation intensity (RI).

Operating Temperature (°C)	Reciprocation Intensity (ms^{-2})	Can Headspace (mm)	Liquid Viscosity (Pa.s)	Particle Conc. (%)	Particle Density (kg/m^3)	U (W/m^2K)	h_{fp} (W/m^2K)
i.) Max U	**ii.) Max h_{fp}**	**iii.) Min RI**					
130	18	5	0.001	27	1351	779	1400
130	15	5	0.001	25	1305	759	1380
130	19	5	0.001	23	1336	794	1420
i.) Max U	**ii.) Max h_{fp}**	**iii.) Min RI**	**iv.) T=110 °C (low temperature)**				
110	18	5	0.001	24	1248	786	1400
110	17	5	0.001	27	1294	779	1390
110	18	5	0.001	26	1328	781	1400
i.) Max U	**ii.) Max h_{fp}**	**iii.) Min RI**	**iv.) T=130 °C (high temperature)**				
130	20	5	0.001	24	1294	805	1350
130	21	5	0.001	27	1229	811	1360
130	20	5	0.001	20	1346	803	1370
i.) Max U	**ii.) Max h_{fp}**	**iii.) Min RI**	**iv.) LV = 0.001 Pa.s (low viscosity fluid)**				
130	16	5	0.001	24	1401	765	1390
130	16	5	0.001	26	1415	754	1370
110	15	5	0.001	28	1462	738	1350
i.) Max U	**ii.) Max h_{fp}**	**iii.) Min RI**	**iv.) LV = 0.011 Pa.s (medium viscosity fluid)**				
130	23	5	0.011	24	1262	608	1210
130	23	5	0.011	24	1275	608	1210
130	23	5	0.011	23	1231	612	1220
i.) Max U	**ii.) Max h_{fp}**	**iii.) Min RI**	**iv.) LV = 0.94 Pa.s (high viscosity fluid)**				
130	16	5	0.94	24	1401	490	1020
130	16	5	0.94	26	1415	483	1010

	110		15		5	0.94	28	1462	473	1000
i.)	**Max U**	**ii.)**	**Max h_{fp}**	**iii.)**	**Min RI**	**iv.)**	**PC = 0.1% v/v (single-particle/liquid-only cans)**			
	110		20		5	0.001	0.1	1264	660	1280
	110		22		5	0.001	0.1	1278	673	1310
	110		20		5	0.001	0.1	1232	651	1270
i.)	**Max U**	**ii.)**	**Max h_{fp}**	**iii.)**	**Min RI**	**iv.)**	**PC = 45% v/v (tightly packed can)**			
	110		28		5	0.001	45	1307	751	1400
	110		29		5	0.001	45	1253	733	1360
	110		31		5	0.001	45	1361	766	1450
i.)	**Max U**	**ii.)**	**Max h_{fp}**	**iii.)**	**Min RI**	**iv.)**	**PD=830 kg/m^3 (polypropylene)**			
	110		24		5	0.001	21	830	772	1355
	110		23		5	0.001	19	830	768	1350
	110		23		5	0.001	22	830	770	1350
i.)	**Max U**	**ii.)**	**Max h_{fp}**	**iii.)**	**Min RI**	**iv.)**	**PD=1130 kg/m^3 (Nylon)**			
	130		18		5	0.001	22	1130	779	1390
	130		21		5	0.001	25	1130	810	1430
	130		19		5	0.001	24	1130	793	1410
i.)	**Max U**	**ii.)**	**Max h_{fp}**	**iii.)**	**Min RI**	**iv.)**	**PD=2210 kg/m^3 (Teflon)**			
	130		19		5	0.001	35	2210	535	988
	130		21		5	0.001	28	2210	542	1020
	130		20		5	0.001	31	2210	538	989

8.5 Conclusions

A composite model was developed by combining data from various designs in Chapters 6 and 7 and the process variables were optimized by maximizing heat transfer coefficients and minimizing reciprocation intensity. Highest reciprocation intensity (37-45 ms^{-2}) was optimal for enhancing U and h_{fp} alone, however, a lower reciprocation intensity (16-19 ms^{-2}) was desirable on simultaneous optimization. Temperature and headspace did not significantly affect optimization results. For very high viscosity liquids, a lower reciprocation intensity (15-17 ms^{-2}) is preferred due to possibility of formation of clumps at higher agitation. In liquid-only cans, lower reciprocation intensity (20-23 ms^{-2}) was required, while very compact packing of particles resulted in higher reciprocation intensity (28-32 ms^{-2}) requirements. Heavier particles like Teflon required higher particle concentration (28-35% v/v), as compared to Nylon (22-25% v/v) and polypropylene (19-22 % v/v) since, due to their weight these particles form clumps at bottom of the can, and higher concentration of particles increases the availability of particles for creating agitation inside the can. This study shall be helpful in establishing optimal processing conditions for reciprocating agitation thermal processing of liquid particulate mixtures.

PREFACE TO CHAPTER 9

In Chapters 4-7, heat transfer coefficients (U and h_{fp}) associated with liquid particulate mixtures were evaluated in detail for reciprocating cans. Effect of various processing conditions and product properties on U and h_{fp} were studied providing a good database of heat transfer coefficients under different modes and conditions of heat transfer. However, the treatment of data and models developed to describe the effect of variables, while useful for recognizing the effect of these parameters, may be somewhat limited to the test conditions studied. In order to extend these results to other systems and for scale-up considerations, dimensionless correlations are traditionally used to model heat transfer coefficients. Therefore the objective of chapter 9 was to develop dimensionless correlations for the heat transfer coefficients (U and h_{fp}) for liquid-only and liquid-particulate canned mixtures subjected to reciprocating agitation thermal processing.

Parts of this chapter have been submitted for publication as an article "*Dimensionless correlations for heat transfer coefficients during reciprocating agitation thermal processing of Newtonian liquid/particulate mixtures*" in Food and Bioproducts Processing.

The experimental work and data analysis was carried out by the candidate under the supervision of Dr. H. S. Ramaswamy.

CHAPTER 9

DIMENSIONLESS CORRELATIONS FOR PREDICTING THE HEAT TRANSFER ASSOCIATED WITH RECIPROCATING CONTAINER AGITATION THERMAL PROCESSING OF PARTICULATE FLUIDS.

9.1 Abstract

Data on overall heat transfer coefficient U and fluid to particle heat transfer coefficients h_{fp}, obtained for several processing conditions from Chapters 4-7, were used to develop dimensionless correlations for liquid-particle and liquid-only conditions. Different dimensionless numbers considered appropriate for the type of agitation and heat transfer involved were employed in the analysis. Sum of amplitude of reciprocation and dimension of can along the axis of reciprocation ($A+D_{axis}$) was found to be most suitable as characteristic length in correlations for overall heat transfer coefficient (U), while for fluid-to-particle heat transfer coefficient (h_{fp}) sum of amplitude of reciprocation and diameter of particle ($A+D_p$) was most desirable. Using these characteristic lengths, the ratio of Groshof (Gr) and square of Reynolds (Re) number [Gr/Re^2] during reciprocating agitation fell between 0.01-4.46 for U and 0.02-6.86 for h_{fp} suggesting mixed convection mode for some conditions. In mixed convection mode, Nusselt number (Nu) was correlated to Rayleigh number (Ra), Peclet number (Pe), Froude number (Fr), relative density of particle to liquid (ρ_p/ρ_l), particle concentration ($\varepsilon/(100-\varepsilon)$), ratio of headspace to height of can (h_s/H) and aspect ratio of can (AR). Aspect ratio was included in the dimensionless correlations to take into account the change in orientation of the can and is defined as ratio of dimension of can along axis of reciprocation to its dimension perpendicular to axis of reciprocation. For particulate fluids, an excellent correlation of R^2 between 0.93-0.95 was obtained between the Nu and the other dimensionless groups, when considering the effect of both forced and natural convection in the following general form: $Nu = A_1(Ra)^{A2}+A_3(Pe)^{A4}(Fr)^{A5}(\rho_p/\rho_l)^{A6}(\varepsilon/(100-\varepsilon))^{A7}(h_s/L_c)^{A8}(AR)^{A9}$. However, on a modeling only forced convection scenario, R^2 was only 0.88-0.89, indicating the presence of some natural convection even with reciprocating agitation. For liquid-only cans, correlations were obtained by ignoring the density and particle concentration terms from above mode. Here, the contribution of natural convection was found higher than that in multiple-particle scenario.

9.2 Introduction

Process modeling for thermal processing of liquid/particulate canned food requires data on the overall heat transfer coefficient from the heating medium to the can liquid (U), and the fluid-to-particle heat transfer coefficient (h_{fp}), besides the relevant thermo-physical properties (Sablani *et al.*, 1997). However, there are many operating conditions and liquid and particle properties which may vary during the thermal process and it is very difficult to experimentally collect data for each processing condition. In this context, researchers have widely used dimensionless correlations for the prediction of U and h_{fp} for a wide variety of scenarios using a limited set of experimental data. This technique is highly effective in generalizing data because it limits the number of variables that must be studied and permits the grouping of physical variables that affect the process of heat transfer (Ramaswamy and Zareifard, 2003). Dimensional analysis not only helps us to generate predictive models, but also helps in obtaining a better understanding of the physical phenomenon and can also be easily used for scale-up purposes. In this context, reciprocating agitation thermal processing is one of the emerging technologies in the field of thermal processing for reducing quality loss due to detrimental effects of heat. Reciprocating agitation is different from the well-analyzed rotary agitation as there is a possibility of changing frequency, amplitude and container orientations, as compared to only rotation speed and reel radius during rotation. Due to absence of any pertinent literature on dimensional analysis during reciprocating mode of agitation, there is still a need to understand the heat transfer phenomenon in greater detail.

An excellent review of earlier works on dimensional analysis in the field of thermal processing has been presented by Rao and Anantheswaran (1988). Mostly, these works were focused on development of dimensionless correlations for evaluating U only (Lenz and Lund, 1978; Anantheswaran and Rao, 1985a, 1985b; Deniston *et al.*, 1987) or h_{fp} only (Fernandez *et al.*, 1988l Alhamdan and Sastry, 1990; Alhamdan *et al.*, 1990). Later, researchers (Sablani *et al.*, 1997; Garrote *et al.*, 2006; Meng and Ramaswamy, 2007c; Dwivedi and Ramaswamy, 2010d) have developed dimensionless correlations for both U and h_{fp}. These studies have correlated Nusselt number (Nu) (a dimensionless measure of convective heat transfer coefficient) with several other dimensionless numbers like Reynolds number (Re), Prandtl number (Pr), Grashof number (Gr), Rayleigh number (Ra), Froude number (Fr), Archimedes number (Ar), ratio of headspace of can

to length of can (H_s/L_c), ratio of particle to liquid concentration ($\frac{\varepsilon}{100-\varepsilon}$) etc., the ratio of equivalent particle diameter to the diameter of the can ($\frac{d_p}{D_c}$), particle sphericity (ψ), density simplex $\left(\frac{\rho_p-\rho_l}{\rho_l}\right)$ etc. Most of these studies involve model food particle like Nylon, Teflon, polypropylene etc., however, other researchers (Fernandez *et al.*, 1988; Garrote *et al.*, 2006; Carino-Sarabia and Velez-Ruiz, 2013) have also developed dimensionless correlations using data from thermal processing of real food particles. More recently, researchers (Kannan and Sandaka, 2008; Kurian *et al.*,2009) have also used CFD simulations to generate time-temperature data for generating dimensionless correlations. Kannan and Sandaka (2008) have incorporated fourier number (τ) in their correlations to predict time-dependent heat transfer coefficients, while Kannan and Sandaka, and Kurian *et al.* (2009) used CFD simulations to model can foods and developed correlations for inclined cans by including a dimensionless constant in terms of sine and cosine functions of angle of inclination (θ). Apart from these, Fernandez *et al.* (1988) have used the fluidized bed and packed bed approaches and the modified Stanton number and Colburn j-factor in empirical correlations for h_{fp} in cans with axial rotation. In order to model changes in viscosity on agitation of non-Newtonian fluids, researchers (Anantheswaran and Rao, 1985b; Meng and Ramaswamy, 2007c) have used generalized Reynolds number (GRe) and generalized Prandtl number (GPr) by replacing viscosity term in these numbers with apparent viscosity in respective dimensionless numbers.

Characteristic length to be used in various dimensionless numbers is one of the most crucial parameter for developing dimensionless correlations. Lenz and Lund (1978) used reel radius as the characteristic length in the dimensionless correlation with axial rotation. Anantheswaran and Rao (1985b) used the sum of diameter of rotation and the length of the can as the characteristic length for correlation for U values. Deniston *et al.* (1987) used the diameter of the can in correlations to describe the heating behavior of liquid in the presence of multiple particles. Fernandez *et al.* (1988) used the diameter of the particle in the development of a dimensionless correlation for h_{fp}. Sablani *et al.* (1997) found that using the sum of the rotation diameter and the diameter of the can as the characteristic length was most appropriate for U correlations and the particles shortest dimension was most appropriate for h_{fp} correlations.

Agitation processing involves forced convection for enhancing heat transfer inside food containers, yet some degree of natural convection may also be present due to natural heat induced

convection currents (Dwivedi and Ramaswamy, 2010d). Earlier studies on agitation processing (Sablani *et al.*, 1997; Meng and Ramaswamy, 2007c) primarily developed the correlations on the assumption that forced convection was the dominant mechanism for heat transfer and ignored the role of natural convection. However, much earlier, Fand and Keswani (1973) had established that even in forced convection situations, the natural convection phenomenon would continue as buoyant forces resulting from density differences exist. Marquis *et al.* (1982) acknowledged that natural convection was important during the heating of liquids in bottles subjected to axial rotation. Hence, some researchers (Lenz and Lund, 1978; Dwivedi and Ramaswamy, 2010d) correlated their data with a two-term model which can be interpreted as the sum of natural and forced convection contributions. Dwivedi and Ramaswamy (2010d) concluded that modeling the dimensionless correlations developed on the basis of the heat transferred to canned particulate liquids as a sum of natural and forced convection can help in determining the contribution of each mode of convection.

The objective of this study was, therefore, to develop the dimensionless correlations for both U and h_{fp} in canned particulate fluids subjected to thermal processing with reciprocation agitation. Separate models were developed for liquid-only cans and liquid-particulate scenarios. Effect of container orientation was also included in the models by choosing the characteristic length on the basis of container orientation. Additionally, the objective was to evaluate the role of natural convection during reciprocating mode of agitation.

9.3 Materials and Methods

The experimental data obtained from Chapters 4-7 for different levels of glycerin concentration (contributing to liquid viscosities between 0.001-0.94 Pa.s) and different particle densities (Polypropylene – 880 kg/m^3, Nylon – 1130 kg/m^3 and Teflon – 2210 kg/m^3) under different operating conditions were used for the development of dimensionless correlations. The range of parameters related to liquid, particles and retort operating conditions are summarized in Table 9.1. The experimental and mathematical procedures to determine overall heat transfer coefficient and fluid to particle heat transfer coefficient and together with the gathered data, are detailed in Chapters 6 and 7 for liquid-only and liquid-particulate scenarios.

9.3.1 Dimensionless numbers

Heat transfer during thermal processing is a combination of natural and forced convection scenarios. The dimensionless form of heat transfer coefficient is Nusselt number (Nu), given by Equation (9.1), which is defined as the ratio of convective to conductive heat transfer across (normal to) the boundary.

Table 9.1. Range of processing conditions and product properties used in the determination of convective heat transfer coefficients (U and h_{fp}).

No	Parameter	Symbol	Experimental Range
1	Retort Temperature	T	110 - 130 ºC
2	Reciprocation Frequency	F	0.3 - 4 Hz
3	Reciprocation Amplitude	A	0.05 - 0.25 m
4	Can Headspace	H	0.002, 0.015 m
5	Liquid Viscosity	LV	0.001-0.94 Pa.s
6	Particle Density	PD	830-2210 kg/m^3
7	Particle Concentrations	PC	Single Particle, 10, 20, 30, 40% (v/v)

$$Nu = \frac{hl}{k} \tag{9.1}$$

where, h is the overall (U) or fluid-to-particle heat transfer coefficient (h_{fp}); l is the characteristic dimension and k is the thermal conductivity of fluid.

In natural convection heat transfer, Rayleigh number (Ra) is the most important dimensionless number used to describe the intensity of heat transfer. It is defined as the product of the Grashof number, which describes the relationship between buoyancy and viscosity within a fluid, and the Prandtl number, which describes the relationship between momentum diffusivity and thermal diffusivity. Hence the Rayleigh number itself may also be viewed as the ratio of

buoyancy and viscosity forces times the ratio of momentum and thermal diffusivities (Equation 9.2).

$$Ra = Gr.Pr = \frac{g\beta\Delta T l^3}{\nu\alpha} \tag{9.2}$$

where, l is the characteristic dimension, g is the acceleration due to gravity, β is the thermal expansion coefficient, ΔT is the average temperature difference between the surface temperature and bulk temperature, ν is the kinematic viscosity of the liquid and α is the thermal diffusivity of the liquid.

Peclet number (Pe) plays the role in heat transfer that is similar to that of the Reynolds number in fluid mechanics and is often used to characterize forced convection scenarios. Defined as the product of Reynolds (Re) and Prandtl number (Pr) (Equation 9.3), Peclet number tells us the relative importance of convective transport of thermal energy when compared with molecular transport of thermal energy (conduction).

$$Pe = Re.Pr = \frac{ul}{\alpha} \tag{9.3}$$

where, l is the characteristic dimension, u the local flow velocity, and α is the thermal diffusivity of liquid. Apart from Rayleigh number and Peclet number, Nusselt number was also correlated with other dimensionless numbers of interest. Froude number (Fr) was included in the dimensional analysis as it explains the effect of reciprocation forces, which is described as the ratio of the inertial force to the gravitational force. From its definition, Fr is ratio of acceleration during reciprocating agitation or reciprocation intensity (RI) (defined in Equation 8.1), and acceleration due to gravity. Thus, Fr was calculated using Equation (9.4).

$$Fr = RI/g = \frac{\omega^2 l(1 + (l/2r))}{2g} \tag{9.4}$$

where, g is the acceleration due to gravity, ω is angular velocity in radian/s (2*π*frequency), l is the characteristic length, and r is the length of connecting rod (0.4 m).

To account for the effect of particle concentration and particle density in correlations for liquid-particulate mixtures, the ratio of the particle volume to the volume of the liquid ($\frac{\varepsilon}{100-\varepsilon}$) and the ratio of the particle density to the liquid density ($\frac{\rho_p}{\rho_l}$) was included. The effect of headspace of can was taken into account using the ratio of headspace to length of can ($\frac{h_s}{L_c}$).

Aspect ratio (AR) of the can with respect to the reciprocation axis was also taken into account to take into account the effect of orientation of can. Aspect ratio was defined as the dimension of can along the axis of reciprocation to the dimension of can vertically perpendicular (horizontally perpendicular if the axis of reciprocation in vertical) to the axis of reciprocation. Thus, for HA orientation it was defined as length of can (L_c)/diameter of can (D_c), for HP orientation, it was equal to 1 and for V orientation it was equal to D_c/L_c. The magnitudes of the dimensionless groups were calculated using the physical and thermal properties of materials at the average bulk temperature of the process and detailed in Table 9.2.

Table 9.2. Thermo-physical properties of materials used in development of dimensionless correlations.

Material	**Density, ρ (kg/m^3)**	**Heat capacity, c_p (J/kg.K)**	**Thermal conductivity, k (W/m.K)**	**Thermal diffusivity, α (m^2/s)**	**Kinematic viscosity, ν (m^2/s)**	**Thermal expansion coefficient, β (1/K)**
Nylon	1130	2070	0.37	$1.5x10^{-7}$		-
Polypropylene	830	1840	0.36	$2.3x10^{-7}$	-	-
Teflon	2210	980	0.29	$1.3x10^{-7}$	-	-
Glycerin (100%)	1260	2430	0.28	$0.9x10^{-7}$	$7.5x10^{-4}$	$5.1x10^{-4}$
Glycerin (80%)	1210	2720	0.33	$1.0x10^{-7}$	$7.5x10^{-5}$	$5.0x10^{-4}$
Glycerin (50%)	1130	3340	0.41	$1.1x10^{-7}$	$9.7x10^{-6}$	$4.5x10^{-4}$
Glycerin (20%)	1050	3760	0.53	$1.3x10^{-7}$	$2.8x10^{-6}$	$3.4x10^{-4}$
Glycerin (0%)/ Water	1000	4180	0.60	$1.4x10^{-7}$	$1.0x10^{-6}$	$2.5x10^{-4}$

9.3.2 Characteristic Dimensions

Various dimensionless groups used in this study (Nu, Ra, Pe, Gr, Pr, Re) are widely affected by the characteristics dimensions to diversified degree of magnitude; therefore, one should be careful while selecting the appropriate one when the comparison is to be made with published correlations (Awuah *et al.*, 1995). Different parameters were tested for their suitability to be used as a characteristic length. Any parameter which yields dimensionless correlations with high coefficient of determination (R^2), low mean squared error (MSE) and low coefficient of variation (CoV) was considered to be suitable to be used as characteristic dimension.

Since, U is affected more by the dimension of can as it is the heat transfer coefficient at can wall and h_{fp} is affected more by particle dimensions as it is the heat transfer coefficient between fluid and particle, diameter of particle (D_p) was used as a possible characteristic length for U correlations and diameter of particle (D_p) was used as a possible factor for h_{fp} correlations.

Amplitude of reciprocation is another important factor which may affect the heat transfer in reciprocating agitation. Since heat transfer at both the can wall (U) and particle-fluid interface is affected by change in amplitude, amplitude was chosen as a factor to be tested for suitability as characteristic length for both U and h_{fp}.

The placement of can inside the reciprocating cage is bound to affect the nature of heat transfer occurring in the system. To take the effect of different orientations into consideration, diameter of can along the axis of reciprocation, or simply the axial dimension of can (D_{axis}) was also considered as a possible choice for characteristic length. D_{axis} was equal to the length of can (L_c) for cans with its longer axis along the axis of reciprocation (HA orientation), and was equal to the diameter of can (D_c) for cans placed vertically (V orientation) or horizontally perpendicular to the axis of reciprocation (HP orientation).

To summarize, different combinations of A, D_c and D_{axis} were evaluated as characteristics dimensions for correlations of U, while different combinations of A, D_p and D_{axis} were evaluated as characteristics dimensions for correlations of h_{fp}.

9.3.3 Regression Analysis

The general form of the dimensional correlations used to accommodate the complex combination of natural and forced convection heat transfer mechanisms in the case of reciprocating cans filled with liquid particulate mixtures can be given as Equation (9.5).

$$Nu = A_1(Ra)^{A_2} + A_3(Pe)^{A_4} * (Fr)^{A_5} * \left(\frac{\rho_p}{\rho_l}\right)^{A_6} * \left(\frac{\varepsilon}{100-\varepsilon}\right)^{A_7} * \left(\frac{h_s}{L_c}\right)^{A_8} * (AR)^{A_9} \quad (9.5)$$

While modeling pure forced convection regime, the term of Ra was dropped from Equation (9.5). While modeling liquid only scenario, the terms of ratio of the particle volume to the volume of the liquid ($\frac{\varepsilon}{100-\varepsilon}$) and the ratio of particle density to liquid density ($\frac{\rho_p}{\rho_l}$) were dropped.

A multiple nonlinear regression analysis (solver) was performed to evaluate the values of coefficients from A_1 to A_9, by employing tangent as an estimate and Newton as a search method. Coefficient of determination (R^2), coefficient of variation (MSE) and mean square error (MSE) were evaluated to analyze the goodness of fit of the correlation model.

9.4 Results and discussion

9.4.1 Characteristic length

The characteristic length to be used in the generation of dimensionless numbers is a crucial factor which not only helps to improve model accuracy, but also shines a light on the inherent nature of the physical phenomenon (Sablani *et al.*, 1997).

In this study, diameter of can (D_c), amplitude of reciprocation (A) and dimension of can along the axis of reciprocation (D_{axis}), individually and in combination with each other, were tested for their suitability to be used as characteristic length in correlations for the overall heat transfer coefficient (U). For fluid-to-particle heat transfer coefficient (h_{fp}), diameter of particle (D_p) was used instead of D_c in testing for a suitable characteristic length.

Tables 9.3 and 9.4 list the values of mean square error (MSE), coefficient of variation (CoV) and coefficient of determination (R^2) for each of the six combinations of the three lengths studied for U and h_{fp}.

Table 9.3. Results of regression analysis with various characteristic dimensions for dimensionless correlations of overall heat transfer coefficient (U)

Characteristic dimension	Correlation	R^2	MSE	CoV (%)
Diameter of can (D_c)	$Nu=112.94Ra^{-0.028}+8.52Pe^{0.45}Fr^{0.87}(\frac{\rho_p}{\rho_l})^{-0.96}(\frac{\varepsilon}{100-\varepsilon})^{0.13}(\frac{h_s}{L_c})^{-0.012}AR^{0.17}$	0.87	1330	20.90
Amplitude (A)	$Nu=31.06Ra^{0.026}+0.061Pe^{0.65}Fr^{0.33}(\frac{\rho_p}{\rho_l})^{-0.77}(\frac{\varepsilon}{100-\varepsilon})^{0.079}(\frac{h_s}{L_c})^{-0.076}AR^{-0.0029}$	0.93	1400	9.41
Axial dimension of can (D_{axis})	$Nu=83.22Ra^{-0.013}+2.49Pe^{0.54}Fr^{0.86}(\frac{\rho_p}{\rho_l})^{-0.98}(\frac{\varepsilon}{100-\varepsilon})^{0.14}(\frac{h_s}{L_c})^{-0.019}AR^{-0.038}$	0.85	662	21.43
$A+D_c$	$Nu=94.21Ra^{0.0089}+0.021Pe^{0.72}Fr^{0.41}(\frac{\rho_p}{\rho_l})^{-0.83}(\frac{\varepsilon}{100-\varepsilon})^{0.092}(\frac{h_s}{L_c})^{-0.047}AR^{-0.0024}$	0.90	3650	10.95
$A+D_{axis}$	$Nu=73.35Ra^{0.0090}+0.031Pe^{0.56}Fr^{0.48}(\frac{\rho_p}{\rho_l})^{-0.84}(\frac{\varepsilon}{100-\varepsilon})^{0.098}(\frac{h_s}{L_c})^{-0.055}AR^{0.10}$	0.95	756	9.52
D_c+D_{axis}	$Nu=205.62Ra^{-0.021}+1.73Pe^{0.52}Fr^{0.87}(\frac{\rho_p}{\rho_l})^{-0.97}(\frac{\varepsilon}{100-\varepsilon})^{0.13}(\frac{h_s}{L_c})^{-0.013}AR^{0.10}$	0.86	2760	11.02
$A+D_c+D_{axis}$	$Nu=193.65Ra^{-0.0016}+0.19Pe^{0.59}Fr^{0.61}(\frac{\rho_p}{\rho_l})^{-0.89}(\frac{\varepsilon}{100-\varepsilon})^{0.11}(\frac{h_s}{L_c})^{-0.020}AR^{0.043}$	0.89	7440	15.16

Suitability of any correlation model can be adjudged by considering the values of coefficient of determination (R^2), coefficient of variation (CoV) and mean squared error (MSE). The most desirable model to represent a process must have maximum R^2, minimum CoV and minimum MSE. For correlations of U, lowest CoV (~9.4%) was observed on using amplitude (A) as the characteristic length. On the other hand, lowest MSE (~662) was observed on choosing axial length of can (D_{axis}) as the characteristic length, albeit with considerably low R^2 (~0.85) and

high CoV (~21.4%). However, on using sum of amplitude and axial dimension ($A+D_{axis}$), R^2 (~0.95) was highest and MSE improved tremendously (from 1400 to 756) as compared to using amplitude (A) alone, while CoV (~9.5%) was almost similar. Hence, $A+D_{axis}$ was considered to be most suitable to be used as the characteristic length for correlations of U in reciprocating agitation.

In rotary agitation, researchers (Anantheswaran and Rao, 1985a, Sablani *et al.*, 1997; Meng and Ramaswamy, 2007c; Dwivedi and Ramaswamy, 2010d) have generally found the sum of diameter of rotation and length (or diameter) of can (D_r+D_c) to be the most appropriate choice as characteristic length for U. Here, it must be noted that amplitude of reciprocation is analogous to the diameter of rotation in rotary agitation (Section 5.4.3). Since, Reynolds number and other characteristic numbers are directly affected by the change of speed of can on variation of amplitude (or diameter of rotation), its choice as a characteristic length is plausible. However, earlier researchers did not consider orientation/inclination of containers and, thus, got the length/diameter of can (D_c) directly as an additional constituent of characteristic length. But, in this study, we varied the orientation of containers and hence, inclusion of D_c as characteristic length (individually or in combination with other parameters) failed in predicting the dimensionless number appropriately yielding high MSE and CoV, and low R^2 (Table 9.3).

Change in orientation in reciprocating agitation is analogous to change in mode of rotation (ex: end-over-end mode, axial mode, biaxial mode etc.) or angle of inclination of can in rotary agitation, but, a single dimensionless correlation for all three modes of rotation has not been developed. Yet, Kurian *et al.* (2009), using CFD simulations, did find that dimensionless numbers like Nusselt number varied with change in angle of inclination of can and this variation was proportional to the projection of the dimension of can along the axis. Farid and Ghani (2004) also suggested choosing different characteristic length for different orientations and used radius of can as the characteristic dimension for vertical cans and half of height of can as characteristic dimension for horizontal cans. Thus, suitability of D_{axis} in dimensionless correlation can be explained by the fact that it enables to account for the change in dimension of can along the axis of reciprocation on changing the orientation of the can.

Table 9.4. Results of regression analysis with various characteristic dimensions for dimensionless correlations of fluid-to-particle heat transfer coefficient (h_{fp})

Characteristic dimension	Correlation	R^2	MSE	CoV (%)
Diameter of particle (D_p)	$Nu=-25.03Ra^{-0.097}+0.90Pe^{0.41}Fr^{0.044}(\frac{\rho_p}{\rho_l})^{-0.49}(\frac{\varepsilon}{100-\varepsilon})^{0.036}(\frac{h_s}{L_c})^{-0.10}AR^{-0.82}$	0.85	1040	12.80
Amplitude (A)	$Nu=0.062Ra^{0.25}+0.24Pe^{0.51}Fr^{0.049}(\frac{\rho_p}{\rho_l})^{-0.58}(\frac{\varepsilon}{100-\varepsilon})^{0.039}(\frac{h_s}{L_c})^{-0.11}AR^{0.037}$	0.91	2430	11.64
Axial dimension of can (D_{axis})	$Nu=-0.13Ra^{0.21}+974.85Pe^{-0.035}Fr^{0.30}(\frac{\rho_p}{\rho_l})^{-0.48}(\frac{\varepsilon}{100-\varepsilon})^{0.040}(\frac{h_s}{L_c})^{-0.12}AR^{-0.62}$	0.85	1150	15.43
$A+D_p$	$Nu=0.073Ra^{0.24}+0.21Pe^{0.52}Fr^{0.047}(\frac{\rho_p}{\rho_l})^{-0.59}(\frac{\varepsilon}{100-\varepsilon})^{0.039}(\frac{h_s}{L_c})^{-0.11}AR^{0.03}$	0.93	1090	9.14
$A+D_{axis}$	$Nu=0.22Ra^{0.21}+0.21Pe^{0.52}Fr^{0.053}(\frac{\rho_p}{\rho_l})^{-0.60}(\frac{\varepsilon}{100-\varepsilon})^{0.042}(\frac{h_s}{L_c})^{-0.12}AR^{-0.07}$	0.87	7030	17.29
D_p+D_{axis}	$Nu=-5.80*10^{9}*Ra^{-1.30}+200.85Pe^{0.078}Fr^{0.26}(\frac{\rho_p}{\rho_l})^{-0.57}(\frac{\varepsilon}{100-\varepsilon})^{0.045}(\frac{h_s}{L_c})^{-0.13}AR^{0.82}$	0.81	1640	11.94
$A+D_p+D_{axis}$	$Nu=0.22Ra^{0.21}+0.22Pe^{0.52}Fr^{0.057}(\frac{\rho_p}{\rho_l})^{-0.60}(\frac{\varepsilon}{100-\varepsilon})^{0.042}(\frac{h_s}{L_c})^{-0.12}AR^{-1.06}$	0.86	8162	11.41

For correlations of h_{fp}, sum of diameter of particle and amplitude of rotation ($A+D_p$) gave the best R^2 (=0.93) and lowest CoV (=9.1%) (Table 9.4). The value of MSE (=1090) for $A+D_p$ was also only slightly higher than lowest MSE (=1040) observed on using D_p alone as characteristic length. Since, axial dimension of can was not a suitable choice, it can be seen that the effect of container orientation was not as important for h_{fp} correlations, as it was for U correlations. From the results discussed herein and in Table 9.4, $A+D_p$ was chosen as the characteristic length for correlations of h_{fp} in reciprocating agitation.

In rotary agitation, Fernandez *et al.* (1988) and Sablani *et al.* (1997) used equivalent particle diameter (or radius) as characteristic dimension for dimensionless correlations of h_{fp} in end-over-end mode of agitation. This is in line with our results for reciprocating agitation, except that we obtained an additional factor (A), which suggests the greater impact of amplitude on the

phenomenon of heat transfer in reciprocating agitation. Similar to our results, Dwivedi and Ramaswamy (2010d) found the sum of diameter of particle and radius of rotation (D_p+D_r) as optimum characteristic length in free and fixed axial modes, and in line with results of other researchers, they found D_p to be more suitable than D_r when considered individually. However, in our study, amplitude alone gave better R^2 and CoV than D_p (Table 9.4). Hence, importance of amplitude in h_{fp} correlations for reciprocating agitation was found to be far greater than that of particle diameter.

9.4.2 Role of natural and forced convection during reciprocating agitation

The dimensionless group Gr/Re^2 describes the ratio of buoyant forces to inertia forces and governs the relative importance of free to forced convection regimes. When $Gr/Re^2 << 1$, Nusselt number can be considered to be a function of only Peclet number (Pe=Re*Pr) and effects of free convection due to Rayleigh number (Ra=Gr*Pr) may be ignored, while when $Gr/Re^2 >> 1$, forced convection mechanisms due to Pe can be ignored. However, when $Gr/Re^2 \approx 1$, combined effects of free and forced convection must be considered resulting in mixed convection scenarios. Johnson *et al.* (1988) prescribed this zone of mixed convection to be between 0.8 and 5.10 while Awuah and Ramaswamy (1996) suggested the limit to be 1.3-23.5. The ratio of Gr/Re^2 during reciprocating agitation fell between 0.01-4.46 for U and 0.02-6.86 for h_{fp}. The lower limit of the ratio fell below the limits suggested by both Johnson *et al.* (1988) and Awuah and Ramaswamy (1996), indicating the dominance of forced convection in reciprocating agitation.

Both upper and lower limits of Gr/Re^2 were far lower than that found by Dwivedi and Ramaswamy (2010d) in free-axial (U: 0.26-13.51; h_{fp}: 0.22-13.51) and fixed-axial (U: 0.38-18.7; h_{fp}: 0.27-16.79) mode of rotary agitation, suggesting that forced convection effects were much more predominant in reciprocating agitation as compared to rotary agitation.

Fig 9.1 presents the variation of Gr/Re^2 with Froude number (Fr) for U and h_{fp} correlations. It is clear that Gr/Re^2 was very strongly correlated with Fr, which is the measure of maximum acceleration felt by the moving can and its particles. As soon as Fr increased beyond 0.5-0.6, Gr/Re^2 fell below the lower limit of 0.8 for mixed convection (Jonhnson *et al.*, 1988) and forced convection dominated heat transfer regime became predominant. This is also evident from the

fact that Nu was very high (>100) when Gr/Re^2 ratio was less than 0.8 (Fig. 9.2). Hence, heat transfer was modelled initially as pure forced convection.

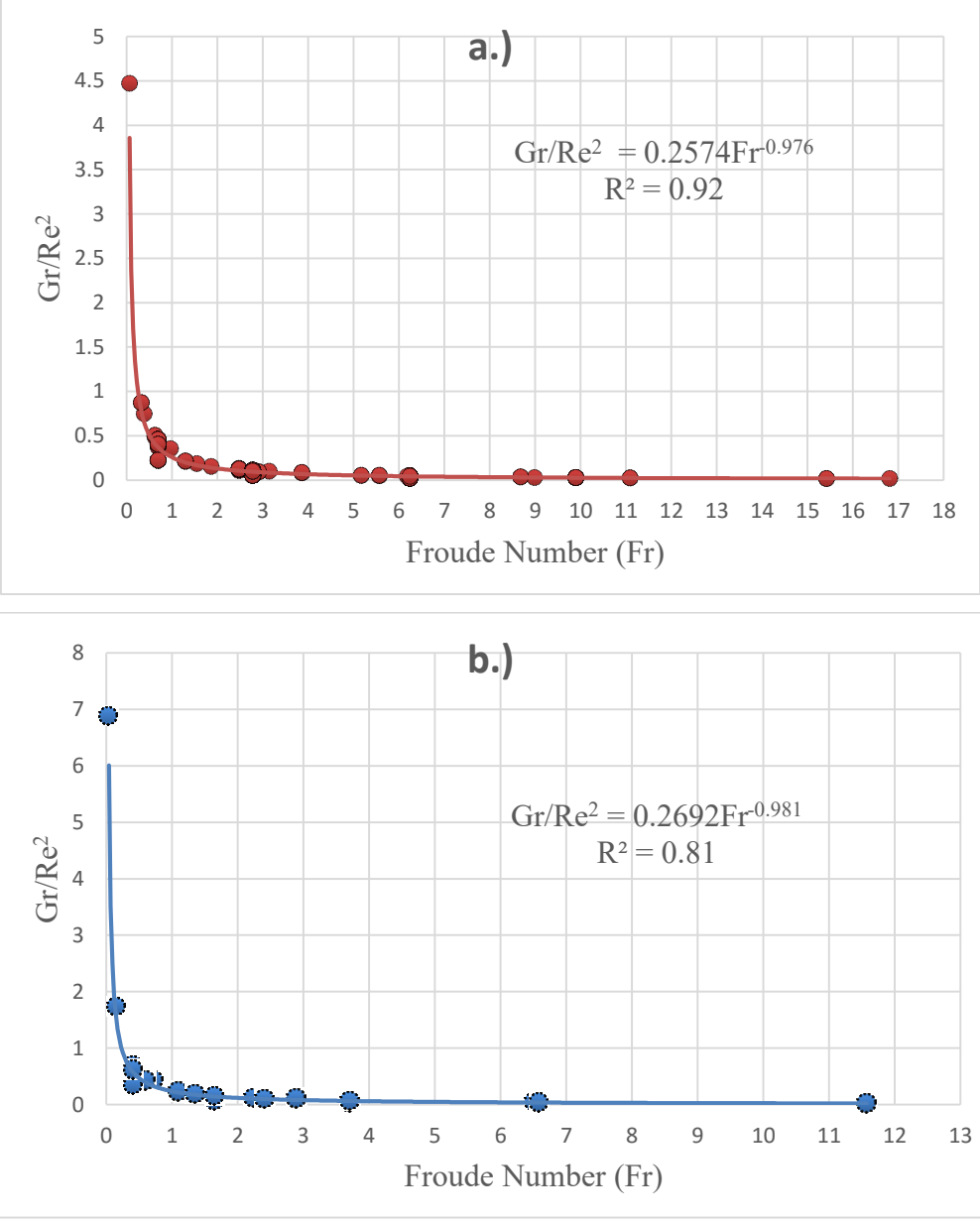

Fig. 9.1. Plot between Gr/Re^2 and Froude number (Fr) for a) overall transfer coefficient (U) and b) fluid-to-particle heat transfer coefficient (h_{fp}) correlations.

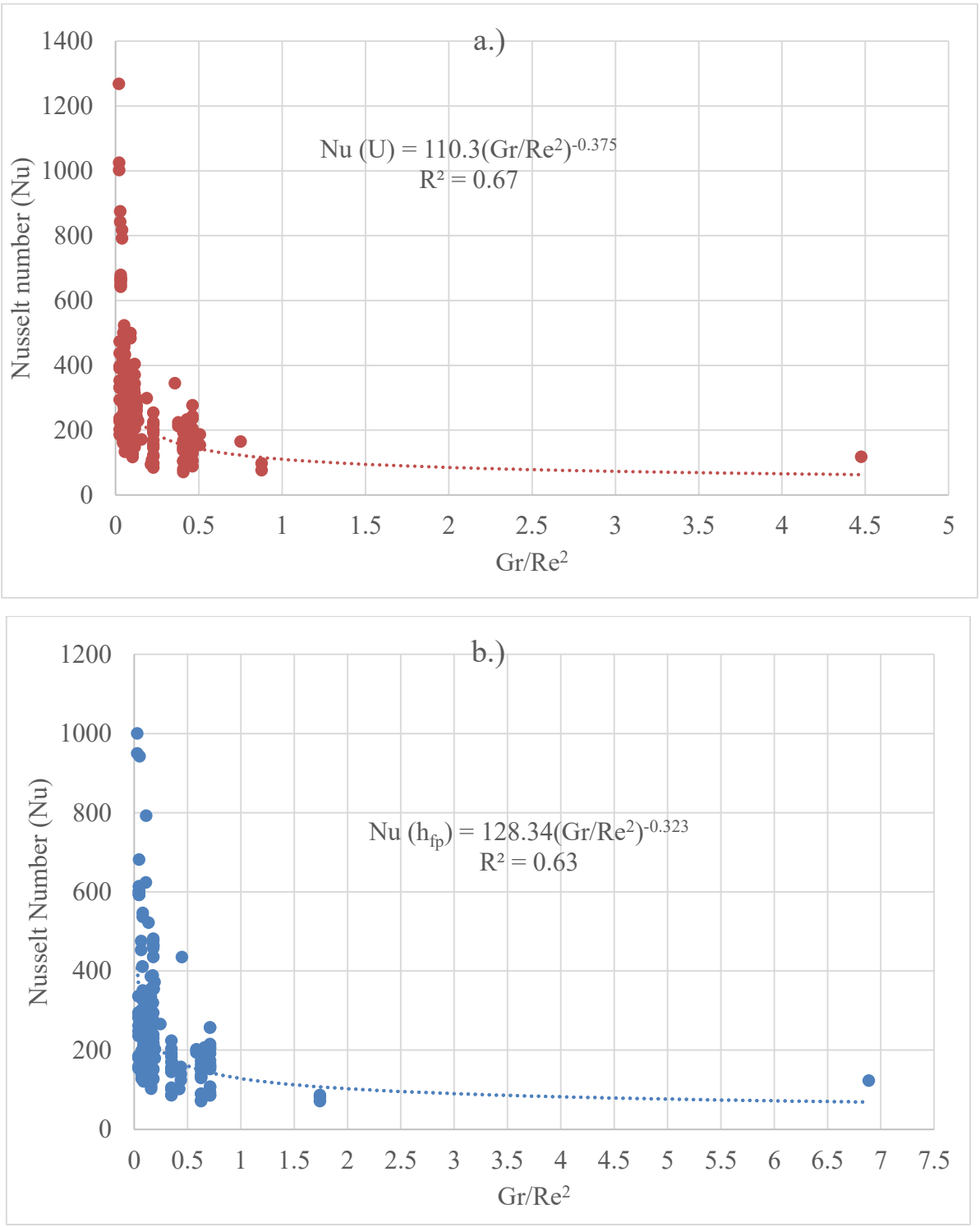

Fig. 9.2. Plot between Nusselt number (Nu) and Gr/Re^2 for a) overall transfer coefficient (U) and b) fluid-to-particle heat transfer coefficient (h_{fp}) correlations.

Equations (9.6) and (9.7) represent the dimensionless correlations assuming pure forced convection for U and h_{fp}. These models gave a good fit with experimental data (Fig. 9.3) with MSE and CoV of 4420 and 12.3% respectively for U correlations, and of 3140 and 13.9% for h_{fp} correlations.

$$Nu\ (U)=0.048Pe^{0.58}Fr^{0.21}\left(\frac{\rho_p}{\rho_l}\right)^{-0.53}\left(\frac{\varepsilon}{100-\varepsilon}\right)^{0.061}\left(\frac{h_s}{L_c}\right)^{-0.036}AR^{0.13} \qquad R^2 = 0.88 \quad (9.6)$$

$$Nu\ (h_{fp})=0.25Pe^{0.50}Fr^{0.050}\left(\frac{\rho_p}{\rho_l}\right)^{-0.52}\left(\frac{\varepsilon}{100-\varepsilon}\right)^{0.038}\left(\frac{h_s}{L_c}\right)^{-0.10}AR^{0.08} \qquad R^2 = 0.89 \quad (9.7)$$

However, some of the data points in Figs. 9.1 and 9.2 fell in the region of mixed convection. Also, there was some scatter recorded in Fig. 9.3. Hence, it was decided to include mixed convection mode in the analysis. The contributions from natural convection were accounted by introducing additive terms in the model for Rayleigh number resulting in Equations (9.8) and (9.9) for U and h_{fp} respectively.

$$Nu\ (U) =73.35Ra^{0.0090}+0.031Pe^{0.56}Fr^{0.48}\left(\frac{\rho_p}{\rho_l}\right)^{-0.84}\left(\frac{\varepsilon}{100-\varepsilon}\right)^{0.098}\left(\frac{h_s}{L_c}\right)^{-0.055}AR^{0.10} \qquad R^2 = 0.95 \quad (9.8)$$

$$Nu\ (h_{fp})=0.073Ra^{0.24}+0.21Pe^{0.52}Fr^{0.047}\left(\frac{\rho_p}{\rho_l}\right)^{-0.59}\left(\frac{\varepsilon}{100-\varepsilon}\right)^{0.039}\left(\frac{h_s}{L_c}\right)^{-0.11}AR^{0.03} \qquad R^2 = 0.93 \quad (9.9)$$

For the mixed convection model, CoV was 9.5% and 9.1% for U and h_{fp} correlations respectively and MSE was 756 and 1090 respectively. Dimensionless correlations for U (Equations 9.6 and 9.8) were valid in the range $2.21*10^3 < Gr < 4.14*10^9$; $7 < Pr < 8180$; $5.02*10^1 < Re < 4.06*10^5$; $1.81*10^7 < Ra < 2.90*10^{10}$; $3.73*10^5 < Pe < 1.13*10^7$; $0.062 < Fr < 16.8$; $0.66 < \frac{\rho_p}{\rho_l} < 2.21$; $0.001 < \frac{\varepsilon}{100-\varepsilon} < 0.82$; $0.018 < \frac{h_s}{L_c} < 0.14$; $0.79 < AR < 1.26$. Dimensionless correlations for h_{fp} (Equations 9.7 and 9.9), on the other hand, were valid in the range $2.82*10^2<Gr<1.14*10^9$; $7 < Pr < 8180$; $1.27*10^1 < Re< 1.71*10^5$; $2.31*10^6 < Ra < 7.96*10^9$; $1.04*10^5<Pe<6.33*10^6$; $0.037<Fr<11.6$; $0.66<\frac{\rho_p}{\rho_l}<2.21$; $0.001<\frac{\varepsilon}{100-\varepsilon} < 0.82$; $0.018 < \frac{h_s}{L_c} < 0.14$; $0.79 < AR < 1.26$.

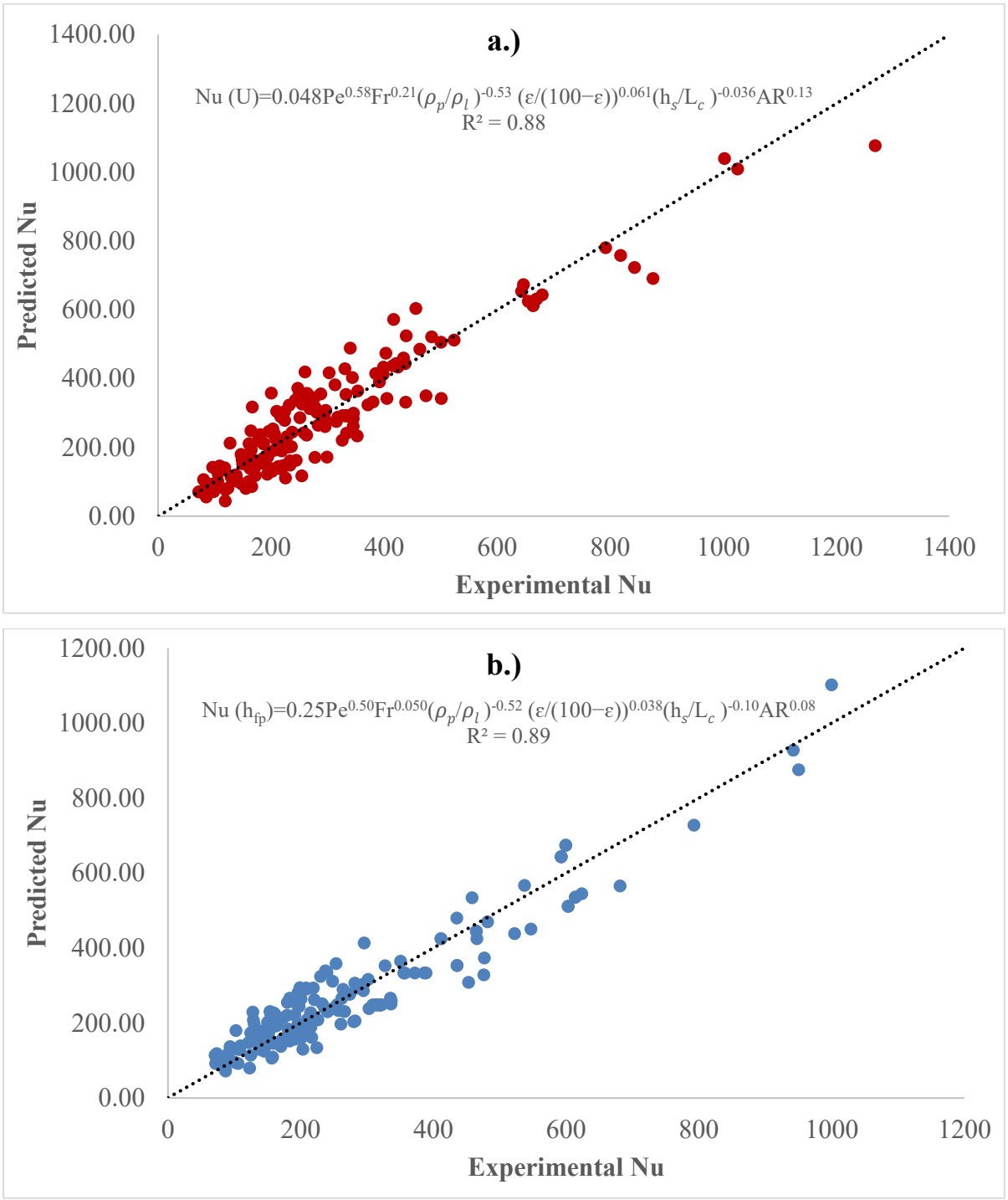

Fig. 9.3. Experimental versus predicted (Nu) for liquid-particulate mixtures subjected to reciprocating agitation thermal processing for dimensionless correlations derived using pure forced convection model from a) Equation (9.6) for overall heat transfer coefficient (U) and b) Equation (9.7) for fluid-to-particle heat transfer coefficients (h_{fp}).

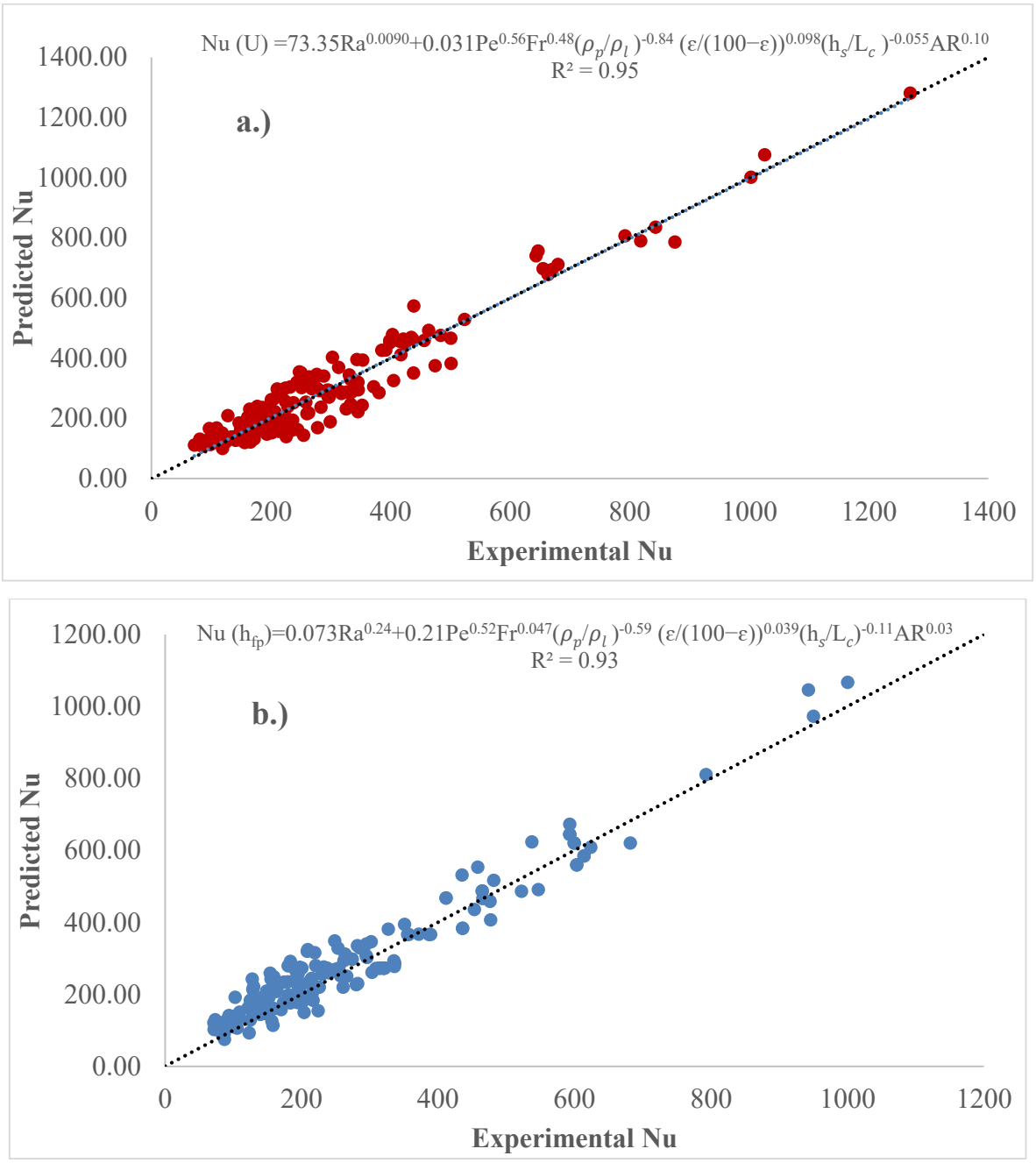

Fig. 9.4. Experimental versus predicted (Nu) for liquid-particulate mixtures subjected to reciprocating agitation thermal processing for dimensionless correlations derived using mixed convection model from a) Equation (9.8) for overall heat transfer coefficient (U) and b) Equation (9.9) for fluid-to-particle heat transfer coefficients (h_{fp}).

Better R^2, CoV and MSE, on including the natural convection term, show better suitability of Equations (9.8 and 9.9) as compared to Equations (9.6 and 9.7) to model the heat transfer phenomenon during reciprocating agitation thermal processing. Also, the experimental v/s predicted plot of Nusselt number for the mixed convection model is shown in Fig. 9.4 and shows a better fit than the forced convection model (Fig. 9.3). Better fits using a mixed convection model were also observed by Dwivedi and Ramaswamy (2010d) for correlations involving rotary modes of agitation.

Fand and Keswani (1973) postulated that natural convection continues to operate in all forced convection situations, as buoyant forces resulting from density differences are always present. Hence, in order to quantify the contribution of natural convection towards heat transfer during reciprocating agitation thermal processing, contribution from the first term on the right hand side of Equation (9.8) and Equation (9.9) was evaluated. This contribution ranged between 2-26% and 0.3-11% for U and h_{fp} correlations respectively. The contribution of natural convection happening was also found significant strongly correlated with the term Gr/Re^2 (Fig. 9.5). The contribution of natural convection increased with Gr/Re^2 very rapidly and is in accordance with the observations of other researchers (Johnson *et al.*, 1988; Awuah and Ramaswamy, 1996; Sablani *et al.*, 1997; Dwivedi and Ramaswamy, 2010d).

From Fig. 9.5, it is clear that the contribution of natural convection was much more significant for U as compared to h_{fp}. This may be attributed to the fact that forced convection helped in enhancing heat transfer at the liquid-particle interface more tremendously due to motion of particles, as compared to the heat transfer through can wall. Dwivedi and Ramaswamy (2010d) also found similar trends with the minimum contribution of natural convection in heat transfer in free axial mode of rotation to be 3.24% for U and 1.96% for h_{fp} and in fixed axial mode of rotary agitation to be 21.50% for U and 15.5% for h_{fp}. However, other researchers (Sablani *et al.*, 1997; Meng and Ramaswamy, 2007c) did not consider natural convection in their models for end-over-end agitation, and hence our results could not be compared with end-over-end mode of rotation. Thus, while forced convection was the more predominant mechanism in reciprocating agitation as compared to rotary agitation, still, consistent with the argument of Fand and Keswani (1973), natural convection phenomenon cannot be ignored.

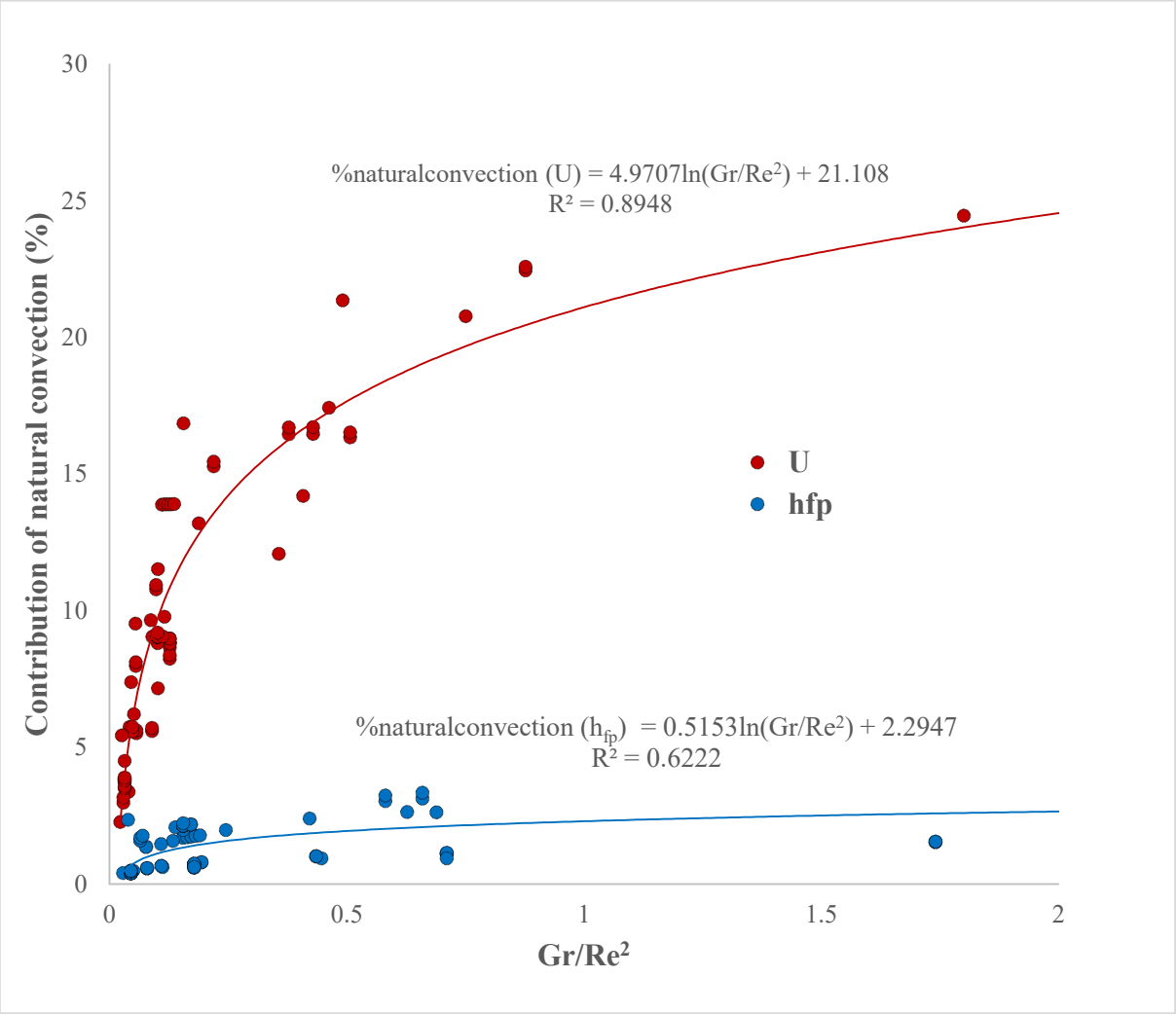

Fig. 9.5. Contribution of natural convection towards heat transfer at the can wall (U) and at the liquid-particle interface (h_{fp})

9.4.3 Heat transfer in liquid particulate mixtures subjected to reciprocating agitation.

Equations (9.8 and 9.9) represent the dimensionless correlations for liquid-particulate food products and can be used to predict the heat transfer coefficients (U and h_{fp}) under a wide variety of processing conditions, based on the validity of the respective equations (discussed in Section 9.4.2). In previous section, the role of contribution of natural convection (due to Ra) and forced convection (due to Pe) towards heat transfer in liquid particulate mixtures has also been discussed. In this section, we focus on the effect of individual terms.

The Nusselt number (Nu) for U correlation was proportional to $Fr^{0.48}$ and for h_{fp} correlation was proportional to $Fr^{0.047}$, which implies that the Nusselt number increased with increase in Froude number. Froude number is proportional to the reciprocation intensity and it is obvious that Nu increased with increasing reciprocation intensity. This is mainly due to increase in turbulence on increase in reciprocation intensity. However, in rotary agitation, researchers (Meng and Ramaswamy, 2007c; Dwivedi and Ramaswamy, 2010d) have observed that Nu decreases with increase in Fr. Here, it is worth mentioning that, Fr in rotary agitation is defined on the basis of ratio of centrifugal forces and gravity forces, while in reciprocating agitation, Fr is the ratio of reciprocating force and gravity force. In this context, it must be noted that centrifugal forces are restrictive to the amount of heat transfer as they force the particles to clump against the can wall, thus decreasing the intensity of agitation. No such detrimental effect is associated with reciprocating forces and the intensity of agitation increases uninhibited during reciprocating motion. This may be the cause of difference in trends in the effect of Fr during reciprocating agitation, as compared to rotary agitation.

The Nusselt number (Nu) was proportional to $(\frac{\varepsilon}{100-\varepsilon})^{0.098}$ and $(\frac{\varepsilon}{100-\varepsilon})^{0.039}$ (terms signifying particle concentration) for U and h_{fp} respectively, implying that with the increasing particle concentration, Nu increased slightly. Similar to our results, Meng and Ramaswamy (2007c) also reported a slight increase in Nu with the increase in particle concentration $(V_p/V_l/)^{0.091}$. With multiple particles in Newtonian fluids during end-over-end rotation, Sablani *et al.* (1997) reported that increasing particle concentration reduced the heat transfer to the liquid and a negative component of $(e/100\text{-}e)^{-037}$ was obtained. In the correlation developed by Lenz and Lund (1978) with axial rotation, it was found that Nu was proportional to $(1\text{-}V_p/V_l)^{-0.46}$, which is similar to the trends in our study that Nu increased on increasing V_p/V_l.

The Nusselt number (Nu) was proportional to $(\frac{\rho_p}{\rho_l})^{-0.84}$ and $(\frac{\rho_p}{\rho_l})^{-0.59}$ for U and h_{fp} correlations respectively. This implies that with an increase in ratio of particle to liquid density, U and h_{fp} decreased. This is in contrast with the results of Meng and Ramaswamy (2007c) and Dwivedi and Ramaswamy (2010d) for rotary agitation. They observed that Nu increased with increase in this ratio. This discrepancy in trends with rotary agitation may be attributed to the fact that high density particles settled at the bottom of the can during horizontal reciprocation in this study, leading to a

decrease in heat transfer. This has been discussed in detail in Sections 6.4.4 and 7.4.2. On the other hand, higher density particles aided heat transfer during rotating motion as they fell more efficiently from the top of the container during rotary motion (Dwivedi and Ramaswamy, 2010d).

The effect of headspace was very slightly significant with the coefficient of only -0.055 and -0.11. This is far less as compared to the coefficient of 1.56 observed by Sablani *et al.* (1997), and coefficients of 0.655 and 0.35 observed by Garrote *et al.* (2006) for U and h_{fp} correlations respectively for end-over-end mode of agitation. This shows that the effect of headspace was less significant during reciprocating agitation than rotary agitation. Dwivedi and Ramaswamy (2010d) also found headspace very less significant and was eliminated from their dimensionless correlation during stepwise regression.

Aspect ratio of the can was a new term introduced by us to take into account the placement of can and its aspect ratio simultaneously. Aspect ratio was found significant with coefficient of 0.10 and 0.03 for U and h_{fp} correlations respectively. Thus, it is clear that Nu increased with increase in aspect ratio. This is in line with results in Chapter 5, where HA orientation was found to have higher heat transfer rate, followed by HP and V orientations respectively. Also, this is in accordance with the results that orientation affected U correlations more significantly as compared to h_{fp}.

9.4.4 Heat transfer in liquid-only cans subjected to reciprocating agitation.

Dimensionless correlations were also developed to model heat transfer in liquid-only cans. For this purpose, the values of overall heat transfer coefficient *U* available for single-particle scenario from chapters 4 and 6 were used. The characteristic length was same as that in the liquid-particulate scenario i.e. sum of amplitude of reciprocation and axial dimension of can ($A+D_{axis}$). Correlations were developed using the general equation Eq. 9.5 but the effect of the particle's physical properties ($\frac{\rho_p}{\rho_l}$ and$\frac{\varepsilon}{100-\varepsilon}$) were excluded as can content did not include particles. Equation (9.10) depicts the developed correlation.

$$Nu\ (U) = 24.17Ra^{0.012} + 1.61Pe^{0.39}Fr^{0.41}\left(\frac{h_s}{L_c}\right)^{0.7}AR^{0.40} \qquad R^2 = 0.96 \quad (9.10)$$

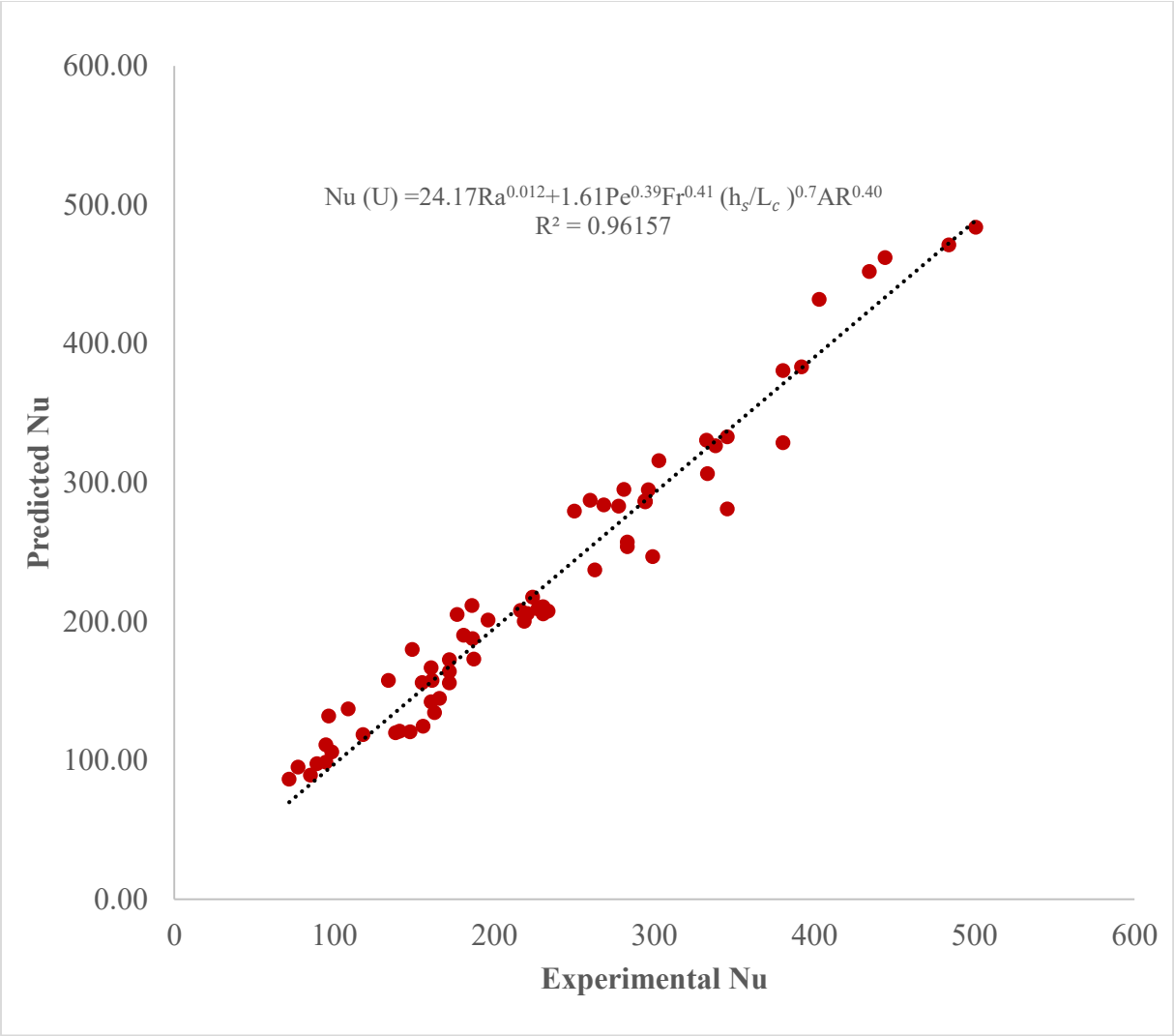

Fig. 9.6. Experimental versus predicted Nu for liquid-only cans subjected to reciprocating agitation thermal processing for dimensionless correlations in Equation (9.9).

Coefficient of determination (R^2) was 0.96, mean square error (MSE) was 645 and coefficient of variation was 6.9%. Thus, it was seen that Equation (9.9) presented a better fit than the general correlation for liquid-particulate mixtures in Equation (9.7). Experimental vs. predicted data from Equation (9.9) is presented in Fig. 9.6, which depicts a good correlation of the values. The validity of Equation 9.7 is limited to $1.51*10^4 < Gr < 4.14*10^9$; $7 < Pr < 8180$; $1.81*10^2 < Re < 4.06*10^5$; $1.23*10^8 < Ra < 2.90*10^{10}$; $7.36*10^5 < Pe < 4.46*10^6$; $0.062 < Fr < 6.24$; $0.018 < \frac{h_s}{L_c} < 0.14$; $0.79 < AR < 1.26$.

The contribution of natural convection to the total heat transfer was calculated from the first term of Equation (9.9), which was found to be 6-31%. Higher natural convection was achieved in comparison to the overall heat transfer coefficient correlation when used with particles (Eq. 9.7). There could be two main reasons; firstly the particles inside the can could have given secondary agitation to the other contents, and the other reason could be that the range of Re and Fr studied was higher in the multiple particles scenario.

This percentage contribution of natural convection was higher in rotary mode of agitation. Dwivedi and Ramaswamy (2010d) found the contribution in liquid-only/single-particle cans processed in free axial mode to be 51%. Rao and Anantheswaran (1988) reported that the percentage of natural convection varied between 47% and 99% for canned Newtonian liquid without particles processed in steritort between 2 to 8 rpm. These comparison suggest that reciprocating agitation was more efficient in enhancing the effect of forced convection, as contribution of natural convection was lower.

9.5 Conclusions

Dimensionless correlations for mixed (combination of natural and forced) and pure forced convection were developed for liquid-only and liquid-particulate canned foods processed using reciprocating agitation thermal processing. Sum of amplitude of reciprocation and axial dimension of can ($A+D_{axis}$) was found to be most suitable as characteristic length in U correlations, while sum of amplitude of reciprocation and diameter of particle ($A+D_p$) was most desirable for h_{fp} correlations. The developed equations gave higher coefficients of determination (R^2 ranging from 0.93 to 0.96), lower mean square (MSE ranging from 645 to 1191) and lower coefficient of variation (CoV ranging betweern 6.9% to 9.5%) as compared to pure forced convection model (R^2 ranging from 0.88 to 0.89, MSE from 3140 to 4420 and CoV from 12.3% to 13.9%). The ratio of Gr/Re^2 during reciprocating agitation fell between 0.01-4.46 for U and 0.02-6.86 for h_{fp} and this ratio was strongly correlated with Froude number (Fr) and Nusselt number (Nu). It was concluded that there was a contribution from natural convection existing during reciprocating agitation thermal processing, although the contribution was much lower than in rotary mode of agitation. This contribution was higher for liquid-only cans as compared to liquid-particulate cans due to mixing produced by movement of particles.

PREFACE TO CHAPTER 10

Flow visualization studies can be used to gain a further understanding of the mixing behavior of particulate systems and for understanding their influence on associated heat transfer within cans. In this chapter, a flow visualization study was carried out to observe the relative movement of partic1es in viscous fluids in containers subjected to simulated flow conditions representing thermal processing of cans under reciprocating agitation thermal processing conditions. Since the heat transfer coefficient associated with particulate fluids depends on the relative movement between liquid and solid surface, a visual observation study would give a better insight to this phenomenon.

Parts of this chapter have been submitted for publication as an article "*Visualization and quantification of particle-motion and particle-mixing during reciprocating mode of agitation*" in Journal of Food Engineering.

The experimental work and data analysis was carried out by the candidate under the supervision of Dr. H. S. Ramaswamy.

CHAPTER 10

VISUALIZATION AND QUANTIFICATION OF PARTICLE-MOTION AND PARTICLE-MIXING DURING RECIPROCATING MODE OF AGITATION

10.1 Abstract

A flow visualization study was carried out to observe the relative movement of particles in viscous fluids in containers subjected to simulated flow conditions representing thermal processing of cans under reciprocating agitation. The effects of various processing parameters on particle motion/mixing were investigated experimentally with single and multiple particles, in transparent glass containers. The containers were held inside the reciprocating cage, at room temperature with the door held in an open position for video taping of particle motion in the container. The concentration of covering liquid (glycerin) was adjusted to match the viscosity profile of the fluid at higher temperatures so that particle mixing behavior prevailing at thermal processing conditions could be visualized at room temperature processing conditions (neglecting temperature effects on physico chemical properties of the particle). Results showed that the particle and liquid movement was much more rapid in HA orientation as compared to V orientation. In HA orientation, the mixing was more uniform and particles moved throughout the container, while in V orientation, most of the mixing and motion was concentrated in the upper half of the container. Visualization of the motion of the particles revealed that higher density particles sank at the bottom of the container and had lower level of mixing. Mixing time was calculated using multiple particle case by observing the movement of the center mass of particles of two colors. Mixing time was only 15-70 s for HA orientation, as compared to 150-420 s for V orientation. Mixing time was also affected significantly by reciprocation frequency, liquid viscosity and particle concentration. These results implied that the heat transfer could be easily influenced by particle to fluid relative motion and that observed differences in heat transfer in the different particulate fluid systems could be related in sorne way to particle motion in the cans.

10.2 Introduction

It is well recognised that agitation is imparted during thermal processing to generate forced convection, produced due to movement of can contents, for enhancing the extent of heat transfer (Ramaswamy and Sablani, 1997). The movement of liquid and particles inside agitating cans helps

in achieving enhanced mixing conditions and increased turbulence. This aids in speeding up the process of heat transfer to the cold-spot and achieving greater temperature uniformity inside the can, both of which are highly desirable to reduce processing times. Thus, the phenomenon of heat transfer during agitation thermal processing is strongly correlated with the extent of particle motion and particle mixing achieved due to agitation. In this context, flow visualization studies can be a perfect tool to better understand the flow pattern of liquid and mixing behavior of particulates and their influence on associated heat transfer coefficients (Rao and Anantheswaran, 1988).

Various studies have been conducted to investigate the effect of liquid and particle motion during agitation processing. Hiddink (1976) studied the flow visualization of liquids (water, 75% glycerin and silicon oil) in cans during natural convection heating using a particle-streak method to observe the flow patterns. Later, Stoforos and Merson (1990) studied the motion of spherical particles in axially rotating cans and characterized the relative particle-to-fluid velocity under idealized conditions of particle motion in rotating cans. Their results also revealed that particles followed much more complicated path (flow pattern) than idealized in mathematical analyses. In another study Stoforos and Merson (1992) attempted to use this technique to explain the decrease of h_{fp} values when increasing rotational speed or decreasing liquid viscosity for a heavier particle (Teflon sphere in 350 cst silicone oil) in axial rotation. Ramaswamy and Sablani (1997) studied the motion of a single particle in a can during end-over-end rotation and explained the differences in h_{fp} between various experimental conditions. Sablani and Ramaswamy (1998) studied the multiple particle mixing behavior in water and oil subjected to end-over-end rotation and discussed the effects of various operating parameters on heat transfer coefficients. Sablani and Ramaswamy (1996) also conducted particle motion studies on nylon particles using different particle concentrations, particle size, particle shape and rotational speeds in end-over-end mode of rotation. Meng and Ramaswamy (2007d) analyzed the relative movement of particles in viscous fluids in containers subjected to simulated flow conditions representing thermal processing of cans under end-over-end agitation. They used carboxymethyl cellulose as a covering fluid and adjusted the concentration to match those at higher temperatures so that particle mixing behavior prevailing at thermal processing conditions could be observed at room temperatures. They observed that with low viscous fluids, the particle mixing was rapid and the particle rotation was more frequent and with high viscous fluid, the particle mixing was slow due to restricted motion. However, in

reciprocation agitation there is paucity of scientific literature on visualization of particle mixing behavior. The last study in this area was carried out over 8 years ago (Meng and Ramaswamy, 2007d) and with a different type of container agitation than what was used in this study.

In Chapters 4-7, the effect of various processing conditions and product properties on U and h_{fp} has been quantified with single and multiple particles in cans during reciprocating mode of agitation. In the agitation processing of cans containing liquid and solid particles, both the overall heat transfer coefficient and fluid-to-particle coefficients are influenced by particle motion. Various flow visualization studies have revealed that the differences in the heat transfer coefficients could be explained by the particle mixing behavior. The objective of the present work was, therefore, to carry out a flow visualization study to observe particle/fluid motion in Newtonian fluids to enable a better understanding of heat transfer problem associated with liquid-particulate cans during reciprocation agitation thermal processing.

10.3 Materials and methods

10.3.1 Materials

Experiments were carried out in a pilot scale reciprocating retort described in Chapter 3. All the experiments were conducted at room temperature, with the retort door held open for visual observation and video recording. For this purpose, glass containers, 7.5 cm diameter and 10 cm height were used in place of metal cans. Experiments were conducted for both single and multiple particles containing various concentrations of covering liquid (glycerin) under vertical (V) and horizontal (HA) container orientations. 19mm Nylon, polypropylene and Teflon particles were used to simulate particles of different densities. The thermophysical properties of these materials lie close to that of real food and have been detailed in Table 6.1.

10.3.2 Viscosity adjustment

Since the experiments were conducted at room temperature, the concentration of covering liquid (glycerin) was adjusted to match the fluid viscosity at the bulk average temperature during the equilibration time of a typical thermal process. The bulk average temperature was assumed to be 85 ºC. This was done so that particle mixing behavior prevailing at thermal processing conditions could be observed at room temperatures. For this, viscosity of glycerin was measured

using a controlled stress rheometer (AR 2000, TA Instruments, New Castle, DE, USA) with attached computer software (Rheology Advantage Data Analysis Program, TA version 2.3 s). 2 ml of different glycerin solutions were placed on the flat plate of the cone and plate geometry (60mm, 2^o steel cone) with the instrument programmed at 20°C. Zero gap and instrument rotational mapping was efficiently performed before executing the experiments so as to get reliable results. Each test was conducted using the flow procedure consisting of temperature ramp from 20ºC to 90ºC at the rate of 5ºC/min at the constant shear rate of 0.1768 Pa.

10.3.3 Visualization and Quantification

In the single particle study, effect of particle density was studied using 19 mm spherical particles of three different materials i.e. Polypropylene, Nylon, and Teflon representing different densities of particles in equivalent concentrations of 50 and 100% glycerin. These experiments were conducted at 2 Hz and 15 cm amplitude with a headspace of 12 mm.

With multiple particles in the containers, 19 mm spherical Nylon particles were used to study the effect of particle concentration (20, 30 and 40%) liquid viscosity (glycerin concentrations representative of 50 and 100% at 85ºC) and reciprocation frequency (1, 2 and 3 Hz). These experiments were conducted at 15 cm amplitude with a headspace of 12 mm. For observing the multi-particle mixing behavior under different processing conditions, at the beginning of the experiment, the glass containers were filled with two layers of particles of different colors (black and white) and appropriate fluid.

All experiments were performed under two orientations (HA – longer axis of can placed horizontally along the axis of reciprocation; V – longer axis of can placed vertically perpendicular to the axis of reciprocation). HP orientation (longer axis of can placed horizontally perpendicular to the axis of reciprocation) was not considered as it was difficult to videotape the cans when it was placed in this orientation and as the heat transfer in this orientation was found in between the HA and V orientations (Chapter 5).

All the experiments were videotaped, played subsequently on computer in slow motion and photographed for characterization of the particle motion and mixing. In each run, the experiment was conducted for sufficient time to allow sufficient mixing of the particles. Snapshots for analysis

of particle motion and particle mixing were taken at every 15s for V orientation and every 5s for HA orientation cans. In single particle scenario, the position of single particle inside the can was traced every 15 s and was presented to reveal the movement of the particle inside the container. In multiple particle scenario, the mixing of the two color particles was observed by the movement of the black and white particles. For this, the center of mass of the particles of two color was calculated for each snapshot and evaluated using Equation (10.1). The movement of the center of mass of each color demonstrated the motion of the particles while the distance between the center of mass of each color demonstrated the progress of mixing. The mixing time was characterized as the instant at which the distance between the center of mass of the particles reduced to zero for the first time.

$$x_c = \frac{\sum_{i=1}^{n} x_i}{n} \tag{10.1}$$

where n is the number of particles of a particular color, x_c is the position of center of mass from the base of can and x_i is the position of individual particle from the base of can.

10.4 Results and discussion

10.4.1 Adjustment of viscosity to match thermal processing conditions

In this study, experiments were conducted at room temperature to enable visual observation of reciprocation cans. Hence, it was important to adjust the experimental conditions to simulate actual thermal processing conditions. Since, viscosity of most liquids decrease with increase in temperature, the viscosity of covering fluid was adjusted to match that the the bulk average temperature of the process. Here, the process is not the total cook time, but rather the equilibration time of the cold-spot i.e. the time required for the cold spot to reach operating temperature. Only the temperature till the equilibration time of the cold-spot was considered. Time-temperature data for various processing conditions presented in Fig. 4.1 (Single particle under various reciprocating conditions) and Fig. 5.3 (Multiple particle under various container orientations) were considered and the average temperature of the process was found out to be 85 ºC.

The variation of viscosities of glycerin v/s temperature curve is shown in Fig. 10.1. It was seen that a straightline fit could be obtained between the logarithmic of viscosity and temperature curve. The fitted equations are presented in Fig 10.1 alongside each curves. These equations can thus be used to find the equivalent concentration of glycerin at room temperature which would give the same viscosity as that under the thermal processing scenario.

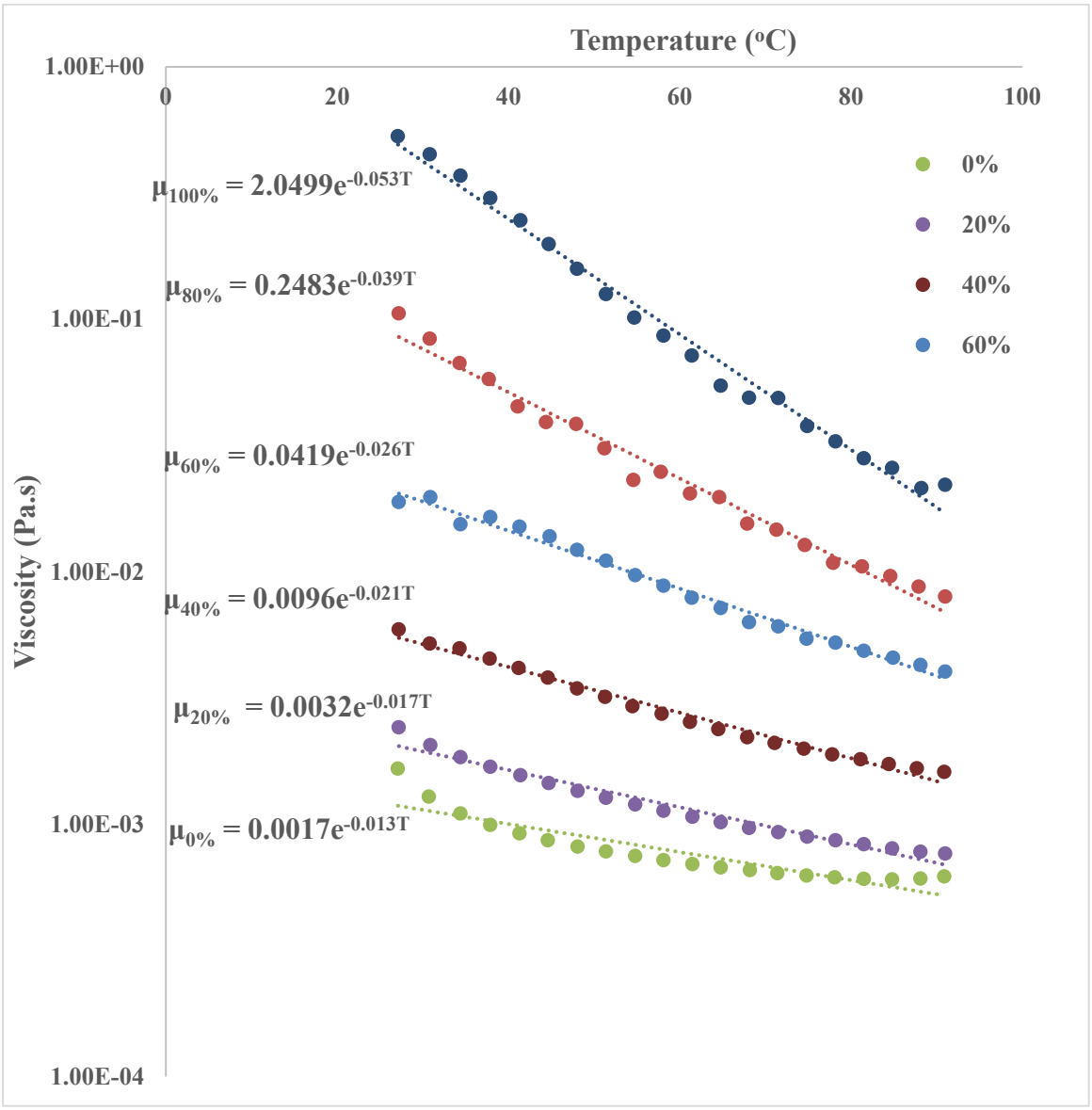

Fig. 10.1. Viscosity v/s temperature cuve for different concentrations of glycerin with correlations between viscosity (in Pa.s) and temperature (in ^{O}C)

Using interpolation of data from Fig. 10.1, it was found that 70% glycerin at room temperature exhibited similar viscosity at room temperature as that of 100% glycerin at bulk average temperature of the thermal process (85 ºC). Thus, 70% glycerin was used to simulate processing with 100% glycerin. Similarly, 30% glycerin was used at room temperature to simulate processing with 50% glycerin during the actual process. Similar method was also used by Meng and Ramaswamy (2007d) in their visualization studies. Although, it must be kept in mind that viscosity constantly varies with temperature, nevertheless, using equivalent viscosity during particle motion and visualization studies shall help in throwing better light on the agitation process.

10.4.2 Visualization of mixing and motion in different container orientations

In order to account the effect of container orientation, both single and multiple particle cans were filled with 50% glycerin concentrations and processed at 2 Hz. Results of this study revealed that container orientation was the most significant factor which affected particle motion and mixing. The phenomenon of mixing and motion of cans was found very different in the V and HA orientation and is discussed for single and multiple particle cans.

Single particle in can

Snapshot illustrations of a can, filled with single Nylon particle and equivalent of 50% glycerin concentration, processed under the two container orientations at 2 Hz are shown in Fig. 10.2 for various time instants. Under vertical orientation, most of the shaking and mixing was in the upper half of the can. There were small eddies and vortexes forming, although, most of them were concentrated near the top portion of covering liquid. On the other hand, during HA orientation, turbulence observed was much greater as compared to the V orientation. Liquid motion was very vigorous and there were many eddy currents and local vortexes forming throughout the container. Higher mixing during HA orientation may be attributed to the fact that the headspace was completely transferred to the sides during reciprocation (t=15s in Fig. 10.2b) resulting in the back and forth motion of the entire liquid. On the other hand, in V orientation the headspace movement reached only upto half the height of the can. Also, when the reciprocating liquid striked the curved surface of the side wall in V orientation, there were only slights deflections produced, as compared to HA orientation where the liquid bounced back after striking the wall. As a result, the motion of liquid in HA orientation was much more severe.

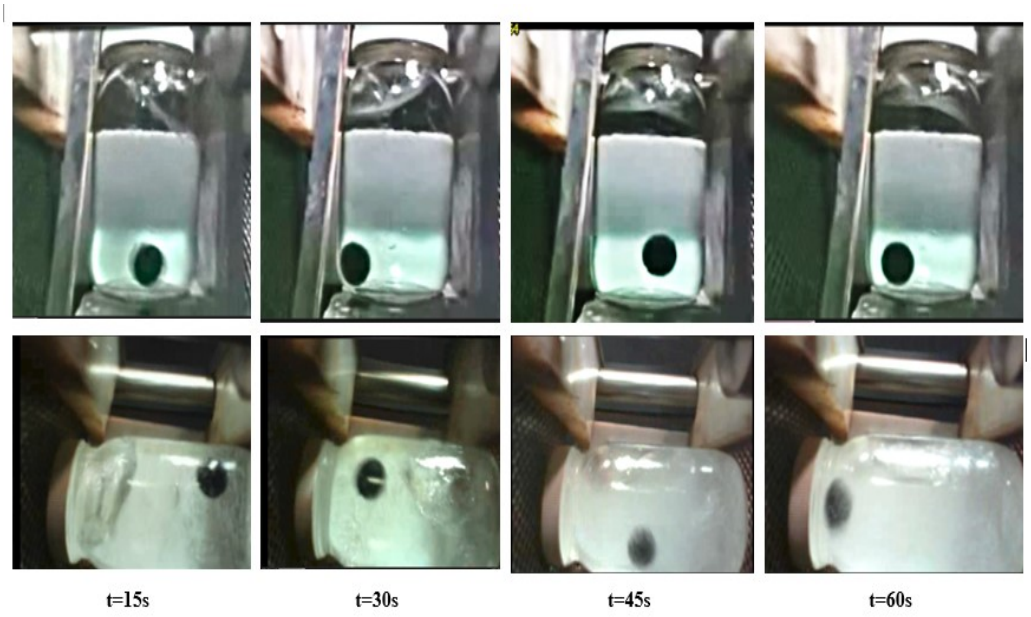

Fig. 10.2. Snapshots illustrations at t=15s, 30s, 45s and 60s of single particle cans (19 mm Nylon sphere) filled with equivalent concentration of 50% glycerin and processed at 2 Hz by placing the can inside the reciprocating cage with its longer axis vertically perpendicular (V – top row) and b) horizontally along the axis of reciprocation (HA – bottom row).

With regards to the particle motion in a single-particle can, Fig. 10.3 shows a schematic of the various positions of the particle observed inside the can in V and HA orientation over the first 3 min of reciprocation. The Nylon particle, which was heavier than the covering liquid, sunk to the bottom of the container and moved back and forth along the base of the can. Occasionally, the nylon particle would rise a little and then sink down again (Fig. 10.3). The single particle inside the can also moved randomly across the entire volume during HA orientation, as compared to its localized movements near the bottom half of can in V orientation. Thus, in the single particle case, HA orientation was found to exhibit better mixing conditions than the V orientation.

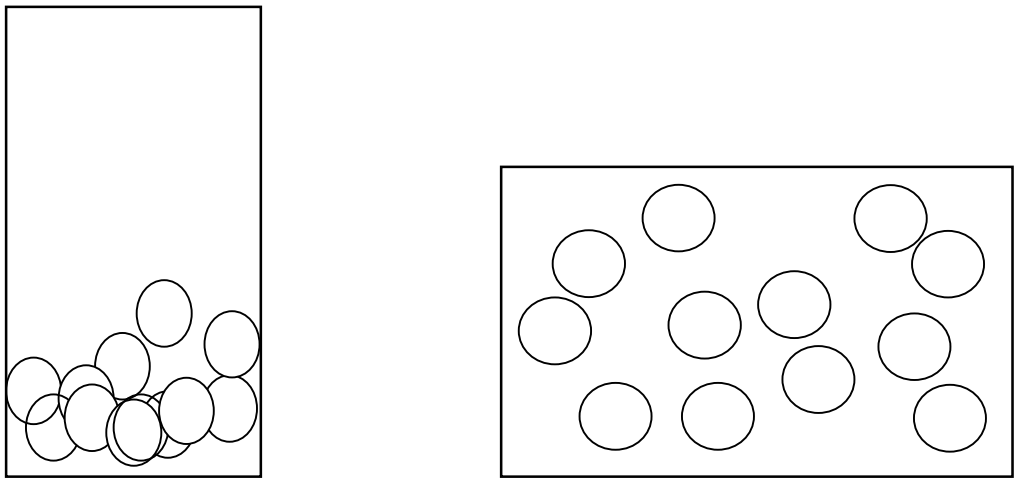

a) **b)**

Fig. 10.3. Schematic of particle position during the 1st 3 min of reciprocations in a single particle can (19 mm Nylon sphere) filled with equivalent concentration of 50% glycerin and processed at 2 Hz by placing the can inside the reciprocating cage with its longer axis a) vertically perpendicular (V) and b) horizontally along the axis of reciprocation (HA)**.**

Multiple Particles in can

Fig. 10.4 shows the snapshots of cans, filled with multiple particles (30% v/v 19mm nylon spheres) and the equivalent of 50% glycerin concentration, processed under the two orientations at 2 Hz. It was seen that in vertical orientation, particles were stacked at bottom of the container due to their weight. The motion of black particles at top of the can was more intense as compared to white particles at the bottom of the can. This particle motion demonstrated that agitation in the liquid was more intense towards the top near the headspace and was considerably low at the bottom of the container. As mixing progressed, black particles started moving down through the center of the container, and white particles started rising near the wall. Also, there was a slight rotation of particles observed due to the rocking motion in the containers.

In the HA orientation, the mixing was very severe and within the first 15s, all particles had been dispersed evenly throughout the container. The particles moved randomly throughout the can and there was no regional accumulation seen. Particles constantly collided with each other and with the walls of the container, unlike in V orientation Very severe particle movement during HA orientation, as compared to V orientation, may be attributed to the fact that there was more void

space available when the can was placed along its length and hence, particle packing was not so intense. Also, the particles bounced back on collision against the flat surface during HA orientation resulting in higher velocity generation, as compared to V orientation where the particles got deflected by the curved surface of the vertical wall.

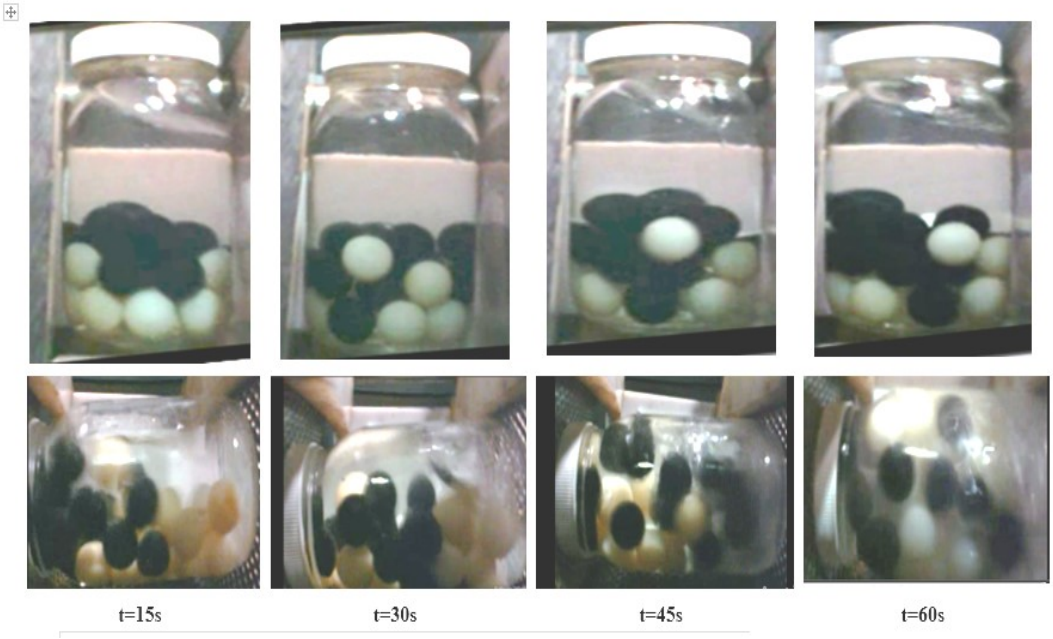

Fig. 10.4. Snapshots illustrations at t=15s, 30s, 45s and 60s of multiple particle cans (30% v/v 19mm Nylon spheres) filled with equivalent concentration of 50% glycerin and processed at 2 Hz by placing the can inside the reciprocating cage with its longer axis vertically perpendicular (V – top row) and horizontally along the axis of reciprocation (HA – bottom row).

From the results presented in this section, it can be seen that HA orientation had a higher intensity of particle motion and mixing, as compared to V orientation. This is in alignment with the results presented in Chapter 5, where HA orientation was found to be better for increasing the heat transfer coefficients U and h_{fp}. However, it must be mentioned that constant collision amongst the particles observed in HA orientation is not desirable for soft textured products, and under those scenarios, V orientation may be a better alternative.

10.4.3 Motion of particle as affected by particle density and liquid viscosity

To investigate the effect of particle density and liquid viscosity on the particle mixing behavior, one can was filled with three particles – one each of 19mm Nylon, polypropylene and

Teflon spheres and were filled with equivalent concentrations of 50 and 100% glycerin. These cans were processed at 2 Hz reciprocation frequency. The Teflon particle was colored black, Nylon particle was colored half black and half red, while the polypropylene particle was colored white. Fig. 10.5 shows the positions of the three particles inside a vertical can under equivalent concentrations of 50 and 100% glycerin, while Fig. 10.6 shows the schematics of the position of the three particles over a period of 3 min.

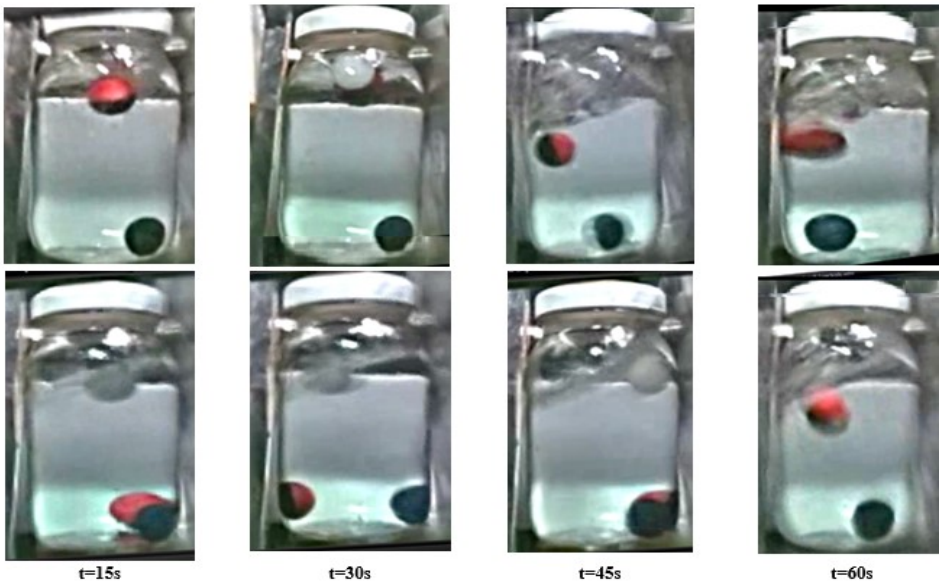

Fig. 10.5. Snapshots illustrations at t=15s, 30s, 45s and 60s of cans processed with Nylon (half red, half black), polypropylene (white) and teflon (black) spheres in 100% (top row) and 50% (bottom row) glycerin concentrations at 2 Hz.

It is seen from Fig. 10.5 that while Teflon particles sunk and sat at the bottom of the container for all concentrations of glycerin, polypropylene particles floated at the top of the container throughout the motion. The Nylon particle, on the other hand, was found at the bottom for 50% glycerin and was floating at the top for 100% glycerin. The motion of the high density Teflon was severely restricted due to its weight and it reciprocated at the base of the container. On the other hand, polypropylene and Nylon particles showed more movement. The Nylon particle showed most movement and was found to reach almost the height of the container in both 50 and 100% glycerin cans (Fig. 10.6).

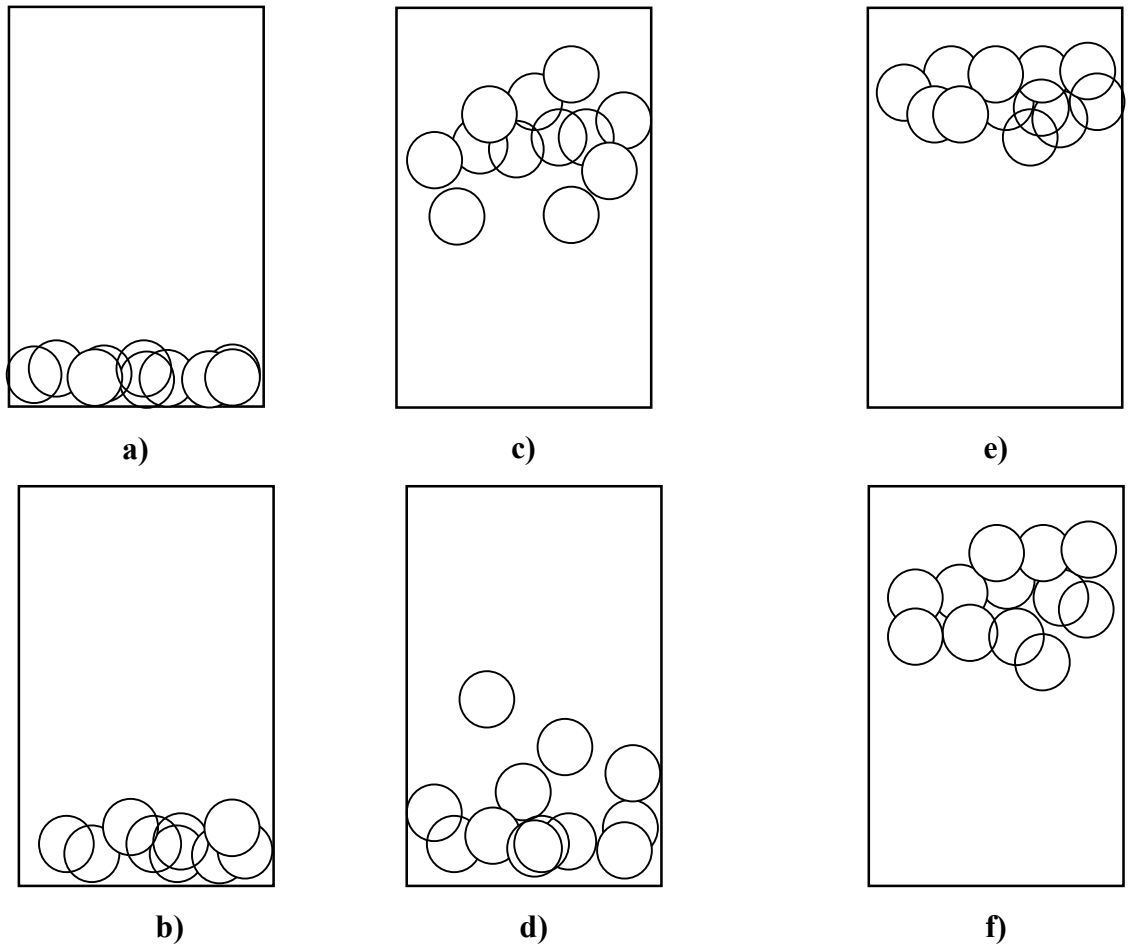

Fig. 10.6. Schematic of particle position during the 1st 3 min of reciprocations in cans processed with a) Teflon in 100% glycerin; b) Teflon in 50% glycerin; c) Nylon in 100% glycerin; d) Nylon in 50% glycerin; d) polypropylene in 100% glycerin; and f) polypropylene in 50% glycerin**.**

With regards to the effect of liquid viscosity, it is clear from Fig. 10.6 that the range of motion of all particles was much more in 50% glycerin as compared to 100% glycerin. This is mainly because of the lower resistance offered by lower viscous liquid to particle motion as compared to higher viscous liquid. Also, the amount of turbulence produced in higher viscous liquid is lower than that that in low viscosity liquid. However, the range of motion of Nylon particles in 100% glycerin solution was almost similar to that of the 50% glycerin solution, wherein most of the motion was in the top half of the container for the former condition and in the bottom half of the container for the latter. Thus, Nylon particle's range of motion did not decrease even on increase in liquid viscosity. This was due to higher agitation in the top of the can as a result of headspace effects discussed in Section 10.4.2, which aided Nylon particle motion under high

viscosity glycerin solution. This explains the phenomenon that h_{fp} of single Nylon particle was close to 500 W/m^{2}K in Chapter 6, even with 100% glycerin solution.

Sablani (1996) suggested that particle movement behavior reflects the flow pattern inside the can and the intensity of particle movement would be directly proportional to the intensity of heat transfer taking place inside the system. Thus, the results presented in this section help to explain the trends in the heat transfer coefficients observed in Chapters 6 and 7 wherein U and h_{fp} were found in the order: Nylon>polypropylene>Teflon.

10.4.4 Quantification of Multi-particle mixing behavior

Multiple particle mixing behavior was quantified by the movement of the center of mass of the white and black spheres. At time t=0, the center of mass of white and black particles are at maximum distance from each other. As reciprocation sets in, the amount of mixing progresses and this distance decreases. When the center of mass of white and black particles coincided with each other, the mixing was assumed to be complete and the time taken to achieve this was characterized as the mixing time. Fig. 10.7 presents the movement of the center of mass of the black and white spheres inside a can filled with 30% v/v Nylon particles and 50% glycerin solution and processed at 2 Hz with the longer axis of the can placed along the axis of reciprocation.

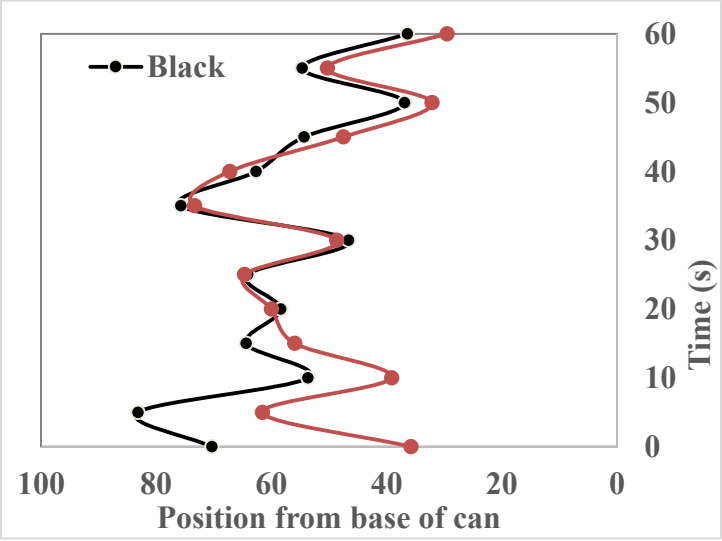

Fig. 10.7. Movement of the center of mass of the black and white spheres inside a can filled with 30% v/v Nylon particles and 50% glycerin solution and processed at 2 Hz reciprocation frequency with the longer axis along the axis of reciprocation (HA orientation).

In Fig. 10.7, it was seen that the center of mass of the particles also changed to and fro during each reciprocations. Hence, this plot could not be directly used to find out the mixing time. However, we observed from Fig. 10.7 that the distance between the centers of mass of the white particles did not get affected due to reciprocation and decreased progressively with increased mixing, proving an opportunity to be used as a measure of the intensity of mixing. Thus, to find mixing time, the distance between the center of mass of the two colors was plotted versus time and the point where the curve met the x-axis was taken as the mixing time. The mixing time for different parameters studied has been provided in Table 10.1. It was found that the mixing time was affected significantly by all the parameters studied viz. container orientation, liquid viscosity, particle concentration and reciprocation frequency.

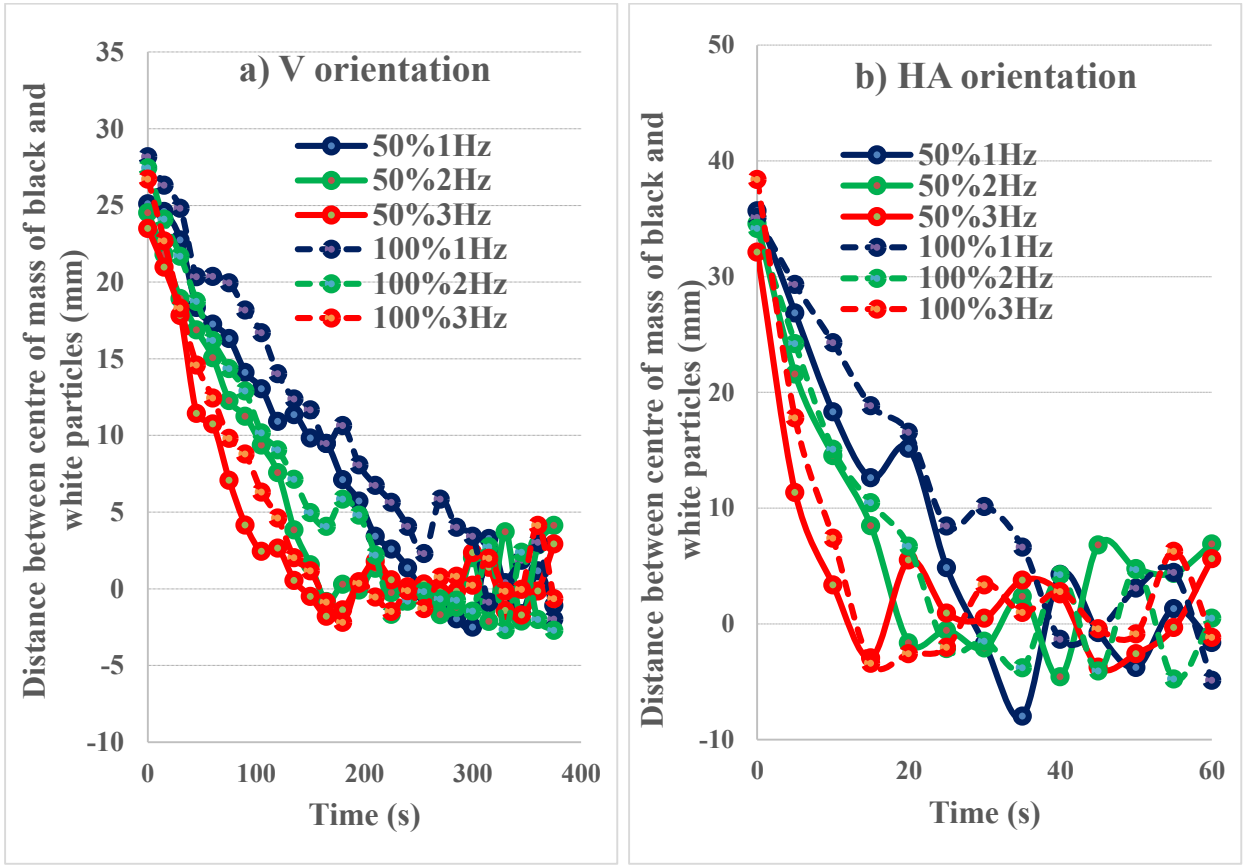

Fig. 10.8. Distance between centre of mass of black and white particles (mm) inside cans filled with various levels of liquid viscosity and processed at various frequency of reciprocation by keeping the longer axis of can along: a) V orientation; and b) HA orientation.

The distance between the center of mass of the particles of two colors for a multiple-particle can filled upto 30% v/v by equal number of white and black 19mm Nylon spheres has been plotted versus time for the two container orientations at various liquid viscosities and reciprocation frequency in Fig. 10.8. Here, it is noteworthy that the intensity of mixing during HA orientation was far greater than V orientation and hence, the mixing time was very low. Thus, during HA orientation, snapshots for calculation of mixing time was taken every 5s, while in V orientation, snapshots after every 15s ware considered. During HA orientation, the mixing time varied between 15-50 s, while during V orientation, longer mixing times of 90-480 s was observed (Table 10.1). The shorter mixing times was due to better particle and liquid motion observed during HA orientation as discussed in Section 10.4.2.

Table 10.1. Mixing time observed at various reciprocation frequency, particle concentration, liquid viscosity and container orientation.

Reciprocation Frequency (Hz)	Particle Conc. (% v/v)	Equivalent Glycerin Conc. (% v/v)	Mixing time (s)	
			HA orientation	V orientation
1	20	50	40	275
1	30	50	30	255
1	40	50	50	210
2	20	50	30	190
2	30	50	25	165
2	40	50	40	285
3	20	50	25	170
3	30	50	20	150
3	40	50	35	255
1	20	100	45	335
1	30	100	40	315
1	40	100	60	420
2	20	100	35	275
2	30	100	30	255
2	40	100	55	340
3	20	100	20	165
3	30	100	15	165
3	40	100	30	265

10.4.5 Effect of reciprocation frequency, liquid viscosity and particle concentration

The effect of reciprocation frequency, liquid viscosity and particle concentration was studied on mixing time for the two orientations using a full factorial design. The results for the mixing time have been presented in Table 10.1.

As expected, reciprocation frequency was found to be the most influential parameter which affected the amount of mixing and mixing time. As seen in Fig. 10.8, in both V and HA orientation, the distance between the center of mass of the two particles decreased at the fastest rate for 3 Hz frequency (red colored line) and at the slowest rate for 1 Hz frequency (blue colored line). The mixing time varied between 30-60 s and 255-420 s for HA and V orientation respectively at 1 Hz. However, on increasing the frequency to 3 Hz, the mixing time reduced drastically to 15-35 s for HA and 150-265 s for V orientation respectively. Liquid viscosity also affected the mixing time considerably. At 2 Hz frequency, mixing time was upto 50% more for can processed with equivalent of 100% glycerin concentration as compared to 50% glycerin concentration cans. These results are in agreement with the results of Sablani and Ramaswamy (1998) and Meng and Ramaswamy (2007d), who also demonstrated the decrease in mixing in higher viscous liquid and at lower agitation intensity due to a decrease in the Reynolds number.

With reference to particle concentration, it was seen that mixing time was found to slightly decrease from 20% to 30% but it was lowest for 40% particle concentration. The effect was more significant in V cans as compared to HA cans, as in V cans the particles were stacked at the bottom and motion was more difficult and particle concentration dependent. Increase in particle concentration from 20% to 30% resulted in greater number of particles and hence there was an increase in secondary agitation, which increased the turbulence and hence mixing due to their motion. At higher particle concentration (40% v/v) the container was packed tightly which restricted the free particle movement, and hence mixing time was higher. These results agree well with the effect of particle concentration on the trends in heat transfer coefficients presented in Chapters 6 and 7. Similar results in terms of mixing time was observed by Sablani (1996) and Meng (2006).

10.5 Conclusions

In this study, a methodology was suggested to conduct visualization studies at room temperature by taking the equivalent viscosity at the average temperature of the thermal process (85^{o}C). Further, the concept of the motion of the center of mass of particles of two different colors was suggested to study the particle mixing phenomenon during agitation thermal processing. The phenomenon of mixing was strongly affected by the container orientation and was markedly different for horizontal and vertical orientations. In vertical orientation, most of the movement of the can liquid and particles was concentrated near the headspace of the container, whereas in HA orientation, the entire can had turbulence and the mixing was very enhanced. This resulted in significantly lower mixing times as well for HA orientation as compared to V orientation. The extent of particle motion/mixing in the containers varied depending on the processing conditions. With a single particle in the container, the liquid viscosity and particle density influenced the particle motion in the container in each orientation, apart from reciprocation frequency. On increasing particle concentration in a multiple particle can, higher mixing was obtained. Although, very high packing was detrimental to mixing. The particle mixing time was shortened at higher reciprocation frequency and lower liquid viscosity. These results help to explain sorne variations in the heat transfer coefficients detailed in preceding Chapters.

CHAPTER 11

GENERAL CONCLUSIONS, CONTRIBUTION TO THE KNOWLEDGE AND RECOMMENDATIONS

11.1 General conclusions

Demand for better quality and safe products has prompted development of systems which can sterilize canned liquid particulate foods in a short period of time. With the promotion of Shaka® retorts, 'reciprocating agitation' has piqued the interest of thermal processing industry as a measure to deliver high quality end products. This study was focused on characterization of heat transfer during reciprocating agitation thermal processing of liquid particulate mixtures. A few of the notable conclusions are highlighted herein.

1. A lab-scale reciprocating retort (capacity: 4 cans) was developed by modifying an existing still retort to incorporate reciprocating motion by the aid of slider crank mechanism. It was demonstrated that the system works well within the range of operation conditions relevant to thermal processing applications. Issues in control of key variables (ex: temperature, frequency, amplitude, container orientation etc) were addressed. In-retort and in-container temperature distribution studies revealed better temperature distribution scenario in reciprocating retorts as compared to still retorts, which improved with increasing reciprocation intensity (by increasing frequency/amplitude).

2. The developed reciprocating retort was used to compare heating rates associated with reciprocating agitation vs. static mode of processing. It was found that reciprocating agitation helped to obtain faster heating rates (low temperature equilibration time, , low $f_{h\text{-}p}$ and $f_{h\text{-}l}$) with 2-7 times improvement in the values of heat transfer coefficients (U and h_{fp}), as compared to the conventional static retort. Due to the rapid heating conditions, process time requirements could be reduced by 46-62% as compared to static mode of processing. With 26-36% lower values of a quality degradation index, reciprocating agitation thermal processing was shown to have a good potential for high quality retention in processed products.

3. Further analysis into the effects of container orientation during thermal processing, cans placed with their longer axis along the axis of reciprocation (HA orientation) were demonstrated to have the highest heat transfer rates due to intensive turbulence in this orientation, which may

not always be desirable for some fragile products. On the other hand, cans placed vertically (V orientation) had the slowest heat transfer rates. Reduction in process time was not significant beyond 30 ms^{-2} reciprocation intensity for HA cans and of 60 ms^{-2} reciprocation intensity for HP and V cans. Based on the results, it was concluded that HA orientation must be selected for achieving lowest process times. HA orientation was best for processing products where turbulence was not a problem (like soups, sauces, pet foods etc.). It was also noted that HP and V orientation are more suitable for processing food products, where this intensive turbulence might be a concern.

4. In liquid-only/single-particle cans, heat transfer coefficients (U and h_{fp}) were found to be influenced significantly by various processing conditions. In general, higher U and h_{fp} values were obtained at lower liquid viscosity, higher reciprocation frequency, higher reciprocation amplitude, higher operating temperature, and higher headspace. In the single-particle case, 'comparable density' particles (Nylon) were found to have highest h_{fp} than other heavier/ lighter particles, due to their ability to move throughout the liquid.

5. Under all processing conditions and product properties, U and h_{fp} values of liquid-particulate mixtures were found higher for reciprocation agitation processing than rotary and still thermal processing and they increased with an increase in frequency. Although some headspace was necessary in all conditions, changes in headspace was not significant. Operating temperature had little effect on U and h_{fp}. In terms of product properties, U and h_{fp} were found to increase on increasing particle concentration till an optimal level, beyond which U and h_{fp} decreased due to dominance of conduction based heating. Higher liquid viscosity resulted in inhibition of movement of particles due to viscous forces and hence agitation and heat transfer decreased. Consistent with results from single-particle/liquid-only study, U and h_{fp} decreased at higher liquid viscosity and followed the trend: Nylon>polypropylene>Teflon.

6. Optimization studies on reciprocating agitation thermal processing suggested that application of high reciprocation intensities (37-45 ms^{-2}) were instrumental for maximing heat transfer. However, inclusion of agitation quality loss consideration presented lower reciprocation intensity (16-19 ms^{-2}) regimes as optimal processing scenarios. Temperature and headspace did not significantly affect optimization results. Other optimization results were also presented on applications of other constraints on product properties.

7. Dimensionless correlations for mixed (combination of natural and forced) and pure forced convection were developed for liquid-only and liquid-particulate canned foods using heat transfer data for reciprocating agitation thermal processing. Amplitude of reciprocation influenced the heat transfer phenomenon significantly as it was found to be most suitable as a parameter for the characterstic length in both U and h_{fp} correlations. The heat transfer phenomenon was best demonstrated using a mixed convection model, although the contribution of forced convection was found higher than all modes of rotary agitation.

8. Visualization studies were conducted to analyse the liquid/particle motion and particle mixing inside reciprocating containers. Results show that the mixing phenomenon was strongly affected by container orientation and explained various trends observed in Chapter 5. Particle mixing studies were conducted using a new concept of the motion of the center of mass of particles of two different colors. Single particle studies explained the effect of particle density and liquid viscosity observed earlier (Chapter 6), while multiple particles studies helped to explain the effect of addition of particles in a reciprocating can (Chapter 7). Mixing time was found to explain the effects of various processing conditions on heat transfer observed earlier in this study. Thus, the trends in heat transfer phenomenon observed in earlier chapters (Chapters 4-9) strongly correlated with trends in fluid flow and particle motion phenomenon observed in the visualization study (Chapter 10).

11.2 Contribution to knowledge

1. There was no detailed literature available investigating the heat transfer phenomenon during reciprocating mode of agitation. This study is the first scientific investigation of the heat transfer phenomenon during reciprocating agitation thermal processing. Comparison of this novel mode of agitation with other agitation techniques (like rotary agitation etc.) helps to express certainty about existence of better heat transfer conditions during reciprocating mode of thermal processing.

2. Modifications were made to a conventional static vertical retort to simulate reciprocating agitation conditions. Temperature distribution studies revealed that better temperature uniformity and rapid heat transfer rates exist inside reciprocating retorts. The study also demonstrates that it

is possible to install simple reciprocatory mechanism in existing static retorts for establishing and optimizing processing conditions for reciprocation agitation thermal processing.

3. Process time and a quality degradation index during reciprocating agitation thermal processing were compared under various processing conditions. Better heat transfer conditions during reciprocation helped to obtain very low process times. Thus, reciprocating agitation can be recommended as a suitable choice for obtaining high quality products.

4. Container orientation is an important choice while imparting reciprocating agitation. Effects of various container orientations are reported in this study. A concept of critical reciprocation intensity, beyond which increasing reciprocation intensity are insignificant, is discussed in detail.

5. For the first time, a comprehensive study was carried out to understand the effects of various processing conditions and product variables on associated heat transfer coefficients (U and h_{fp}) in liquid-only, single-particle and multiple-particle cans subjected to reciprocating agitation thermal processing. The values of U and h_{fp} under a various combination of these parameters are reported in this study.

6. Based on the results of U and h_{fp} available from study, optimal processing conditions under different constraints were suggested for using reciprocating agitations of cans during thermal processing.

7. Dimensionless correlations are established to predict heat transfer coefficients U and h_{fp} for liquid-only and liquid-particulate canned foods subjected to reciprocating agitation processing. Comparison with correlations on rotary mode of agitation is available, which demonstrates better forced convection conditions in reciprocating retorts.

8. A new concept of visualization of particle mixing by observing the motion of center of mass of the particles of various colors is used in this study. This method helps to predict mixing times for studying the phenomenon of particle mixing.

11.3 Recommendations for future research

This research work has demonstrated several important findings. Further, the detailed studies also showed some areas of interests for future research and development, which could be summarized as follows:

1. Investigation of other types of motions of container (ex: oscillating, rocking, tumbling etc.) which can produce better mixing and heat transfer coefficients.

2. Investigation of reciprocating mode of agitation during processing of thin profile semi-rigid and plastic food containers.

3. Extending this study to quantify the heat transfer coefficient (U and h_{fp}) during reciprocating agitation thermal processing of canned products containing non-Newtonian fluids and various commercial food products.

4. Quantifying the influence of other parameters (like particle shapes and sizes, can sizes and materials, particle shape and different retort heating mediums like water, steam etc.) on U and h_{fp} and more detailed comparison of reciprocating agitation with rotary agitation techniques.

5. Conducting biological validations of reciprocating agitation thermal process using predicted heat transfer coefficients.

6. Quality influence studies on various food products and investigation of the optimal processing schedules.

7. Relating the evaluated heat transfer coefficients to the conventional thermal processing heat penetration parameters, heating rate index and lag factor.

REFERENCES

Abbatemarco, C., & Ramaswamy, H. S. (1993). Heating behavior and quality factor retention in a canned model food as influenced by thermal processing in a rotary retort. *Journal of Food Quality*, 16, 273-285.

Abdullah A., Talib A. R. A., Jaafar A. A., Salleh M. A. M., & Chong W. T. (2010). The basics and issues of Thermochromic Liquid Crystal Calibrations. *Experimental Thermal and Fluid Science*, 34(8), 1089-1121.

Alhamdan, A., & Sastry, S. K. (1990). Natural convection heat transfer between non-Newtonian fluids and an irregular-shaped particle. *Journal of Food Process Engineering*, 13, 113–124.

Alhamdan, A., Sastry, S. K., & Blaisdell, J. L. (1990). Natural convection heat transfer between water and an irregular-shaped particle. *Transactions of the American Society of Agricultural and Biological Engineers*, 33, 620-624.

Anantheswaran, R. C., & Rao, M. A. (1985a). Heat transfer to model Newtonian liquid foods in cans during end-over-end rotation. *Journal of Food Engineering*, 4, 1-19.

Anantheswaran, R. C., & Rao, M. A. (1985b). Heat transfer to model Newtonian liquid foods in cans during end-over-end rotation. *Journal of Food Engineering*, 4, 21-35.

Angalet S. M. (2011). *Shaka: A new and novel processing technology to produce commercially sterile canned foods*. MSc Thesis, Kansas State University, Manhattan, Kansas

Atherton, D., & Thorpe, R. H. (1980). The processing of canned fruits and vegetables. In *Technical Bulletin No. 4. Campden Food Preservation Research Association*, Chipping Campden, Gloucestershire, UK.

Awuah, G. B., & Ramaswamy, H. S. (1996). Dimensionless correlations for mixed and forced convection heat transfer to spherical and finite cylindrical particles in an aseptic processing holding tube simulator. *Journal of Food Process Engineering*, 19, 269–287.

Awuah, G. B., Ramaswamy, H. S., & Simpson, B. K. (1995). Comparison of two methods for evaluating fluid to-surface heat transfer coefficients. *Food Research International*, 28, 261–271.

Awuah, G. B., Ramaswamy, H. S., & Economides, A. (2007a). Thermal processing and quality: Principles and overview. *Chemical Engineering and Processing: Process Intensification*, 46, 584–602.

Awuah, G. B., Khurana, A., Weddig, L. M., & Balestrini, C. G. (2007b). A comparative study of heat penetration data using remote sensors and needle or rod-in-tube thermocouples. *Journal of Food Process Engineering*, 30, 458–471.

Balasubramaniam, V. M., & Sastry, S. K. (1994a). Liquid-to-particle heat transfer in a continuous flow through a horizontal scraped surface heat exchanger. *Food and Bioproducts Processing*, 72, 189-196.

Balasubramaniam, V. M., & Sastry, S. K. (1994b). Liquid-to-particle convective heat transfer in non-Newtonian carrier medium during continuous tube flow. *Journal of Food Engineering,* 23, 169-187.

Balasubramaniam, V. M., & Sastry, S. K. (1994c). Method for non-invasive estimation of convective heat transfer coefficients in continuous flow. *American Society of Agricultural and Biological Engineers*, Paper No. 946543, 1-11.

Balasubramaniam, V. M., & Sastry, S. K. (1995). Use of liquid crystals as temperature sensors in food processing research. *Journal of Food Engineering*, 26, 219-230.

Ball, C. O. (1923). Thermal process times for canned foods. *Bulletin Natural Research Council (U. S.),* 7.

Ball, C. O., & Olson, F. C. W. (1957*). Sterilization in Food Technology*. McGraw-Hill, New York, NY, USA.

Balsa-Canto, E., Banga, J. R., & Alonso, A. A. (2002). A novel, efficient and reliable method for thermal process design and optimization. Part II: applications *Journal of Food Engineering*, 52, 235–247.

Barrett, D. M., Somogyi, L., & Ramaswamy, H. S. (2004). *Processing Fruits: Science and Technology*. CRC Press, Boca Raton, FL, USA.

Bee, G. R., & Park, D. K. (1978). Heat penetration measurement for thermal process design. *Food Technology*, 32, 56-58.

Berry, M. R., & Bradshaw, J. G. (1980). Heating characteristic of condensed cream of celery soup in a steritort: heat penetration and spore count reduction. *Journal of Food Science*, 45, 869-874.

Berry, M. R., & Kohnhorst, A. L. (1983). Critical factors for thermal processing of institutional pouches. *Journal of Food Protection*, 46, 487–489.

Berry, M. R., & Kohnhorst, A. L. (1985). Heating characteristic of homogeneous milk based formulas in cans processed in an agitating retort. *Journal of Food Science*, 50, 209-214.

Bhamidipati, S., & Singh, R. K. (1994). Fluid to particle heat transfer coefficient determination in a continuous system. *American Society of Agricultural and Biological Engineers*, Paper No. 946542, 1-13.

Bhamidipati, S., & Singh, R. K. (1995). Determination of fluid particle convective heat transfer coefficient. *Transactions of the American Society of Agricultural and Biological Engineers*, 38, 857- 862.

Boz, Z., & Erdogdu, F. (2013). Evaluation of two-dimensional approach for computational modelling of heat and momentum transfer in liquid containing horizontal cans and experimental validation. *Food and Bioproducts Processing*, 91, 37–45.

Breidt, F., Hayes, J, & McFeeters, R. F. (2007). Determination of 5-log reduction times for food pathogens in acidified cucumbers during storage at 10 and 25 ºC. *Journal of Food Protection*, 70, 2638-2641.

Britt, I., Zhang, Z., and Tung, M. A. (1997). Influence of temperature measuring systems on heat penetration results. Presented at *The Institute for Thermal Processing Specialists (IFTPS) Annual Meeting*, November 18–20. Arlington, VA.

Brown, K. L. (2000). Control of bacterial spores. *British Medical Bulletin*, 56, 158-171.

Cariño-Sarabia, A., & Vélez-Ruiz, J. F. (2013). Evaluation of convective heat transfer coefficient between fluids and particles in suspension as food model systems for natural convection using two methodologies. *Journal of Food Process Engineering*, 115, 173–181.

CFPRA. (1997). Guidelines for the Establishment of Scheduled Heat Processes for Low-Acid Foods. *Technical Manual No. 3. Campden Food Preservation Research Association*, Chipping Campden, Gloucestershire, UK.

Chandarana, D., & Gavin, A. (1989). Modeling and heat transfer study of heterogeneous foods processed aseptically. Presented at *The First International Congress on Aseptic Processing Technologies*, March 19-21, pp. 1-23. Indianapolis, IN.

Chandarana, D., Gavin, A., & Wheaton, F. W. (1990). Particle/Fluid Interface Heat Transfer under UHT Conditions at Low Particle/Fluid Relative Velocities. *Journal of Food Process Engineering*, 13, 191–206.

Chang, S. Y., & Toledo, R. T. (1989). Heat transfer and simulated sterilization of particulate solids in a continuously flowing system. *Journal of Food Science*, 54, 1017-1023.

Chang, S. Y., & Toledo, R. T. (1990). Simultaneous determination of thermal diffusivity and heat transfer coefficient during sterilization of carrot dices in a packed bed. *Journal of Food Science,* 55, 199-205.

Chau, K. V., & Snyder, G. V. (1988). Mathematical model for temperature distribution of thermally processed shrimp. *Transactions of the American Society of Agricultural and Biological Engineers*, 31, 608-612.

Clifcorn, L. E., Peterson, G. T., Boyd, J. M., & O'Neil, J. H. (1950). A new principle for agitating in processing of canned foods. *Food Technology*, 4, 450–460.

Conley, W., Kaap, L., & Shuhmann, L. (1951). The application of "End-Over-End" agitation to the heating and cooling of canned food products. *Food Technology,* 5, 457-460.

Damay, L., & Pain, J. P. (1993). Mesure du coefficient d' échange de chaleur entre une particule et un fluide en écoulement. *Rapport du Diplôme d' Etudes Approfondies en Génie des Procédes Industriels*, Villetaneuse, France.

De Cordt, S., Avila, S., Hendrickx, M., & Tobback, P. (1994). DSC and protein-based time-temperature indicators: case study of α-amylase stabilized by polyols and/or sugar. *Biotechnology and Bioengineering*, 44, 859–865.

De Cordt, S., Hendrickx, M., Maesmans, G., & Tobback, P. (1992). Immobilized α-amylase from Bacillus licheniformis: a potential enzymic indicator for thermal processing. *International Journal of Food Science and Technology*, 27, 661–673.

Deniston, M. F., Hassan, B. H., & Merson, R. L. (1987). Heat Transfer Coefficients to Liquids with Food Particles in Axially Rotating Cans. *Journal of Food Science*, 52, 962-966.

Dhayal, P., Chhanwal, N., & Anandharamakrishnan, C. (2013). Heat Transfer Analysis of Sterilization of Canned Milk Using Computational Fluid Dynamics Simulations. *Journal of Food Science and Engineering*, 3, 571-583

Dimou, A., Stoforos, N. G., & Yanniotis, S. (2014). Effect of Particle Orientation during Thermal Processing of Canned Peach Halves: A CFD Simulation. *Foods*, 3, 304-317.

Dwivedi, M. (2008). *Heat transfer to canned Newtonian liquid-particulate mixture subjected to axial agitation processing*. PhD Thesis, McGill University, Montreal, Canada.

Dwivedi, M., & Ramaswamy, H.S. (2010a). An empirical methodology for evaluating the fluid to particle heat transfer coefficient in bi-axially rotating cans using liquid temperature data. *Journal of Food and Bioprocess Technology*, 3, 716-731.

Dwivedi, M., & Ramaswamy, H. S. (2010b). Comparison of heat transfer rates during thermal processing under end-over-end and axial modes of rotation. *Journal of Food Science and Technology*, 43, 350–360.

Dwivedi, M., & Ramaswamy, H. S. (2010c). Comparative study of wireless versus standard thermocouples for data gathering and analyses in rotary cookers. *Journal of Food Processing and Preservation*, 34, 557-574.

Dwivedi, M., & Ramaswamy, H. S. (2010d). Dimensionless correlations for convective heat transfer in canned particulate fluids under axial rotation processing. *Journal of Food Process Engineering*, 33, 182–207.

Ecklund, O.F. (1956). Correction factors for heat penetration thermocouples. *Food Technology*, 10(1), 43-44.

Erdogdu, F., & Tutar, M. (2011). Velocity and temperature field characteristics of water and air during natural convection heating in cans. *Journal of Food Science*, 76, 119-129.

Evans, D. E. (1992). *Hydrostatic cooker discharge*. U.S. patent 5,161,457, Nov 10.

Farid, M., & Ghani, A. G. (2004). A new computational technique for the estimation of sterilization time in canned food. *Chemical Engineering and Processing*, 43, 523–531

Fernandez, C. L., Rao M. A., Rajavasireddi S. P., & Sastry S. K. (1988). Particulate heat transfer to canned snap beans in a steritort. *Journal of Food Process Engineering*, 10, 183–198.

Francesco, M., & Vittorio, R. (2003). Industrial assessment and control of canned food sterilization. Presented at *AIChE Annual Meeting*, November, 16-21. San Francisco, CA, USA,.

Gadonna, J. P., Pain, J. P., & Barigou, M. (1996). Determination of the convective heat transfer coefficient between a free particle and a conveying fluid in a horizontal pipe. *Food and Bioproduct Processing*, 74, 27-39.

Garrote, R. L., Silva, E. R., Roa, R. D., & Bertone R. A. (2006). Heat transfer coefficients to canned green peas during end-over-end sterilisation. *International Journal of Food Science and Technology*, 41, 1016-1022.

Gerber, F. (1938). *Reciprocating cooker*. U.S. patent 2,134,817, Nov 1.

Ghani, A. G., Farid, M. M., & Chen, X. D. (2002). Numerical simulation of transient temperature and velocity profiles in a horizontal can during sterilization using computational fluid dynamics. *Journal of Food Engineering*, 51, 77-83.

Ghani, A. G., Farid, M. M., & Zarrouk, S. J. (2003). The effect of can rotation on sterilization of liquid food using computational fluid dynamics. *Journal of Food Engineering*, 57, 9–16.

Ghiron, K., & Litchfield, J. B. (1997). Magnetic thermometry in the aseptic processing of multiphase foods. In *Engineering and Food at ICEF 7*, pp. 77-80. Jowitt, R., Eds., Sheffeld Academic Press, Sheffeld, UK.

Gillespy, T. G. (1953). Estimation of the sterilizing values of processes as applied to canned foods. II – Packs heating by conduction: complex processing conditions and value of coming-up time of retort. *Journal of Science of Food and Agriculture*, 4, 553–565.

Guiavarc'h, Y. P., Deli, V., Van Loey, A. M., & Hendrickx, M.E. (2002a). Development of an enzymic time temperature integrator for sterilization processes based on Bacillus licheniformis a-amylase at reduced water content. *Journal of Food Science,* 67, 285–291.

Guiavarc'h, Y. P., Dintwa, E., Van Loey, A. M., Zuber, F. T., & Hendrickx, M. E. (2002b). Validation and use of an enzymic time-temperature integrator to monitor thermal impacts inside a solid/liquid model. *Food and Biotechnology Progress*, 18, 1087–1094.

Gultekin D. H., & Gore, J. C. (2006). Measurement of thermal diffusivity by magnetic resonance imaging. *Magnetic Resonance Imaging*, 24, 1203-1207.

Gultekin D. H., & Gore, J. C. (2008). Measurement of heat transfer coefficients by nuclear magnetic resonance. *Magnetic Resonance Imaging,* 26, 1323-1328.

Haentjens, T. H., Van Loey, A. M., Hendrickx, M. E., & Tobback, P. P. (1998). The use of a-amylase at reduced water content to develop time temperature integrators for sterilization processes. *LWT- Food Science and Technology*, 31, 467–472.

Hassan, B. H. (1984). *Heat transfer coefficients for particles in liquid in axially rotating cans*. PhD thesis, University of California, Davis, CA, USA, 1984.

Hassan, H. F. & Ramaswamy, H. S. (2013). Bio-validation of bi-axial rotary thermal processing. *LWT-Food Science and Technology,* 53(2), 418-425.

Hassan, H. F., Ramaswamy, H. S., & Dwivedi, M. (2012). Overall and Fluid-to-particle Heat Transfer Coefficients associated with Canned Particulate non-Newtonian Fluids during Free Bi-axial Rotary Thermal Processing. *International Journal of Food Engineering*, 8, 1556-3758.

Hayakawa, K. I. (1964). *Development of formulas for calculating the theoretical temperature history and sterilizing value in a cylindrical can of thermally conductive food during heating*. PhD thesis, Rutgers State University, New Brunswick, NJ, USA, 1964.

Hayakawa, K. I. (1977). Mathematical methods for estimating proper thermal processes and their computer implementation. *Advances in Food Research*, 23, 75-141.

Heinz, G., & Hautzinger, P. (2007). *Meat processing technology for small-to medium-scale producers*. RAP (Food and agriculture organization of the United Nations) Publication, Bangkok, Thailand.

Hendrickx, M., Maesmans, G., De Cordt, S., Noronha, J., Van Loey, A., & Tobback, P. (1995). Evaluation of the integrated time-temperature effect in thermal processing of foods. *Critical Reviews in Food Science and Nutrition*, 35, 231–262.

Hersom, A. C., & Hulland, E. D. (1980). *Canned foods: Thermal processing and microbiology (7th Ed.)*. Churchill-Livingstone: Edinburgh, London, UK.

Hiddink J, Schenk J, & Bruin S. (1976). Natural convection heating of liquids in closed containers. *Applied Scientific Research*, 32, 217–37.

Higgins, K. T. (2012). Reciprocating retorts. *Food Engineering Magazine*, August 2012, 95-96.

Holdsworth, S. (1985). Optimization of thermal processing – a review. *Journal of Food Engineering*, 4, 89–116.

Holdsworth, S., & Simpson, R. (2007). *Thermal Processing of Packaged Foods, (2nd ed.)*. Springer, New York, USA.

Hotani, S., & Mihori T. (1983). Some thermal engineering aspects of the rotation method in sterilization. In *Heat Sterilization of Food*. T. Motohito and K. I. Hayakawa (Eds.). Koseisha-Koseikaku Co., Ltd., Tokyo, Japan, pp. 121–129.

IFTPS (1992). Temperature Distribution Protocol for Processing in Steam Still Retorts, Excluding Crateless Retorts. *Institute for Thermal Processing Specialists (IFTPS) Annual Meeting*, Fairfax, VA, USA.

IFTPS (2015). Lateral Agitation Effects on Shelf-Stable Food Products In Flexible and Semi-Rigid Containers. *Institute for Thermal Processing Specialists (IFTPS) Annual Meeting*, March 3-6, San Antonio, TX, USA.

Incropera, F. P., & DeWitt, D. P. (2000). *Fundamentals of Heat and Mass Transfer (4th ed.)*. John Wiley and Sons, New York, USA.

Incropera, F. P., & DeWitt, D. P. (2011). *Introduction to Heat Transfer, (6th ed.)*. John Wiley and Sons, New York, USA.

Institut-Appert. (1979). *Barèmes de Sterilisation pour Aliments Appertisés*. Institut Appert., Paris, France.

James, P. W., Hughes, J. P., Jones, T. E. R., & Tucker, G. S. (2006). Numerical Simulations of Non-Isothermal Flow in Off-Axis Rotation of a Can Containing a Headspace Bubble. *Chemical Engineering Research and Design*, 84, 311–318.

Johnson, A.G., Kirk, G., & Shin, T. (1988). Numerical and experimental analysis of mixed forced and natural convection about a sphere. *Transactions of American Society of Agricultural Engineers*, 31, 293–299, 304.

Joseph, S. J., Speers, R. A., & Pillay, V. (1996). Effect of Head Space Variation and Heat Treatment On the Thermal and Rheological Properties of Nonagitated, Conduction-Heated Materials. *LWT - Food Science and Technology*, 29, 556-560.

Kakade, V. U., Lock, G. D., Wilson, M., Owen, J. M., & Mayhew, J. E. (2009). Accurate heat transfer measurements using thermochromic liquid crystal. Part 1: Calibration and characteristics of crystals. *International Journal of Fluid Flow*, 30, 939-949.

Kannan, A., & Sandaka, P. C. (2008). Heat transfer analysis of canned food sterilization in still retort. *Journal of Food Engineering,* 88, 213–228.

Kurian, V, Varma, M. N., & Kannan, A. (2009). Numerical studies on laminar natural convection inside inclined cylinders of unity aspect ratio. *International Journal of Heat and Mass Transfer*, 52, 822–838.

Larousse, J, & Brown B. (1996). Heat Penetration in Canned Foods - Theoretical Considerations. In *Food Canning Technology*, pp. 383-423. Larousse, J., and Brown, B., Eds., Wiley-VCH, New York, USA.

Lekwauwa, A. N., & Hayakawa, K. I. (1986). Computerized model for the prediction of thermal responses of packaged solid-liquid food mixture undergoing thermal processes. *Journal od Food Science*, 51, 1042-1049.

Lenz, M. K., & Lund, D. B. (1978). The lethality-fourier number method heating rate variations and lethality confidence intervals for forced-convection heated foods in containers. *Journal of Food Process Engineering*, 2, 227-271.

Lesley, D. R. (1987). Update on Ball Electronic Systems Division's (BESD) detraces temperature environment measurement system as applied to food thermal processing. Presented at *The IFTPS Annual meeting*, Anaheim, California, USA.

Lowe, F.W., Poindexter, F.E. (1952). *Horizontal retort with reciprocating agitator*. U.S. patent 2,615,834, Oct 28.

Lund, D. B. (1982). Application of optimization in heat processing. *Food Technology*, 36(7), 97-100.

Maesmans, G., Hendrickx, M., De Cordt, S., & Tobback, P. (1993). Theoretical considerations on design of multicomponent time temperature integrators in evaluation of thermal processes. *Journal of Food Processing and Preservation*, 17, 369–389.

Maesmans, G., Hendrickx, M., De Cordt, S., & Tobback, P. (1994). Feasibility of the use of a time–temperature integrator and a mathematical model to determine fluid-to-particle heat transfer coefficients. *Food Research International*, 27, 39–51.

Marquis, F., Bertch, A.J., & Cerf, O. (1982). Stérilisation des liquides dans des bouteilles d'axe horizontal. *Influence de la vitesse de rotationsur le transfert de chaleur*, 62, 220–231.

May, N. (1997). *Guidelines for performing heat penetration trials for establishing thermal processes in batch retort systems (Guideline No.16)*. Campden and Chorleywood Food Research Association, Chipping Campden, Gloucestershire, UK.

Meng, Y. (2006). *Heat Transfer Studies on Canned Particulate Viscous Fluids during End-Over-End Rotation*. PhD Thesis, McGill University, Montreal, Canada.

Meng, Y., & Ramaswamy, H. S. (2005). Heat transfer coefficients associated with canned particulate/non-Newtonian fluid (CMC) system during end-over-end rotation. *Food and Bioproducts processing*, 83, 229-237.

Meng, Y., & Ramaswamy, H. S. (2007a). System variables affecting heat transfer in a canned particle in Newtonian fluid system during end-over-end rotation. *LWT-Food Science and Technology*, 40, 1240–1245.

Meng, Y., & Ramaswamy, H. S. (2007b). Effect of system variables on heat transfer to canned particulate non-Newtonian fluids during end-over-end rotation. *Food and Bioproducts processing,* 85, 34-41

Meng, Y., & Ramaswamy, H. S. (2007c). Dimensionless heat transfer correlations for high viscosity fluid-particle mixtures in cans during end-over-end rotation. *Journal of Food Engineering,* 80, 528-535.

Meng, Y., & Ramaswamy, H. S. (2007d). Visualization of particle/liquid movements in high viscous fluids during end-over-end rotation. *Journal of Food Engineering*, 80 (2), 545-552.

Mohamed, I. O. (2007). Determination of an effective heat transfer coefficients for can headspace during thermal sterilization process. *Journal of Food Engineering*, 79, 1166-1171

Montville, T. J., & Sapers, G. M. (1981). Thermal resistance of spores from pH elevating strains of Bacillus licheniformis. *Journal of Food Science*, 4, 710-1712.

Mwangi, J. M., Rizvi, S. S. H., & Datta, A. K. (1993). Heat transfer to particles in shear flow: application in aseptic processing. *Journal of Food Engineering*, 19, 55-74.

National Canners Association Research Laboratories. (1968). *Laboratory Manual for Food Canners and Processors*. AVI Pub. Co., Westport, CT, USA.

Naveh, D., & Kopelman, I. J. (1980). Effect of some processing parameters on the heat transfer coefficients in a rotating autoclave. *Journal of Food Processing and Preservation*, 4, 67-77

Nelson, P, & Tressler, D. (1980). *Fruit and Vegetable Juice Processing Technology*. AVI Pub. Co., Westport, CT, USA.

NFPA. (1971). Processes for low-acid canned foods in glass containers. In *Bulletin 30-L. National Food Processors' Association*, Washington, DC, USA.

NFPA. (1982). Processes for low-acid canned foods in metal containers. In *Bulletin 26-L, (12th ed.) National Food Processors' Association*, Washington, DC, USA.

NFPA. (1985). *Guidelines for Thermal Process Development for Foods Packaged in Flexible Containers*. National Food Processors' Association, Washington, DC, USA.

Ochoa, A. D., Baughn, J. W., & Byerley, A. R. (2005). A new technique for dynamic heat transfer measurements and flow visualization using liquid crystal thermography. *International Journal of Heat and Fluid Flow*, 26, 264-275

Odlaug T. E., & Pflug I. J. (1978). Clostridium Botulinum and Acid Foods. *Journal of Food Protection,* 41(7), 566-573.

Oharenko, L. (1958). *Retort Shaking Apparatus*. U.S. patent 2,834,585, May 13.

Pflug, I. J. (2003). *Microbiology and Engineering of Sterilization Processes (11th ed.)*. Environmental Sterilization Laboratory, Minneapolis, MN, USA,.

Pflug, I. J., Jones, A. T., & Blanchett, R. (1980a). Performance of bacterial spores in a carrier system in measuring the F_o-value delivered to cans of food heated in a steritort. *Journal of Food Science,* 45, 940-945.

Pflug, I. J., Smith, G., Holcomb, R., & Blanchett, R. (1980b). Measuring sterilizing values in containers of food using thermocouples and biological indicator units. *Journal of Food Protection,* 43, 119-123.

Pham, Q. T. (1989). Calculation of thermal process lethality for conduction-heated canned foods. *Journal of Food Science*, 52, 967 -974.

Prickett, M. E. (1958). *Can Retort*. U.S. patent 2,849,944, Sep 2.

Ramaswamy, H. S., & Abbatemarco, C. (1996). Thermal processing of fruits. In *Processing of Fruits - Science and Technology, Volume 1*. Somogyi, L. P., Ramaswamy, H. S., and Hui, Y. H., Eds., Technomic Publishing Company, Lancaster, Pennsylvania, USA.

Ramaswamy, H. S., & Dwivedi, M. (2011). Effect of Process Variables on Heat-Transfer Rates to Canned Particulate Newtonian Fluids during Free Bi-axial Rotary Processing. *Food and Bioprocess Technology*, 4(1), 61-79.

Ramaswamy, H. S., & Grabowski, S. (1996). Influence of entrapped air on the heating behavior of a model food packaged in semi-rigid plastic containers during thermal processing. *LWT - Food Science and Technology*, 29, 82–93.

Ramaswamy, H. S., & Sablani, S. S. (1997). Particle motion and heat transfer in cans during end-over-end rotation: influence of physical properties and rotational speed. *Journal of Food Processing and Preservation,* 21, 105-127.

Ramaswamy, H. S., & Zareifard, R. (2002). Dimensionless correlations for forced convection heat transfer to spherical particles under tube-flow heating conditions. In *Transport Phenomena in Food Processing*, J. Welti-Chanes, J. F. Velez-Ruiz., G. Barbosa-Canovas (Eds.), pp. 505-520. CRC Press, Boca Raton, FL, USA.

Ramaswamy, H. S., Abbatemarco, C., & Sablani, S. S. (1993). Heat transfer rates in a canned food model as influenced by processing in an end-over-end rotary steam-air retort. *Journal of Food Processing and Preservation*, 17, 269-286.

Ramaswamy, H. S., Awuah, G. B. & Simpson, B. K. (1997). Heat transfer and lethality considerations in aseptic processing of liquid/particle mixtures: a review. *Critical Reviews in Food Science and Nutrition*, 37, 253-286.

Ramaswamy, H. S., Awuah, G. B., Kim, H. J., & Choi, Y. M. (1996). Evaluation of a chemical marker for process lethality measurement at 110ºC in a continuous flow holding tube. *Journal of Food Processing and Preservation,* 20, 235-249.

Rao, M. A., & Anantheswaran, R. C. (1988). Convective heat transfer to fluid foods in cans. *Advances in Food Research*, 32, 39-84.

Rattan, N. S., & Ramaswamy, H. S. (2014). Quality optimization of canned potatoes during rotary autoclaving. *Journal of Food Quality*, 37, 168-176.

Rodriguez, A. C., & Teixeira, A. A. (1988). Heat transfer in hollow cylindrical rods used as bioindicator units for thermal process validation. *Transactions of the American Society of Agricultural and Biological Engineers*, 31, 1233–1236.

Rönner, U. (2002). Validation of heat processes using bio-indicators (polymer beads). In *Second international symposium on thermal processing – Thermal processing: validation challenges (Session 2:3)*. Tucker, G. S., Eds., Campden and Chorleywood Food Research Association, Chipping Campden, Gloucestershire, UK.

Sablani, S. S. (1996). *Heat transfer studies of liquid particle mixtures in cans subjected to end-over-end processing*, PhD thesis, McGill University, Montreal, Canada.

Sablani, S. S., & Ramaswamy, H. S. (1995). Fluid-to-particle heat-transfer coefficients in cans during end-over-end processing. *LWT - Food Science and Technology*, 28(1), 56-61.

Sablani, S. S., & Ramaswamy, H. S. (1996). Particle heat transfer coefficients under various retort operating conditions with end-over-end rotation. *Journal Food Process Engineering*, 9, 403-424.

Sablani, S. S., & Ramaswamy, H. S. (1997). Heat transfer to particles in cans with end-over-end rotation: Influence of particle size and concentration. *Journal of Food Process Engineering*, 20(4), 265-283.

Sablani, S. S., & Ramaswamy, H. S. (1998). Multi-particle mixing behavior and its role in heat transfer during end-over-end agitation of cans. *Journal of Food Engineering*, 38(2), 141-152.

Sablani, S. S., & Ramaswamy, H. S. (1999). End-over-end agitation processing of cans containing liquid particle mixtures: Influence of continuous versus oscillatory rotation. *Journal of Food Science Technology*, 5, 385-389.

Sablani, S. S., Ramaswamy, H. S., & Mujumdar, A. S. (1997). Dimensionless correlations for convective heat transfer to liquid and particles in cans subjected to end-over-end rotation. *Journal of Food Engineering*, 34, 453–472.

Sastry, S. K., Beelman, R. B., & Speroni, J. J. (1985). A three-dimensional finite element model for thermally induced changes in foods: application to degradation of agaritine in canned mushrooms. *Journal of Food Science*, 50, 1293–1299.

Sastry, S. K., Shen, G. Q., & Blaisdell, J. L. (1989). Effect of ultrasonic vibration on fluid-to-particle convective heat transfer coefficients. *Journal of Food Science*, 54, 229-230.

Sielaff, H. (1996). *Technologie der Konservenherstellung (12th ed.)*. Behr's Verlag, Hamburg, Germany.

Silva, C. L. M., Oliveira, F. A. R., Lamb, J., Torres, A. P., & Hendrickx, M. (1994). Experimental validation of models predicting optimal surface quality sterilization temperatures. *International Journal of Food Science and Technology*, 29, 227–241.

Silvestrini, J. A. (2008). *Thermal conditioning system having continuous conveyor*. U.S. patent 7,337,707, Mar 4.

Smout, C., Avila, I., Loey, A. M. L., Hendrickx, M. E. G., & Silva, C. (2000). Influence of rotational speed on the statistical variability of heat penetration parameters and on non-uniformity of lethality in retort processing. *Journal of Food Engineering,* 45, 93–102.

Steele, R. J., & Board, P. W. (1979). Thermal process calculations using sterilizing ratios. *Journal of Food Technology*, 14, 227-235.

Stoforos, N. G. (1988). *Heat Transfer in Axially Rotating Canned Liquid/Particulate Food Systems*. PhD Thesis, University of California, Davis CA, USA, 1988.

Stoforos, N. G., & Merson, R. L. (1990). Estimating heat transfer coefficients in liquid particulate canned foods using only liquid temperature data. *Journal of Food Science*, 55, 478-483.

Stoforos, N. G., Merson, & R. L. (1991). Measurement of heat transfer coefficients in rotating liquid/particulate systems. *Biotechnology Progress*, 7, 267-271.

Stoforos, N. G., & Merson, R. L. (1992). Physical property and rotational speed effects on heat transfer in axially rotating liquid/particulate canned foods. *Journal of Food Science*, 57, 749–754

Stoforos, N. G., & Reid, D. S. (1992). Factors influencing serum separation of tomato ketchup. *Journal of Food Science*, 57(3), 707-713.

Stoforos, N. G., Noronha, J., Hendrickx, M., & Tobback, P. (1997). Inverse superposition for calculating food product temperatures during in-container thermal processing. *Journal of Food Science*, 62, 220-224.

Stumbo, C. R. (1973). *Thermo bacteriology in Food Processing (2nd ed.)*. Academic press, New York, USA.

Stumbo, C. R., Purohit, K. S., & Ramakrishnan, T. V. (1975). Thermal process lethality guide for low-acid foods in metal containers *Journal of Food Science*, 40, 1316–1323.

Sun, G., Hewitt, G. F., Wadekar, V. V., & Hewitt, G. F. (1994). Heat transfer in horizontal slug flow. *Institute of Chemical Engineers*, 271-276.

Tattiyakul, J., Rao, M. A., & Datta, A. K. (2002). Heat transfer to three canned fluids of different thermo-rheological behaviour under intermittent agitation. *Food and Bioproduct Processing*, 80, 20–27

Tucker, G. S. (1999). A novel validation method: application of time-temperature integrators to food pasteurization treatments. *Food and Bioproduct Processing*, 77, 223–231.

Tucker, G. S. (2004). Improving rotary thermal processing. In *Improving the Thermal Processing of Foods*, pp. 125–137. Richardson, P., Eds., CRC Press, Boca Raton, FL, USA.

Van Loey, A. (1996). *Enzymic time temperature indicators for the quantification of thermal processes in terms of food safety*. PhD Thesis, University of Leuven- KU Leuven, Belgium.

Van Loey, A., Ludikhuyze, L., Hendrickx, M., De Cordt, S., & Tobback, P. (1995). Theoretical consideration on the influence of the z-value of a single component time temperature integrator on thermal process impact evaluation. *Journal of Food Protection*, 58, 39–48.

Van Loey, A. M., Haentjens, T. H., Hendrickx, M. E., & Tobback, P. P. (1997). The development of an enzymic time temperature integrator to assess the lethal efficacy of sterilization of low-acid canned foods. *Food Biotechnology*, 11, 169–188.

Van Loey, A., Guiavarc'h, Y., Claeys, W., & Hendrickx, M. (2004). The use of time temperature indicators (TTIs) to validate thermal processes. In *Improving the thermal processing of foods*, pp. 365–384. Richardson, P., Eds., Woodhead Publishing, Cambridge, London, UK.

Veltman, J. (1995). *Sterilizer with reduced surface contamination*. U.S. patent 5,458,261, Oct 17.

Walden, R. (1999). *Thermal processing method and apparatus for use with packaging containers*. U.S. patent 5,857,312, Jan 12.

Walden, R., & Emanuel, J. (2010). Developments in in-container retort technology: the Zinetec Shaka process. **In** *Case studies in novel food processing technologies: Innovation in*

processing, packaging, and predictive modeling, Chapter 16, pp. 359-406. Doona, C. J., Kustin, K., and Feeherry, F.E., Eds., Woodhead Publishing Ltd., Cambridge, UK,

Wang, N., Zhang, N., & Wang, M. (2006). Wireless sensors in agriculture and food industry - Recent development and future perspective. *Computers and Electronics in Agriculture*, 50, 1-14.

Weng, Z. J., Hendrickx, M., Maesmans, G., & Tobback, P. (1992). The use of a time temperature integrator in conjunction with mathematical-modeling for determining liquid particle heat-transfer coefficients. *Journal of Food Engineering, 1*6, 197-214.

Zitoun, K. B., & Sastry, S. K. (1994). Determination of convective heat transfer coefficient between fluid and cubic particles in continuous tube flow using non-invasive experimental techniques. *Journal of Food Process Engineering*, 17, 209-228.